

BIOMASS CHAR AS AN IN-SITU CATALYST FOR TAR REMOVAL IN GASIFICATION SYSTEMS

Ziad Abu El-Rub

Doctoral Committee

Chairman and secretary:	Prof.dr. F. Eising	University of Twente
Promotor:	Prof.dr.ir. G. Brem	University of Twente
Co- promotor:	Prof.dr.ir. Th. H. van der Meer	University of Twente
Members:	Prof.dr.ir. W.P.M. van Swaaij	University of Twente
	Prof.dr.ir. J.J.H. Brouwers	TU Eindhoven
	Prof.Dr.-Ing. H. Spliethoff	TU Munich
	Prof.dr.ir. L. Lefferts	University of Twente
	Dr.ir. A.I. van Berkel	TNO

Title: Biomass Char as an In-Situ Catalyst for Tar Removal in Gasification Systems

Author: Ziad Abu El-Rub

PhD thesis, Twente University, Enschede, The Netherlands

March 2008

ISBN: 978-90-365-2637-1

Copyright © 2008 by Ziad Abu El-Rub, Enschede, The Netherlands

Printed by Gildeprint Drukkerijen, Enschede, The Netherlands, 2008

BIOMASS CHAR AS AN IN-SITU CATALYST FOR TAR REMOVAL IN GASIFICATION SYSTEMS

DISSERTATION

to obtain

the degree of doctor at the University of Twente,

on the authority of the rector magnificus,

prof.dr. W.H.M. Zijm

on account of the decision of the graduation committee,

to be publicly defended

on Friday 7th of March 2008 at 13.15

by

Ziad Yousef Kamel Abu El-Rub

born on April 21st, 1975

in Rusaifah, Jordan

This dissertation is approved by:

Prof.dr.ir. G. Brem

Prof.dr.ir. Th.H. van der Meer

Promotor

Co-promotor

To my parents and my wife Maisa'a

Summary

The contribution of biomass to the world's energy supply is presently estimated to be around 10 to 14 %. The European Union set a firm target of cutting 20% of the EU's greenhouse gas emissions by 2020 - the EU will be willing to put this goal up to 30% if the US, China and India make similar commitments. EU leaders also set a binding overall goal of 20% for renewable energy sources by 2020, compared to the present 6.5 %. It is expected that biomass gasification will play an important role in meeting these goals. The gasification technology for biomass conversion is still in the development stage and cannot be considered as proven technology for small and medium scale applications. The main technical barrier remains the efficient removal of tars from the produced gases in gasification systems. Tars are defined as a generic term comprising all organic compounds present in the producer gas excluding gaseous hydrocarbons (C_1 - C_6) and benzene.

Biomass char was noticed to have a good catalytic activity for tar removal. However, a comprehensive study on biomass char for tar removal is not found. Therefore, the objective of this thesis is to find out how active and useful biomass char is for tar removal and to design an innovative application of biomass char for in-situ tar removal in a biomass gasifier.

To achieve this objective, the first step was to carry out a literature review for the various types of catalysts that have been used in several investigations on tar reduction. It was found that biomass char could be a good alternative catalyst for tar removal. The attractiveness of the biomass char for solving the tar problem is related to its low cost, natural production inside the biomass gasifier, catalytic activity for tar reduction and the possibility to be integrated in the gasification process itself.

The most important catalysts found in the literature review were compared with biomass chars by measuring the conversion of naphthalene and phenol, as model tar components. Tests were carried out in a fixed catalyst bed at a temperature range of 700–900 °C under atmospheric pressure, a gas residence time in the empty reactor of 0.3 s and an atmosphere of carbon dioxide and steam. Thus, biomass chars were compared with calcined dolomite, olivine, used fluid catalytic cracking (FCC) catalyst, biomass ash and commercial nickel catalyst. The biomass chars gave the highest naphthalene conversion among the low cost catalysts. A simple first order kinetic model was proposed to describe the naphthalene conversion for the biomass char in the temperature range of 700-900 °C. The first order kinetic rate constant was found to have an activation energy of ($E_a = 61 \text{ kJ/mol}$) and a pre-exponential factor of ($k_o = 1 \cdot 10^4 \text{ s}^{-1}$).

Further, the catalytic activity of the biomass char for tar reduction and the simultaneous char conversion was studied in a fixed bed reactor experimentally. For both naphthalene, as model tar component, and real tar almost complete conversions at temperatures ≥ 800 °C, 0.3 s gas residence time and 500-630 μm char particle size were reached. It was found that the pore structure of the char particle and the mineral content are key elements for the biomass char activity. Although the exact mechanism of tar removal by char is not yet clear it can be assumed that when the tar in the producer gas passes through the char bed, the tar molecule is adsorbed on the char particle active sites to enter parallel gasification and polymerization reactions. The char catalyzes the gasification reactions of the adsorbed tars with steam and carbon dioxide. Moreover, it catalyzes the formation of tar radicals that enter heavy hydrocarbon polymerization reactions where the products are deposited as coke on the surface of the char. Despite the coke formation on the char particle, its catalytic activity was found to be constant during time at temperatures above 800 °C. This was related to the refreshment of the active surface area by the gasification reactions of coke and char with steam and carbon dioxide. Thus, the char consumption by the gasification reactions was not a disadvantage for the char as a catalyst but on the contrary an advantage because of its continuous (re-)activation.

The knowledge gained from the fixed bed experiments is incorporated in a single char particle model to get a better understanding of the performance of char for tar reduction. The char particle was found to be isothermal under the standard conditions. Moreover, the effect of internal and external mass transfer resistances were minor and the reactions can be considered as kinetically controlled. The particle model is further extended to a fixed bed reactor model. The reactor model results were validated with fixed bed experimental results. It was found that the bulk temperature and gas residence time are the main parameters having a significant effect on the naphthalene conversion. As far as the carbon conversion (gasification) is concerned the bulk temperature, gas residence time, bulk steam concentration and time on stream were the dominating process parameters.

The performance of biomass char for tar removal was also investigated in a bubbling fluidized bed reactor. The naphthalene removal in a bubbling fluidized char bed was modeled and validated with experiments. It was found that the mass transfer of the naphthalene between the bubble and the dense phase is the main mechanism that controls the naphthalene removal in bubbling fluidized bed conditions. The model results agree well with the experimental results.

Finally, a novel experiment was carried out that combined biomass gasification and tar removal by char in one reactor. Here, biomass was fed in a bubbling bed where biomass char was used as the bed material. It was found that this in-situ tar removal seems to be very promising for a significant reduction of the tar problem: more than 97 % tar conversion at 850 °C was measured. Based on these results, a preliminary design of a gasification system with in-situ tar removal by char is presented. The next step for future research would be the development of an optimum reactor for gasification with in-situ tar removal.

Samenvatting

De huidige bijdrage van biomassa aan de energievoorziening in de wereld wordt geschat op 10 tot 14%. De Europese Unie streeft naar het bereiken van 20% duurzame energie voor elektriciteitsopwekking in het jaar 2020. Het is de verwachting dat biomassavergassing een belangrijke bijdrage zal leveren aan de realisatie van deze doelstellingen. Ondanks de aanzienlijke inspanning aan onderzoek en ontwikkeling is de vergassingstechniek echter nog steeds in de demonstratiefase. De belangrijkste technologische barrière voor commercialisatie van biomassavergassing is de efficiënte verwijdering van teer uit het productgas. Teer is een algemene term voor alle “condenseerbare” organische componenten die aanwezig zijn in het productgas, met uitzondering van gasvormige koolwaterstoffen (C_1 - C_6) en benzeen.

Behalve gas wordt ook kool (char) geproduceerd bij biomassavergassing. De char van biomassa blijkt een goede katalytische werking te bezitten voor de reductie van teer. Incidentele aanwijzingen en resultaten in de literatuur toonden de katalytische rol van char in teerverwijdering reeds aan. Een omvattende studie op deze werking, die zou bijdragen in de oplossing van het “teerprobleem”, is echter niet beschikbaar. De huidige studie heeft daarom tot doel te onderzoeken hoe actief biomassa char is en hoe biomassa char zo efficiënt mogelijk gebruikt kan worden om de hoeveelheid teer, die uit een biomassa vergasser komt, te reduceren.

De eerste stap in dit onderzoek was het maken van een literatuuroverzicht van de diverse types katalysatoren die al zijn toegepast in de verschillende onderzoeken gericht op teerreductie in vergassingsprocessen. Uit de vergelijking bleek dat biomassa char een goede alternatieve katalysator voor teerverwijdering zou kunnen zijn door de lage kosten, de natuurlijke productie van char in de biomassa vergasser, de katalytische activiteit en de mogelijkheid tot integratie in het vergassingsproces zelf (“in-situ”). Vervolgens zijn de belangrijkste katalysatoren voor teerverwijdering uit het literatuuroverzicht (dolomiet, olivijn, spent ‘Fluid Catalytic Cracking’(FCC) katalysator, as van biomassa en een commerciële nikkel katalysator) zijn in een experimenteel onderzoek vergeleken met biomassa char. Hiertoe zijn testen uitgevoerd in een vastbed buisreactor in het temperatuurbereik van 700-900 °C, atmosferische druk en een verblijftijd van het gas in het lege katalysatorbed van 0.3 s. Om de teren te simuleren is gebruik gemaakt van de modelcomponenten naftaleen en phenol in een matrix van kooldioxide en waterdamp. De resultaten laten zien dat onder de zogenaamde “low-cost” katalysatoren, biomassa char de hoogste naftaleen conversie heeft. Een eenvoudig eerste orde kinetisch model is afgeleid voor de naftaleen conversie door biomassa char in het temperatuurbereik van 700-900 °C. De activeringsenergie is bepaald op $E_a=61 \text{ kJ/mol}$ en de pre-exponentiële factor op $k_o=1 \cdot 10^4 \text{ s}^{-1}$. Vervolgens is een experimentele parameterstudie in een vastbedreactor uitgevoerd waarbij zowel de katalytische activiteit van de biomassa char voor

teerreductie als de gelijktijdige charconsumptie door vergassingsreacties gemeten zijn. Bij gebruik van zowel naftaleen als een volledig teermengsel, werd een nagenoeg volledige conversie (>99%) bereikt bij temperaturen ≥ 800 °C, 0.3s verblijftijd van het gas en 500-630 μm deeltjesgrootte van de char. Het blijkt dat de poreuze structuur en het mineraalgehalte van de chardeeltjes belangrijk zijn voor de katalytische activiteit. De charconsumptie is beperkt en kan voldoende aangevuld worden door de natuurlijke productie van char in een vergassingsproces.

Een mogelijke verklaring voor de katalytische activiteit van de char kan als volgt geformuleerd worden: de teren in het productgas stromen door het vastbed waar ze in contact komen met de chardeeltjes; de “teermolekullen” adsorberen vervolgens aan de actieve locaties in de poriën van de chardeeltjes en nemen deel aan parallelle vergassings- en polymerisatie reacties. De char treedt op als katalysator van de vergassingsreacties van de geadsorbeerde teren met waterdamp en kooldioxide. Daarnaast versnelt de char het kraken en de polymerisatie van teermolekullen naar uiteindelijk roet (cokes) dat op het oppervlak van de char kan neerslaan. Ondanks deze cokesvorming op de chardeeltjes blijkt uit de experimenten dat de katalytische activiteit bij temperaturen boven de 800 °C vrijwel constant blijft. Dit komt omdat de neergeslagen cokes samen met de char voortdurend vergast door de aanwezigheid van waterdamp en CO₂. Hierdoor is de consumptie van char door de vergassingsreacties juist geen nadeel voor char als katalysator, maar eerder een voordeel vanwege de continue re-activatie van het (inwendige) oppervlak van de chardeeltjes.

Een model voor een enkel chardeeltje is ontwikkeld om beter inzicht te krijgen in de sleutelparameters voor de teerverwijdering door chardeeltjes. Het chardeeltje blijkt isotherm te zijn onder typische vergassingsomstandigheden, en bovendien blijken de overall effecten van intern en extern massatransport, veroorzaakt door deeltjesgrootte en gas snelheid, minimaal te zijn. Het deeltjesmodel is verder uitgebreid naar een model voor een vastbed reactor. De resultaten van het reactormodel zijn gevalideerd met de eerder genoemde resultaten van de experimenten in de vastbed reactor. De overeenkomst tussen model en metingen is redelijk goed en gebleken is dat de bedtemperatuur en de verblijftijd van het gas een dominante invloed hebben op de naftaleen conversie. Wat de charconsumptie betreft is gebleken dat, naast de twee hiervoor genoemde parameters, de waterdampconcentratie in het inkomende gas dominant is.

Vervolgens is de prestatie van biomassa char voor teerverwijdering ook onderzocht in een stationaire wervelbed reactor. De naftaleenreductie in een wervelbed van chardeeltjes is zowel gemodelleerd als experimenteel onderzocht. Het massatransport van naftaleen (teer) tussen de bellen- en dichte fase blijkt de dominante processtap voor de naftaleenreductie te zijn. Model- en experimentele resultaten komen goed met elkaar overeen. De gemeten naftaleenreducties waren maximaal 90%. De lagere reductie in vergelijking tot de vastbed reactor wordt grotendeels veroorzaakt door de “kortsluiting” van teren via de bellen in het wervelbed.

Tenslotte is een aantal experimenten uitgevoerd waarbij biomassa direct is toegevoerd aan een wervelbed bestaande uit chardeeltjes. Hierbij vindt simultaan in één reactor de vergassing van biomassa en het reduceren van de teren plaats (in-situ

teerverwijdering in de vergasser). Bij deze experimenten met een 'charbed' is gebleken dat bij bed temperaturen van ca. 850 °C meer dan 97% teerreductie plaatsvindt in vergelijking met een wervelbed bestaande uit zanddeeltjes. Deze laatste resultaten bieden een goed startpunt voor verder onderzoek naar de ontwikkeling van een optimaal systeem voor biomassavergassing in een wervelbed bestaande uit char als bedmateriaal.

Table of Contents

Chapter 1 Introduction.....	1
Abstract.....	1
1.1 Biomass Gasification.....	2
1.2 State of the Art.....	3
1.3 Tar Problem.....	4
1.4 Why Biomass Char?.....	6
1.5 Objective of the Thesis.....	6
1.6 Organization of the Thesis.....	6
References.....	7
Chapter 2 A Review of Catalysts for Tar Reduction in Biomass Gasification.....	9
Abstract.....	9
2.1 Introduction.....	10
2.2 Catalysts.....	11
2.2.1 Minerals.....	12
2.2.1.1 Calcined rocks.....	12
2.2.1.2 Olivine.....	14
2.2.1.3 Clay minerals.....	16
2.2.1.4 Iron ores.....	17
2.2.2 Synthetic catalysts.....	18
2.2.2.1 Char.....	18
2.2.2.2 Fluid catalytic cracking (FCC) catalysts.....	19
2.2.2.3 Alkali metals based catalysts.....	20
2.2.2.4 Activated alumina.....	21
2.2.2.5 Transition metals-based catalysts.....	22
2.3 Concluding Remarks.....	25
References.....	26

Chapter 3 Experimental Comparison of Biomass Char with other Catalysts for Tar Reduction.....31

Abstract.....	31
3.1 Introduction.....	32
3.2 Experimental.....	34
3.2.1 Setup.....	36
3.2.2 Tar sampling method.....	37
3.2.3 Gas analysis.....	38
3.2.4 Test procedure.....	38
3.2.5 Tested Catalysts.....	39
3.2.6 Experimental data evaluation.....	40
3.3 Results and Discussion.....	42
3.3.1 Phenol conversion.....	42
3.3.2 Naphthalene conversion.....	46
3.3.3 Reaction rate for naphthalene removal with char.....	47
3.4 Evaluation.....	51
3.4.1 Results.....	51
3.4.2 Biomass char as a catalyst.....	51
3.5 Concluding Remarks.....	52
References.....	53

Chapter 4 Tar Reduction in a Fixed Char Bed.....57

Abstract.....	57
4.1 Introduction.....	58
4.2 Experimental.....	58
4.2.1 Synthetic tar setup.....	58
4.2.2 Real tar setup.....	60
4.2.3 Char properties.....	62
4.3 Experimental results on naphthalene reduction with char.....	64
4.3.1 Reference experiment.....	64
4.3.2 Effect of the char bed temperature.....	65
4.3.3 Effect of the gas residence time.....	67
4.3.4 Effect of the particle size.....	70
4.3.5 Effect of the inlet naphthalene concentration.....	71

4.3.6 Effect of the gas composition.....	72
4.3.7 Effect of the char properties and source.....	74
4.4 Experimental results on real tar reduction with char.....	76
4.5 Discussion.....	81
4.6 Concluding remarks.....	85
References.....	86
Chapter 5 Modeling of Naphthalene Reduction with Char Particles.....	89
Abstract.....	89
5.1 Introduction.....	90
5.2 Single particle model.....	90
5.2.1 Kinetics.....	91
5.2.2 Mass balance.....	95
5.2.3 Energy balance.....	99
5.2.4 Physical properties and parameters estimation.....	102
5.2.5 Numerical solution.....	105
5.2.6 Reference conditions.....	106
5.2.7 Results of the single particle model.....	106
5.3 Reactor model.....	110
5.3.1 Reactor model validation.....	113
5.3.2 Key parameters for optimal design.....	120
5.4 Evaluation.....	125
5.5 Concluding Remarks.....	129
References.....	129
Chapter 6 Tar Reduction in a Bubbling Fluidized Char Bed.....	133
Abstract.....	133
6.1 Introduction	134
6.2 Model Development.....	134
6.2.1 Hydrodynamics.....	135
6.2.2 Solving the mass balances.....	137
6.3 Model results.....	139
6.3.1 Effect of particle size.....	140
6.3.2 Effect of bed temperature.....	142

6.3.3 Effect of the bed height.....	143
6.4 Experimental results.....	145
6.4.1 Experimental setup.....	145
6.4.2 Synthetic tar results.....	146
6.4.2.1Effect of particle size.....	146
6.4.2.2Effect of bed height.....	147
6.5 Validation of the model.....	148
6.6 In-situ Real Tar Reduction.....	149
6.6.1 Gasifier.....	149
6.6.2 Experimental results.....	151
6.7 Evaluation.....	153
6.7.1 Naphthalene removal in a secondary fluidized bed.....	153
6.7.2 Comparison of the naphthalene removal in a fixed and a fluidized bed	154
6.7.3 Biomass gasification in a char bed.....	155
6.8 Application.....	159
6.9 Concluding Remarks.....	159
References.....	160
Chapter 7 Conclusions and Recommendations.....	163
7.1 Conclusions.....	163
7.2 Recommendations.....	166
Nomenclature.....	167
Appendix A.....	175
List of Publications.....	183
Acknowledgment.....	185
Curriculum Vitae.....	187

Chapter 1

Introduction

Abstract

In this chapter, a general introduction is given on the research described in this thesis. As a start the importance of biomass gasification, its major applications and the state-of-the-art are presented. The main technological obstacle for the commercialization of this technology is the presence of tar in the produced gas and its condensation in the downstream equipment. Some background on tar, its impact and the present solutions are discussed. New process-integrated solutions are required for the further penetration of gasification in the market. In this work, biomass char as a catalyst for tar reduction was chosen. Finally, the objective of the research and the organization of the thesis are presented.

1.1 Biomass Gasification

Biomass can be defined as any organic material of a plant origin. The contribution of biomass to the world's energy supply is presently estimated to be around 10 to 14 % [1]. The European Union leaders also set a binding overall goal of 20% for renewable energy sources by 2020, compared to the present 6.5 % [2].

Biomass can be converted to energy carriers by biological or thermochemical processes. It is expected that the biomass gasification technologies may play an important role in meeting the set goals for renewable energies. This is because of the higher efficiencies that may be produced by gasification compared to other technologies such as combustion.

Gasification involves the partial combustion of biomass to produce gaseous fuels (fuel gases or synthesis gases) in a gasification medium such as air, oxygen or steam. The fuel gas produced is called "producer gas". These gaseous products have many possible applications such as [3, 4] generation of heat or electricity, synthesis of liquid transportation fuels, production of hydrogen, synthesis of chemicals and generation of electricity in fuel cells. Prime movers that can be coupled to gasification plants for power production are internal combustion engines, stirling engines, (micro-) turbines and fuel cells.

The gaseous products of the biomass gasification need to be cleaned from different types of impurities such as [5] (a) solid impurities (dust); (b) inorganic impurities such as nitrogen compounds (NH_3 and HCN); sulfur compounds (H_2S), ash and metal compounds and (c) organic impurities (tars). Table 1-1 shows the gas quality requirement for power generation [6].

Table 1-1 The gas quality requirement for power generation [6]

		IC engine	Gas turbine
Particles	mg/Nm ³	<50	<30
Particle size	µm	<10	<5
Tar	mg/Nm ³	<100	n.i
Alkali metals	mg/Nm ³	n.i	0.24

n.i: not indicated

The main types of biomass gasifiers are updraft, downdraft, fluid bed and entrained flow gasifiers. The updraft gasifiers show the highest tar production while the downdraft gasifiers show the lowest. Fluid bed gasifiers show intermediate tar production. For large-scale applications, the preferred type is the entrained flow gasifier while for small scale applications the downdraft gasifier is often used. The bubbling and circulating fluidized bed gasifiers can be competitive in medium scale applications.

1.2 State of the Art

Biomass gasification is still in the development stage despite the significant efforts devoted for the commercialization of this technology [7, 8]. This is mainly because the biomass gasification process is still relatively expensive in comparison to fossil fuel based energy systems. Moreover, the technology has a low reliability for long-term operation [7] and the main technical barrier for its commercialization still remains the efficient removal of tar. Biomass gasification can be seen in several applications and implementations in the following market segments listed in Table 1-2 [8, 9]:

Table 1-2 Markets of applications and implementations of biomass gasification [8, 9]

Application	State of art
Heat gasifiers	<p>Commercially available.</p> <p>No need for tar removal.</p> <p>The most well-known technologies are those of Bioneer (fixed-bed, updraft), PRM Energy (fixed-bed, updraft), Ahlstrom (now FosterWheeler) and Lurgi Umwelt (both CFB).</p> <p>Mostly, the gas is used for combustion in boilers and district heating purposes.</p>
Cofiring gas from a gasifier in existing power plants	<p>The first gasifier coupled with a power plant was installed in Zeltweg, Austria, followed by others in Lahti in Finland, Amer in the Netherlands, Vermont in the USA and Ruien in Belgium.</p> <p>The Zeltweg, Lahti and Amer plants have the simplest gas cleaning; a cyclone solids separator at the outlet of the gasifier and no (or limited) product gas cooling.</p>
IGCC: integrated gasification and combined cycle	<p>IGCC is seen as the total final concept of a biomass-to-electricity system.</p> <p>The development and implementation is complex.</p> <p>The European Commission has identified the potential of this technology, and called for proposals for Targeted Projects on this subject in 1993.</p> <p>Three projects were selected, Arbre, Bioflow and Bioelettrica.</p> <p>Arbre plant in Selby, England is being realized and the combined cycle has been in operation. The gasification technology was supplied by TPS which used dolomite as a catalyst for gas cleaning. However, the owner (Kelda group) has sold the plant to EPRI for unknown reasons in 2002. Negotiations are on going about the future of Arbre.</p> <p>The cofiring project in Vermont is seen as a development towards an IGCC plant.</p> <p>The Värnamo pressurized gasifier of Foster Wheeler (formerly Ahlström) was also mothballed after positive results of the demonstration project. The plant has high temperature gas cleaning in a metallic filter. The capacity was too small for commercial operation.</p> <p>Within the sixth EU framework program, a new project is approved recently for syngas production using the Värnamo gasifier. It is an integrated project called CHRISGAS.</p>
CFB with gas engine	<p>A relatively new application is the combination of circulating fluid bed technology coupled with gas engines.</p>

Fixed bed gasification for power production

Many small-scale, fixed bed gasifiers are either in operation or under development around the world.

Some of these are based on old technologies (N-Ireland, Harboore) but also recent successful R&D results have been implemented (ESP, tar crackers, 2-stage gasifiers).

Most of the units are CHP plants where heat is used for district heating.

Entrained flow gasification for syngas production

The European Directive on liquid biofuels for the transportation sector has been an important driver to develop new technologies for syngas production using entrained flow gasification.

In Freiberg, Germany, three entrained flow gasifiers are in operation for syngas, methanol, hydrogen and Fisher-Trops diesel production from biomass. Pyrolysis oil gasification is also considered as an alternative route for this purpose (CHOREN Project).

More details on the state of art and recent projects for biomass gasification are given by Maniatis [7] and Kwant et. al. [9].

1.3 Tar Problem

Tars are defined as a generic term comprising all organic compounds present in the producer gas excluding gaseous hydrocarbons (C_1-C_6) and benzene[10]. Figure 1-1 shows the typical composition of the biomass tars [11]. However, this composition depends on the type of fuel and the gasification process.

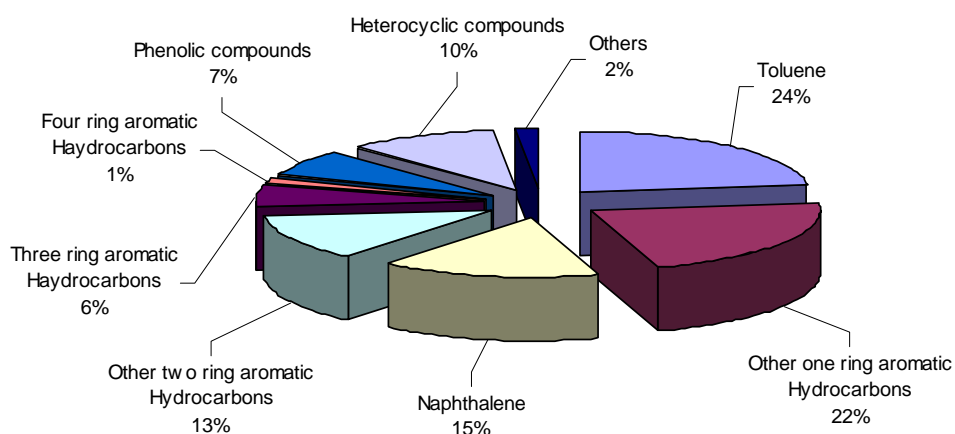


Figure 1-1 Typical composition of biomass tars (wt %) [11] (modified)

Different classifications for tars are found in literature [3, 12-15]. In general, these classifications are based on: properties of the tar components, and the aim of the producer gas application. The tar components can be segregated and classified into five classes based on their chemical, condensation and solubility behavior, as given in Table 1-3. This classification system has been developed by Padban [16] in the framework of the project "Primary measures for the reduction of tar production in

fluidized-bed gasifiers", funded by the Dutch Agency for Research in Sustainable Energy (SDE).

Table 1-3 Classification of tars [3, 12-15]

Class	Class name	Tar components	Representative compounds
1	GC Undetectable Tars	The heaviest tars, cannot be detected by GC	None
2	Heterocyclic	Tars containing hetero atoms; highly water-soluble compounds	Pyridine, phenol, cresols, quinoline, soquinoline, dibenzophenol
3	Light Aromatic Hydrocarbons (LAH)	Aromatic components. Light hydrocarbons with single ring. Important from the point view of tar reaction pathways, do not pose a problem on condensability and solubility	Toluene, ethylbenzene, xylenes, styrene
4	Light Poly Aromatic Hydrocarbons (LPAHs)	Two and three rings compounds; condense at low temperature even at very low concentration	Indene, naphthalene, methylnaphthalene, biphenyl, acenaphthalene, fluorine, phenanthrene, anthracene
5	Heavy Poly Aromatic Hydrocarbons (HPAHs)	Larger than three-rings, condense at high temperatures at low concentrations	Fluoranthene, pyrene, chrysene, perylene, coronene

The presence of tars in the fuel gas is one of the main technical barriers in the biomass gasification development. These tars can cause several problems, such as [17] cracking in the pores of filters, forming coke and plugging the filters, and condensing in the cold spots and plugging the lines, resulting in serious operational interruptions. Moreover, these tars are dangerous because of their carcinogenic character, and they contain significant amounts of energy which should be transferred to the fuel gas as H₂, CO, CH₄, etc. In addition, high concentration of tars can damage or lead to unacceptable levels of maintenance for engines and turbines. The tar levels and composition varies with gasifier type, process conditions, and biomass type.

Tars can be removed by [18] physical (e.g., scrubbing), non-catalytic (e.g., thermal cracking), and catalytic tar removal processes. The catalytic tar conversion is technically and economically interesting approach for gas cleaning. It has the potential to increase conversion efficiencies while simultaneously eliminating the need for the collection and disposal of tars. The catalytic conversion of tars is commonly known as hot gas cleaning. In literature, the research on catalytic hot-gas cleanup has involved

[18, 19]: (a) incorporating or mixing catalyst with the biomass feed to achieve catalytic gasification or pyrolysis, (also called in-situ), (b) treatment of gasifier raw gas in a second bed of calcined rocks catalysts, and (c) three steps process (gasifier + guard bed of calcined rocks catalysts + bed of a nickel-based catalyst). In this thesis, biomass char was studied as a low cost alternative catalyst that can be used for both in-situ or downstream tar reduction.

1.4 Why Biomass Char?

The products of biomass gasification process are producer gas, ash and tars. The ash produced from wood biomass gasifiers contains mainly char because of the low ash content in the wood biomass. The char was noticed to have a good catalytic activity for tar removal. In a downdraft gasifier, both fuel and gas flow downwards through the reactor enabling pyrolysis gases to pass through a throated hot bed of char [20]. This results in cracking of most of the tars into non-condensable gases and water [21]. The two stage gasifier developed by the Technical University of Denmark (DTU) gives almost complete tar conversion ($< 15 \text{ mg/Nm}^3$) [22]. The high tar removal is related to passing the volatiles through a partial oxidation zone followed by a char bed.

The feasibility of the catalytic cleaning of producer gas from the biomass gasification is mainly determined by economics [22]. The economics of the overall gasification process is affected by the cost of the catalyst downstream of the biomass gasifier, lifetime of the catalyst, and gas cleaning temperature. The attractiveness of biomass char for solving the tar problem comes from its low cost, its catalytic activity for tar reduction and natural production inside the gasifier. The last characteristic gives the biomass char the possibility to be integrated in the gasification process itself. However, there are no significant data or comprehensive studies that explain the performance of biomass char for tar reduction.

1.5 Objective of the Thesis

There are scattered efforts and signs that show a catalytic role for biomass char in tar removal. However, a complete and comprehensive study on biomass char for solving the tar problem is not found in literature. The objective of this thesis is to study the mechanisms and key parameters of tar reduction using biomass char and how to integrate the findings in a biomass gasification process.

1.6 Organization of the Thesis

In chapter two, a literature review is given about the catalysts used for tar removal in biomass gasification. In chapter three, the most important catalysts found in the literature review are experimentally compared with biomass char for the reduction of model tar components such as naphthalene and phenol. Biomass char was found to

have a high catalytic activity and was further studied in chapter four by investigating its performance in a fixed bed reactor for synthetic tar and real tar reduction. It was found that biomass char is highly active and has a high potential for tar removal. In chapter five, the char particle was investigated by developing a single char particle model for naphthalene removal. This model was used as a base for a fixed bed reactor model to validate the experiments performed in a fixed bed reactor. In chapter six, the performance of biomass char for tar removal was investigated in a bubbling fluidized bed reactor, which has larger scale application than a fixed bed reactor. A two-phase mathematical reactor model was developed to study naphthalene conversion in a fluidized char bed. The model was validated with experiments. Moreover, a novel experiment was made that combines the char natural production inside the bubbling bed gasifier and its catalytic activity. The biomass char was used as a bed material inside the bubbling fluidized bed biomass gasifier (in-situ tar reduction). It was found that the in-situ tar reduction in a biomass gasifier seems to be very promising for solving the tar problem. Biomass char has the potential of more than 97 % tar reduction at 850 °C.

References

1. McKendry, P., *Energy Production from Biomass (Part 1): Overview of Biomass*. Bioresource Technology, 2002. **83**: p. 37-46.
2. Yang, M., *Climate Change Drives Wind Turbines*. Energy Policy, 2007. **35**: p. 6546-6548.
3. Milne, T.A., N. Abatzoglou, and R.J. Evan, *Biomass Gasifier "Tars": Their Nature, Formation and Conversion*. 1998, National Renewable Energy Laboratory (NREL).
4. Stevens, D.J., *Hot Gas Conditioning: Recent Progress with Larger-Scale Biomass Gasification Systems, Update and Summary of Recent Progress*. 2001, Pacific Northwest National Laboratory: Richland: Washington.
5. Simell, P. and J.B.-s. Bredenberg, *Catalytic Purification of Tarry Fuel Gas*. Fuel, 1990. **69**(10): p. 1219-1225.
6. Hasler, P. and T. Nussbaumer, *Gas Cleaning for IC Engine Applications from Fixed Bed Biomass Gasification*. Biomass and Bioenergy, 1999. **16**: p. 385-395.
7. Maniatis, K. *State of the Art on Thermochemical conversion technologies*. in *2nd World Conference on Biomass for Energy, Industry and Climate Protection*,. 2004. Rome, Italy: Eta-Florence.
8. Morris, M. and L. Waldheim. *Status and Development of Biomass Gasification*. in *International Nordic Bioenergy Conference*. 2003. Javaskyla, Finland.
9. Kwant, K.W. and H. Knoef, *Status of Biomass Gasification in Countries Participating in the IEA Bioenergy Task 33 Biomass Gasification and EU Gasnet*. 2004.

10. Neeft, J.P.A., et al. in *12th European Conference for Energy, Industry and Climate Protection*. 17-21 June 2002. Amsterdam, The Netherlands.
11. Coll, R., et al., *Steam Reforming Model Compounds of Biomass Gasification Tars: Conversion at Different Operating Conditions and Tendency towards Coke Formation*. Fuel Processing Technology, 2001. **74**(1): p. 19-31.
12. Maniatis, K. and A.A.C.M. Beenackers, *Introduction: Tar Protocols*. IEA Gasification Tasks. Biomass and Bioenergy, 2000. **18**: p. 1-4.
13. Padban, N., *Tars in Biomass Thermochemical Conversion Processes. Progress Report SDE Project Primary Measures for Reduction of Tars during Fluidized Bed Gasification of Biomass*. 2001, Department of Thermal Engineering, University of Twente: Enschede, The Netherlands.
14. van Passen, S.V.B., et al. *Primary Measures for Tar Reduction, Reduce the Problem at the Source*. in *12th European Conference and Technology Exhibition on Biomass for Energy, Industry and Climate Protection*. 2002. Amsterdam, The Netherlands.
15. Devi, L., et al., *Catalytic Decomposition of Biomass Tars: Use of Dolomite and Untreated Olivine*. Renewable Energy, 2005. **30**: p. 565-587.
16. Padban, N., *Tars in Biomass Thermochemical Conversion Processes. Progress Report SDE Project Primary Measures for Reduction of Tars during Fluidized Bed Gasification of Biomass*. 2001, Department of Thermal Engineering, University of Twente: Enschede, The Netherlands.
17. Corella, J., A. Orio, and M.P. Aznar, *Biomass Gasification with Air in Fluidized Bed: Reforming of the Gas Composition with Commercial Steam Reforming Catalysts*. Ind. Eng. Chem. Res., 1998. **37**: p. 4617-4624.
18. Bridgwater, A.V., *Catalysts in Thermal Biomass Conversion*. Applied Catalysis A: General, 1994. **116**: p. 5-47.
19. Orio, A., J. Corella, and I. Narvaez, *Performance of Different Dolomites on Hot Raw Gas Cleaning from Biomass Gasification with Air*. Ind. Eng. Chem. Res., 1997. **36**: p. 3800-3808.
20. Ekstrom, C., N. Lindman, and R. Pettersson, *Fundamentals of Thermochemical Biomass Conversion*. 1985, London and New York: Elsevier Applied Science. 601-618.
21. Dogru, M., et al., *Gasification of Hazelnut Shells in a Downdraft Gasifier*. Energy, 2002. **27**: p. 415-427.
22. Delgado, J., P.M. Aznar, and J. Corella, *Calcined Dolomite, Magnesite, and Calcite for Cleaning Hot gas from a Fluidized Bed Gasifier with Steam: Life and Usefulness*. Ind. Eng. Chem. Res., 1996. **35**: p. 3637-3643.

Chapter 2

A Review of Catalysts for Tar Reduction in Biomass Gasification

Abstract

This chapter presents a review of the various types of catalysts that have been used in several research works to reduce the tars in the producer gas generated by the biomass gasification process. The studied catalysts are divided into two classes according to their production method: minerals and synthetic catalysts. Biomass char is concluded to be a catalyst of high potential for tar reduction.

2.1 Introduction

In general, tars can be removed by [1] physical, non-catalytic (e.g., thermal cracking), and catalytic tar reduction processes. Catalytic tar conversion is a technically and economically interesting approach for gas cleaning. It has the potential to increase conversion efficiencies while simultaneously eliminating the need for downstream collection and disposal of tars. The catalytic conversion of tars is commonly known as hot gas cleaning. The research on catalytic tar conversion involves two approaches [2, 3]:

(a) Primary measures: the catalyst is incorporated or mixed with the feed biomass to achieve the so-called catalytic gasification or pyrolysis (also called in-situ) to remove the tar in the gasifier itself.

(b) Secondary measures: the gasifier producer gas is treated downstream of the gasifier in a secondary reactor to remove the tar outside the gasifier.

Bridgwater et al. [1] reviewed three groups of catalysts for biomass gasification: dolomites, fluid catalytic cracking catalysts, and nickel and other precious metals such as platinum, palladium and rhodium. Later, Sutton et al. [4] reviewed three groups of catalysts for biomass gasification. These catalysts are dolomites, alkali metals, and nickel.

This chapter presents a review of nine catalysts that have been used in literature to reduce tars in producer gas obtained from gasification processes. The catalysts are reviewed based on the following points: (a) chemical composition, (b) factors of catalytic activity for tar reduction, (c) factors of catalytic deactivation, (d) advantages and disadvantages, and (e) references to experimental results. The catalysts are here divided into two classes based on their production method: minerals and synthetic catalysts. Figure 2-1 shows the different reviewed catalysts that belong to these classes.

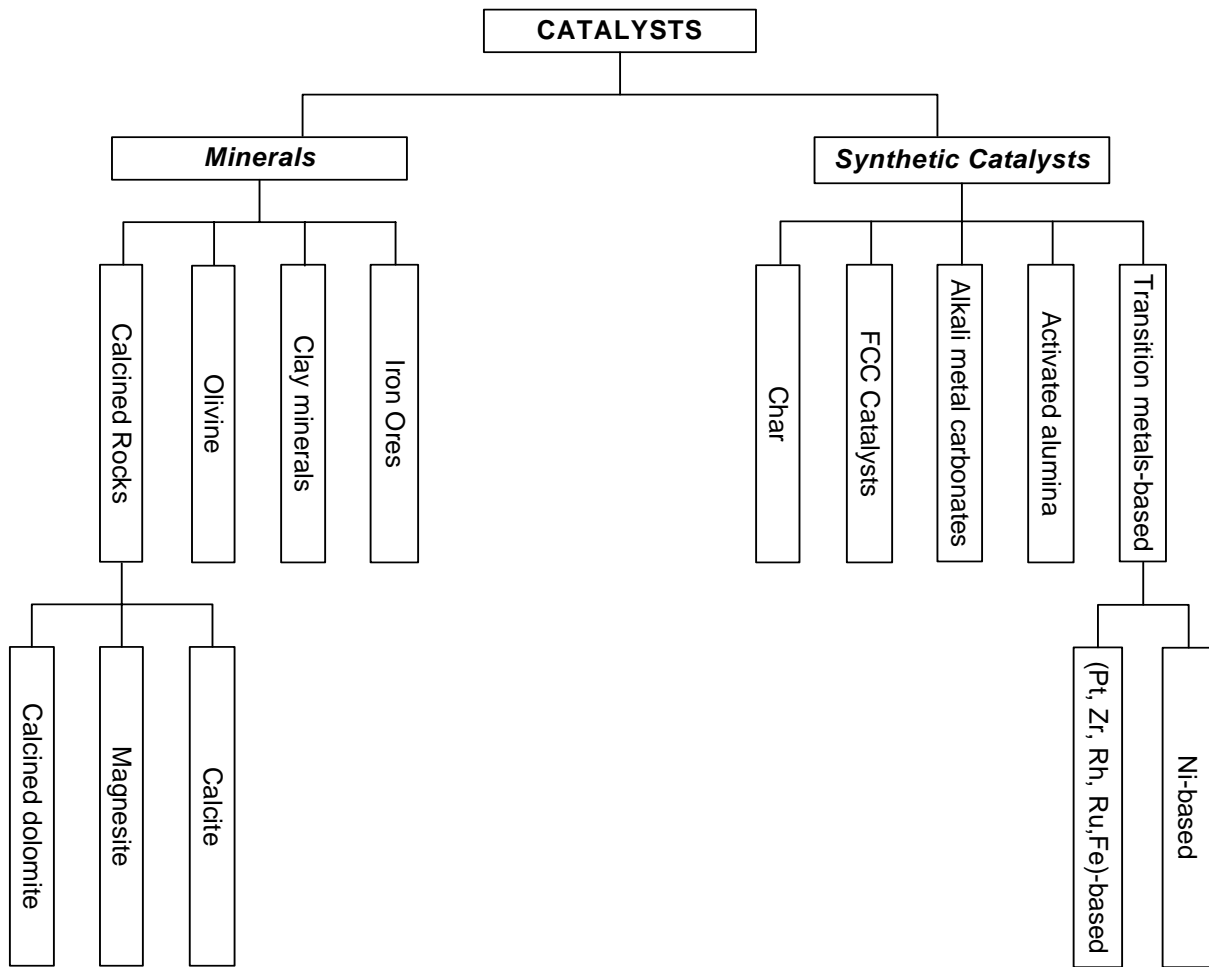


Figure 2-1 Classification and types of catalysts used for tar reduction

2.2 Catalysts

Tar reduction reactions are often kinetically limited. Therefore, the reaction rates can be increased by increasing the temperature and/or using a catalyst. However, catalysts can only increase the rate of a reaction that is thermodynamically feasible. Several reactions can occur in a secondary catalytic reactor downstream of the gasifier. The most important reactions are listed in Table 2-1.

Table 2-1 Important reactions in a secondary catalytic reactor downstream the gasifier

Reference	Reaction type	Reaction	No.
[5, 6]	Steam reforming	$C_nH_m + nH_2O \rightleftharpoons nCO + (n + \frac{m}{2})H_2$	(2-1)
[5, 6]	Dry reforming	$C_nH_m + nCO_2 \rightleftharpoons 2nCO + (\frac{m}{2})H_2$	(2-2)
[7]	Thermal cracking	$C_nH_m \rightarrow C^* + C_xH_y + gas$	(2-3)
[8, 9]	Hydrocracking or hydroreforming of tars	$C_nH_m + xH_2 \rightleftharpoons CO + H_2 + CH_4 + \dots + coke$	(2-4)
[7]	Water gas shift reaction	$CO_{(g)} + H_2O_{(g)} \rightleftharpoons CO_{2(g)} + H_{2(g)}$	(2-5)

C_nH_m hydrocarbons that represents tars

C_xH_y hydrocarbons that represents lighter tars

This section discusses the two classes of catalysts used in tar reduction for biomass gasification in the order presented in Figure 2-1.

2.2.1 Minerals

Minerals are natural, homogeneous solids with a definite, but generally not fixed, chemical composition and an ordered atomic arrangement [8]. The catalysts belonging to this class are available in nature and can be used directly or with some physical treatment (such as heating). In general, it can be noted that mineral catalysts are relatively cheap compared with synthetic catalysts. Below, different minerals that have catalytic activity for tar reduction are discussed.

2.2.1.1 Calcined rocks

Calcined rocks contain alkaline earth metal oxides (CaO and/or MgO). Alkaline earth metals include any of the divalent electropositive metals beryllium, magnesium, calcium, strontium, barium, and radium, belonging to group 2A of the periodic table. Calcined rocks include calcites, magnesites, and calcined dolomites. Simell et al. [9] classified such catalysts according to the CaO/MgO ratio as shown Table 2-2. These catalysts have other names such as alkaline earth oxides, stones, minerals, and naturally occurring catalysts. The uncalcined forms of these materials are called limestone ($CaCO_3$), magnesium carbonate ($MgCO_3$), and dolomite ($CaCO_3.MgCO_3$), respectively.

Table 2-2 Classification of calcined rocks based on Ca/MgO weight ratio as presented by Simell et al. [9]

Type	CaO/MgO Ratio
Limestone	> 50
Dolomitic limestone	4-50
Calcitic dolomite	1.5-4
Dolomite	1.5

Table 2-3 lists some examples of the chemical compositions of these materials [10]. These materials show catalytic activity for tar reduction when calcined. Calcination occurs because of the loss of bound carbon dioxide when the material is heated. The reactions involved in tar reduction over these materials are not well known. However, these reactions at least include reactions 1-4 listed in Table 2-1.

Table 2-3 Chemical composition (wt. %) examples of limestone, magnesium carbonate and dolomite [10]

Component	Calcite Morata (Zaragoza, Spain)	Magnesite Navarra (Navarra, Spain)	Dolomite Norte (Bueras, Cantabria, Spain)
CaO	53.0	0.7	30.9
MgO	0.6	47.1	20.9
CO ₂	41.9	52.0	45.4
SiO ₂	2.7		1.7
Fe ₂ O ₃	0.8		0.5
Al ₂ O ₃	1.0		0.6

Simell et al. [9] related the catalytic activity for tar reduction of the calcined rocks to several factors such as a large pore size and surface area of the corresponding calcinates and a relatively high alkali metal content (K, Na). Alkali metals could act as promoters present in commercial steam-reforming catalysts by enhancing the gasification reaction of carbon intermediates deposited on the catalyst surface. The activity of these rocks can be improved by increasing the Ca/Mg ratio, decreasing the grain size, and increasing the active metal content such as iron [9]. The factors that cause catalytic deactivation of the calcined rocks are related to coke formation and CO₂ partial pressure. Coke causes deactivation of the calcined rocks by covering their active sites and blocking their pores [10]. Coke is produced by the catalytic reactions involving tar-side reactions that occur on the catalyst surface. The CO₂ partial pressure causes deactivation when it is higher than the equilibrium decomposition pressure of the carbonated form of the material under the same conditions [11].

Dolomites have several advantages. They are abundant and considered to be the most popular inexpensive catalysts for tar reduction. Dolomites can provide relatively

high tar conversion (up to 95%). They are often used as guard beds to protect the expensive and sensitive metal catalysts from deactivation caused by tars or other impurities such as H_2S . The main problem with these materials is their fragility. They are soft and quickly eroded in fluidized beds with high turbulence [10].

Delgado et al. [10] found that the reactivity of these catalysts decreases in the order: calcined dolomite > calcite > magnesite. Dolomites can be of different types depending on their origin, and thus, they differ in composition. Simell et al. [9] found that kalkkima dolomite (0.8 wt. % Fe) and Ankerite dolomite (4.6 wt. % Fe) are highly active dolomites. Orio et al. [6] tested the activities of different dolomites and found the following order: Chilches dolomite > Norte dolomite > Malaga dolomite. They related the differences in activity to the iron oxide (Fe_2O_3) content (wt.%), being 0.74-0.84, 0.12 and 0.01, respectively. In-situ use of calcined rocks was employed by Walwander et al. [12] in the U.S, Corella et al. in Spain, and Kurkela et al. in Finland. Also, Finnish companies Tampella Power Oy, Carbona Inc., and VTT prefer in-situ use [10]. The University of Zaragoza (Zaragoza, Spain) found that in-situ use of dolomite is less effective than its use downstream from the gasifier [13]. This was attributed to the higher steam content in the fuel gas from the O_2 -steam gasification process.

Tar contents in the raw flue gas below 1 g/Nm^3 are obtained using a bed with a content between 15 and 30 wt. % of dolomite, with the rest being silica sand [2]. Gil et al. [2] reported that in-situ use of dolomite generates higher carryover of solids from the gasifier bed with correspondingly higher particulates content in the raw producer gas. The in-situ use of dolomite has the lowest cost and the lowest tar reduction. A secondary bed of dolomite is preferred by the Swedish company TPS AB. TPS has demonstrated the success of tar cracking over dolomite in a secondary reactor that is close-coupled with their circulating fluidized bed gasifier. This method seems to be more successful than in-situ addition of dolomite, giving tar reductions of up to 95%. With this method (use of a secondary bed of dolomite downstream from the gasifier), Corella and co-workers obtained a reduction of the tar content in the fuel gas to about 1.2 g/Nm^3 ; tar contents below this limit were never reached with dolomites by these authors [6, 13]. Gil et al. [2] considered a bed of dolomite downstream of the gasifier as the well-known and used method for tar reduction. This method has higher costs than the in-situ use of dolomite but shows higher tar reduction.

2.2.1.2 Olivine

Olivine consists mainly of silicate mineral in which magnesium and iron cations are set in the silicate tetrahedral [14]. Natural olivine is represented by the formula $(\text{Mg,Fe})_2\text{SiO}_4$. Table 2-4 gives the chemical composition of a selected commercial olivine [15].

Table 2-4 Chemical composition of a selected commercial olivine [14]

Component	Wt. %
MgO	48.5-50.0
SiO ₂	41.5-42.5
Fe ₂ O ₃	6.8-7.3
Al ₂ O ₃	0.4-0.5
NiO	0.3-0.35
Cr ₂ O ₃	0.2-0.3
CaO	0.05-0.10
MnO	0.05-0.10

The catalytic activity of olivine for tar reduction can be related to iron oxide (Fe₂O₃), magnesite (MgO), and nickel (Ni) contents. The iron is effective when it is found on the surface of the catalyst. Oxidation and/or calcination of olivine affects bringing the iron to the surface [16].

On that basis, the reactions involved in tar reduction with olivine could be similar to those involved in the same processes with calcined rocks. This has to be further investigated. Olivine is mainly deactivated by the formation of coke, which covers the active sites and reduces the surface area of the catalyst.

The advantages of this catalyst are its low price (similarly to dolomite) and high attrition resistance compared with dolomite. Its mechanical strength is comparable to that of sand, even at high temperatures. Its performance is therefore better than that of dolomite in fluidized bed environments [17]. Olivine is available on the market at a price of about 120 Euro per metric ton [17]. On the other hand, olivine has a lower catalytic activity for tar reduction than dolomite [18].

Devi et al. [16, 19] presented a detailed investigation of the catalytic behavior of olivine. They found that untreated olivine could convert only 46% of the total tar present in a hot gasification gas at 900 °C. They pre-treated olivine by heating it at 900 °C in the presence of air for different times. This pre-treatment affects bringing the iron to the surface of olivine. The pre-treated olivine showed 80 % naphthalene conversion at 900 °C. They observed severe coke formation for steam and dry reforming reactions on the surface of the catalyst. Rapagná et al. [17] tested olivine and dolomite in steam gasification of biomass in a fluidized bed. They reported that the activity of olivine is comparable to that exhibited by dolomite in terms of the destruction of tars and the resulting increase of permanent gases. Courson et al. [18] integrated a small amount of nickel into natural olivine. They found that, at 750 °C, this catalyst has a high activity in dry reforming (95% methane conversion) and steam reforming (88% methane conversion). At 770 °C, the average tar content is decreased from 43 g/Nm³ dry gas with sand to 0.6 for dolomite and 2.4 for olivine [18]. Because of olivine's mechanical strength and catalytic activity, Rósen et al. [20] used it as a bed material for the pressurized gasification of birch.

2.2.1.3 Clay minerals

Most common clay minerals belong to the kaolinite, montmorillonite, and illite groups. The chemical compositions of kaolinite and montmorillonite are reported in Table 2-5 [21].

Table 2-5 Chemical composition of two clay materials [21]

Oxide	Kaolinites	Montmorillonite
SiO ₂	45.20	53.20
Al ₂ O ₃	37.02	16.19
Fe ₂ O ₃	0.27	4.13
FeO	0.06	-
MgO	0.47	4.12
CaO	0.52	2.18
K ₂ O	0.49	0.16
Na ₂ O	0.36	0.17
TiO ₂	1.26	0.20
H ₂ O	14.82	23.15
Total	100	100

Wen et al. [21] related the catalytic activity of clay minerals for tar reduction to (a) effective pore diameter, (b) internal surface area, and (c) number of strongly acidic sites. The catalytic activity increases with pore diameter greater than 0.7 nm, larger internal surface area, and larger number of strongly acidic sites. Simell et al. [22] reported that these materials enhance the tar cracking reaction explained by eq (2-3) and have little effect on other gas-phase reactions such as water-gas shift reaction explained by eq (2-5) and steam and dry reforming reactions explained by eqs (2-1) and (2-2). Adjaye et al. [23] reported that silica-alumina catalyst is amorphous (non-crystalline) and contains acid sites. Most of these sites are buried in inaccessible locations, thus leading to low acidity. Simell et al. [22] reported that, at temperatures above 850 °C most of the aluminium silicates seemed to lose their catalytic activity and act as inert materials.

The advantages of clay minerals are that they are relatively cheap and have no disposal problems because they can be disposed after simple treatment. The main disadvantages of these catalysts are the lower activity compared with dolomite and nickel-based catalysts and the fact that most natural clays do not survive the high temperatures (800-850 °C) needed for tar reduction (they lose their pore structure).

Simell et al. [22] tested the activity of silica-alumina (13 wt. % Al₂O₃, 86.5 wt. % SiO₂, 100 m²/g surface area) in a fixed bed at 900 °C and 0.3-s residence time for tar reduction of a tarry fuel gas from an updraft gasifier. They found the following order of activity: commercial nickel catalyst (Ni on Al₂O₃) > dolomite > activated alumina >

silica-alumina (clay mineral) > silicon carbide (inert). Wen et al. [21] found that Kaolinites and montmorillonite, which have a specific surface area of 15-20 m²/g, are catalytically less active in the catalytic pyrolysis of coal tar than very effective zeolites with pore size greater than 0.7 nm and surface areas of 600-900 m²/g. They exhibited catalytic activities similar to those of zeolites with small pore sizes.

2.2.1.4 Iron ores

Minerals containing appreciable amounts of iron can be grouped according to their chemical compositions into oxides, carbonates, sulfides, and silicates. Table 2-6 lists the main iron minerals commonly used as a source of iron [24]. However, oxide minerals are the most important source of iron, and the others are of minor importance.

Table 2-6 Main iron minerals [24]

Mineral	CAS registry number	Chemical name	Chemical formula	Iron (wt. %)
Hematite	1309-37-1	Ferric oxide	Fe ₂ O ₃	69.94
Magnetite	1309-38-2	Ferrous-ferric oxide	Fe ₃ O ₄	72.36
Goethite	1310-14-1	Hydrous iron oxide	HFeO ₂	62.85
Siderite	14476-16-5	Iron carbonate	FeCO ₃	48.20
Ilmenite	12168-52-4	Iron titanium oxide	FeTiO ₃	36.80
Pyrite	1309-36-0	Iron sulfide	FeS ₂	46.55

Metallic iron (reduced form) catalyzes tar decomposition more actively than the oxides [9, 25]. Simell et al. [9] reported that iron catalyzes the reactions of the main components of the fuel gas (H₂, CO, CO₂, H₂O) such as water-gas shift reaction. Various forms of iron are reported to catalyze coal gasification reactions, pyrolysis, and tar decomposition. Iron is rapidly deactivated in the absence of hydrogen because of coke deposition [25]. Simell et al. [9] tested the activities of two ferrous materials in catalyzing the decomposition of tarry constituents in fuel gas in a tube reactor in the temperature range of 700-900 °C. The ferrous materials tested were iron sinter and pellet in which iron exists as magnetite (Fe₃O₄) and, in smaller amounts, as hematite (Fe₂O₃). The activities of these materials were found to be lower than that of dolomite. Tamhankar et al. [25] studied the catalytic cracking activity and reaction mechanism of benzene on iron oxide-silica. They found that the catalyst in its reduced form has a high activity toward benzene cracking and a high selectivity toward methane formation. They found also that hydrogen plays a critical role in the overall reaction and in suppressing catalysts deactivation. Cypers et al. [26] studied the influence of iron oxides on coal pyrolysis. They found that the presence of iron oxides reduces the tar yield in the coal primary devolatilization zone between 300 and 600 °C. The production of methane increases toward the end of the devolatilization zone of coal in the presence of iron oxide. They found that hematite has a greater effect than magnetite.

2.2.2 Synthetic catalysts

Synthetic catalysts are chemically produced and relatively more expensive than mineral catalysts.

2.2.2.1 Char

Char is a nonmetallic material. It can be produced by the pyrolysis of coal or biomass. In the usual carbonization procedure, heat at 400-500 °C is applied for a prolonged period of time in the absence of air. The proximate and ultimate analyses of two types of chars are reported in Table 2-7.

Table 2-7 Proximate and ultimate analysis of chars produced from charcoal and poplar wood [27, 28]

	Char from poplar wood [27, 28]	Char from charcoal [27, 28]
Proximate dry analysis (wt.%)		
Ash	4.6	1
Volatiles	7.4	9.4
Fixed carbon	88	89.6
Ultimate analysis (wt. %)		
C	85.5	92
H	0.76	2.45
O	8.9	3
N	0.29	0.53
S	-	1

Biomass char properties are not fixed and depend on biomass type and process conditions. Thus, the char catalytic activity for tar reduction can be related to the pore size, surface area, and ash or mineral content of the char. The first two factors are dependent on the char production method, such as the heating rate and pyrolysis temperature. The last factor depends mainly on the char precursor type. The char is deactivated by (a) coke formation, which blocks the pores of char and reduces the surface area of the catalyst, and (b) catalyst loss, as char can be gasified by steam and dry reforming reactions explained by eqs (2-1) and (2-2).

The attractiveness of char as a catalyst originates from its low cost and its natural production inside the gasifier. However, it can be consumed by gasification reactions with steam or CO₂ in the producer gas. Therefore, a continuous external supply depends on the balance of char consumption and production.

Char was noticed to have a good catalytic activity for tar removal. In the downstream gasifier, both the fuel and gas flow downwards through the reactor enabling the pyrolysis gases to pass through a throated hot bed of char. This results in the cracking of most of the tars into non-condensable gases and water [29]. The two

stage gasifier developed by the Technical University of Denmark (DTU) gives almost complete tar conversion ($< 15 \text{ mg/Nm}^3$) [30]. The high tar removal of this gasifier is related to passing the volatiles through a partial oxidation zone followed by a char bed. Zanzi et al. [31] studied the effect of the rapid pyrolysis conditions on the reactivity of char in gasification. They found that the reactivity of char produced in the pyrolysis stage is highly affected by the treatment conditions, and they thought it might significantly increase if high heating rates, small fuel particle sizes, and short residence times at high temperatures were used. Chembukulam et al. [32] found that the conversion of tar and pyroligneous liquor over semicoke/charcoal at $950 \text{ }^\circ\text{C}$ resulted in almost complete decomposition into gas of low calorific value. Seshardi et al. [33] studied the conversion of a coal liquid (tar) over a char-dolomite mixture under different temperatures, pressures, and carrier gases.

2.2.2.2 Fluid catalytic cracking (FCC) catalysts

Zeolites represent a well-defined class of crystalline aluminosilicate minerals whose three-dimensional structures derived from frameworks of $[\text{SiO}_4]^{4-}$ and $[\text{AlO}_4]^{5-}$ coordination polyhedra [34]. Catalytic cracking is a process that breaks down the larger, heavier, and more complex hydrocarbon molecules into simpler and lighter molecules by the action of heat and aided by the presence of a catalyst but without the addition of hydrogen. In this way, heavy oils (fuel oil components) can be converted into lighter and more valuable products (notably LPG, gasoline, and middle distillate components). The catalytic cracking of hydrocarbons is believed to be a chain reaction that follows the carbenium ion theory developed by Whitmore [35]. His mechanism involves three steps: [36], [37] initiation, propagation, and cracking steps.

The acidic properties (Brønsted sites) of zeolites are dependent on the method of preparation, form, temperature of dehydration, and Si/Al ratio. The key properties of zeolites are structure, Si/Al ratio, particle size, and nature of the (exchanged) cation. These primary structure/composition factors influence acidity, thermal stability, and overall catalytic activity.

The catalytic behavior of FCC catalysts differs from that of the previous described catalysts that have low surface acidity or are considered basic, such as calcined rocks. FCC catalysts are used mainly to perform tar cracking reactions, which can be summarized by the general reaction given in eq (2-3). However, de Souza et al. [38] found that zeolites might be appropriate catalysts for water gas shift reaction given by eq (2-5). Seshardi et al. [33] related the activity of zeolites in cracking coal liquid to their large surface areas, large pore diameters, and high densities of acid sites. The loss of catalytic activity is mainly related to the coke formation and substances whose molecules react with the catalyst acidic sites. Coke deposition decreases the surface area and the zeolite micropore volume by blocking its channels. Steam, basic nitrogen compounds, and alkaline metals react with the catalyst acidic sites and poison the catalyst.

The advantages of these catalysts are related to their relatively low price and the knowledge gained about them from long experience with their use in FCC units. The

major disadvantage of these catalysts is their rapid deactivation because of the coke formation.

Radwan et al. [39] characterized the coke deposited from benzene cracking over USY zeolites in the temperature range of 500-800 °C under He or H₂ gas flow at 1.0 and 5.0 MPa. They found that the composition of coke strongly depends on the cracking temperature and that the H/C ratio decreases with increasing temperature. Adjaye et al. [23] examined the relative performance of HZSM-5, H-mordenite H-Y, silicalite, and silica-alumina in the production of the organic distillate fraction (ODF); formation of hydrocarbons; and minimization of char, coke, and tar formation. They found that HZSM-5 was the most effective catalyst for the production of ODF, overall hydrocarbons, and aromatic hydrocarbons. In addition, it provided the least coke formation. Silica-alumina catalyst was the most effective in minimizing char formation. H-Y catalyst was superior in minimizing tar formation as well as maximizing the aliphatic hydrocarbon production. Gil et al. [40] tested a spent “in equilibrium” catalyst in a fluidized bed and found that the FCC catalyst was quickly elutriated from the bed. Herguido et al. [41] tested an “in equilibrium” spent FCC catalyst in a 15 cm-i.d. riser-gasifier with a stable fluidized bed of sand at its bottom. Tar was reduced from 78 to 9 g/Nm³ with recirculation and continuous regeneration of the catalyst.

2.2.2.3 Alkali metals based catalysts

Alkali metals are any of the monovalent metals lithium (Li), sodium (Na), potassium (K), rubidium (Rb), cesium (Cs), and francium (Fr), belonging to group 1A of the periodic table. They are all highly reactive and electropositive. Alkali metals, principally K and to a lesser extent Na, exist naturally in biomass [42]. Their salts are soluble and gained from ashes of plants [1]. Table 2-8 shows the analysis of wood ash after gasification as reported by Sutton et al. [4]. To reduce the tars content, these ashes can be used as primary (in-situ) or secondary (outside the gasifier) catalysts. On the other hand, they can be used directly as catalysts in the form of alkali metal carbonates or supported on other materials such as alumina. Direct addition of alkali materials to biomass is done by dry mixing or wet impregnation.

Table 2-8 Wood ash analysis after gasification [4]

Component	Wt. %
CaO	44.3
MgO	15
K ₂ O	14.5

Alkali metals catalyze gasification reactions. They are considered as effective catalysts for steam and dry gasification of carbon [43]. Padban [44] reported that alkali metals, especially K, act as promoters in unzipping the cellulose chains during the thermal decomposition of woody biomass. Lizzio et al. [45] reported that K is a good

catalyst for the steam gasification of coal because of the formation of a liquid-solid interface between K and carbon. The same authors explained that, when K_2CO_3 is used as the K precursor, it wets and is dispersed well on the coal surface. They lose their activity because of particle agglomeration when added to biomass in fluidized bed gasifiers [4]. They also lose their activity at high temperatures (900 °C) when used in a secondary fixed bed because of melting and agglomeration [46]. Lizzio et al. [45] related the deactivation of K during gasification to several factors including the loss of contact between the catalyst and char, particle sintering, unfavorable reaction with the mineral matter of char, and loss of potassium by vaporization.

The advantage of alkali metals as catalysts comes from their natural production in the gasifier where ashes are produced. The use of ashes as catalysts solve the problem of the handling of ash wastes and gives an added value to the gasification process by increasing the gasification rate and reducing the tar contents in the produced gas. However, the major disadvantage of these catalysts is their loss of activity because of particle agglomeration.

Sutton et al. [4] reported several disadvantages for the direct addition of alkali metal catalysts, such as difficult and expensive recovery of the catalyst, increased char content after gasification, and ash disposal problems. Lee et al. [47] found that the addition of Na_2CO_3 enhances the catalytic gasification of rice straw over nickel catalyst and significantly increases the formation of gas. The same authors found that the formation of gas depends on the nature of alkali metal carbonates used and has the order $Na \geq K > Cs > Li$. Sutton et al. [4] reported that K_2CO_3 is not suitable as a secondary catalyst because the hydrocarbon conversion rarely exceeds 80% when it is used. Lee et al. [48] found that the catalytic activity of single salts in steam gasification depends on the gasification temperature, with the following order of activity: $K_2CO_3 > Ni(NO_3)_2 > K_2SO_4 > Ba(NO_3)_2 > FeSO_4$.

2.2.2.4 Activated alumina

Activated alumina consists of a series of non-equilibrium forms of partially hydroxylated aluminum oxide, Al_2O_3 . Its chemical composition can be represented by $Al_2O_{(3-x)}(OH)_{2x}$, where x ranges from about 0 to 0.8. The porous solid structure of activated alumina is produced by heating (calcining) the hydrous alumina precursor to drive off the hydroxyl groups [49]. Aluminum oxide can be found in several minerals as indicated in Table 2-9 .

Table 2-9 Main minerals contain aluminium oxide [49]

Mineral	CAS registry number	Formula
Aluminum hydroxide	21645-51-2	Al(OH) ₃
Bauxite	1318-16-7	
Boehmite	1318-23-6	AlO(OH)
Corundum	1302-74-5	α -Al ₂ O ₃
Diaspore	14457-84-2	α -AlO(OH)
Gibbsite	14762-49-3	α -Al(OH) ₃
Sapphire	1317-82-4	Al ₂ O ₃

The catalytic activity of alumina is related to the complex mixture of aluminium, oxygen, and hydroxyl ions that are combined in specific ways to produce both acid and base sites [49]. Activated alumina is deactivated by coke formation.

The advantage of activated alumina is its relatively high activity, which is comparable to that of dolomite [9]. The main disadvantage is rapid deactivation by coke compared with dolomite [personal communication with Corella and Simell, 2003].

Simell et al. [9] tested the activity of activated alumina (99 wt. % Al₂O₃) in catalyzing the decomposition of tarry constituents in fuel gas in a tube reactor in the temperature range of 700–900 °C. They found that activated alumina was nearly as effective as dolomite.

2.2.2.5 Transition metals-based catalysts

Transition metals are considered as good catalysts for the steam and dry reforming of methane and hydrocarbons. Nickel catalyst supported on alumina is cheaper and sufficiently active than other metals such as Pt, Ru, and Rh. [50]. Nickel metal is one of the group VIII metals. The general composition of the Ni-based catalysts can be divided into three main components: (a) Ni element, (b) support, and (c) promoters. The Ni represents the active site of the catalyst. The support material gives the catalyst mechanical strength and protection against severe conditions such as attrition and heat. Alumina-based materials are considered the primary support material for most reforming catalysts. Promoters such as alkaline earth metals, e.g., magnesium (Mg), and alkali metals, e.g., Potassium (K), are added to ensure economical operations under severe conditions. Mg is used to stabilize the Ni crystallite size and K to neutralize the support surface acidity and thereby reduce coke deposition on the catalyst surface and enhance catalyst activity [51]. In general, the steam-reforming catalysts can be classified into two types according to the feed: (a) light hydrocarbons (particularly methane), and (b) heavy hydrocarbons (particularly naphtha). Table 2-10 shows examples of the composition of eight commercial Ni-based steam-reforming catalysts used by Caballero et al. [52]. The first four are for light hydrocarbons and the last four (unidentified) are for the heavy hydrocarbons.

Table 2-10 Examples of the composition of some commercial Ni-based steam reforming catalysts [52]

Company	Catalyst	Composition (wt. %)									
		NiO	Al ₂ O ₃	CaO	SiO ₂	K ₂ O	MgAl ₂ O ₄	MgO	Fe ₂ O ₃	MnO	BaO
United Catalysts	C11-9-061	10-15	80-90	<0.1	<0.05				1-5	1-5	1-5
Haldor Topsoe	RKS-1	15			0.1	<500*	85				
ICI	57-3	12	78	10	0.1						
BASF	G1-25S	12-15	>70		<0.2						
	Nickel A	22	26	13	16	7		11			
	Nickel B	15			0.1	<500*	85				
	Nickel D	20			<0.2						
	Nickel E	25	>70		<0.2	1					

* ppm

Steam-reforming catalysts exhibit high activities for tar reduction and gas upgrading in biomass gasification. These catalysts accelerate steam and dry reforming reactions (eqs 2-1 and 2-2), and water-gas shift reaction (eq 2-5). Aznar et al. [53] found that heavy-hydrocarbon steam-reforming catalysts are more active than light-hydrocarbon steam-reforming catalysts. The activity of these catalysts depends on the content of nickel, type of support, and type and content of promoter(s).

Ni-based catalysts can be deactivated in several ways, which can be summarized as follows:

Mechanical deactivation, this normally occurs because of catalytic material loss through attrition and loss of surface area through crushing. This deactivation is irreversible and can be prevented by selecting less severe process conditions. Fluidized bed conditions increase catalyst attrition and mechanical deactivation, so these catalysts are normally used in fixed beds [54].

Sintering, causes loss of surface area and occurs because of the applied severe conditions such as high temperatures.

Fouling, occurs because of physical blockage of the catalyst surface area by coke. Such deactivation is usually reversible and can be reduced or prevented by conditioning the feed gas. Baker et al. [55] reported that on one hand the acidity of the catalyst support affects coke accumulation and catalyst deactivation, on the other hand accelerates the cracking reaction discussed by eq 2-3. Catalytic deactivation because of fouling is also a function of the catalyst placement and the mode of contact (fixed or fluidized bed) [55]. Aznar et al. [53] proposed that the tar content in the fuel gas entering a bed of Ni-based catalyst has to be below 2 g/Nm³ to avoid catalyst deactivation by coke.

Catalyst poisoning, is caused by the strong chemisorption of impurities (mainly H₂S) in the feed onto the catalyst active sites. Engelen et al. [56] reported that typical

gas of biomass gasification contains 20–200 ppm H_2S , depending on the solid fuel used. Poisoning can be prevented by conditioning the feed gas to the catalyst. Sulfur poisoning is reversible and has a temporary effect on the catalyst [57]. Hepola et al. [57] reported that, at 900 °C, the activity of the Ni catalyst recovered rapidly when H_2S was removed from the gas. Forzatti et al. [58] reported that S adsorption decreases with increasing temperature. They reported that 5 ppm sulfur in the feed poisoned a Ni/ Al_2O_3 steam-reforming catalyst working at 800 °C, whereas less than 0.01 ppm poisoned the same catalyst working at 500 °C.

The main advantages of Ni-based catalysts are their ability to attain complete tar removal at temperatures of around 900 °C [59], and to increase the yields of CO and H_2 [52]. Olivares et al. [60] reported that commercial nickel-based catalysts are 8–10 times more active than calcined dolomites under the same operating conditions. The disadvantages of Ni-based catalysts are their rapid deactivation from sulfur and high tar contents in the feed and the need for preconditioning of the feed before it enters the catalyst bed. In addition, Ni-based catalysts are relatively expensive.

Ni-based catalysts have proven to be useful in biomass gasification for gas cleaning and upgrading [61]. Sutton et al. [4] reported that the use of Ni-based catalysts at temperatures higher than 740 °C, generally results in an increase in the H_2 and CO contents, with a decrease in the hydrocarbons (tars) and methane contents. Aznar et al. [53] found that steam-reforming catalysts for heavy hydrocarbons (naphtha) are more active for tar reduction than commercial steam-reforming catalysts for light hydrocarbons (methane). Arauzo et al. [62] studied the catalytic pyrogasification of biomass in a fluidized bed reactor. They found that the addition of Mg in the catalyst crystal lattice improved the resistance to attrition and loss in gasification activity because of increased coke production. However, the same authors found that the addition of potassium had little effect. Lee et al. [47] found that the addition of Na_2CO_3 to a nickel catalyst significantly enhances its activity for catalytic gasification of rice straw and also significantly increased the gas formation. Baker et al. [55] explored the effect of gas-solid contact mode and placement of the catalyst on the performance of a Ni-based catalyst. They found poor catalyst performance because of coke deactivation if the catalyst is placed in the gasifier or in a secondary fixed bed, compared with catalyst placement in a secondary fluidized bed. Yamaguchi et al. [63] tested the performance of alumina-supported nickel catalysts for steam gasification of wood. They found that the activity of the catalyst decreased over time because of coke fouling and sintering of the nickel metal in the catalyst. Hepola et al. [57] reported that the performance of a nickel-based catalyst for tar reduction decreased because of H_2S adsorption whereas the ammonia conversion seemed to be enhanced by H_2S concentrations in the gas. The authors found that high operating temperatures reduced the catalyst deactivation caused by H_2S .

2.3 Concluding Remarks

This survey presented a review of the various types of catalysts that have been used in several research programs on tar reduction in producer gas from a gasification process. It also suggests a classification for catalysts into minerals and synthetic catalysts. This classification is based on the catalyst production method. The advantages and disadvantages of the different catalysts are summarized in Table 2-11.

Table 2-11 Summary of catalysts advantages and disadvantages

Catalyst	Advantages	Disadvantages
Calcined rocks	Inexpensive and abundant Attain high tar conversion ~95% conversion with dolomite Often used as guard beds for expensive catalysts Most popular for tar reduction	Fragile materials and quickly eroded from fluidized beds
Olivine	Inexpensive High attrition resistance	Lower catalytic activity than dolomite
Clay minerals	Inexpensive and abundant Less disposal problems	Lower catalytic activity than dolomite Most natural clays do not support the high temperatures (800-850 °C) needed for tar reduction (lose pore structure)
Iron ores	Inexpensive Abundant	Rapidly deactivated in absence of hydrogen Lower catalytic activity than dolomite
Char	Inexpensive Natural production inside the gasifier High tar conversion comparable to dolomite	Consumption because of gasification reactions Biomass char properties are not fixed and depends on biomass type and process conditions
FCC	Relatively cheap but not cheaper than the above More knowledge is known about it from the experience with FCC unit	Quick deactivation by coke Lower catalytic activity than dolomite
Alkali metals based	Natural production in the gasifier Reduce ash handling problem when used as a catalyst	Particle agglomeration at high temperatures Lower catalytic activity than dolomite
Activated alumina	High tar conversion comparable to dolomite	Quick deactivation by coke

Transition metal-based	Able to attain complete tar reduction at ~ 900 °C Increase the yield of CO and H ₂ Ni-based catalysts are 8 to 10 times more active than dolomite	Rapid deactivation because of sulfur and high tar content in the feed Relatively expensive
------------------------	--	---

It can be concluded that calcined rocks and transition metal-based catalysts give the highest tar reduction. They are used as a reference for the catalytic cleaning methods of most institutions and companies working on biomass gasification.

On the other hand, biomass char can be a good alternative catalyst for tar removal. The attractiveness of biomass char for solving the tar problem is related to its low cost, natural production inside the biomass gasifier, its catalytic activity for tar reduction and the possibility to be integrated in the gasification process itself. Therefore, biomass char can be a catalyst of high potential for tar reduction in biomass gasification process. However, there is no significant data or comprehensive studies that explain the performance of biomass char for tar reduction. In the next chapters the performance of biomass char as a catalyst for tar reduction is discussed.

References

1. Bridgwater, A.V., *Catalysts in Thermal Biomass Conversion*. Applied Catalysis A: General, 1994. **116**: p. 5-47.
2. Gil, J., et al., *Biomass Gasification with Air in a Fluidized Bed: Effect of the on-Bed Use of Dolomite under Different Operation Conditions*. Ind. Eng. Chem. Res., 1999. **38**: p. 4226-4235.
3. Milne, T.A., N. Abatzoglou, and R.J. Evan, *Biomass Gasifier "Tars": Their Nature, Formation and Conversion*. 1998, National Renewable Energy Laboratory (NREL).
4. Sutton, D., B. Kelleher, and J.R.H. Ross, *Review of Literature on Catalysts for Biomass Gasification*. Fuel Processing Technology, 2001. **73**: p. 155-173.
5. Corella, J., J.M. Toledo, and P.M. Aznar, *Improving the Modeling of the Kinetics of the Catalytic Tar Elimination in Biomass Gasification*. Ind. Eng. Chem. Res., 2002. **41**: p. 3351-3356.
6. Orio, A., J. Corella, and I. Narvaez, *Performance of Different Dolomites on Hot Raw Gas Cleaning from Biomass Gasification with Air*. Ind. Eng. Chem. Res., 1997. **36**: p. 3800-3808.
7. Baker, E.G., L.K. Mudge, and M.D. Brown, *Steam Gasification of Biomass with Nickel Secondary Catalysts*. Ind. Eng. Chem. Res., 1987. **26**: p. 1335-1339.
8. Klein, C. and H. Hurlbut, *Manual of Mineralogy*, ed. s. ed. 1993, New York: Wiley.

9. Simell, P.A., J.K. Leppalahti, and J.B.-s. Bredenberg, *Catalytic Purification of Tarry Fuel Gas with Carbonate Rocks and Ferrous Materials*. *Fuel*, 1992. **71**: p. 211-218.
10. Delgado, J., P.M. Aznar, and J. Corella, *Calcined Dolomite, Magnesite, and Calcite for Cleaning Hot gas from a Fluidized Bed Gasifier with Steam: Life and Usefulness*. *Ind. Eng. Chem. Res.*, 1996. **35**: p. 3637-3643.
11. Simell, P., J.K. Leppalahti, and E. Kurkela, *Tar-Decomposing activity of Carbonate Rocks under High CO₂ Partial Pressure*. *Fuel*, 1995. **74**(6): p. 938-945.
12. Walawender, W.P., S. Ganasen, and L. Fan. *Steam Gasification of Manure in Fluidized Bed. Influence of Limestone as Bed Additive*. in *Symposium Papers on Energy from Biomass and Wastes*. 1981. IGT: Chicago, IL.
13. Corella, J., et al., *Biomass Gasification in Fluidized Bed: Where to Locate the Dolomite?* *Energy & Fuels*, 1999. **13**(6): p. 1122-1127.
14. Rapagana, S., et al., *Steam Gasification of Biomass in a Fluidized-Bed of Olivine Particles*. *Biomass and Bioenergy*, 2000. **19**: p. 187-197.
15. Abu El-Rub, Z., E.A. Bramer, and G. Brem. *Removal of Naphthalene as the Model Tar Compound on Calcined Dolomites, Olivine and Commercial Nickel Catalyst in a Fixed Bed Tubular Reactor*. in *21th European Conference for Energy, Industry and Climate Protection*. 2002. Amsterdam, The Netherlands: ETA: Florence and WIP: Munich.
16. Devi, L., et al., *Catalytic Decomposition of Biomass Tars: Use of Dolomite and Untreated Olivine*. *Renewable Energy*, 2005. **30**: p. 565-587.
17. Rapagna, S., et al., *Steam Gasification of Biomass in a Fluidized-Bed of Olivine Particles*. *Biomass and Bioenergy*, 2000. **19**: p. 187-197.
18. Courson, C., et al., *Development of Ni catalysts for gas Production from Biomass Gasification. Reactivity in Steam- and Dry-Reforming*. *Catalysis Today*, 2000. **63**: p. 427-437.
19. Devi, L., *Catalytic Removal of Biomass Tars; Olivine as Prospective in-Bed Catalyst for Fluidized-Bed Biomass Gasifiers*. 2005, Technical University of Eindhoven: Eindhoven, The Netherlands.
20. Rosen, C., et al. *Fundamentals of Pressurized Gasification of Biomass*. in *Developments in Thermochemical Biomass Conversion*. 1997. London, Great Britain: Blackie Academic & Professional.
21. Wen, Y.W. and E. Cain, *Catalytic pyrolysis of a coal tar in a fixed-bed reactor*. *Ind. Eng. Chem. Proc. Des.*, 1984. **23**(4): p. 627-637.
22. Simell, P.A. and J.B.-s. Bredenberg, *Catalytic Purification of Tarry Fuel Gas*. *Fuel*, 1990. **69**: p. 1219-1225.
23. Adjaye, J.D. and N.N. Bakhski, *Production of Hydrocarbons by Catalytic Upgrading of a fast Pyrolysis Bio-Oil. Part II: Comparative Catalyst*

- Performance and Reaction Pathways*. Fuel Processing Technology, 1995. **45**: p. 185-202.
24. Lankford, W.T.J.a.c.-w., *The Making, Shaping, and Treating of Steel*. 10th ed. 1985, Pittsburgh, Pa.: Association of Iron and Steel Engineers.
 25. Tamhankar, S.S., K. Tsuchiya, and J.B.-s. Riggs, *Catalytic Cracking of Benzene on Iron Oxide-Silica: Activity and Reaction Mechanism*. Applied Catalysis A: General, 1985. **16**: p. 103-121.
 26. Cypers, R. and C. Souden-Moinet, *Pyrolysis of Coal and Iron Oxides Mixtures. 1. Influence of Iron Oxides on the Pyrolysis of Coal*. Fuel, 1980. **1980**: p. 48-54.
 27. Zanzi, R., K. Sjostrom, and E. Bjornbom, *Rapid High-Temperature Pyrolysis of Biomass in a Free-Fall Reactor*. Fuel, 1996. **75**(5): p. 545-550.
 28. Chembukulam, S.K., et al., *Smokeless Fuel from Carbonized Sawdust*. Ind. Eng. Chem. Prod. Res. Dev., 1981. **20**: p. 714-719.
 29. Dogru, M., et al., *Gasification of Hazelnut Hhells in a Downdraft Gasifier*. Energy, 2002. **27**: p. 415-427.
 30. Brandt, P., E. Larsen, and U. Henriksen, *High Tar Reduction in a Two-Stage Gasifier*. Energy & Fuels, 2000. **14**: p. 816-819.
 31. Zanzi, R., K. Sjstrm, and E. Bjrnbnom, *Rapid High-Temperature Pyrolysis of Biomass in a Free-Fall Reactor*. Fuel, 1996. **75**(5): p. 545-550.
 32. Chembukulam, S.K., et al., *Smokeless Fuel from Carbonized Sawdust*. Ind. Eng. Chem. Prod. Res. Dev., 1981. **20**: p. 714-719.
 33. Seshardi, K.S. and A. Shamsi, *Effect of Temperature, Pressure, and Carrier gas on the Cracking of Coal Tar over a Char-Dolomite Mixture and Calcined Dolomite in a Fixed Bed Reactor*. Ind. Eng. Chem. Res., 1998. **37**: p. 3830-3837.
 34. Bhatia, S., *Zeolite Catalysis: Principles and Applications*. 1990, Florida: CRC Press, Inc.: Boca Raton.
 35. Whitmore, F.C., *Mechanism of the Polymerization of Olefins by Acid Catalysts*. Ind. Eng. Chem. Proc. Des., 1934. **26**(1): p. 94-95.
 36. Corma, A. and A.V. Orchillés, *Current views of the mechanism of Catalytic Cracking*. Microporous and Mesoporous Materials, 2000. **35-36**: p. 21-30.
 37. Watson, B.A., M.T. Klein, and R.H. Harding, *Catalytic Cracking of Alkylbenzenes: Modeling the Reaction Pathways and Mechanisms*. Applied Catalysis A: General, 1997. **160**: p. 13-39.
 38. de Souza, T.R.O., S.M. Brito, and H.M.C. Andrade, *Zeolite Catalysts for Water Gas Shift Reaction*. Applied Catalysis A: General, 1999. **178**: p. 7-15.

39. Radwan, A.M., T. Kyotani, and A. Tomita, *Characterization of Coke Deposited from Cracking of Benzene over USY Zeolite Catalyst*. Applied Catalysis A: General, 2000. **192**: p. 43-50.
40. Gil, J., et al., *Biomass Gasification with Air in a Fluidized Bed: Effect of the In-Bed Use of Dolomite under Different Operating Conditions*. Ind. Eng. Chem. Res., 1999. **38**: p. 4226-4235.
41. Herguido, J., et al. *Results with a Multisolid Circulating Fluid Bed Pilot Plant for the Improved Steam Gasification of Biomass*. in *Biomass for Energy, Industry and Environment, 6th E.C. Conference*. 1992. London and New York.
42. Turn, S., et al., *Control of Alkali Species in Gasification Systems: Final Report*. 2000.
43. Suzuki, T., H. Ohme, and Y. Watanabe, *Alkali metal catalyzed carbon dioxide gasification of carbon*. Energy & Fuels, 1992. **6**(4): p. 343-351.
44. Padban, N., *PFB Air Gasification of Biomass: Investigation of Product Formation and Problematic Issues related to Ammonia, Tar and Alkali*, in *Department of chemical Engineering II*. 2000, Lund University.
45. Lizzio, A.A. and L.R. Radovic, *Transient Kinetics Study of Catalytic Char Gasification in Carbon Dioxide*. Ind. Eng. Chem. Res., 1991. **30**(8): p. 1735-1744.
46. Abu El-Rub, Z., B. E.A., and G. Brem. *Tar Removal in an Entrained Flow Cracker (EFC) with Application to Biomass Gasification*. in *Pyrolysis and Gasification of Biomass and Waste, Proceeding of an Expert Meeting*. 2002. Strasbourg, France: CPL Press, Liberty House, The Enterprise Centre.
47. Lee, W., et al., *The Effect of Na₂CO₃ on the Catalytic Gasification of Rice Straw over Nickel Catalysts Supported on Kieselguhr Seung*. Korean J. Chem. Eng., 2000. **17**(2): p. 174-178.
48. Lee, W.J., *Catalytic activity of alkali and transition metal salt mixtures for steam-char gasification*. Fuel, 1995. **74**(9): p. 1387-1393.
49. Kirk-Othmer, *Encyclopedia of Chemical Technology*. 2002, New York: Wiley-Interscience.
50. Garcia, L., et al. *Assessment of Coprecipitated Nickel-Alumina Catalysts, for Pyrolysis of Biomass*. in *Development in Thermochemical Biomass Conversion*. 1997. London: Blackie Academic and Professional.
51. Richardson, S.M. and M.R. Gray, *Enhancement of Residue Hydroprocessing Catalysts by Doping with Alkali Metals*. Energy & Fuels, 1997. **11**(6): p. 1119-1126.
52. Caballero, M.A., et al., *Commercial Steam Reforming Catalysts To Improve Biomass Gasification with Steam-Oxygen Mixtures. 1. Hot Gas Upgrading by the Catalytic Reactor*. Ind. Eng. Chem. Res., 1997. **36**(12): p. 227-5239.

53. Aznar, M.P., et al., *Commercial Steam Reforming Catalysts to Improve Gasification with Steam-Oxygen Mixtures. 2. Catalytic Tar Removal*. Ind. Eng. Chem. Res., 1998. **37**: p. 2668-2680.
54. Sada, E., H. Kumazawa, and M. Kudsy, *Pyrolysis of lignins in molten salt media*. Ind. Eng. Chem. Res., 1992. **31**(2): p. 612-616.
55. Baker, E.G., L.K. Mudge, and M.D. Brown, *Steam Gasification of Biomass with Nickel Secondary Catalysts*. Ind Eng. Chem. Res., 1987. **26**: p. 1335-1339.
56. Engelen, K., et al., *A Novel Catalytic Filter for Tar Removal from Biomass Gasification gas: Improvement of the Catalytic Activity in Presence of H₂S*. Chemical Engineering Science, 2003. **58**(3-6): p. 665-670.
57. Hepola, J. and P. Simell, *Sulphur Poisoning of Nickel-Based Hot Gas Cleaning Catalysts in Synthetic Gasification Gas. II. Chemisorption of Hydrogen Sulphide*. Applied Catalysis B: Environmental, 1997. **14**: p. 305-321.
58. Forzatti, P. and L. Lietti, *Catalyst Deactivation*. Catalyst Today, 1999. **52**: p. 165-181.
59. Aznar, M.P., et al., *Improved steam gasification of lignocellulosic residues in a fluidized bed with commercial steam reforming catalysts*. Ind. Eng. Chem. Res., 1993. **32**(1): p. 1-10.
60. Olivares, A., et al., *Biomass Gasification: Produced Gas Upgrading by In-Bed Use of Dolomite*. Ind. Eng. Chem. Res., 1997. **36**: p. 5220-5226.
61. Garcia, L., et al. in *Development in Thermochemical Biomass Conversion*. 1997: Blackie Academic and Professional: London.
62. Arauzo, J., et al., *Catalytic Pyrogasification of Biomass. Evaluation of Modified Nickel Catalysts*. Ind. Eng. Chem. Res., 1997. **36**(1): p. 67-75.
63. Yamaguchi, T., et al., *Deactivation and Regeneration of Catalyst for Steam Gasification of Wood to Methanol Synthesis Gas*. Ind. Eng. Chem. Prod. Res. Dev., 1986. **25**: p. 239-243.

Chapter 3

Experimental Comparison of Biomass

Char with other Catalysts for Tar

Reduction

Abstract

In this chapter the potential of using biomass char as a catalyst for tar reduction is discussed. Biomass char is compared with other known catalysts used for tar conversion as discussed in chapter two. Model tar compounds, phenol and naphthalene, were used to test char and other catalysts. Tests were carried out in a fixed bed tubular reactor at a temperature range of 700–900 °C under atmospheric pressure and a gas residence time in the empty catalyst bed of 0.3 s. Biomass chars are compared with calcined dolomite, olivine, used fluid catalytic cracking (FCC) catalyst, biomass ash and commercial nickel catalyst. The conversion of naphthalene and phenol over these catalysts was carried out in the atmosphere of CO₂ and steam. At 900 °C the conversion of phenol was dominated by thermal cracking whereas naphthalene conversion was dominated by catalytic conversion. Biomass chars gave the highest naphthalene conversion among the low cost catalysts used for tar removal. Further, biomass char is produced continuously during the gasification process, while the other catalysts undergo deactivation. A simple first order kinetic model is used to describe the naphthalene conversion with biomass char.

3.1 Introduction

The review made in chapter two showed that biomass char can be a material of high potential for tar reduction in the biomass gasification process. Therefore, it is important to compare the performance of biomass char for tar reduction with other types of active catalysts under comparable process conditions.

The properties that determine the technical suitability of a catalyst for the tar removal in a gasification process are [1]: (1) activity; how fast one or more reactions (e.g., tar conversion reactions) proceed in the presence of the catalyst, (2) selectivity; the fraction of the starting material (tar) that is converted to the desired product, and (3) stability; the chemical, thermal, and mechanical stability of a catalyst determines its lifetime in industrial reactors. Activity and stability are the most important for tar conversion in the gasification process and to a less extent the selectivity as long as the tar is converted to light gases.

The attractiveness of char as a catalyst originates from its low cost and its natural production inside the gasifier. However, it will be consumed by gasification reactions with steam or CO₂ in the producer gas. The need for a continuous external char supply or withdrawal depends on the balance of char consumption and production in the gasification system.

The tar mixture is classified into five classes by Padban [2]: Undetectable, heterocyclic, light aromatic hydrocarbons (LAH), light polyaromatic hydrocarbons (LPAH) and heavy polyaromatic hydrocarbons (HPAH) as explained in Table 1-3. The distribution of the tar over these classes is very dependent on the gasification temperature as shown in Figure 3-1 [2].

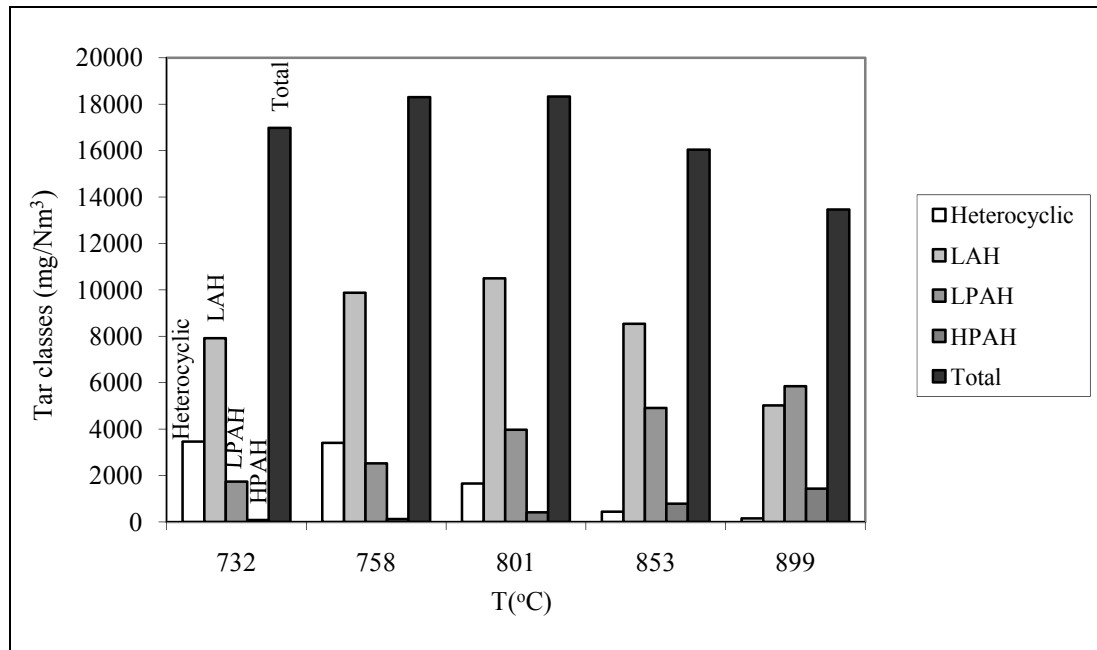


Figure 3-1 Effect of gasification temperature on tar classes concentrations [2], LAH: light aromatic hydrocarbons; LPAH: light polyaromatic hydrocarbons; HPAH: heavy polyaromatic hydrocarbons

Out of these classes, heterocyclic, LAH, LPAH and HPAH tars are the most important as shown in Figure 3-1. The LAH tars are not considered as problematic because they do not condense at typical application temperatures. Therefore, they are not studied in the present comparison. The HPAH are also not studied because of low concentrations in the tar mixture. Finally, the GC-undetectable tars are not studied because they simply cannot be determined.

Table 3-1 characterizes the commonly used model tar compounds in literature [3-7]. It shows that naphthalene and phenol are the best model tar compounds that represent LPAH and heterocyclic tars, respectively.

Table 3-1 Characteristics of the common model tar compounds used in literature [3-7]

Model Tar Compound	Remarks
Naphthalene	The order of thermal reactivity is [3]: toluene >> naphthalene > benzene. Represents the LPAHs tars or tertiary tars. At 900 °C, Naphthalene is the major single compound in the tars [4].
Phenol	Represents heterocyclic tars. Major tar compound at process temperatures lower than 800 °C [5].
Benzene	It represents a stable aromatic structure apparent in tars formed with high-temperature processes [6]. It is not considered as a problematic tar.
Toluene	It represents a stable aromatic structure apparent in tars formed with high-temperature processes [7].

It is not considered as a problematic tar.

Less harmful than most of the other tar compounds [7].

High-temperature chemistry of toluene is fairly well-known [7].

High-temperature tar is more unsaturated than toluene. Thus, with toluene catalyst deactivation because of charring can be less severe and the hydrocarbon conversion to gases is too high in comparison with real tar [7].

Gives higher conversion than real tar would, and based on toluene conversion, results would be unrealistic with respect to the decomposition of the gasifier product tar [7].

Cyclohexane It is not considered as a problematic tar.

n-heptane It is not considered as a problematic tar.

The objective of this chapter is to compare the tar reduction performance of biomass char with other catalysts. This comparison was carried out in a fixed bed tubular reactor using model tar compounds reduction. Biomass char was compared with calcined dolomite, olivine, used fluid catalytic cracking (FCC) catalyst, biomass ash and commercial nickel catalyst. Two reference experiments were carried out, one with an inert bed material (silica sand) and another in an empty reactor in a steam and CO₂ atmosphere.

3.2 Experimental

Testing of the biomass char and the other catalysts was carried out using two model tar compounds phenol and naphthalene. The experimental conditions are given in Table 3-2. The following experiments were performed:

- Measuring reactor temperature profile
- Comparison of catalysts using phenol as a model tar compound
- Comparison of catalysts using naphthalene as a model tar compound

Determining the apparent kinetic constant of the biomass char using naphthalene model tar compound

Table 3-2 Experimental conditions of catalysts screening

		Phenol	Naphthalene
Symbol		C ₆ H ₅ OH	C ₁₀ H ₈
Temperature	°C	700, 900	900
Initial tar component concentration	g/Nm ³	8-13	40, 90
Pressure	atm	1	1
Gas residence time *	s	0.3	0.3
Catalyst bed volume	cm ³	25	25
Catalyst bed height	cm	2	2
Feed gas composition			
CO ₂	Vol. %	6	6
H ₂ O	Vol. %	10	10
N ₂	Vol. %	balance	balance

*See eq. (3-2)

The operating conditions that are commonly used for comparing the catalysts activity for tar conversion are, mostly, 800-900 °C, 0.2-0.4 s gas residence time in the empty catalyst bed, and a steam and CO₂ atmosphere [7-9].

In the thermal cracking approach for tar removal, high temperatures are used (>1000 °C). This approach has the disadvantage of high energy cost. On the other hand, the catalytic approach allows lower temperatures but uses (expensive) catalysts. A temperature of 900 °C was selected for the comparison with other research works. Performing the comparison at higher temperature can lead to thermal cracking of the tars which does not give an accurate measure for the activity of the catalyst.

The tar conversion reaction is not very fast. Thus, we have to insure that the tar has enough time in the catalyst bed to be converted. Several definitions for residence time have been used in literature. The residence time (τ) in the catalyst bed with respect to the empty catalyst bed volume is selected. The value of 0.3 s residence time is a good selection for comparison looking at the results of other research works in literature. In addition, the value of the residence time with respect to the catalyst weight (τ') with the unit (kg·h·m⁻³) was given in Table 3-6 for the sake of comparison. Both residence times were calculated based on the gas flow rate at the inlet of the bed including the steam content in the gas at the bed temperature.

The major components found in the producer gas are H₂O, CO₂, H₂, CO and CH₄. The most important components responsible for tar conversion are H₂O and CO₂ because of the dry and steam reforming reactions explained in chapter two. That is the reason they were used in the feed gas with tar. The inhibitory effect of CO and H₂ on the tar reforming reaction rates [10, 11] was studied in chapter four and was found to be of minor importance for the tar conversion over biomass char.

3.2.1 Setup

The fixed bed reactor is made of a quartz tube, with 75 cm length and 4 cm internal diameter. The bed is supported by a porous quartz disc and heating is done by a tubular electric furnace. The longitudinal temperature profile is measured by a K-type thermocouple which is fitted in a small quartz pipe placed in the center of the reactor. Steam and model tar component are introduced in the gas stream by means of two separate saturation units. The concentrations of steam and model tar component can be altered by changing the saturation temperature. The feeding line as well as the product line is externally heated ($\sim 250\text{ }^{\circ}\text{C}$) to prevent tar condensation. The flow of the feed gases is regulated by critical nozzles and mass flow controllers. Figure 3-2 shows the experimental setup.

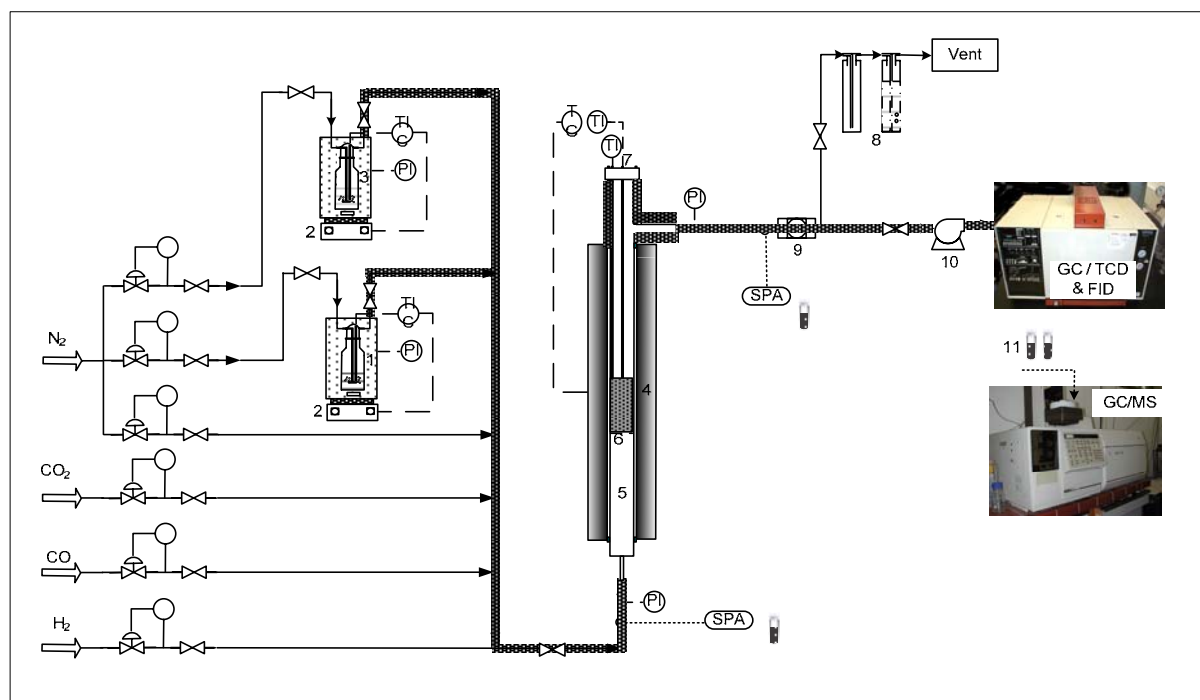


Figure 3-2 Experimental setup for catalysts comparison (1. water saturator; 2. heater; 3. model tar component saturator; 4. tubular furnace; 5. quartz tubular reactor; 6. catalyst bed; 7. quartz tubes for thermocouples; 8. water condenser; 9. filter; 10. heated pump; 11. SPA sample vials; GC: gas chromatography; FID: flame ionization detector; TCD: thermal conductivity detector; MS: mass spectrometry; SPA: solid phase adsorption)

Catalysts screening experiments using naphthalene were performed at a high temperature ($900\text{ }^{\circ}\text{C}$) in order to get a high naphthalene conversion. Catalysts screening experiments using phenol were performed at $700\text{ }^{\circ}\text{C}$ because phenol is thermally unstable at $900\text{ }^{\circ}\text{C}$. Figure 3-3 illustrates the temperature profile inside the reactor. The temperature along the catalyst bed is constant, i.e., model tar component removal occurs at isothermal conditions. Insulation around the reactor especially around the inlet and outlet were made so that the temperature along the reactor was always above the dew point of model tars to prevent condensation.

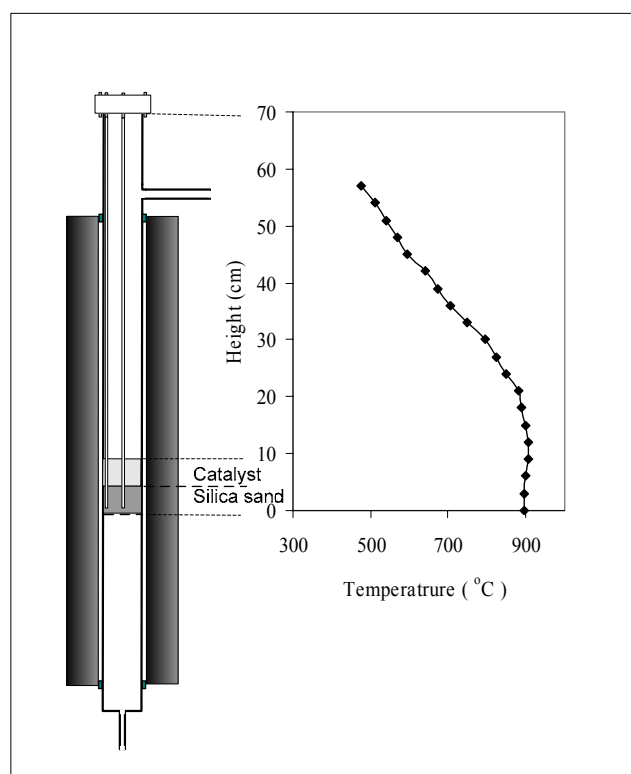


Figure 3-3 Reactor temperature profile

3.2.2 Tar sampling method

There is not yet an international standard method for measuring tar in producer gas from biomass gasifiers. However, in the beginning of the year 2003 a European project named “Tar Measurement standard” started to focus on the standardization at a European level (CEN) of a Guideline for the measurement of the tar [12, 13]. In the present study the tar content in the gas was determined using the solid phase adsorption method (SPA) [14]. The advantages of the SPA method compared with the conventional cold trapping method used by the Guideline [15], are the sampling speed (one sample per minute compared with one sample per hour), simplicity, less solvent consumption, faster workup, accuracy and repeatability. The SPA method is reliable to measure the tar classes 2-5: from xylenes up to tar compounds with a molecular weight of 300 kg/kmol (coronene) [2].

The principle for this method is that tar compounds in the vapor-phase can be trapped on a porous adsorbent (silica-bonded amino-phase) at ambient temperature, as shown in Figure 3-4. Before and after the reactor, a hot gas sample of 100 ml was manually withdrawn through a sorbent tube during approximately 1 min using a gas-tight syringe so that the tar was adsorbed and condensed onto the sorbent. The sampling point was kept at a temperature of 250-300 °C to prevent tar condensation. The adsorbed tar compounds were eluted from the sorbent tube using the solvents dichloromethane for naphthalene or isopropanol for phenol. The amount of solvent was fixed to 1 ml per sample.

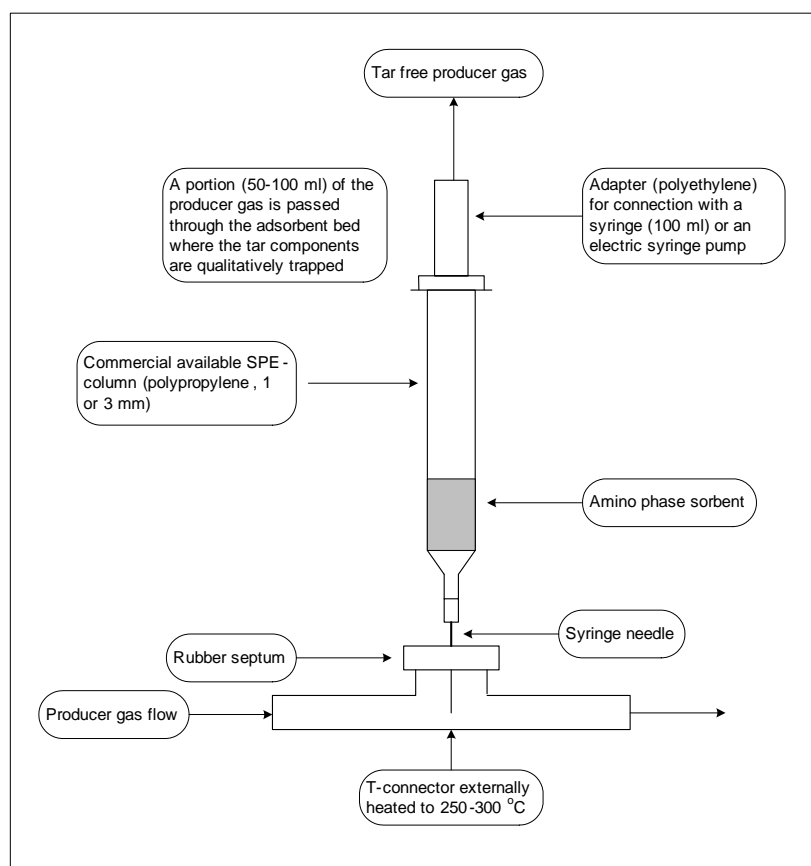


Figure 3-4 SPA tar sampling method [14]

3.2.3 Gas analysis

The tar containing sample from the SPA method was analyzed in a gas chromatograph in combination with a mass spectrometer (GC/MS). When samples from the feed and the product gas are taken, tar conversion can be determined. Measurements on volumetric concentration of H_2 , N_2 , CH_4 , CO can be done online by gas chromatography in combination with a thermal conductivity detector (GC/TCD). CO_2 concentration could only be measured offline using an infrared Maihak Multor 610 detector.

3.2.4 Test procedure

The experimental runs were started by pouring a weighed sample of the bed material (catalyst) on top of a silica bed. The feed gas flow rate was regulated to give the desired space time of 0.3 s. The reactor is preheated to the required temperature with an oven. Calcination required for some catalysts was carried out in-situ at the reactor temperature and atmospheric pressure for 1 h at constant nitrogen flow. After calcination, all the gaseous reagents were fed and the catalysts were then stabilized for at least 15 minutes before the feed and product gas were sampled.

3.2.5 Tested Catalysts

Commercial biomass char (C.B. Char), Calcined dolomite, olivine, and “in-equilibrium” (once used) fluid catalytic cracking (FCC) catalyst were obtained from commercial suppliers. Biomass ash and another biomass char were produced from pinewood biomass in our laboratory. The biomass char was produced by pyrolyzing the pinewood at 500 °C and the biomass ash was produced by burning the produced pinewood char at 600 °C. FCC catalyst had an average particle size of 57 μm. Silica sand (inert material) and commercial nickel catalyst (highly active catalyst) were used as extremes for comparing the activity of the selected catalysts. The particles of dolomite, olivine and char were sieved to a particle size range of 1.4-1.7 mm. Nickel catalyst particles were crushed and sieved to a particle size range of 1.4-1.7 mm. The produced biomass ash was very fine with a particle size less than 0.3 mm. Table 3-3 to Table 3-5 provide some chemical characteristics of the tested catalysts.

Table 3-3 Chemical composition of the compared catalysts (wt. %)

Element	Olivine	Dolomite	Nickel	Biomass Ash
MgO	48.5-50.0	21.5	-	15
CaO	0.05-0.10	30.5	-	44.3
SiO ₂	41.5-42.5	0.15	7	-
Fe ₂ O ₃	6.8-7.3	0.20	-	-
Al ₂ O ₃	0.4-0.5	0.061	12	-
NiO	0.3-0.35	-	70	-
MnO	0.05-0.10	-	-	-
Cr ₂ O ₃	0.2-0.3	-	-	-
NiCO ₃	-	-	5	-
K ₂ O	-	-	-	14.5

Table 3-4 Chemical characteristics of the spent FCC catalyst

APS	SA	MSA	ABD	Fe	Na	C	Ti	ReO	SiO ₂	Mg	Al ₂ O ₃
μ	m ² /g	m ² /g	g/cc	wt.%	wt.%	wt.%	wt.%	wt.%	wt.%	wt.%	wt.%
57	172	79	0.86	0.3	0.15	0.08	0.97	3.73	50.58	0.21	44.3

APS = Average Particle Size

SA = Surface Area

MSA = Matrix Surface Area

ABD = Apparent Bulk Density

Table 3-5 The ultimate analysis of tested biomass char produced by pyrolyzing pinewood at 500 °C and commercial biomass char (wt. %)

	Pinewood char	Commercial biomass char (C.B. Char)
C	87.9	89.03
N	0.3	0.24
H	0.6	0.12
Ash	4.7	9.55
O (by difference)	6.5	1.06

Table 3-6 Bed properties of tested catalysts

Bed material*	Catalyst bed density (g/cm³)	Particle size (mm)	Weight time (kg_{cat}·h/m³)
Olivine	1.97	1.4-1.7	0.27
Raw dolomite	1.93	1.4-1.7	0.27
Silica sand	1.73	1.4-1.7	0.24
FCC (spent)	1.13	0.057	0.16
Nickel	1.03	1.4-1.7	0.14
Commercial biomass char (C.B. Char)	0.52	1.4-1.7	0.04
Biomass char	0.26	1.4-1.7	0.03
Biomass ash	0.09	<0.25	0.01

*The catalyst bed is added on the top of a silica sand bed of the same volume.

3.2.6 Experimental data evaluation

Conversion of the tar model compounds naphthalene and phenol were calculated from their inlet and outlet concentrations as shown in eq (1). This equation is often used in literature [6, 16-18] for ease of results comparison with other research works. The data points that represent the model tar compound conversion were average points. For every point five samples, on average, were taken.

$$X = \frac{(C_{in} - C_{out})}{C_{in}} \quad (3-1)$$

Where,

X = tar conversion

C_{in} = inlet tar concentration

C_{out} = outlet tar concentration

Several definitions for residence time have been used in literature. The residence time (τ) in the catalyst bed with respect to the empty catalyst bed volume is selected and defined as:

$$\tau = \frac{V_{R,cat}}{Q_{in}(T, P_{tot})} \quad (3-2)$$

Where,

$V_{R,cat}$ = Volume of catalyst bed with respect to the volume of empty reactor, m^3

$Q_{in}(T, P_{tot})$ = Inlet volume flow rate, m^3/s

The activity of the catalyst is defined in terms of kinetics. The reaction rate is calculated as the rate of change of the amount of tars with time relative to the reaction volume (used in this study) or mass of the catalyst. A first order kinetic model was used for making a kinetic study. This model is easy for data evaluation and comparison of results with literature. The reaction rates were measured in the temperature and concentration ranges that are common in the industrial gasification processes. Under the selected operating conditions presented in Table 3-2, the naphthalene conversion is kinetically limited where mass transfer has minor effect as will be explained in chapter four and five.

$$-r_{tar} = k_{app} C_{tar} \quad (3-3)$$

Where,

r_{tar} = rate of tar conversion, $kmol/m^3 \cdot s$

k_{app} = apparent kinetic constant, s^{-1}

C_{tar} = tar concentration, $kmol/m^3$

To verify plug flow conditions in the fixed bed, we need to calculate the dimensionless Peclet number (Pe).

$$Pe = v \cdot \frac{L}{D_l} \quad (3-4)$$

$Pe \rightarrow 0$ large dispersion, hence mixed flow

$Pe \rightarrow \infty$ negligible dispersion, hence plug flow

Where,

L = length of the bed, m

ν = velocity, m/s

D_l = dispersion coefficient, m^2/s

Peclet number for the present experiments was found to be very high, hence plug flow conditions can be assumed. Under plug flow conditions, the apparent kinetic constant can be integrated as:

$$k_{app} = \frac{-\ln(1 - X)}{\tau} \quad (3-5)$$

Where,

τ = gas residence time in the empty bed volume based on inlet gas velocity and reactor temperature, s

The apparent rate constant of naphthalene conversion over biomass char was estimated according to the Arrhenius' law. The estimated apparent activation energy for char was assumed to be constant in the studied temperature range (700-900 °C).

$$k_{app} = k_{o,app} e^{(-E_{app} / RT)} \quad (3-6)$$

Where,

$k_{app,o}$ = apparent frequency factor, s^{-1}

E_{app} = apparent activation energy, kJ/kmol

3.3 Results and Discussion

3.3.1 Phenol conversion

Two types of experiments were performed; thermal and catalytic phenol reduction. The thermal experiments were performed in an empty reactor to study the stability of phenol at 700 and 900 °C. The activity of six different catalytic bed materials for phenol conversion was tested. For both types of experiments, dry gas and phenol analysis were performed. The summary of experimental results is given in Table 3-7.

Table 3-7 Dry gas composition at the reactor outlet, inlet and outlet phenol concentrations, and thermal and catalytic conversion of phenol; average feed gas composition: 6 vol. % CO₂, 10 vol. % H₂O and balance N₂, $\tau = 0.3$ s

Catalyst	T (°C)	Dry gas composition (vol. %)				Phenol		
		H ₂	CO	CO ₂	N ₂	out g/Nm ³	in g/Nm ³	Conversion (wt. %)
Empty reactor	700	0.14	8.9·10 ⁻⁴	6.0	93.8	10.9	11.6	6.0
	800	1.16	2.6·10 ⁻³	5.7	93.1	0.2	11.4	98.2
	900	1.60	2.5·10 ⁻³	5.8	92.6	0.2	12.4	98.4
Silica Sand	700	0.23	9.1·10 ⁻⁴	6.4	93.4	7.8	11.9	34.5
	900	1.0	2.6·10 ⁻³	6.0	93.0	0.0	9.1	100
Olivine	700	0.27	7.4·10 ⁻⁴	6.1	93.7	6.3	11.0	42.7
	900	1.0	2.5·10 ⁻³	4.0	95.0	0.0	10.9	100
C.B. Char	700	2.18	1.5	7.2	89.1	1.6	8.7	81.6
	900	5.09	9.2	3.2	82.6	0.0	7.9	100
FCC	700	0.19	9.3·10 ⁻⁴	5.7	94.1	1.1	8.5	87.1
	900	0.89	2.6·10 ⁻³	5.7	93.4	0.0	9.8	100
Dolomite	700	0.85	2.6·10 ⁻³	5.8	93.3	1.0	10	90.0
	900	0.40	2.6·10 ⁻³	6.5	93.1	0.0	13.5	100
Nickel	700	1.90	1.9	6.2	90.0	1.0	11.1	91.0
	900	0.08	1.2·10 ⁻³	6.5	93.5	0.0	10.0	100

Carbon mass balance was based on dry gas analysis that includes phenol content and excludes steam content. Further, nitrogen inlet mole (mass) flow rate should equal nitrogen output mole (mass) flow rate. For all catalysts experiments except char experiments, the closing error of carbon was less than 20 % based on the carbon input (see Figure 3-5).

Carbon mass balance was not verified for experiments with char as a catalyst. The carbon mass balance was not made because the biomass char catalyst is not an inert material as it reacts with steam and CO₂ in the feed gas. At the time of these experiments, it was difficult to measure the carbon loss of the char. Later, the setup was further developed and converted to a sort of a macro reactor where it is connected to a balance (see chapter four, section 4.2.1). For upcoming char experiments the weight of the char could be measured with time and thus the carbon balance could be verified.

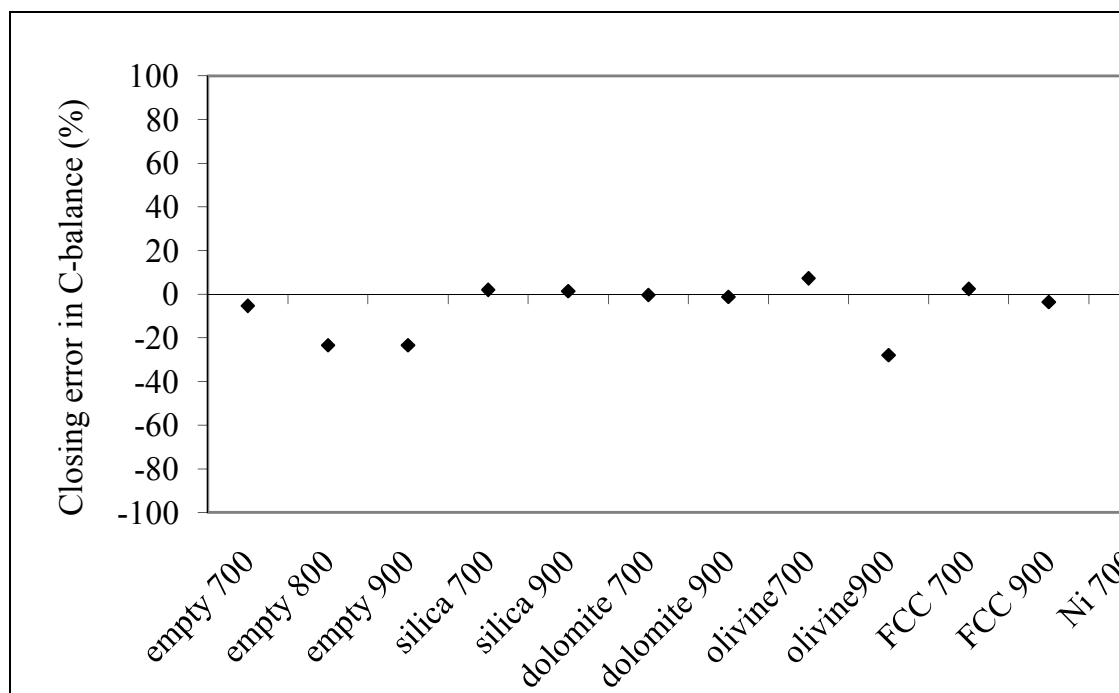


Figure 3-5 Carbon mass balance closing error (%) of the thermal and catalytic conversion of phenol conversion experiments

It is expected that at equilibrium H_2 and CO are produced while CO_2 and H_2O are consumed. Moreover, the amount of H_2 produced is higher than that of CO . Even though, the dry reforming reaction produces more CO than H_2 produced by the steam reforming reaction, it seems that the steam reforming reaction is thermodynamically more favorable.

The steam and dry reforming reactions convert the phenol to CO and H_2 when reacted with H_2O and CO_2 . Phenol is stable at a temperature of $700\text{ }^\circ\text{C}$ with only 6.3 wt. % conversion. However, it loses its stability as temperature increases. The conversion is more than 97 wt. % at $800\text{ }^\circ\text{C}$ and more than 98 wt. % at $900\text{ }^\circ\text{C}$. No significant amounts of other tars in the outlet gas were detected.

The catalytic experiments were performed at two temperatures: 700 and $900\text{ }^\circ\text{C}$. The following results were obtained:

At $900\text{ }^\circ\text{C}$:

All catalysts gave 100 wt. % phenol conversion. It was noted that more than 98 wt. % of phenol was already thermally eliminated.

At $700\text{ }^\circ\text{C}$:

The sequence of the catalysts with respect to decreasing activity is: nickel > dolomite > FCC > char > olivine > sand, see Figure 3-6.

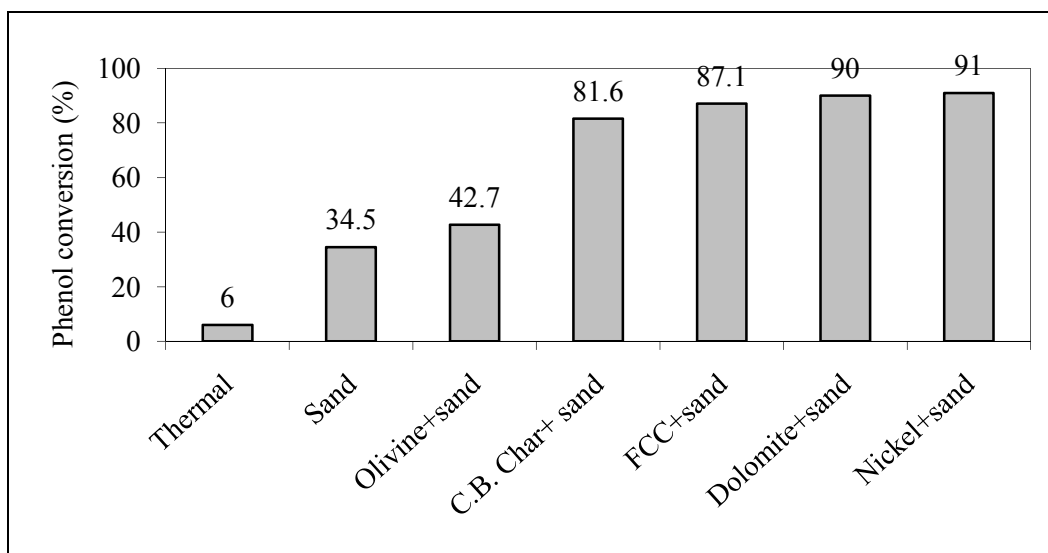


Figure 3-6 Effect of catalysts on phenol conversion. $T = 700\text{ }^{\circ}\text{C}$, $\tau = 0.3\text{ s}$, Feed gas composition: 6 vol. % CO_2 , 10 vol. % H_2O and balance N_2 , inlet phenol concentration: 8-12 g/Nm^3

Dolomite and nickel catalyst gave the highest phenol conversion (90 and 91 wt. %, respectively). They are known to be reforming catalysts and thus catalyze steam and dry reforming reactions of phenol while H_2 and CO are produced. As temperature increased, the produced amount of H_2 decreased for both these catalysts, whereas for other catalysts increases. This confirms that these two catalysts have the same mechanism of tar removal which is expected to be reforming and not cracking.

C.B. char gave moderate phenol conversion (82 wt. %). The carbon in the biomass char catalyst reacts with the steam and CO_2 present in the feed gas. Therefore, the concentrations of both CO and H_2 were higher the amounts produced with other catalysts.

Olivine gave a poor phenol conversion (43 wt. %). The H_2 and CO concentrations in the output gas of the olivine experiments are close to that of FCC and silica sand experiments. This gives an indication that olivine probably has a mechanism of phenol cracking closer to that of FCC and silica sand. This remark is confirmed with the H_2 concentrations that have the same trend of increase with increasing the temperature for the three catalysts. FCC gave a moderate phenol conversion (87 wt. %). The dry gas analysis showed that that the FCC mechanism is not reforming but, as known, cracking catalyst. Obviously, silica sand showed significant catalytic activity for phenol conversion, about 34 wt. %.

No significant amounts of tars other than phenol were detected in the outlet gas. However, phenol could be converted to heavier components that are not detected by SPA.

3.3.2 Naphthalene conversion

The activity of the different catalysts for naphthalene conversion is presented in Figure 3-7.

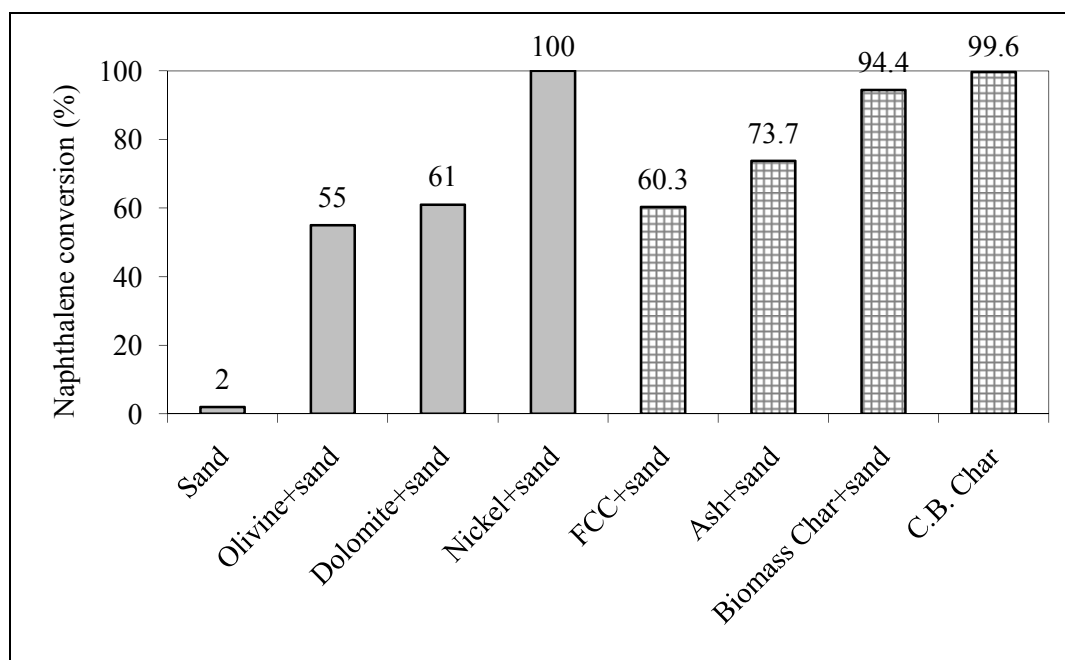


Figure 3-7 Effect of catalyst bed material on naphthalene conversion, $T=900\text{ }^{\circ}\text{C}$, $\tau = 0.3\text{ s}$, Feed gas composition: 6 vol. % CO_2 , 10 vol. % H_2O and balance N_2 , initial naphthalene concentration: 40 g/Nm^3 (■) and 90 g/Nm^3 (▤)

Two inlet naphthalene concentrations were used to see the performance of the catalyst at high naphthalene loadings, such as in updraft fixed bed gasifiers. The ranking of reactivity obtained at 40 g/Nm^3 is: commercial nickel > dolomite > olivine > silica sand. The relative low activity of the tested type of dolomite can be related to the low iron content. The activity of olivine can be increased by carrying out a pretreatment for olivine in order to make the iron active and present on the surface of olivine [19]. Devi et. al. [11] could increase the activity of olivine after pretreatment from 46 % to 80 % naphthalene conversion at comparable experimental conditions. In addition, the large particle size used in the experiments may cause some internal mass transfer limitations. Commercial nickel based catalyst is, as expected, very active, but nickel catalysts are very expensive and more sensitive to deactivation by high tar content and H_2S in the feed gas.

FCC, biomass char, C.B. char and biomass ash were tested at a bed temperature of $900\text{ }^{\circ}\text{C}$, 90 g/Nm^3 initial naphthalene concentration and 0.3 s residence time. The ranking of reactivity obtained is: C.B. char > biomass char > ash > FCC.

The above results agree with the expectations expressed in chapter two, where nickel catalyst, dolomite and char were expected to have the best performance. Nickel catalyst had the highest activity for naphthalene removal. Dolomite gave lower naphthalene conversion than expected because of the low iron content of the tested

type. However, other types with higher content are expected to give better performance. The chars gave the highest activity among the tested catalysts excluding nickel catalyst.

3.3.3 Reaction rate for naphthalene removal with char

From the previous sections, it was found that both biomass chars gave the highest naphthalene conversion excluding the commercial nickel catalyst. The temperature effect on naphthalene conversion was studied for C.B. char (1.4-1.7 mm and 0.5-0.8 mm) in the temperature range of 700 to 900 °C as shown in Figure 3-8. Naphthalene removal increased with increasing bed temperature. On the other hand, the amount of coke formation increased with decreasing bed temperature. The coke covered the catalyst active sites and blocked the pores, which lead to deactivation of the catalyst.

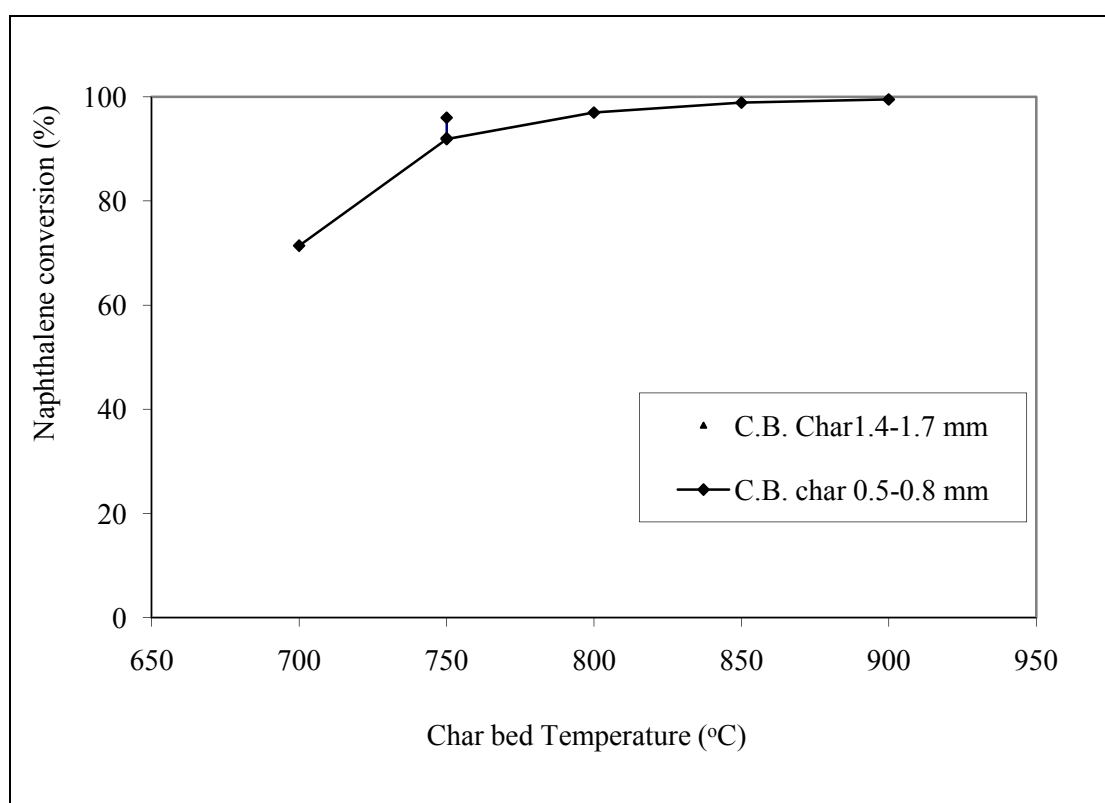


Figure 3-8 Effect of temperature on naphthalene conversion with commercial biomass char, $\tau=0.3$ s, $C_{o,n}=20$ g/Nm³, Feed gas composition: 7% H₂O, 4% H₂, 6% CO, 10% CO₂, 2.4% CH₄, balance N₂,

A reactivity study was done for C.B. char (0.5-0.8 mm) at a temperature range of 700 to 900 °C. The apparent rate constant was varied with temperature by an Arrhenius-type relationship, as shown in Figure 3-9. The apparent activation energy (E_{app}) and the apparent pre-exponential factor ($k_{o,app}$) are listed in Table 3-8.

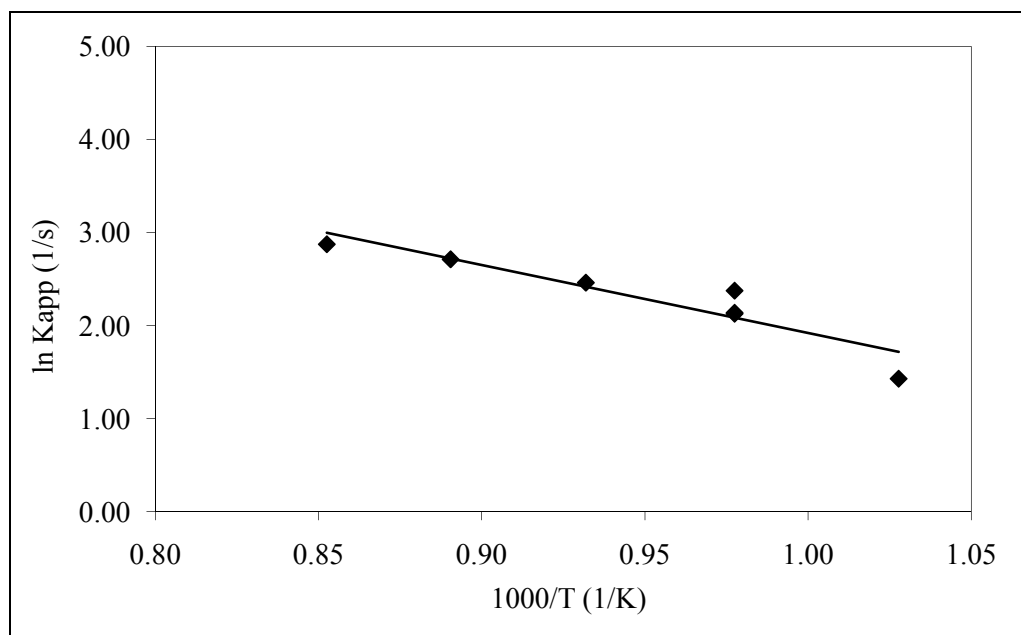


Figure 3-9 Temperature dependency of the apparent reaction rate constant according to Arrhenius' law, τ : 0.3 s, $C_{o,n}$: 20 g/Nm³, Feed gas composition: 7% H₂O, 4% H₂, 6% CO, 10% CO₂, 2.4% CH₄, balance N₂,

Table 3-8 Apparent activation energy (E_{app}) and the apparent pre-exponential factor ($k_{o,app}$) of C.B char, τ : 0.3 s; p.s: 0.5-0.8 mm

Property	Value
E_{app} (kJ/mol)	61
$k_{o,app}$ (s ⁻¹)	1.10^4
$k_{o,app}$ (m ³ .kg ⁻¹ .h ⁻¹)	$7.6 \cdot 10^4$

It would be interesting to compare these results with results of other researchers. However, no comparative research could be found on tar conversion kinetic parameters for biomass char. In Table 3-9 and Table 3-10, a comparison was made with other catalysts usually used in tar reduction. However, the comparison is not simple for the following reasons: (a) different representations of the space time (τ) in terms of catalyst volume/weight and volumetric feed flow rate at normal/reactor temperature, (b) many reported values for the kinetic constant were evaluated under variety of mass transfer limitations, and (c) treatment of different tars compositions originated from different gasification conditions or model tar components.

Table 3-9 Comparison of first order kinetic parameters for different catalysts used for tar elimination

Gasification Conditions		Catalyst Bed		Kinetic Parameters			Ref.
Temperature (°C)	Agent	Type	Temperature (°C)	E_{app} (kJ·mol ⁻¹)	$K_{o,app}$ (Nm ³ ·kg ⁻¹ ·h ⁻¹)	K^* (900 °C)	
	air	Norte dolom ¹	780-920	100±20	(1.51±0.8)·10 ⁶	53	[20] ^a
	air	Chilches dolom.	780-920	100±21	(1.45±0.76)·10 ⁶	51	[20] ^a
	air	Malagan dolom.	780-920	100±22	(1.30±0.54)·10 ⁶	46	[20] ^a
	air	Sevilla dolom.	780-920	100±23	(1.24±0.77)·10 ⁶	44	[20] ^a
750-780	steam	Dolomite	780-910	42	1.96·10 ³	26	[21] ^a
750-780	steam	Magnecite	780-911	42	1.46·10 ³	20	[21] ^a
750-780	steam	Calcite	780-912	42	1.28·10 ³	17	[21] ^a
800-860	steam-O ₂	BASF G1-25S		58±30	1.56·10 ⁵	408	[22] ^a
850	air	Olivine	800-900	114	3.60·10 ⁶	30	[19] ^b
Heavy fraction of mild gasification coal liquids		SiC	500-750	96.9		3.83·10 ⁴	1.9 [23]
		SFCC ^c	500-750	85.8		1.59·10 ⁴	2.4 [23]
		FWC ^d	500-750	81.2		1.30·10 ⁴	3.1 [23]
		CPRD ^e	500-750	76.3		9.26·10 ⁴	37 [23]

* takes the unit of $K_{o,app}$
^a internal diffusion controls
^c SFCC(sorbent-free coal char)
^d FWC(Foster Wheeler char)
^e CPRD =Calcined Plum Run Dolomite

Table 3-10 Comparison of first order kinetic parameters for different catalysts used for naphthalene elimination

Model tar	Agent	Catalyst Bed		Kinetic Parameters			Ref
		Type	Temperature	E_{app} kJ·mol ⁻¹	$K_{o,app}$ m ³ _{Tb,wet} ·kg ⁻¹ ·h ⁻¹ s ⁻¹	K^* (900 °C)	
Naphthalene	H ₂ O+CO ₂ +CO+H ₂	Olivine	825-900	141	1.7·10 ⁷	9	[11]
Naphthalene	H ₂ O+CO ₂	Char	700-900	61	7.6·10 ⁴	199**	this work

* takes the unit of $K_{o,app}$ ** The unit is m³_{Tb,wet}·kg⁻¹·h⁻¹

For ease of comparison, the first order rate constants results of C.B. Char were calculated in two different units. For a temperature of 900 °C, the C.B. Char gives a high rate constant value higher than several different dolomites but less than that of BASF G1-25S CPRD. Therefore, biomass char can be considered as a catalyst of high potential for tar removal.

3.4 Evaluation

In chapter two the most common catalysts used for tar removal were reviewed. These catalysts were used in the present chapter to evaluate how competitive biomass char can be. The comparison is based on both the activity for model tar components removal in a fixed bed reactor and catalyst stability.

3.4.1 Results

The comparison showed that phenol is thermally converted above 800 °C (Table 3-7) which agrees with data from literature (see Figure 3-1). Therefore, the catalysts comparison is made at a temperature where phenol is fairly stable (700 °C). The commercial biomass char gave a moderate phenol conversion (82 %). This is a reasonable result since heterocyclic tars (e.g., phenol) at a gasification temperature of 800 °C or above are cracked thermally. Thus, only small amount of the heterocyclic tars (phenol) remains in the producer gas to be removed catalytically.

Naphthalene is considered as a major tar component at 900 °C. This component is thermally stable at such high temperature as only 2 % was converted over silica sand bed. Therefore, naphthalene needs to be catalytically converted. Biomass chars gave the best naphthalene conversion excluding the nickel catalyst result (Figure 3-7). The latter is a rather expensive catalyst and sensitive to deactivation as explained in chapter two. It is used in this investigation as a reference for high activity since the interest of this research is towards low cost and active catalysts.

The apparent rate constant of naphthalene conversion over char was estimated according to the Arrhenius' law. The estimated apparent activation energy of char was assumed to be constant in the studied temperature range (700-900 °C). The reported activation energies and pre-exponential factors in literature for tar component reduction over the same type of catalyst were reported to have a wide range as shown in Table 3-9 and Table 3-10. This is related to the different operating conditions and different units used. These differences make the comparison difficult to be made. However, the performed experimental comparison showed that char has a high catalytic activity.

3.4.2 Biomass char as a catalyst

Char is a general word and it is not enough to be used when comparing its performance with other research works. The source material of char and method of production affect its physical and chemical properties. Therefore, it should be always accompanied by the ultimate analysis, proximate analysis, mineral content, BET

internal surface area, pore size distribution and porosity. This allows a better comparison and repeatability of the results.

The gas analysis in Table 3-7 showed that biomass char reacts with the reactive gases in the feed gas (steam and CO₂). This explains the relatively high CO and H₂ content in the output gas from the char bed. Whereas the other catalysts were not consumed (inert). On the other hand, while the other catalysts have limited lifetime because of deactivation, char is continuously activated by the gasification reactions with steam and CO₂ even though it has limited lifetime. Moreover, the char consumption by the gasification reactions can be balanced by the gasification process where some char is produced. One kg of biomass can produce 2 Nm³ of producer gas [24]. The char consumption per hour at 850 °C for complete tar removal was found in chapter four to be 1.1 g per 23 NI/h (94 l/h) (Figure 4-26). Thus, the total char consumption per 1 kg biomass becomes 96 g. Assuming that the char production in the gasifier is 10 % of the fed biomass, this is equivalent to 100 g char. Thus, no external supply of char is needed. The char production inside the gasifier can be influenced by manipulating the gasification process parameters, such as, temperature, particle size, moisture content...etc. The continuous biomass char activation and continuous supply of the char to the tar cracker makes the biomass char more stable than the other catalysts. For a self-sustained gasification process with char as a tar catalyst, a model is required to balance the amount of char consumed in the tar cracker with the amount of char produced in the biomass gasifier. The next chapters will show the modeling results.

3.5 Concluding Remarks

The catalysts comparison was based on the activity of the catalyst in a fixed bed reactor. The activity of the catalyst was investigated by naphthalene and phenol conversion, residence time in the catalyst bed, and apparent kinetic constant for a first order kinetic model.

From the experimental comparison of phenol conversion, the following conclusions can be drawn:

- At 900 °C the conversion of phenol is dominated by thermal cracking.
- At 700 °C the ranking of the different catalysts activity for phenol conversion is nickel > dolomite > FCC > char > olivine > sand.
- The output gas analysis of phenol conversion at 700 °C suggests that the dolomite and nickel share a phenol conversion mechanism which is probably reforming. On the other hand, FCC, olivine and silica sand share a different phenol conversion mechanism which can be cracking.

From the experimental comparison of naphthalene conversion, the following remarks can be concluded:

- At 900 °C, the naphthalene is thermally stable.
- The ranking of the different catalysts activity for naphthalene conversion at 900 °C is: nickel > C.B. char > biomass char > biomass Ash > FCC > dolomite > olivine > silica sand.
- The first order kinetic rate constant of biomass char for naphthalene conversion in the temperature range 700-900 °C was found to have an apparent activation energy (E_{app}) of 61 kJ/mol and pre-exponential factor ($k_{o,app}$) of 1.10^4 s^{-1} (equivalent $7.6 \cdot 10^4 \text{ m}^3 \text{ kg}^{-1} \text{ h}^{-1}$).
- Among the low cost material catalysts used for naphthalene conversion, biomass char shows the highest activity. In the next chapters, biomass char will be studied further and tested with real tar.

The continuous activation of the biomass char by the steam and CO₂ content in the producer gas and the continuous external supply of the biomass char from the gasifier to the cracker make the biomass char more stable than the other catalysts.

In the next chapter a clarification is given about the naphthalene removal mechanism over char and the effect of char consumption on the naphthalene conversion. Moreover, the main parameters that affect naphthalene conversion downstream the gasification process are studied and a comparison with real tar conversion will be made.

References

1. Hagen, J., *Industrial Catalysis: a practical approach*. 1999, Weinheim: Wiley-VCH.
2. Kiel, J.H.A., et al., *Primary Measures to Reduce Tar Formation in Fluidized-Bed Biomass Gasifiers*. 2004: The Netherlands.
3. Jess, A., *Mechanics and Kinetics of Thermal Reactions of Aromatic Hydrocarbons from Pyrolysis of Solid Fuels*. *Fuel*, 1996. **75**(12): p. 1441-1448.
4. Milne, T.A., N. Abatzoglou, and R.J. Evan, *Biomass Gasifier "Tars": Their Nature, Formation and Conversion*. 1998, National Renewable Energy Laboratory (NREL).
5. Spliethoff, H., *Status of Biomass Gasification for Power Production*. *IFRF Combustion Journal*, Article No. 200109, 2001.
6. Simell, P.A., E.K. Hiirvensalo, and V. Smolander, *Kinetics, Catalysts, and Reaction Engineering: Steam Reforming of Gasification Gas Tar over Dolomite with Benzene as a Model Compound*. *Ind. Eng. Chem. Res.* 1999. **38**: p. 1250-1257.

7. Simell, P., J.K. Leppalahti, and E. Kurkela, *Tar-Decomposing activity of Carbonate Rocks under High CO₂ Partial Pressure*. *Fuel*, 1995. **74**(6): p. 938-945.
8. Simell, P. and J.B.-s. Bredenberg, *Catalytic Purification of Tarry Fuel Gas*. *Fuel*, 1990. **69**(10): p. 1219-1225.
9. Delgado, J., P.M. Aznar, and J. Corella, *Calcined Dolomite, Magnesite, and Calcite for Cleaning Hot gas from a Fluidized Bed Gasifier with Steam: Life and Usefulness*. *Ind. Eng. Chem. Res.*, 1996. **35**: p. 3637-3643.
10. Ye, D.P., J.B. Agnew, and D.K. Zhang, *Gasification of a South Australian Low-Rank Coal with Carbon Dioxide and Steam: Kinetics and Reactivity Studies*. *Fuel*, 1998. **77**(11): p. 1209-1219.
11. Devi, L., *Catalytic Removal of Biomass Tars; Olivine as Prospective in-Bed Catalyst for Fluidized-Bed Biomass Gasifiers*. 2005, Technical University of Eindhoven: Eindhoven, The Netherlands.
12. Coda, B., et al. *Standardization of the 'Guideline' method for measurement of tars and particles in biomass producer gases*. in *Science in Thermal and Chemical Biomass Conversion*. 2005. Vancouver, Canada.
13. <http://www.tarweb.net/>.
14. Brage, C., et al., *Use of Amino Phase Adsorbent for Biomass Tar Sampling and Separation*. *Fuel*, 1997. **76**(2): p. 1237-42.
15. Simell, P., et al., *Provisional Protocol for the Sampling and Analysis of Tar and Particulates in the Gas from Large-Scale Biomass Gasifiers. Version 1998*. *Biomass and Bioenergy*, 2000. **18**(3): p. 19-38.
16. Peñerez, P., et al., *Hot Gas Cleaning and Upgrading with a Calcined Dolomite Located Downstream a Biomass Fluidized Bed Gasifier Operating with Steam - Oxygen Mixtures*. *Energy & Fuels*, 1997. **11**(1194-1203).
17. Duo, B., et al., *High-Temperature Removal of NH₃, Organic Sulfur, HCl, and Tar Component from Coal-Derived Gas*. *Ind. Eng. Chem. Res.*, 2002. **41**: p. 4195-4200.
18. Zhao, H., D.J. Draelants, and G.V. Baron, *Performance of a Nickel-Activated Candle Filter for Naphthalene Cracking in Synthetic Biomass Gasification Gas*. *Ind. Eng. Chem. Res.*, 2000. **39**: p. 3195-3201.
19. Devi, L., et al., *Catalytic Decomposition of Biomass Tars: Use of Dolomite and Untreated Olivine*. *Renewable Energy*, 2005. **30**: p. 565-587.
20. Orio, A., J. Corella, and I. Narvaez, *New Developments on the Effectiveness of Dolomites of Different Origin for Hot Raw Gas Cleaning in Biomass Gasification with Air*. *Ind. Eng. Chem. Res.*, 1997. **36**: p. 3800-3808.
21. Delgado, J., P.M. Aznar, and J. Corella, *Biomass Gasification with Steam in Fluidized Bed: Effectiveness of CaO, MgO and CaO-MgO for Hot Raw Gas Cleaning*. *Ind. Eng. Chem. Res.*, 1997. **36**(5): p. 1535-1543.

22. Aznar, P.M., et al., *Commercial Steam Reforming Catalysts To Improve Biomass Gasification with Steam-Oxygen Mixtures. 2. Catalytic Tar Removal*. Ind. Eng. Chem. Res., 1998. **37**(7): p. 2668-2680.
23. Shamsi, A., *Catalytic and Thermal Cracking of Coal-Derived Liquid in a Fixed-Bed Reactor*. Ind. Eng. Chem. Res., 1996. **35**(4): p. 1251-1256.
24. Chen, G., J. Andries, and H. Spliethoff, *Biomass Conversion into Fuel Gas using Circulating Fluidized Bed Technology: the Concept Improvement and Modeling Discussion*. Renewable Energy, 2003. **28**: p. 985-994.

Chapter 4

Tar Reduction in a Fixed Char Bed

Abstract

In the previous chapter, the catalytic activity of biomass char was compared with well-known alternative catalysts for tar reduction. In this chapter the results of an extensive experimental study on the activity of biomass char for tar reduction in a fixed bed are presented and discussed. Experiments were carried out for different temperatures, gas residence times, particle sizes, gas compositions, and char properties. For both naphthalene as a model tar component and real tar almost complete conversion (>99%) at temperatures ≥ 800 °C, 0.3 s gas residence time and 500-630 μm char particle size was reached. Char deactivation could be expected because of pore blocking and char consumption by gasification reactions. However, during the experiments the activity of the char for tar reduction was not significantly influenced by the time on stream. Char gasification appears to refresh the active char surface area. Thus, char can be seen as a promising catalyst for tar removal, also because char is produced during the gasification itself.

4.1 Introduction

Because of incomplete gasification, tar and solid char may be formed. The formed solid char, usually, is partially combusted in the gasifier and the remaining unburned char is captured in a dust filtering system. The conditions during the pyrolysis (the early stage of gasification) and also the composition of the biomass affect the char reactivity and burnout [1]. Achieving the highest char reactivity in pyrolysis and the lowest residual char is a target for the gasification process [2]. In literature, char was already noticed to have a good catalytic activity for tar removal in downdraft gasifiers and the two-stage gasifier, developed by the Technical University of Denmark [3], uses char for tar reduction. In these systems high tar removal is realized by passing the volatiles through a combustion or partial oxidation zone followed by a char bed. However, no detailed study on the tar reduction by char has been published in literature.

The catalytic activity of char for tar reduction can be related to its pore size distribution, internal surface area, and mineral content. The first two parameters are dependent on the pyrolysis conditions, such as the heating rate and final pyrolysis temperature. The last parameter depends mainly on the char source type. The char can be deactivated during catalytic reduction because of (a) coke formation that blocks the pores of the char and reduces its surface area and probably covers the ash; hindering its catalytic effect, and (b) consumption of the char, since its fixed carbon is gasified by steam and dry reforming reactions.

In this chapter an experimental study on the char activity for tar reduction is described. Experiments have been carried out in fixed char bed with both naphthalene, as a model tar component, and real tar in a fuel gas matrix.

4.2 Experimental

An experimental program has been carried out in a fixed bed setup. The goal of this experimental study was to reveal the mechanism and key parameters of the tar reduction process with char. Naphthalene was chosen as model compound for tar [4]. In this section, the experimental setups and char properties are described. Two different setups were used for carrying out the experiments. The naphthalene reduction experiments were carried out in the “synthetic tar setup” and the real tar reduction experiments were carried out in the “real tar setup”.

4.2.1 Synthetic tar setup

The fixed bed setup presented in chapter three was used here with some modifications (see Figure 4-1). A gas mixing station is used to compose a gas consisting of CO₂, H₂O, CO, H₂, N₂ and/or naphthalene. The gas is fed to the heated fixed bed reactor. In the reactor, the gas reacts with the biomass char. The naphthalene conversion is measured by sampling the in- and outgoing gas with the solid phase adsorption (SPA) method [5] and analyzing the samples in a gas chromatograph-mass

spectrometer (GC-MS). To study the effect of the carbon conversion in the biomass char on naphthalene conversion, the weight of the char bed as a function of time was measured which is similar to the well-known thermogravimetric analysis (TGA). However, instead of using a microbalance with a small amount of char, a balance was used for the complete fixed bed reactor. The top of the reactor that contains the catalyst bed was hanged on a balance that measures the char weight loss with time. The initial weight of the char bed was measured at room temperature. Then the reactor is heated up to the desired temperature under the flow of N₂, the change of weight is monitored because of 1) the loss of humidity from the reactor wall and char bed and 2) the pyrolysis vapors that evolve from the char bed. The resulting weight of the char bed at the desired reactor temperature is used as the starting char bed weight of the experiment for naphthalene conversion. The experiment started as soon as the feeding of the naphthalene-gas mixture to the reactor was started. The char bed is weighed regularly by disconnecting the inlet and outlet of the reactor and hanging the top of the reactor on the balance.

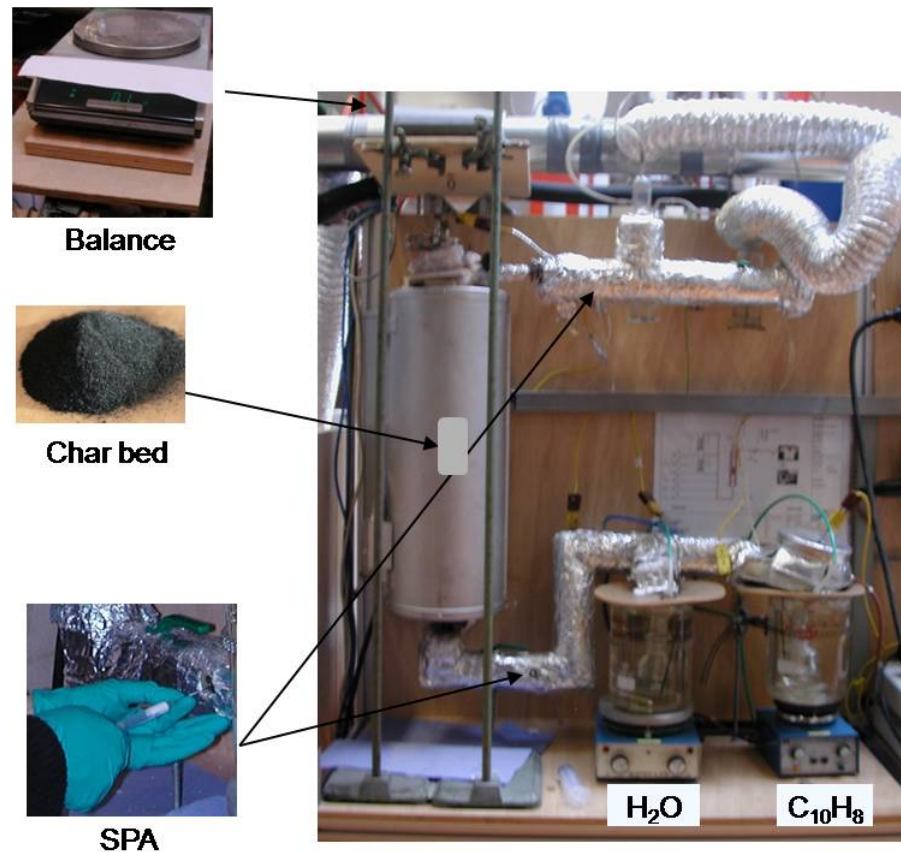


Figure 4-1 Synthetic tar setup

The carbon conversion is measured by weighing the reactor before, during and after the experiment. The biomass carbon conversion is calculated as shown in eq (4-1).

$$X_{c,t} = \frac{W_0 - W_t}{w_c \times W_0} \quad (4-1)$$

Where,

$X_{c,t}$ = Carbon conversion at a certain time

W_o = Weight of char at the reactor temperature at time zero

W_t = Weight of char at reactor temperature and at a certain time

w_c = Carbon content of the treated char

4.2.2 Real tar setup

The real tar setup is shown as a scheme in Figure 4-2 and as a photograph in Figure 4-3. The setup consists of the following main parts:

- Biomass feeder
- Primary reactor (gasifier)
- Secondary reactor (fixed bed tar cracker)
- Gas cleaning system: condensers and filters
- Gas flow regulator: pump and flow meter
- Gas analysis: GC/TCD for dry and tar free gas and GC/MS for SPA tar samples analysis

Biomass is fed to the gasifier through a biomass screw feeder. Two slip streams of the producer gas were taken from the gasifier and the rest was burned before sent to the vent. The first slip stream was used to measure the dry and tar free composition of the producer gas after cooling and filtering. The second slip stream is sent to the secondary reactor via a heated stainless steel line at 300 °C. SPA samples before and after the secondary reactor were taken. The output gas from the secondary reactor is cooled in a condenser and filtered before sent for dry gas and tar free analysis. The gas flow through the secondary reactor is controlled by a pump and calibrated flow meter. In all the experiments, air leaking was checked for the two slip streams.

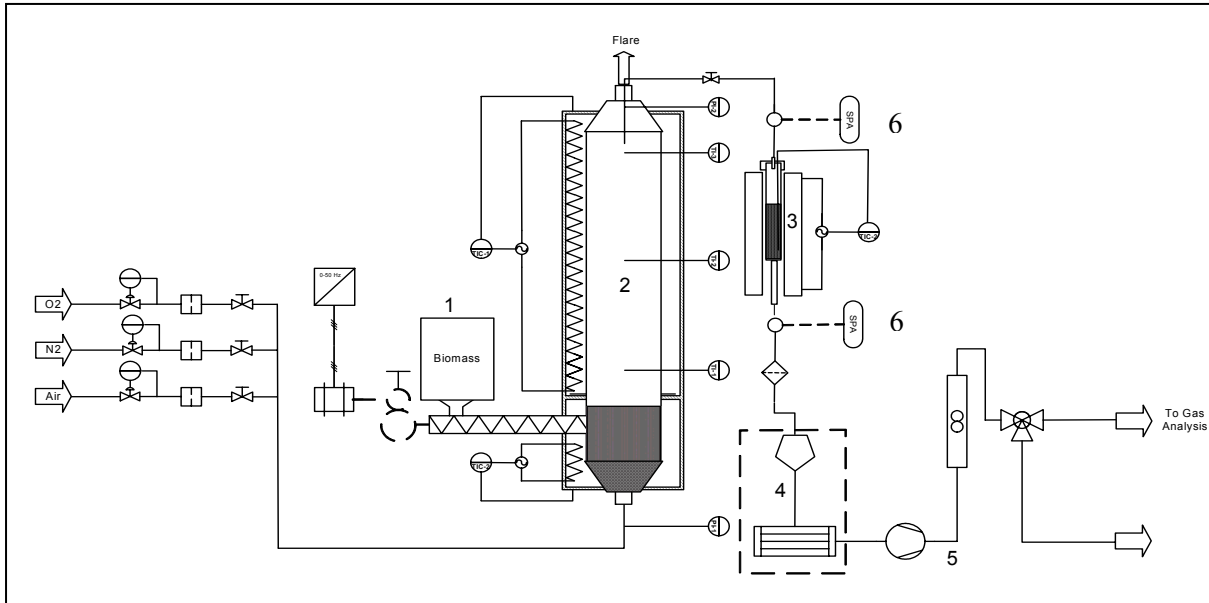


Figure 4-2 Real tar elimination setup, 1. biomass feeder; 2. BFB gasifier; 3. Fixed bed tar cracker; 4. gas cleaning; 5. gas flow regulator; 6. tar SPA sampling points



Figure 4-3 Picture of the biomass gasifier and the fixed char bed reactor during one of the experiments, 1. biomass feeder; 2. BFB gasifier; 3. Fixed bed tar cracker

Primary reactor

The gasification was carried out in a 10 kW_{th} biomass gasifier (primary reactor). This gasifier is a bubbling fluidized bed gasifier with an inner diameter of 12 cm and a height of 120 cm. The gasifier is surrounded by three electrically heated furnaces.

Therefore, the bed and freeboard temperature can be controlled separately between 700 and 950°C, independent of the equivalence ratio (ER). The fuel is continuously fed to the gasifier by a screw feeder at a level of 30 cm above the gasifier bottom. The screw feeder is equipped with a cooling mantle for air or water. Air, which is used as both fluidization and gasification medium, was introduced through a porous distribution nozzle located at the bottom of the gasifier. With this porous nozzle, a uniform distribution over the whole bed area was achieved.

All gasification experiments were carried out at an equivalence ratio (ER) of 0.3. The air flow to the reactor was 2 Nm³/h and the biomass flow rate was 1.56 kg/h. The bed and the freeboard temperatures of the gasifier were controlled by temperature controllers.

The gasifier bed material was silica sand with a mean particle size of about 200 µm. The dynamic bed height was approximately 30 cm. The biomass used for the experiments was birch wood with a particle size of 1.5-3.0 mm (J. Rettenmaier & Sohne, LIGNOCEL, Type: HBR 1500/3000).

Secondary reactor

The fixed char bed reactor (secondary reactor) was made of a stainless steel pipe with an outside diameter of 25 mm and a height of 325 mm as shown in Figure 4-4. The inner diameter of the reactor is 21 mm. At the top, there is T-connection with one inlet for the gasifier and another for the thermocouple. The reactor and the T-connection were attached with flanges, so that they can be simply taken apart in case of refilling the reactor with the catalyst. At the bottom of the reactor, situated a glass wool filter on which the catalyst is placed. The producer gas comes from the top, passes through the catalyst bed and filter and finally exits through an 8 mm stainless steel pipe. The exit of the reactor is connected to a filter-condenser system followed by a pump and flow controller.



Figure 4-4 Secondary reactor (fixed char bed reactor)

4.2.3 Char properties

The biomass char was obtained from a commercial supplier and pre-treated by heating up to 850 °C and soaking for 30 minutes. The chemical and physical properties of the treated biomass char are given in Table 4-1. The main ash metal

components in the treated commercial biomass char are alkali metals (Na and K), alkaline earth metals (Mg and Ca) and transition metals (Fe and Ti). These metals play an important role in promoting the char and tar conversion reactions.

Table 4-1 Chemical and physical properties of treated biomass char

Component biomass char	Wt. (%)	Error (%)
Water	0.2	± 0.00
Ash	9.55	± 0.09
Volatiles	2.01	± 0.06
Fixed carbon	88.24	(Balance)
C	89.03	± 0.13
N	0.24	± 0.01
H	0.12	± 0.01
S	<0.01	
Cl	0.02	± 0.00
Br	< 0.01	
F	0.40	± 0.05
O	10	(balance)
Component ash	Wt. (%)	Error (%)
Na	1.09	±0.01
K	0.48	±0.01
Mg	12.4	±0.1
Ca	29.9	±0.5
Al	2.21	±0.08
Ti	0.81	±0.00
Fe	9.10	±0.01
Si	0.66	±0.02
C	0.17	±0.02
Physical properties	Value	
BET-surface area	353 m ² /g	
Total pore volume	0.19 cm ³ /g	
Adsorption average pore width (4V/A by BET)	29 Å	

The BET-surface area of the biomass char is comparable with that of activated alumina (299 m²/g) and zeolite (350 m²/g) tested by Namioka et al. [6]. On the other hand, it is much higher than the surface area of other active known catalysts such as dolomites (5-20 m²/g) [7] and steam reforming catalysts which have a typical specific surface area of (16-23 m²/g) and a total pore volume of (0.14-0.18 cm³/g) with average pore diameter of (200-500Å) [8]. The large surface area of biomass char is formed during the fast devolatilization of biomass at the initial stage of gasification.

4.3 Experimental results on naphthalene reduction with char

The objective of these experiments is to investigate the influence of the different process parameters on the naphthalene reduction by biomass char. The parameters that have been studied are:

- Char bed temperature
- Gas residence time
- Particle size of the char
- Inlet naphthalene concentration
- Gas composition (H_2O , H_2 , CO , CO_2 , CH_4)
- Char properties and source

4.3.1 Reference experiment

The naphthalene experiments have been carried out to study the catalytic activity of the biomass char for naphthalene reduction and the simultaneous carbon conversion of the char. Table 4-2 shows the experimental conditions of the so-called reference experiment.

Table 4-2 Process conditions of the reference experiment

Parameter	Symbol	Value
Pressure	P (atm)	1
Tar	C_{10}H_8	Naphthalene
Temperature	T_R ($^{\circ}\text{C}$)	900
Gas residence (space) time	τ (s)	1.2
Gas weight time	τ' ($\text{kg}\cdot\text{h}\cdot\text{m}^{-3}$)	0.18
Gas flow rate	v_0 (l/min)	0.39
Bed height	H (cm)	2.5
Char particle size	d_p (μm)	500-630
Standard gas mixture composition (STD)		(vol. %)
CO		6
CO ₂		10
H ₂ O		7
H ₂		4
CH ₄		2.4
N ₂		Balance
Naphthalene		10-20 (g/Nm^3)

The naphthalene reduction during the reference experiment at a bed temperature of 900 °C was high (>99 %) and remains so high during the time on stream for more than eight hours. The carbon conversion after eight hours was about 31%.

4.3.2 Effect of the char bed temperature

In the reference experiment a char bed temperature of 900 °C was chosen and the naphthalene reduction turned out to be >99 %. Figure 4-5 shows the naphthalene reduction for lower temperatures. It is noted that for these experiments a larger particle size and a shorter gas residence time than in the reference experiment were chosen. Despite these changes, the naphthalene reduction at 900 °C stayed high at 100 %. At lower temperatures, the naphthalene reduction decreases slightly to about 90 % at 750 °C. Below this temperature the naphthalene reduction decreases more sharply till about 70 % at 700 °C. Based on these data, a first order kinetic model for naphthalene conversion is applied to calculate the kinetic constants. The apparent activation energy (E_{app}) and the pre-exponential factor (k_{app}) can be calculated as 61 kJ/mol and $1 \cdot 10^4 \text{ s}^{-1}$, respectively.

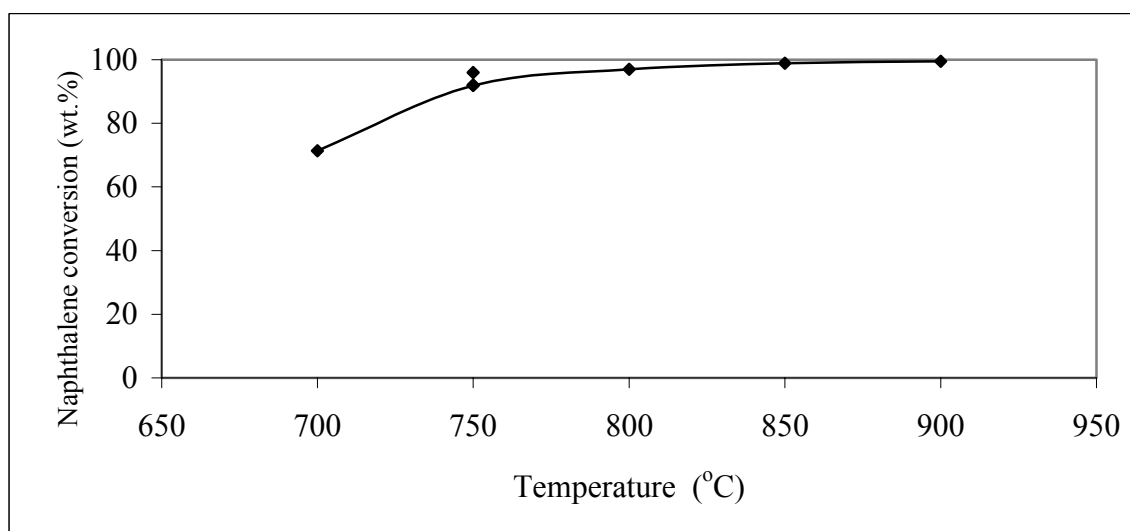


Figure 4-5 Naphthalene conversion as function of char bed temperature, v_0 : 1.57 l/min; τ : 0.3 s; d_p : 500-800 μm ; Gas mixture: Table 4-2; time on stream: 15 min

The corresponding carbon conversions for the different temperatures are presented in Figure 4-6. Here, it can be seen that the carbon conversion strongly increases at temperatures above 800 °C.

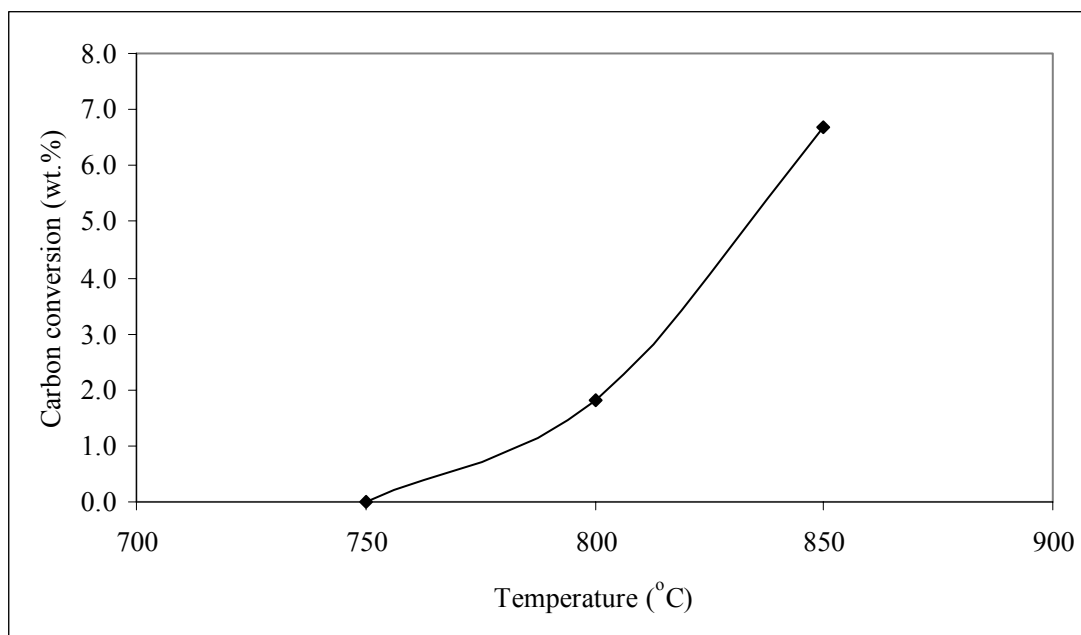


Figure 4-6 Influence of the bed temperature on carbon conversion, v_o : 0.39 l/min; τ : 1.2 s; d_p : 500-630 μm ; Gas mixture: Table 4-2; time on stream: 60 min

Figure 4-7 shows the naphthalene conversion at 750 °C and 900 °C as function of the time on stream under reference conditions as given in Table 4-2. Here it can be seen that, as was already discussed in section 4.3.1, the naphthalene reduction at 900 °C remains constant at >99 %, while the naphthalene reduction at 750 °C decreases with time from about 95% to 80% over eight hours. For the other temperature no longer time on stream data was available.

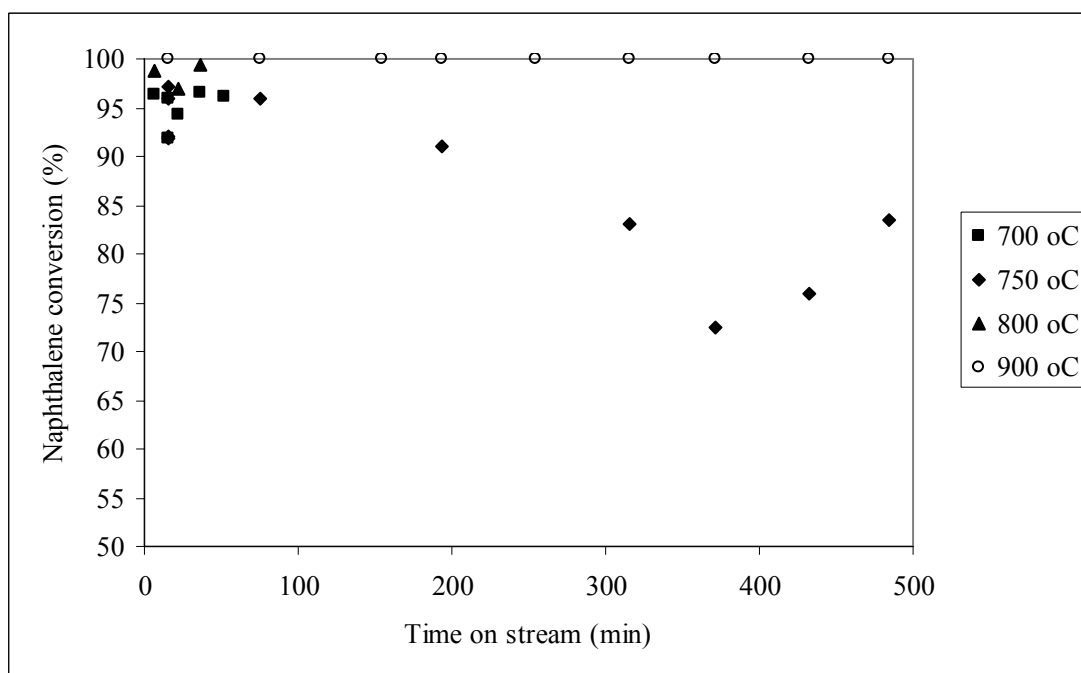


Figure 4-7 Time on stream influence of temperature on naphthalene conversion, v_o : 0.39 l/min; τ : 1.2 s; d_p : 500-630 μm ; Gas mixture: Table 4-2

Figure 4-8 shows the carbon conversion for the same set of experiments. For 900 °C, only two data points are given: the initial value and the carbon conversion after eight hours: 31%. For a bed temperature of 750 °C, two experiments have been carried out; the carbon conversion is negligible over a period of eight hours. This can be explained by two different mechanisms: 1) at 750 °C the carbon gasification rate is very low, or 2) at 750 °C there is a balance between the carbon gasification rate and the coke formation rate caused by the naphthalene reduction reaction. In section 4.3.5 more information about the influence of the naphthalene on the carbon conversion will be presented.

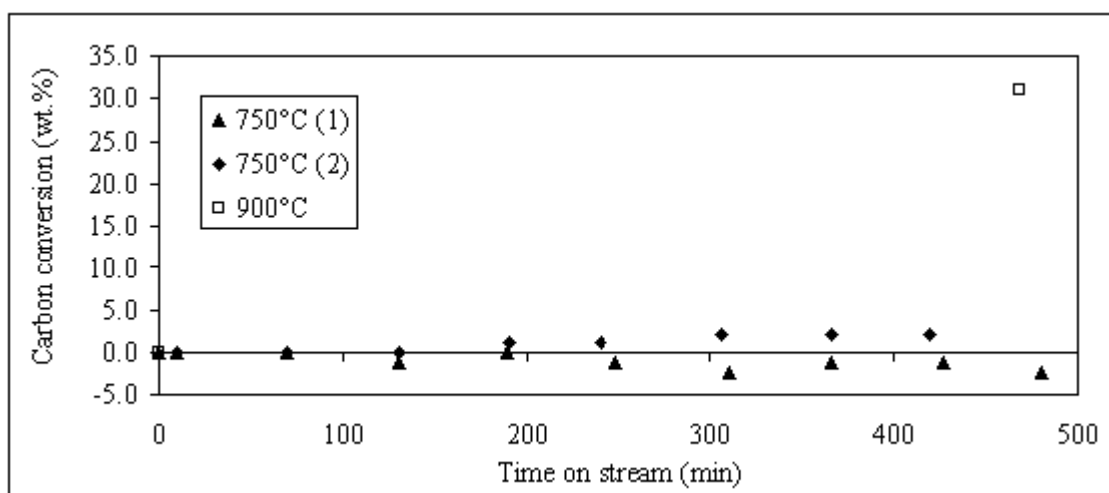


Figure 4-8 Time on stream influence on carbon conversion at 750 °C and 900 °C, v_0 : 0.39 l/min; τ : 1.2 s; d_p : 500-630 μm ; Gas mixture: Table 4-2

4.3.3 Effect of the gas residence time

The gas residence time in the fixed bed was varied by changing the gas flow rate, keeping the amount of catalyst constant. As the gas residence time decreases (standard was 1.2 s), reactions in the char bed have a lower opportunity to proceed toward equilibrium. Figure 4-9 shows the naphthalene conversion at 900 °C for two different gas residence times: 0.4 s and 1.2 s. It can be seen that the naphthalene conversion remains high (> 99 %) for a residence time of 1.2 s. For the shortest gas residence time of 0.4 s, the naphthalene conversion initially slightly increased to almost 100% after two hours on stream, and then decreases with time on stream to 97 % after four hours. Also here, a competition between carbon conversion (increase of internal surface area) and coke deposition (pore plugging) may be suspected.

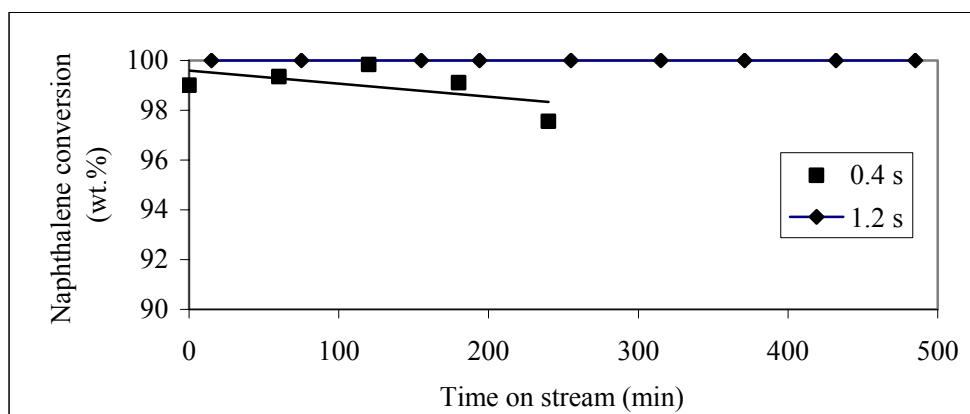


Figure 4-9 Time on stream naphthalene conversion at 1.2 and 0.4 s gas residence times, T_R : 900 °C; v_o : 1.17 l/min; d_p : 500-630 μ m; Gas mixture: Table 4-2

Figure 4-10 shows the naphthalene conversion for different gas residence times at a char bed temperature of 850 °C. There is a general trend that the naphthalene conversion has a minimum after one hour time on stream. This may also be related to the coke formation that deactivates the catalytic activity of the char. On the other hand, the gasification reactions probably remove the coke and generate new reactive surface area and thus the naphthalene conversion increases. For the three tested gas residence times, the naphthalene conversion is the highest at 2.4 s gas residence time. For longer gas residence times the coke formation (pore plugging) may dominate more and for shorter residence time the reaction rate limits the naphthalene conversion.

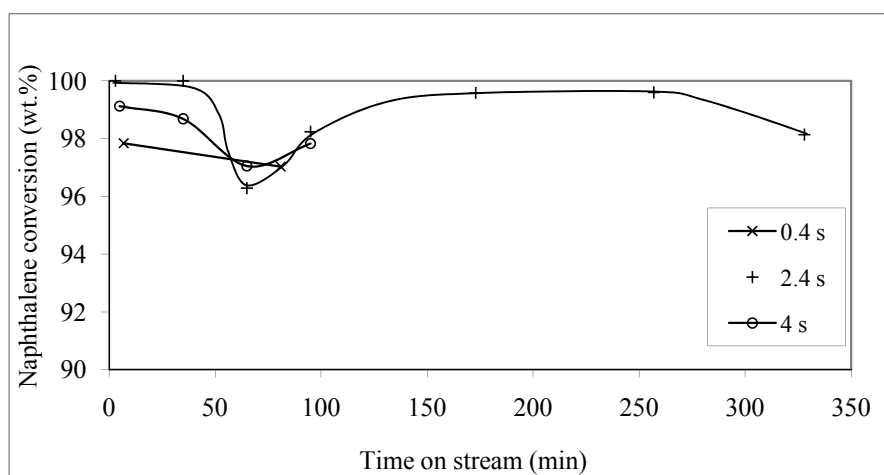


Figure 4-10 Time on stream naphthalene conversion at different residence times, T_R : 850 °C; d_p : 500-630 μ m; Gas mixture: Table 4-2

Figure 4-11 shows the influence of the gas residence time on the naphthalene conversion at 750 °C. Comparable with the experimental results at 850 °C, the naphthalene conversion increases with the gas residence time. No data is available for gas residence times longer than 1.2 s, but it may be expected that the conversion will decrease again for higher gas residence time values.

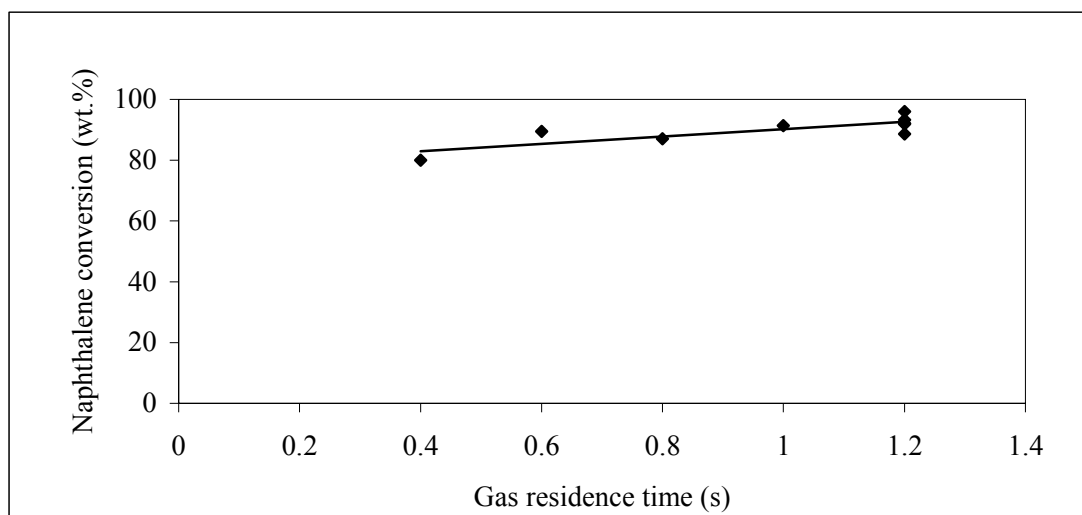


Figure 4-11 Effect of gas velocity on naphthalene reduction, T_R : 750 °C; d_p : 1000-1180 μm ; Gas mixture: Table 4-2; time on stream: 15 min

Figure 4-12 shows the carbon conversion as function of the gas residence time after 60 minutes on stream. It was found that when the residence time increases the carbon conversion decreases. This is mainly caused by the fact that the residence time was increased by decreasing the gas flow to the char bed, and thus for higher residence times less reactive components (H_2O and CO_2) are available for gasification and so less carbon can be gasified.

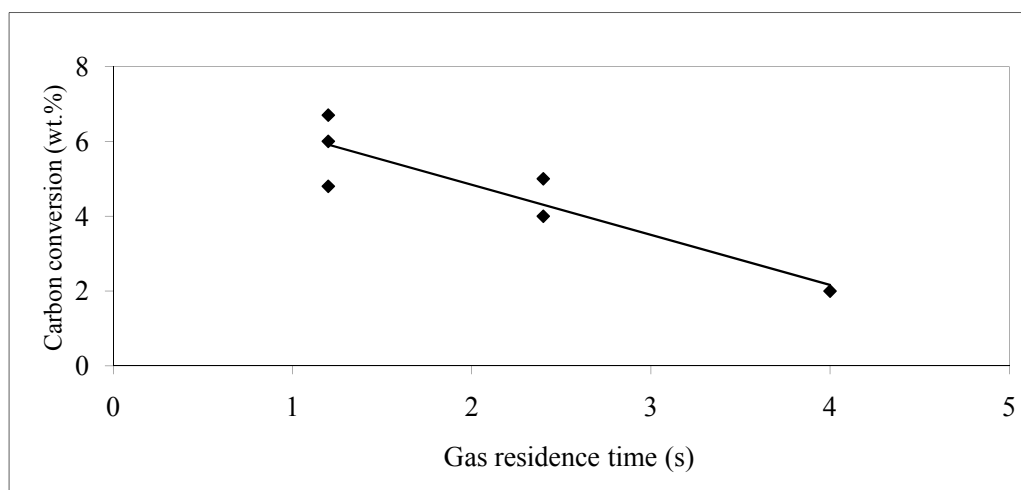


Figure 4-12 Effect of gas residence time on carbon conversion, T_R : 850 °C; d_p : 500-630 μm ; Gas mixture: Table 4-2; time on stream: 60 min

Figure 4-13 shows the carbon conversion as a function of the time on stream for a longer residence time of 2.4 s. The carbon conversion increased linearly with the time on stream. As was seen in Figure 4-10, after one hour a sharp decrease in the naphthalene conversion occurred. Here almost no deviation of the linear relationship between the carbon conversion and the time on stream was seen around one hour of

time on stream. It seems that the carbon gasification prevails the carbon deposition caused by the naphthalene conversion.

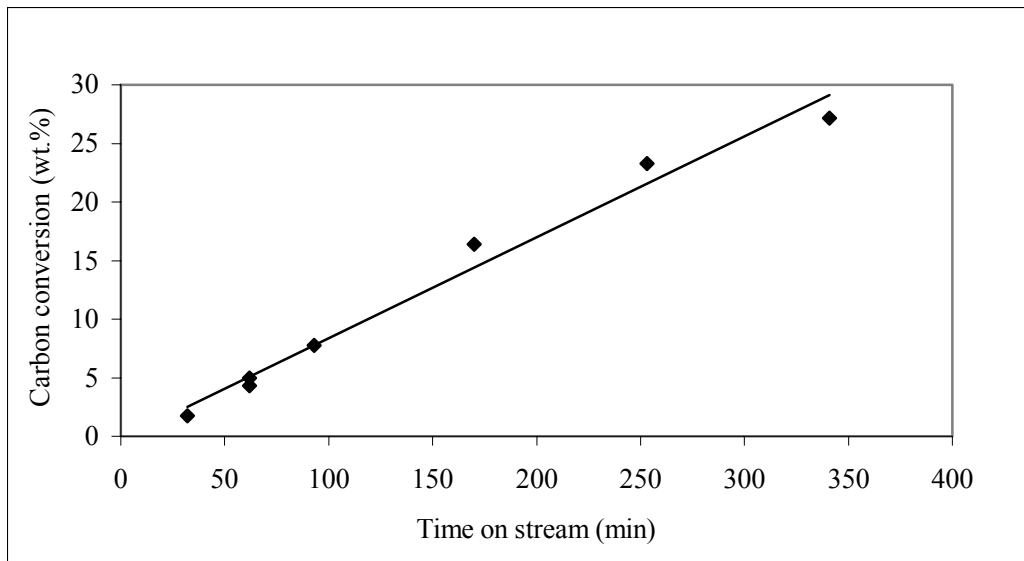


Figure 4-13 Time on stream carbon conversion at different gas residence times, T_R : 850 °C; v_0 : 0.195 l/min; τ : 2.4 s; d_p : 500-630 μm ; Gas mixture: Table 4-2

4.3.4 Effect of the particle size

The particle size affects the rate of mass transfer of naphthalene and reactive gases to the active surface of the char particle. A strong influence of the particle size would mean that the reaction rate is mass transfer or pore diffusion controlled and no influence would mean a kinetically controlled reaction. Figure 4-14 shows only a weak relationship between the naphthalene conversion and the particle size of the char at 750 °C. Therefore, it can be concluded that at 750 °C the naphthalene-char reaction is mainly controlled by kinetics and the internal and external mass transfer because of the particle size are of minor effect.

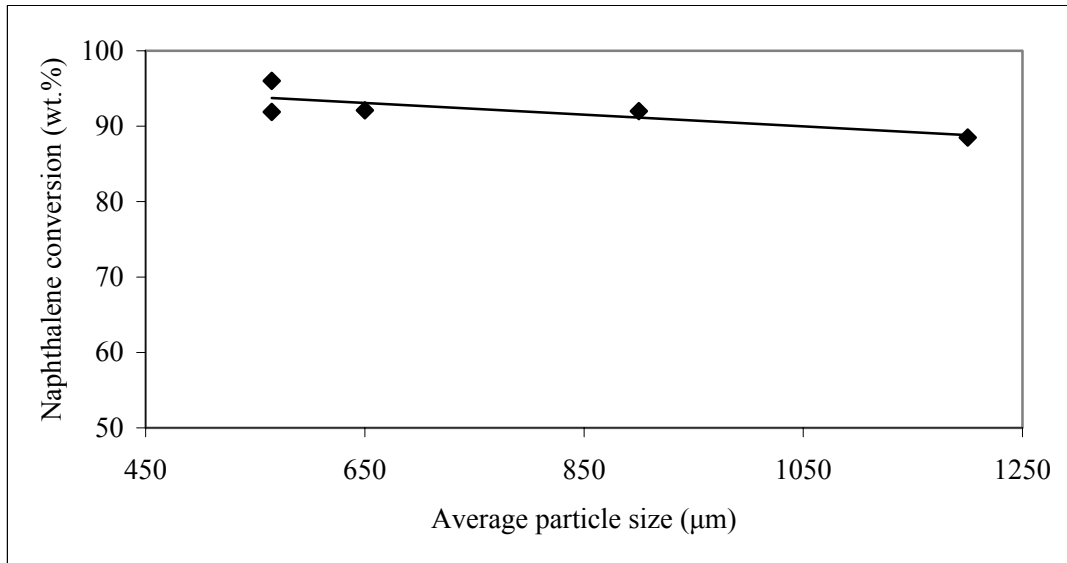


Figure 4-14 Effect of particle size on naphthalene reduction, T_R : 750 °C; v_o : 0.39 l/min; τ : 1.2 s; Gas mixture: Table 4-2; time on stream: 15 min

For the carbon conversion two particle sizes were tested; 500-630 μm and 1400-1700 μm . The rest of the parameters were set on the reference conditions (Table 4-2). The particle size was found to have only a slight effect on the carbon conversion as shown in Figure 4-15. This indicates that the char gasification at 850 °C is mainly kinetically controlled.

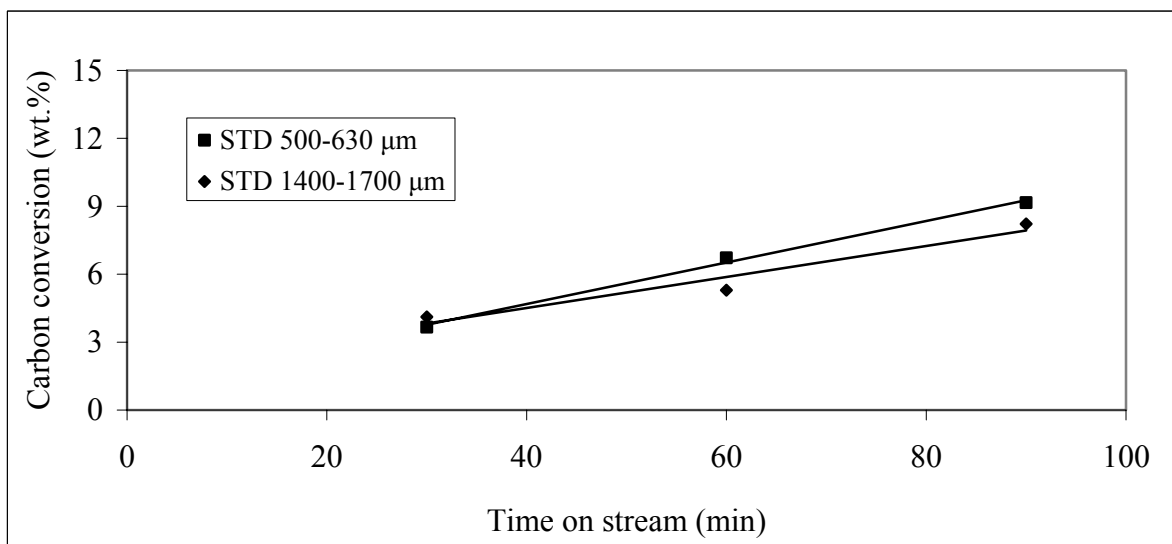


Figure 4-15 Time on stream influence of particle size on carbon conversion, T_R : 850 °C; v_o : 0.39 l/min; τ : 1.2 s; Gas mixture: Table 4-2

4.3.5 Effect of the inlet naphthalene concentration

The effect of the inlet naphthalene concentration on its conversion over char was investigated. It was found that the naphthalene conversion was almost constant (89%-91%) for inlet naphthalene concentrations in the range from 6 to 18 g/Nm^3 at a gas

residence time of 0.15 s, a temperature of 900 °C, and a particle size of 1400-1700 µm. This means that the naphthalene-char reaction is first order in the initial naphthalene concentration for these process conditions. For longer gas residence times and lower temperatures, the deposition of coke [9] may influence the activity of the char, and the higher the initial naphthalene concentration, the more coke may be formed and this may influence the naphthalene reduction.

The influence of the presence of naphthalene in the carrier gas on the carbon conversion was separately tested in two one-hour-experiments. The process conditions for these experiments were: 850 °C bed temperature, 0.3 s gas residence time, 500-630 µm particle size, 60 minute time on stream and a gas mixture according to Table 4-2. It was found that the carbon conversion was more than doubled in the experiment without naphthalene (65%) than the one with naphthalene (30%). There may be two possible explanations: i) the naphthalene is partially converted to coke and thus the net carbon conversion is less or ii) the coke formed on the char surface reduces the rate of the char gasification reaction. To validate these explanations an extreme situation is assumed: all naphthalene is converted into coke and the rate of the char gasification reaction is not affected. Therefore, the maximum difference between the remaining carbon in the two cases can be the amount of carbon in the supplied naphthalene. The measured difference was (1.3 g) whereas the amount of naphthalene carbon fed was (0.9 g) and this means that still (0.4 g) was not gasified. In real circumstances, not all naphthalene will be converted to coke, and thus, it can be concluded that when naphthalene is present in the gas, the rate of carbon gasification becomes lower. So, coke formation decreases the carbon gasification rate. For better char performance, it is important to improve the process conditions such that naphthalene or tar decomposition decreases and the rate of reforming of naphthalene increases. From above, it may be concluded that there is a competition between the coke formation and gasification. When the rate of coke formation is higher than the rate of gasification, the resulted weight of char increases and the char activity decreases.

4.3.6 Effect of the gas composition

Char and naphthalene are consumed by the steam and dry reforming reactions as explained in [10-13]. The effect of the H₂O- and CO₂-concentration in the producer gas was studied. For each component two concentrations were tested, 10 vol. % and 20 vol. %, as they are considered common concentrations in a producer gas. The exact mechanisms of the steam and dry reforming of naphthalene decomposition reactions are not well known. Nevertheless, naphthalene can have longer residence time when adsorbed on the surface of the char. The metal content of the char catalyzes the different reactions. The naphthalene can be gasified by the steam and the dry reforming reactions as can be seen from the results of Table 4-3. The experimental results show that naphthalene is not only converted by the steam (H₂O) reforming reaction but can also be converted by the dry reforming reaction (CO₂). It was found that the gas composition affects the naphthalene conversion and that the CO₂-N₂ mixture gave the highest naphthalene conversion whereas the steam-N₂, the steam-CO₂-N₂ and the standard gas mixtures gave a comparable but lower naphthalene conversion.

Table 4-3 Effect of the ambient gas components on naphthalene conversion, T_R : 750 °C;
 v_0 : 0.39 l/min; τ : 1.2 s; d_p : 500-630 μm ; gas balance is N_2

Gas composition (vol. %)					Naphthalene conversion
H_2O	CO_2	H_2	CO	CH_4	(wt.%)
10	-	-	-	-	93
-	10	-	-	-	97
10	10	-	-	-	93
7	10	4	6	2.4	93*

* average value for 4 experiments

The (10 vol. % CO_2 , N_2) gas mixture shows a higher naphthalene conversion than the other gas mixtures. This could mean that CO_2 creates more active sites on the char surface for naphthalene adsorption and reaction than the steam and the other gas components. The naphthalene-char reaction is a very complex reaction as the reactive components (CO_2 , H_2O) are adsorbed at the (internal) char surface, they react with naphthalene and at the same time they react with the carbon on the char surface. This makes the char surface not constant because of the destroyed and created active surface sites.

The presence of the other components in the producer gas (H_2 , CO , CH_4) showed in Table 4-3 a lower naphthalene conversion. Because CO and to a less extent H_2 do not participate in the conversion reactions with the adsorbed naphthalene, their presence in the gas may cause occupation of the char surface and thus causes an inhibitory effect for the naphthalene conversion. This behavior is also confirmed by the work of Devi et. al [14]. They studied the kinetics of naphthalene conversion as function of the different reactive gases (H_2O , CO_2 , CO , H_2) over olivine. They found that the steam reforming of the naphthalene gave slightly higher conversion than the dry reforming of the naphthalene at 900 °C over olivine. They found also an inhibiting effect of H_2 reducing the naphthalene conversion while CO has only a small inhibitory influence. Because of the water gas shift reaction, the inhibiting H_2 can be produced out of the other components: $\text{H}_2\text{O} + \text{CO} \leftrightarrow \text{H}_2 + \text{CO}_2$. More CO_2 produces less H_2 and allows a higher naphthalene conversion and more H_2O produces more H_2 resulting in a lower naphthalene conversion. The experiment where no H_2 could be formed (gas with 10 vol. % CO_2 , N_2) has the highest naphthalene conversion. Moreover, the naphthalene reforming reactions can be catalyzed by dual site mechanism [15] where the naphthalene and the reactive gas component are adsorbed on the neighboring sites and react with each other.

The effect of the gas composition on the carbon conversion for a period of time on stream of 90 minute is given in Figure 4-16. It can be seen that the carbon conversion with only 10 or 20% H_2O (and N_2) in the gas is almost twice as high as for the other gas compositions. The levels of the concentration of H_2O and CO_2 itself have almost no influence on the carbon conversion degree. So, it may be concluded that the gasification reaction of carbon is almost zero order in the different gas components under the measured conditions. The above results can be explained by the fact the kinetics of the steam reforming rate of carbon is faster than the CO_2 gasification of

carbon. Ye et. al. [16] related that to the larger number of active sites generated by the steam rather than by the CO₂.

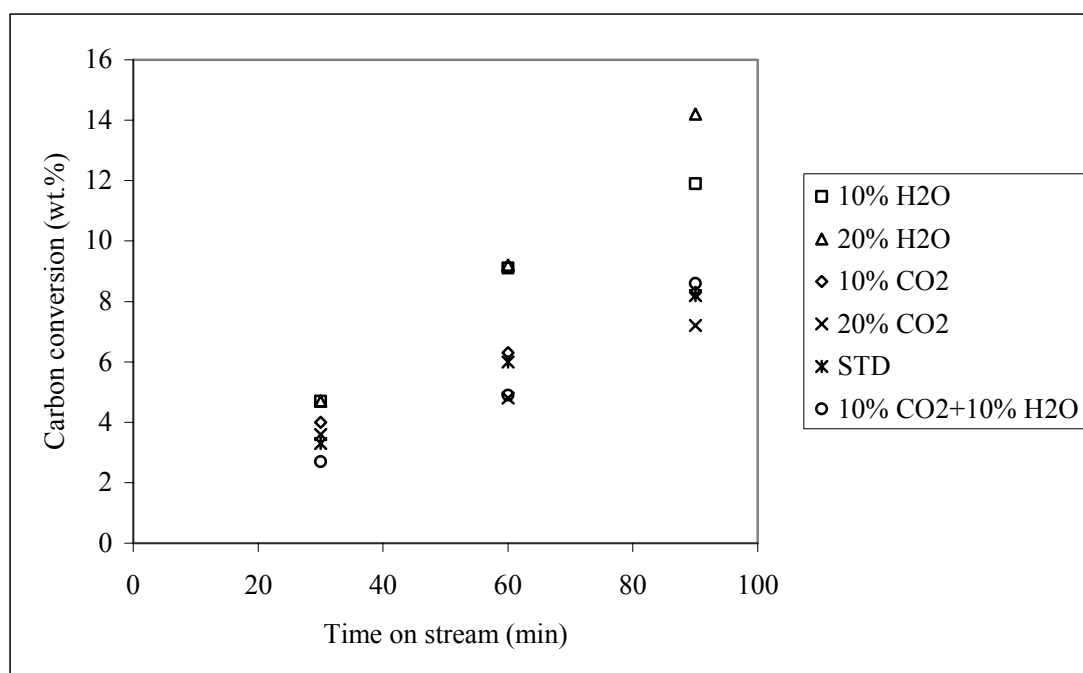


Figure 4-16 Time on stream influence of H₂O concentration on char conversion, T_R: 850 °C; τ: 1.2 s; d_p: 500-630 μm;

4.3.7 Effect of the char properties and source

The two factors that give char such a high activity are expected to be: the internal surface area and the metal content. The results in Table 4-4 show the effect of the pyrolysis conditions on the produced pinewood char surface area and the naphthalene conversion. The char surface area was determined by N₂ adsorption and desorption isotherms providing the BET surface area. The effect of the internal surface area was investigated by producing the biomass char at different pyrolysis conditions. These conditions are represented by the heating rate and the final pyrolysis temperature. The pyrolysis conditions affected the BET surface area of the produced biomass char. The fixed bed tar reduction conditions used resulted in high naphthalene conversions 97.8-99.8 %. At these high conversion degrees no clear influence for the BET surface area can be noticed. It can be expected that at lower temperatures a more visible relationship can be found.

Table 4-4 Effect of Pinewood char production conditions on char BET surface area and naphthalene conversion, T_R : 900 °C; τ : 0.25 s; particle size: 100-500 μm , Gas mixture: Table 4-2.

Heating rate (°C /min)	Final char production temperature (°C)	(BET) (m^2 / g)	Naphthalene Conversion (%)
10	700	200	97.8
10	900	330	98.2
10	950	38.2	97.8
25	700	159	99.9
25	900	56.0	98.2
25	950	89.3	99.6
≥ 50 °C /s	900	n.a	98.9

In general, it can be said that larger pores (meso pores or macro pores) provide a better access of the tar components to the internal surface area of the particle which may cause a higher conversion. The highest produced surface area of the biomass char was 330 m^2/g (see Table 4-4) which is comparable with surface area of activated alumina (299 m^2/g) and zeolite (350 m^2/g) [6]. However, these catalysts have different mechanisms for tar reduction where the tar is cracked on the acid sites of the FCC or on the acid and base sites of the alumina. What makes the surface area of the char important is its capacity for tar adsorption. This is indicated by the known adsorption capacity of the activated carbon and also the work of Hanaoka et. al. [17] who used carbonaceous materials, such as, activated carbon and char coal for the purification of a producer gas in the gas cleaning temperature range of 200 to 400 °C. They found that the ability for tar removal was largely dependent on the type of the carbonaceous material used and the gas cleaning temperature. Further, they found that active carbon with a large specific surface area and a large average pore diameter was the most effective for tar removal at 300 °C. Therefore, the specific surface area and the average pore diameter of active carbon affected the capacity for tar removal. The measured BET surface area of the different biomass chars includes micro pores which might not be accessible for the tar component. Thus, the BET surface area is not the only property that should be investigated but also the pore structure which includes, besides the specific internal surface area, the specific internal pore volume and distribution of the internal volume.

At temperatures used for catalytic tar conversion, the metal content of the char catalyzes the gasification reactions. To investigate these effects, experiments with char from different sources have been carried out. The sources used for the production of the char were pinewood biomass, rietspruyt coal and brown coal. The char particle size was ranging from 100 to 500 μm . The ultimate analysis of the char produced from the three sources is given in Table 4-5.

Table 4-5 Ultimate analysis and mineral content of pinewood char and commercial coal chars (wt.%)

	Pinewood char	Rietspruyt coal char	Brown coal char
C	87.9	82.3	89.6
N	0.3	2.0	0.8
H	0.6	0.4	1.1
Ash	4.7	15.3	7.8
O (by difference)	6.5	0	0.7
MgO	0.203	0.285	0.086
Al ₂ O ₃	-	4.700	0.318
K ₂ O	0.846	0.059	0.006
CaO	1.81	0.793	2.353
Fe ₂ O ₃	0.114	0.275	0.852

It was found that the chars from coal (rietspruyt and brown coal) gave higher naphthalene conversion than the char from biomass (Table 4-6). This is mainly caused by the high content of ash (metals) in the coal chars [18]. For other catalysts such as dolomites and olivine, iron was found to be an important catalyst for tar gasification reactions [19, 20]. The dolomite activity increases with the iron content and the olivine becomes more effective when its iron content is treated. Among the here tested types of chars, the brown coal has the highest iron content and it gave the highest naphthalene conversion (Table 4-6). Therefore, not only alkali content in the char is important but also the iron content. In the biomass char, alkali metals are considered effective for catalyzing the steam and dry reforming reactions of carbon [21]. Lizzio et al. [22] reported that potassium is a good catalyst for the steam gasification of coal.

Table 4-6 Effect of char source type on char BET surface area and naphthalene conversion, T_R : 900 °C; v_o : 1.88 l/min; τ : 0.25 s; particle size: 100-500 μ m, Gas mixture: Table 4-2.

Char Source	BET¹ (m² / g)	Naphthalene Conversion (%)
Pinewood	330	97.8
Rietspruyt coal	25.3	99.4
Brown coal	210	99.8

¹Char production temperature: 900 °C ; heating rate: 10 °C/min

4.4 Experimental results on real tar reduction with char

Experiments with real tar in fuel gas from a gasifier have been carried out in the setup described in section 4.2.2. A slip stream of the gasifier was supplied to an external fixed bed of char. The temperature of the char bed can be varied.

Figure 4-17 shows the influence of the char bed temperature on the real tar reduction. It can be seen that the tar conversion is almost complete at a char bed temperature of 800 °C or higher. A temperature of 750 °C can be considered as too low for real tar conversion with char (58%).

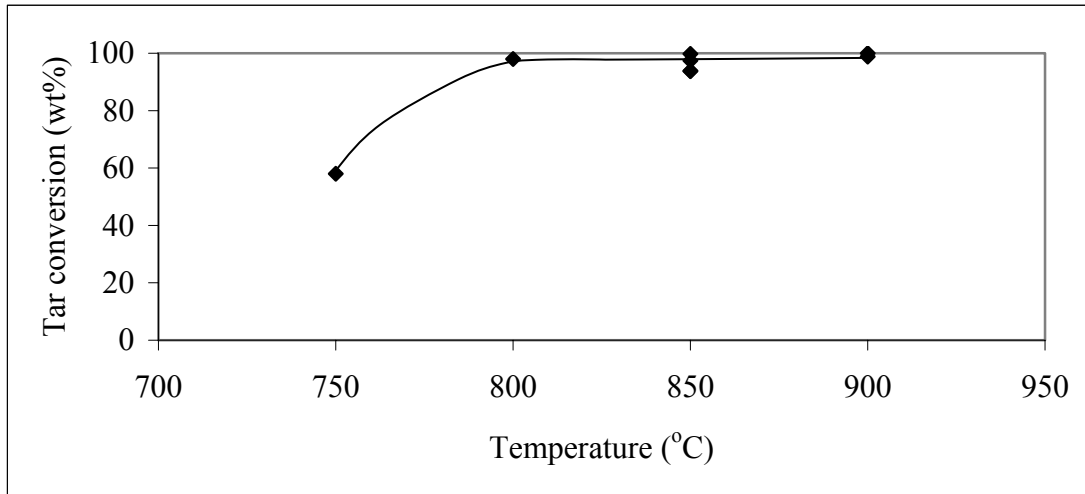


Figure 4-17 Tar reduction temperature influence on tar conversion, v_0 : 1.57 l/min; τ : 0.3 s; d_p : 500-630 μm ; Gas mixture: 13% CO, 10.8% CO₂, 5.6% H₂, 3.9% CH₄, N₂ (balance); time on stream: 15 min

A carbon mass balance was done for the above experiments. It is based on the dry and tar free gas analysis and the amount of carbon converted. The increase in the amount of carbon in the total gas exits from the fixed bed tar cracker should equal the amount of carbon consumed after the experiment. The carbon mass balance results (closing error $\pm 20\%$), shown in Figure 4-18, are acceptable for this kind of measurements.

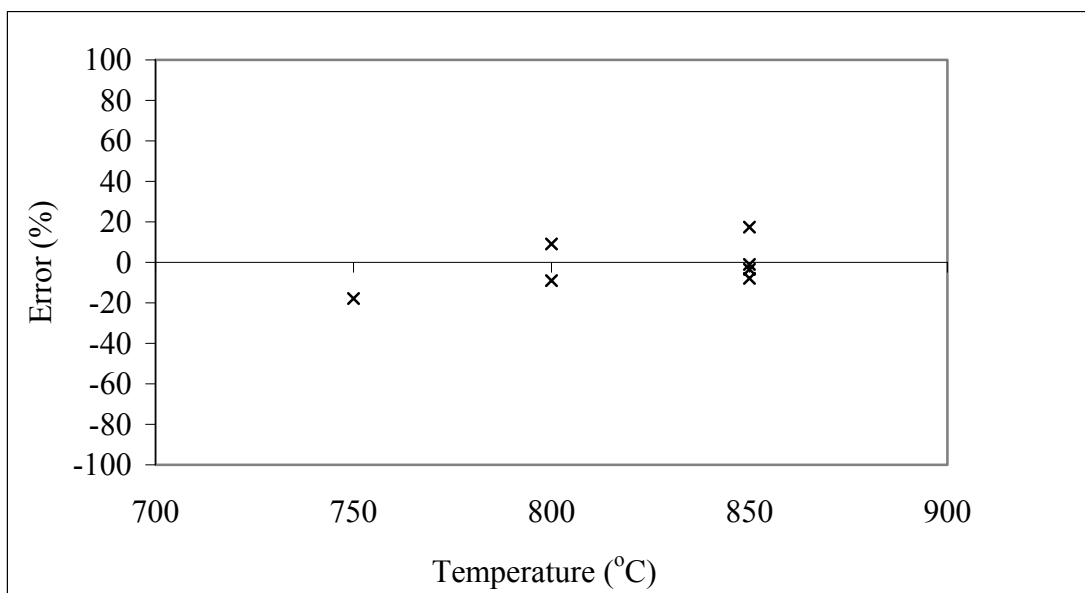


Figure 4-18 Closing error in the carbon mass balance at for experiments carried out at different tar reduction temperatures, v_0 : 1.57 l/min; τ : 0.3 s; d_p : 500-630 μm ; Gas mixture: 13% CO, 10.8% CO₂, 5.6% H₂, 3.9% CH₄, N₂ (balance); time on stream: 60 min

The average tar content in the raw producer gas from the biomass bubbling fluidized bed gasifier was about 9000 mg/Nm³. The tar composition of the producer gas contained mainly naphthalene (40 wt.% on average) and acenaphthylene (20 wt.% on average) as shown in Figure 4-19.

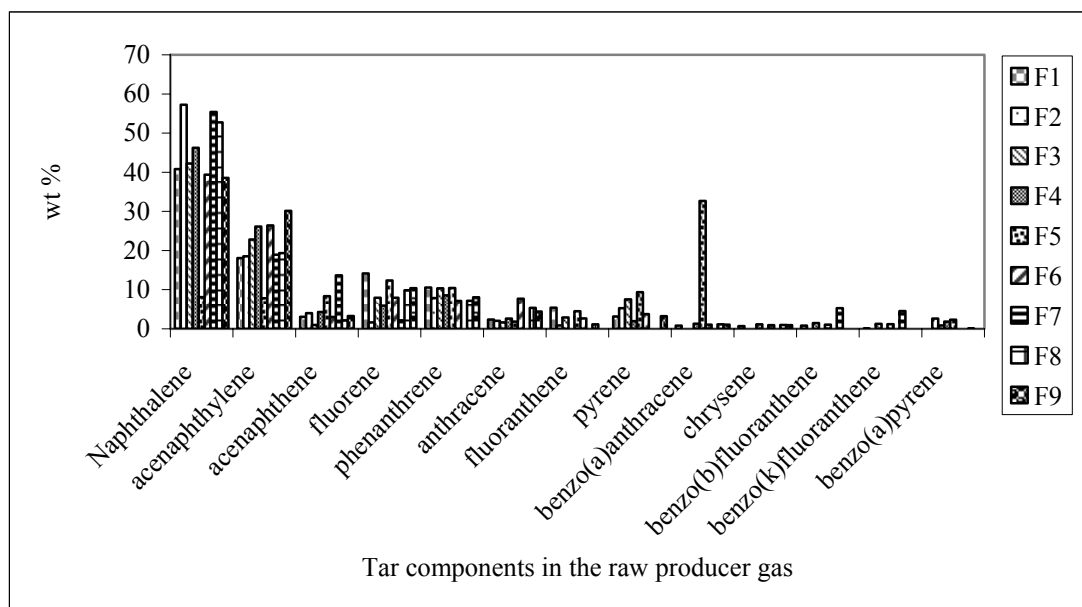


Figure 4-19 Tar composition of raw producer gas samples from the biomass gasifier (100 % \approx 9000 mg/Nm³); F1-F9 are 9 different samples of the same experiment

The tar composition of the outlet gas from the secondary reactor contains a lower number of tar components. The major tar components in the gas that came out of the secondary reactor at 850 °C are shown in Figure 4-20. In this figure the 100% value corresponds to an average tar content of 115 mg/Nm³. Only acenaphthylene, benzo(b)fluoranthene and benzo(k)fluoranthene could be found in the outlet gas of the tar cracker. At 800 °C only benzo(a)pyrene (100 mg/Nm³) was found and at 750 °C only naphthalene was found. The latter experiment had a high inlet tar concentration (17000 mg/Nm³) out of which only (7000 mg/Nm³) naphthalene were left in the outlet gas.

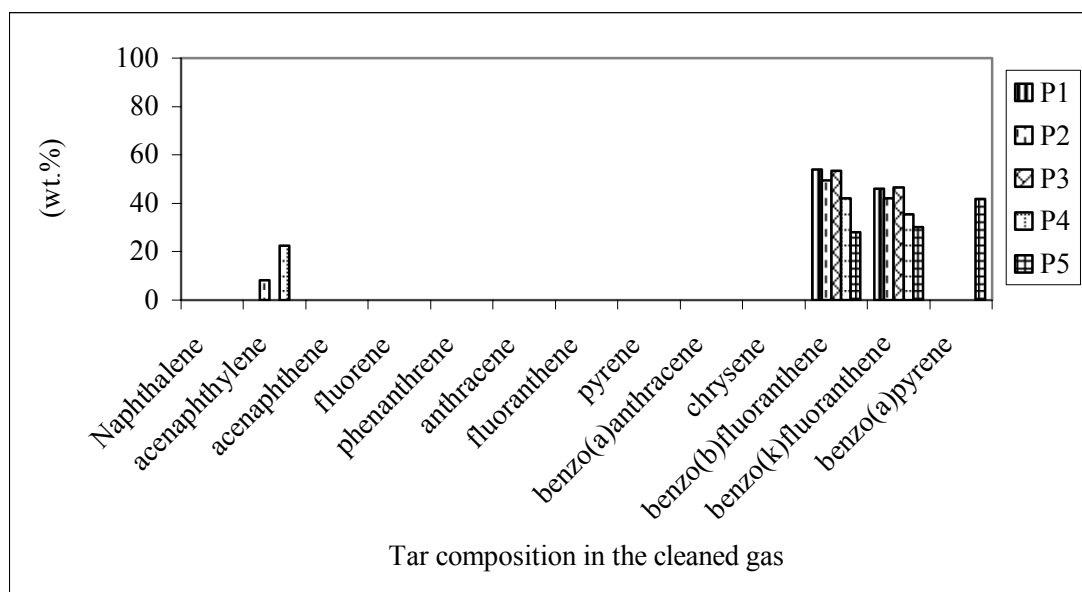


Figure 4-20 Tar composition of 5 cleaned gas samples from the secondary reactor at 850 °C, (100% \approx 115 mg/Nm³), T_R : 850 °C; v_o : 1.57 l/min; τ : 0.3 s; d_p : 500-630 μ m; Gas mixture: 13% CO, 10.8% CO₂, 5.6% H₂, 3.9% CH₄, N₂ (balance); time on stream: 15 min

The results given in the Figure 4-19 and Figure 4-20 showed that most of the components in the feed tar disappeared and only some of the heaviest tars were left. It is not seen that the concentration of any component increased but all of them decreased. In the naphthalene experiments, described in section 4.3, no other tar components in the outlet gas were detected than naphthalene. Moreover, this does not rule out the conversion of these tars to light aromatic tars such benzene, toluene and xylene. These components were found in the real tar analysis results but were not quantified since they are not considered as tars. It might be expected that light polyatomic hydrocarbons are polymerized to form larger poly-aromatic hydrocarbons and converted to coke deposited on the char surface.

As shown in Figure 4-21, the carbon conversion increases with bed temperature. At 850 °C the carbon conversion is about 25 wt.% after 1-hour time on stream. This is because the kinetics of the steam and dry reforming reactions of the char increase with temperature. The carbon conversion may affect the density of both the char particle and the bed. Figure 4-21 shows that the char bed density decreases by about 18 wt.% in the same temperature range. This means that the reaction does not proceed uniformly in the char particle, in this case, the particle volume remains constant and thus, the density should have been decreased with 25%. On the other hand, it is not a shrinking particle reaction, in this case, the particle volume should decrease and thus, the density should remain constant. So, the reaction between tar and char is somewhere in between the two cases.

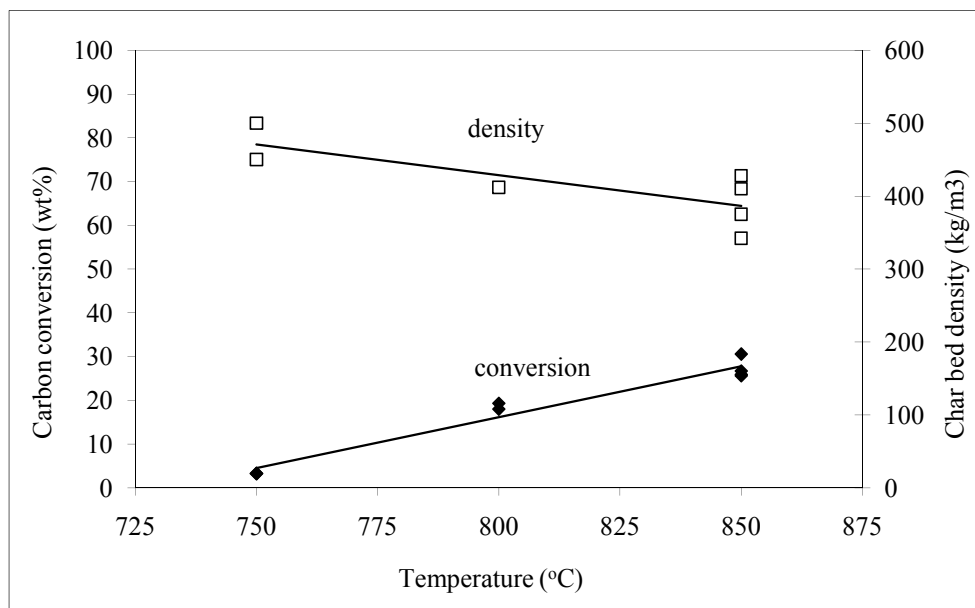


Figure 4-21 Bed temperature influence on carbon conversion and char density, v_0 : 1.57 l/min; τ : 0.3 s; dp: 500-630 μm ; Gas mixture: 13% CO, 10.8% CO₂, 5.6% H₂, 3.9% CH₄, N₂ (balance); time on stream: 60 min

One of the major problems related to the operation of heterogeneous catalysts is the loss of activity (deactivation) with time on stream [23]. The biomass char is a material that can be produced within the gasification process and there is no need for a long lifetime when a continuous internal production of char is achieved. The char is tested for 5 hours and the results showed 100 % tar removal during five hours of experimental time (Figure 4-22). The carbon conversion increased with the time on stream during four hours to 90 wt.%. From the char bed density data it can be seen that the density decreases with char conversion.

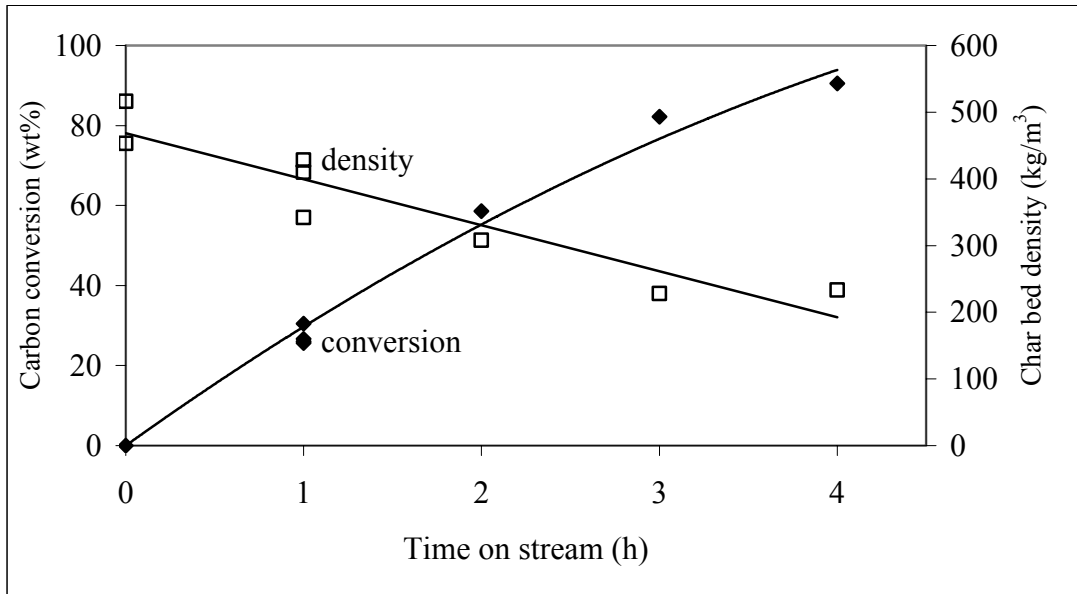


Figure 4-22 Time on stream influence on the carbon conversion, T_R : 850 °C; v_0 : 1.57 l/min; τ : 0.3 s; d_p : 500-630 μm ; Gas mixture: 13% CO, 10.8% CO₂, 5.6% H₂, 3.9% CH₄, N₂ (balance)

4.5 Discussion

It is common in the research on tar removal to use model tar components as was described in section 4.3. Naphthalene is the most applied representative model component. A comparison between the effect of char on the conversion of naphthalene and real tar is discussed below. Figure 4-23 gives a comparison of the tar and naphthalene reduction results as function of the char bed temperature. The naphthalene conversion is comparable with the real tar reduction at temperatures above 800 °C, but clearly higher at lower temperatures (700-750 °C). It can be expected that at lower temperatures the carbon deposition during tar conversion is larger than the carbon deposition during naphthalene conversion, and this will influence the availability of the char for the reduction of naphthalene/tar. In general, higher temperatures result in higher tar conversion, but also in a higher char conversion. A temperature of 800-850 °C seems to be optimal for high tar conversion degrees and a limited carbon conversion degree.

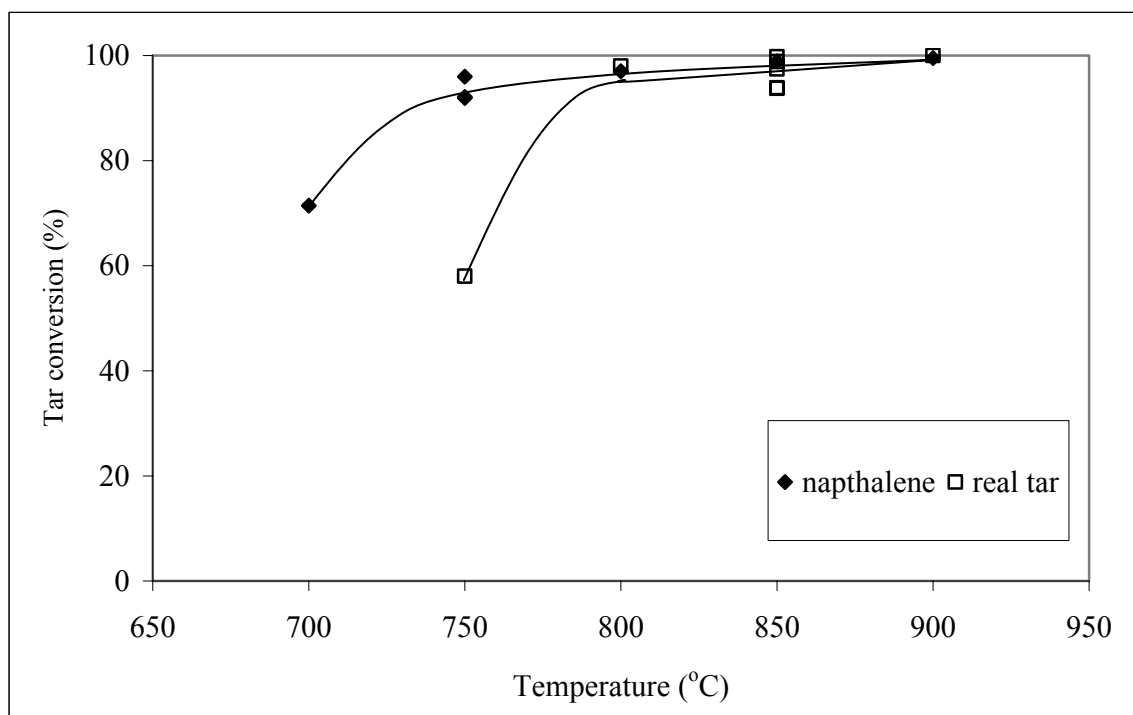


Figure 4-23 Naphthalene and real tar results comparison, Naphthalene: v_0 : 1.57 l/min; τ : 0.3 s; d_p : 500-800 μm ; Gas mixture: Table 4-2; time on stream: 15 min. Real tar: v_0 : 1.57 l/min; τ : 0.3 s; d_p : 500-630 μm ; Gas mixture: producer gas; time on stream: 15 min

The gas residence time has also an important influence on the tar reduction. From Figure 4-10 it could be seen that the tar conversion increases with the gas residence time until a certain value and above that value, the tar conversion decreases with the gas residence time probably because of coke deposition and deactivation of the char. At higher residence times, more coke deposition is expected and this will decrease the net carbon conversion degree. The gas residence time also influences the char conversion because of changes in the gas flow. This is mainly related to the higher gas flow for smaller residence times. In case of a higher flow rate more reactants (CO_2 and H_2O) are supplied that can react with the char, which results in a higher char conversion (see Figure 4-24).

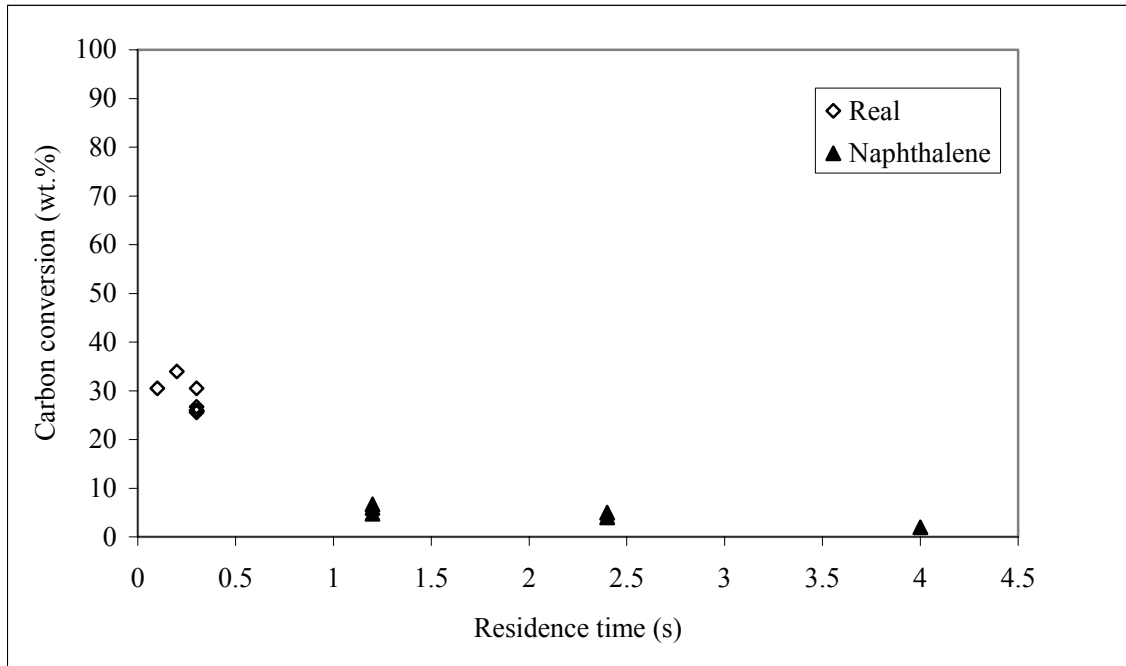


Figure 4-24 Results comparison of effect of gas residence time on synthetic tar (naphthalene) and real tar carbon conversion, Naphthalene: T_R : 850 °C; d_p : 500-630 μm ; Gas mixture: Table 4-2; time on stream: 60 min. Real: T_R : 850 °C; d_p : 500-630 μm ; Gas mixture: producer gas; time on stream: 60 min

Other process parameters like the char particle size and the inlet naphthalene concentration turned out to have less influence on the naphthalene conversion. The composition of the producer gas has no significant influence on the naphthalene conversion, except for the presence of H_2 . It might be concluded that H_2 has an inhibiting effect on the tar reduction reaction. Unfortunately, it is not easy to influence the H_2 -concentration in the producer gas of a gasifier.

The char source is another important parameter for the tar reduction. Especially the presence of metals like iron and alkalis in the ash have a major influence on the tar reduction. Also the way of char production seems to be important. Although, because of the high naphthalene conversion degrees, no influence of the heating rate and the final pyrolysis temperature could be recognized in the present experiments, these parameters will certainly influence the tar-char reaction. More research in this area is required.

The mechanism of the tar reduction by char was investigated. The tar or naphthalene is adsorbed on the active sites of the char particle surface. The adsorbed tars can have two parallel pathways. The first path is a catalytic conversion to CO and H_2 by the steam and dry gasification reactions. The second path is a decomposition to form free radicals that enter polymerization reactions and form coke deposited on the char surface.

It is noted from the experimental results that the char activity for naphthalene reduction did not decrease during the carbon conversion process. Possible explanations are: 1) during the conversion of the carbon, the char micropores grow to meso pores and macro pores which are more effective for the removal [24], and 2) the

metal content concentration of the remaining char increases with the char conversion. Thus, the decrease in the total surface area is (partly) compensated by the increase of the effective surface area for tar conversion or by an increase of the kinetic constant of the reaction. A modeling study has been carried out on this subject and the results will be presented in chapter five.

The biomass char is considered as a catalyst with respect to tar reduction, i.e. it does not react with the tar but catalyzes the tar conversion reactions. However, it is subjected to similar gasification reactions that the tar is subjected to. The char has the activity to remove the hydrogen atom from the tar component to form a free radical [25]. This free radical participates in the heavy hydrocarbon polymerization reactions while the reaction products are deposited as coke on the surface of the char. The tendency toward coke formation is related to the number of aromatic rings in the tar component [9, 26, 27]. The larger the number of aromatic rings, the larger the tendency was found for coke formation. Moreover, naphthalene is reported to have the highest tendency for coke formation [26]. Bartholomew [28] reported that the chemical structure of cokes formed in catalytic processes vary with reaction type, catalyst type, and reaction conditions. The catalytic reactions accompanied by coke formations were classified as coke-sensitive or coke-insensitive [27]. Coke-sensitive reactions, such as catalytic cracking, produce unreactive deposits on active sites leading to the activity decline. On the other hand, coke-insensitive, such as catalytic reforming, produce relatively reactive coke precursors formed on active sites are readily removed by hydrogen or other gasification agents. Tar is expected to be removed over char by the steam and the dry reforming reactions. These reactions probably produce insensitive coke which can be effectively controlled by adapting the operating conditions in such a way that the gasification rate of coke is higher than the production rate.

Circulating fluidized bed reactors are interesting for medium and large scale biomass gasification. In existing biomass fuelled CFB-gasifiers, about 90 % (on average) of the incoming carbon is converted to gaseous products [29]. This means that, on average, 10 % of the carbon is lost in the ash and could be used as a catalyst in a tar-char cracker. This solves both the tar problem and increases the carbon efficiency of the gasifier. The char production inside the gasifier can be influenced by manipulating the gasification process parameters [29, 30], such as, temperature, equivalence ratio, particle size, steam addition, moisture content...etc. Thus, these parameters can be optimized to give the required amount of char in the gasifier. The char consumption in the tar cracker can be balanced by the char produced in the gasifier. For a self-sustained process with char, a model is required to balance the amount of char consumed in the tar cracker with the amount of char produced in the biomass gasifier [29]. Such a model is given the next chapter (see section 5.4).

4.6 Concluding remarks

Biomass char was found to be a catalyst of high potential for tar removal. For a successful design of a process that uses biomass char as a catalyst, several parameters were studied. This study was done with a model tar component (naphthalene) and a real tar mixture. The following conclusions can be drawn:

- The char produced from wood biomass and coals could achieve almost complete naphthalene conversion at temperatures of 800 °C or higher.
- Lower temperatures than 800 °C are not recommended because of the relatively low conversion for real tar. Moreover, naphthalene causes some deactivation of the char with time on stream. This is related to the high amount of coke produced with naphthalene conversion.
- Among the tested types of chars, the brown coal has the highest iron (Fe) content and it gave the highest naphthalene conversion. Therefore, not only alkali content in the char is important but also the iron content. Moreover, the pore structure which includes, the specific internal surface area, the specific internal pore volume and the distribution of the internal volume affect the activity of the char for tar removal.
- The feed gas composition affects both the naphthalene and the simultaneous carbon conversion. The CO₂-N₂ gas mixture gives the highest naphthalene conversion. Whereas, the H₂O-N₂ gas mixture gives the highest carbon conversion. Moreover, H₂ (and CO) has an inhibitory effect that is responsible for decreasing the tar and carbon conversion.
- Low residence times slightly decreases the naphthalene and real tar conversion above 800 °C but it increases the carbon conversion because of the high supply of gas.
- On base of these data a first order kinetic model for naphthalene conversion is used to calculate the kinetics constants. The apparent activation energy (E_{app}) and the pre-exponential factor (k_{app}) can be calculated as 61 kJ/mol and $1 \cdot 10^4 \text{ s}^{-1}$, respectively.
- The conversion of real tar in a char bed at 850 °C was about 97% and the outlet gas contains a less number of tar components with an average tar content of 115 mg/Nm³. At 800 °C only benzo(a)pyrene and at 750 °C only naphthalene was found in the outlet gas.
- The carbon conversion without naphthalene in the feed gas was much higher than the one with naphthalene in the feed gas. This is related to the coke formation that hinders char gasification or coke deposition on the char and gives a lower net conversion. It may be concluded that there is a competition between the coke formation and the carbon gasification. When the rate of coke formation is higher than the rate of gasification, the weight of char increased and the activity of char decreases.

References

1. Zanzi, R., K. Sjostrom, and E. Bjornbom, *Rapid Pyrolysis of Agricultural Residues at High Temperatures*. Biomass and Bioenergy, 2002. **23**(5): p. 131-137.
2. Zanzi, R., K. Sjostrom, and E. Bjornbom. *Rapid Pyrolysis of Bagasse at High Temperature*. in *Third Asia-Pacific International Symposium on Combustion and Energy Utilization*. 1995. Hong Kong.
3. Brandt, P., E. Larsen, and U. Henriksen, *High Tar Reduction in a Two-Stage Gasifier*. Energy & Fuels, 2000. **14**: p. 816-819.
4. Jess, A., *Mechanics and Kinetics of Thermal Reactions of Aromatic Hydrocarbons from Pyrolysis of Solid Fuels*. Fuel, 1996. **75**(12): p. 1441-1448.
5. Brage, C., et al., *Use of Amino Phase Adsorbent for Biomass Tar Sampling and Separation*. Fuel, 1997. **76**(2): p. 1237-42.
6. Namioka, T., et al., *High Tar Reduction With Porous Particles for Low Temperature Biomass Gasification: Effects of Porous Particles on Tar and Gas Yields during Sawdust Pyrolysis*. Journal of Chemical Engineering of Japan, 2003. **36**(12): p. 1440-1448.
7. Yeboah, Y.D., et al., *Effect of Calcined Dolomite on the Fluidized Bed Pyrolysis of Coal*. Ind. Eng. Chem. Process Des. Dev., 1980. **19**: p. 646-653.
8. Brown, R.C., et al., *Biomass-Derived Hydrogen from a Thermally Ballasted Gasifier*. 2005, Center for Sustainable Environmental Technology, Iowa State University: Ames. p. 37.
9. Messenbk, R.C., D.R. Dugwell, and R. Kandiyoti, *CO₂ and Steam-Gasification in a High-Pressure Wire-Mesh Reactor: The Reactivity of Daw Mill Coal and Combustion Reactivity of its Chars*. Fuel, 1999. **78**: p. 781.
10. Orio, A., J. Corella, and I. Narvaez, *Performance of Different Dolomites on Hot Raw Gas Cleaning from Biomass Gasification with Air*. Ind. Eng. Chem. Res., 1997. **36**: p. 3800-3808.
11. Corella, J., J.M. Toledo, and P.M. Aznar, *Improving the Modeling of the Kinetics of the Catalytic Tar Elimination in Biomass Gasification*. Ind. Eng. Chem. Res., 2002. **41**: p. 3351-3356.
12. Barrio, M., et al. *Steam Gasification of Wood Char and the Effect of Hydrogen inhibition on the Chemical Kinetics*. in *Progress In Thermochemical Biomass Conversion*. 2001. Tyrol, Austria: Blackwell Science Ltd.
13. Barrio, M. and J.E. Hustad. *CO₂ Gasification of Birch Char and the Effect of CO Inhibition on the Calculation of Chemical Kinetics*. in *Progress In Thermochemical Biomass Conversion*. 2001. Tyrol, Austria: Blackwell Science Ltd.

14. Devi, L., *Catalytic Removal of Biomass Tars; Olivine as Prospective in-Bed Catalyst for Fluidized-Bed Biomass Gasifiers*. 2005, Technical University of Eindhoven: Eindhoven, The Netherlands.
15. Levenspiel, O., *Chemical Reaction Engineering*. Second Edition ed. 1972, Singapore: Wiley & Sons, Inc. 472.
16. Ye, D.P., J.B. Agnew, and D.K. Zhang, *Gasification of a South Australian Low-Rank Coal with Carbon Dioxide and Steam: Kinetics and Reactivity Studies*. Fuel, 1998. **77**(11): p. 1209-1219.
17. Hanaoka, T., K. Sakanishi, and T. Minowa. *Purification of Hot Producer Gas From Biomass Gasification using Carbonaceous Materials*. in *Second World Conference on Biomass for Energy, Industry and Climate Protection*. 2004. Rome, Italy: ETA-Florence.
18. Akyurtlu, J.F. and A. Akyurtlu, *Catalytic Gasification of Pittsburgh Coal Char by Potassium Sulphate and Ferrous Sulphate Mixtures*. Fuel Processing Technology, 1995. **43**: p. 71-86.
19. Devi, L., et al., *Catalytic Decomposition of Biomass Tars: Use of Dolomite and Untreated Olivine*. Renewable Energy, 2005. **30**: p. 565-587.
20. Simell, P.A., J.K. Leppalahti, and J.B.-s. Bredenberg, *Catalytic Purification of Tarry Fuel Gas with Carbonate Rocks and Ferrous Materials*. Fuel, 1992. **71**: p. 211-218.
21. Suzuki, T., H. Ohme, and Y. Watanabe, *Alkali metal catalyzed carbon dioxide gasification of carbon*. Energy & Fuels, 1992. **6**(4): p. 343-351.
22. Lizzio, A.A. and L.R. Radovic, *Transient Kinetics Study of Catalytic Char Gasification in Carbon Dioxide*. Ind. Eng. Chem. Res., 1991. **30**(8): p. 1735-1744.
23. Forzatti, P. and L. Lietti, *Catalyst Deactivation*. Catalysis Today, 1999. **52**: p. 165-181.
24. Pisa, J.J., et al., *Preparation of active carbons from coal, Part III: Activation of char*. Fuel Processing Technology, 1998. **57**: p. 149-161.
25. Greensfelder, B.S., H.H. Voge, and G.M. Good, *Catalytic and Thermal Cracking of Pure Hydrocarbons*. Ind. Eng. Chem. . 1949. **41**(11): p. 2573.
26. Tenser, P.A. and S. S.V., *Soot Formation during Pyrolysis of Naphthalene, Anthracene, and Pyrene*. Combustion Science and Technology, 1997. **126**: p. 139-151.
27. Menon, P.G., *Coke on Catalysts-Harmful, Harmless, Invisible and Beneficial Types*. J. Mol. Cat., 1990. **59**(2): p. 207-220.
28. Bartholomew, C.H., *Mechanism of Catalyst Deactivation*. Applied Catalysis A: General, 2001. **212**: p. 17-60.
29. van der Drift, A., C.M. van der Meijden, and S.D. Srating-Ytsma. *Ways to Increase Carbon Conversion of a CFB-Gasifier*. in *12th European Conference*

on Biomass for Energy, Industry and Climate Protection. 2002. Amsterdam, The Netherlands: ETA-Florence.

30. Kersten, S.R.A., et al., *Experimental Fact-Finding in CFB Biomass Gasification for ECN's 500 kWth Pilot Plant*. *Ind. Eng. Chem. Res.*, 2003. **42**: p. 6755-6764.

Chapter 5

Modeling of Naphthalene Reduction with Char Particles

Abstract

In the previous chapter, biomass char showed a good performance for the tar reduction in a fixed bed reactor. In this chapter, both a single char particle and a fixed bed reactor model are presented to get a better understanding of tar reduction with char. In the particle model, the effect of the kinetics and heat and mass transfer resistances were investigated. The char particle was found to be isothermal and the effect of internal and external mass transfer resistances are minor in relation to the kinetics. The particle model was further extended to a fixed bed reactor model. The reactor model results were validated with the experimental results presented in chapter four, and they were found to be in good agreement. It was found that the temperature and the gas residence time are the main parameters that have a significant effect on the naphthalene and carbon conversion. These parameters control the coke formation, which affects both naphthalene and char conversion. Finally, a preliminary design for an integrated fixed bed tar cracker downstream of a downdraft fixed bed biomass gasifier was developed. It was calculated that tar reduction of more than 98% could be reached.

5.1 Introduction

In the previous chapters, the biomass char showed high activity for tar removal under fixed bed conditions. It was found that the pore structure and mineral content of the char particle are the key elements for the char activity. The tar in the producer gas is adsorbed on the active sites of the char particles and it undergoes gasification and polymerization reactions. The char catalyzes the gasification reactions of the adsorbed tars with steam and CO_2 . Moreover, the char catalyzes the formation of tar radicals that take part in heavy hydrocarbon polymerization reactions, while the reaction products are deposited as coke on the surface of the char. Despite the coke formation on the char particle, its catalytic activity was found to be constant at temperatures above $800\text{ }^\circ\text{C}$. This was related to the gasification reactions of the coke and char with steam and CO_2 . Thus, char consumption in the tar cracker, caused by gasification reactions, is advantageous because it reactivates the effective char surface area.

Several char particle gasification models are available in literature. Most of these models are concerned with the rate of gasification of a single particle [1, 2] and the evolution of the particle pore structure during gasification [3]. The importance of the model presented in this chapter is the focus on tar conversion over active char and the simultaneous carbon conversion in the char particle.

The here presented single char particle model is developed for naphthalene reduction using a porous char particle in an environment of N_2 , H_2O , H_2 , CO , CO_2 and CH_4 . The effect of different parameters on naphthalene and carbon conversion were investigated. The investigated parameters are: particle size, temperature, environment gas composition and time on stream (time of experiment). Then, the particle model is further extended to a fixed bed reactor model to be able to simulate the experiments of the previous chapter. The reactor model was validated with these experimental results and subsequently used to investigate the key parameters that control the naphthalene and char conversion in a fixed bed reactor. Finally, the model was used for the design of an integrated fixed bed tar cracker downstream of a downdraft fixed bed biomass gasifier.

5.2 Single particle model

In this model, the char particle is considered as a sphere surrounded by a gas film in a bulk producer gas with a constant composition. The model deals with the intrinsic gasification reaction kinetics, external and internal mass transfer, and changing particle properties during gasification. The following assumptions are incorporated in the model:

1. The char particle is spherically symmetric. This allows a simplified one-dimensional solution to the species conservation equations.
2. The char particle has a constant external diameter. This assumption is an approximation to the findings of chapter four. It is found that the char conversion reaction does not proceed uniformly in the char particle and is not

a shrinking particle reaction. Hence, the reaction between tar and char is somewhere in between.

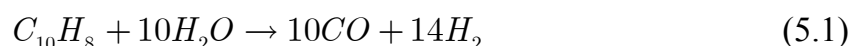
3. The tar is represented by naphthalene as a model tar component. This assumption is justified by the comparison made in chapter four between the naphthalene and the real tar conversion over the char. It shows that the naphthalene is a good representative for the real tar.
4. Only the catalytic conversion of naphthalene to permanent gases is considered. In chapter four, it was found that the naphthalene is converted to permanent gases and coke. Subsequently, the formed coke is gasified to light gases with lower rates than the char. The influence of the coke on both the naphthalene and char conversion is simplified in the model and lumped in the kinetics.
5. An overall first order kinetic rate of naphthalene conversion is assumed. This assumption is justified for two reasons. Firstly, the sensitivity of naphthalene conversion on the char for different gas compositions is low as found in chapter four (Table 4-9). Secondly, the amount of naphthalene (< 0.5 vol. % of the producer gas) compared with the other gases is small. Therefore, in the kinetics of naphthalene conversion, the other gases are assumed to be in excess and lumped in the global pseudo-first order kinetics: ($k = k' [H_2O]^a [CO_2]^b [H_2]^c$).
6. The naphthalene can be converted by parallel reactions with CO₂, steam and to a less extent with H₂. The extent of these reactions is not known. Therefore, for the mass balance of the different species, the naphthalene was assumed to be converted because of its reaction with steam. This assumption is justified for the reasons given in the previous assumption.

In the following sections, the main parts of the model are discussed. The main reactions in the tar cracker are presented in the kinetics section (5.2.1). The species concentration profiles and temperature profile inside the particle are estimated by solving mass balances of the species (5.2.2) and the energy balance equations of the particle (5.2.3). Further, the physical properties and the estimated parameters used in the model are presented in section (5.2.4).

5.2.1 Kinetics

Tar in the producer gas is catalytically converted when passed over a char bed. Char particles catalyze the tar reforming reactions. However, char particles are not inert in the producer gas atmosphere and undergo gasification reactions in the environment inside the gasifier. The gasification reactions are extensively studied in literature [1, 4-8]. However, the kinetic constants of these reactions have many forms and few are based on the active surface area of the particle. In the following sections, the main reactions that occur in the char particle are discussed. The considered kinetic constants are only those valid for producer gas in the temperature range of 700-900 °C at atmospheric pressure.

Naphthalene steam reforming



This reaction is an endothermic and heterogeneous reaction. The naphthalene does not react with the carbon in the char particle like other reactants such as CO_2 , H_2O or H_2 . However, it needs to be adsorbed on the active sites located on the surface of the char particle for faster rate of reaction with steam.

The kinetic rate equation of naphthalene decomposition on the char is not found in literature. However, the catalytic conversion of naphthalene over other catalysts was studied in literature. Devi et al. [9] have developed an overall kinetic rate equation for naphthalene conversion over olivine. This kinetic rate equation is function of the different reactive components in the producer gas:

$$-r_n = k [H_2O]^a [CO_2]^b [H_2]^c [CO]^d [C_{10}H_8]^e \quad (5.2)$$

This equation is only valid when all reactive components are present in the gas within a given range [9]. For the present situation, if one of the components is totally consumed (i.e. $C_i = 0$), then the rate of reaction becomes also zero which may not be valid. Jess [10] has studied the conversion of naphthalene on a nickel catalyst (Ni-MgO) in the presence of about 30 vol. % H_2 and 13 vol. % steam in the temperature range of 660-800 °C. He found that the decomposition reaction is 0.2 order with respect to naphthalene, 0.3 order with respect to hydrogen and zero order with respect to steam. This rate equation will not be used here as nickel catalyst has a different mechanism for naphthalene conversion compared with char as explained in chapter two.

As was shown in the previous chapter during a five-hours lasting experiment, the tar conversion did not change while the final char conversion was more than 90 %. The decrease in the char bed density was compensated with the increase of the active surface area for tar conversion. Because the experimental results showed constant tar conversion, a constant effective char surface area for tar reduction can be assumed. More details on the surface area are given in section (5.2.4). Using the kinetic constants found in the previous chapter (4.3.2) and assuming a first order reaction with respect to naphthalene (4.3.5), the following overall kinetic rate equation of naphthalene decomposition was used in the model:

$$-r_n = k_{n,app} C_n \quad (5.3)$$

$$k_{n,app} = 1 \cdot 10^{-4} e^{-61000/RT} \quad (5.4)$$

Where,

$-r_n$ = overall rate of naphthalene conversion, $kmol/m^3 \cdot s$

$k_{n,app}$ = apparent kinetic rate constant, s^{-1}

C_n = local naphthalene concentration within the particle, $kmol/m^3$

Steam and dry gasification of the char



Steam and dry gasification reactions of char are endothermic and heterogeneous reactions. The gasification reactions of biomass char are not studied extensively in literature as coal char reactions. The n^{th} order kinetics found by Barrio et al. [4, 5] were used here since they were estimated for biomass char (birch wood) in the temperature range 750–950 °C. The type of biomass and gasification temperature range are close to our experimental conditions.

The overall rate of the steam gasification reaction is expressed in grams of carbon gasified per second per gram of carbon present:

$$-r_{H_2O} = k_{H_2O} P_{H_2O}^{0.57} \quad (g \cdot g^{-1} \cdot s^{-1}) \quad (5.7)$$

$$k_{H_2O} = 2.62 \cdot 10^8 e^{(-237000/(RT))} \quad (s^{-1} \cdot bar^{-0.57}) \quad (5.8)$$

Similarly, the overall rate of the dry gasification reaction is expressed in grams of carbon gasified per second per original gram of carbon present:

$$-r_{CO_2} = k_{CO_2} P_{CO_2}^{0.38} \quad (g \cdot g^{-1} \cdot s^{-1}) \quad (5.9)$$

$$k_{CO_2} = 3.1 \cdot 10^6 e^{(-215000/(RT))} \quad (s^{-1} \cdot bar^{-0.38}) \quad (5.10)$$

In chapter four, it was found that the rate of the char gasification is not constant but decreases with time (Figure 4-22) because of the changing surface area of the char particle with time. Thus, the effect of the relative internal surface area of the char particle (see section 5.2.4) is included in the model for the gasification reactions of the carbon.

The following modifications were made on the steam and dry gasification equations to be compatible with our findings and the model units:

- the units of the equations are converted to (kmol/m³.s): multiplying by the concentration of the char (C_C)
- the concentration of the char is expressed in terms of the char particle density ($C_C = w_b \rho_C / M_C$)
- the gas component pressure is expressed in terms of concentration ($P_i = C_i RT$)
- The rate constant is multiplied by the relative surface area $a(X_C)$

Thus, the gasification equations take the following form:

$$-r = k \cdot (C_i RT)^n \cdot a(X_C) \cdot \frac{w_C \cdot \rho_C(X_C)}{M_C} \quad (5.11)$$

Where ,

- r = intrinsic volumetric gasification rate, $\text{kmol.m}^{-3}.\text{s}^{-1}$
- n = apparent reaction order with respect to the gas component
- k = global rate coefficient, $\text{s}^{-1}.\text{bar}^{-n}$
- C_i = gas reactant (H_2O or CO_2) concentration, kmol.m^{-3}
- R = gas constant, $0.08314 \text{ bar.m}^3.\text{kmol}^{-1}.\text{K}^{-1}$
- a = relative surface area of char particle, see eq. (5.47)
- w_C = carbon content in the char particle
- $\rho_C(X_C)$ = density of the char particle that is function of carbon conversion, kg.m^{-3}
- M_C = molecular weight of the carbon, kg.kmol^{-1}

Hydrogasification of the char



The hydrogasification reaction is an exothermic reaction. The first order kinetic data obtained for coconut chars is used where the kinetic constant is based on the internal surface area available for the reaction [11].

$$-r'_{H_2} = k'_{H_2} P_{H_2} \quad (\text{kmol.m}^{-2}.\text{s}^{-1}) \quad (5.13)$$

$$k_{H_2} = 9.14 \cdot 10^{-10} e^{(-149050)/(RT)} \quad (\text{kmol.s}^{-1} \cdot \text{Pa}^{-1} \cdot \text{m}^{-2}) \quad (5.14)$$

The following modifications were done on the hydrogasification equation to be compatible with our model.

- The rate equation is converted and based on unit volume of the particle: multiplying by ($S_o \cdot \rho_C \cdot w_b$)
- The rate constant is multiplied by the relative surface area $a(X_C)$
- The pressure of H_2 is converted and based on concentration ($P_i = C_i RT$)

Thus, the hydrogasification equation can be written as follows:

$$-r_{H_2} = k'_{H_2} \cdot (C_{H_2} RT) \cdot S_o \cdot a(X_C) \cdot \rho(X_C) \cdot w_C \quad (5.15)$$

Where ,

$-r_{H_2}$ = intrinsic volumetric hydrogasification rate, $kmol.m^{-3}.s^{-1}$

k'_{H_2} = intrinsic rate coefficient on area basis, $kmol.s^{-1}.Pa^{-1}.m^{-2}$

C_{H_2} = local concentration of H_2 within the particle, $kmol.m^{-3}$

R = gas constant, $8314 J.kmol^{-1}.K^{-1}$

S_o = initial total surface area of the char, $m^2.kg^{-1}$

Water gas shift reaction



The water gas shift reaction is a homogeneous reaction and exothermic in the direction of the forward reaction. The rate of the gas shift reaction is not catalyzed by the char. Thus, it is a kinetically limited reaction. The forward and backward reactions are used in the model mass balance calculations [12].

$$r_{sh} = k_{sh}C_{H_2O}C_{CO} - k_{-sh}C_{H_2}C_{CO_2} \quad (kmol.m^{-3}.s^{-1}) \quad (5.17)$$

$$k_{sh} = 2780e^{(-12560/(RT))} \quad (m^3.kmol^{-1}.s^{-1}) \quad (5.18)$$

$$k_{-sh} = 1.05 \cdot 10^5 e^{(-45466/(RT))} \quad (m^3.kmol^{-1}.s^{-1}) \quad (5.19)$$

5.2.2 Mass balance

Gas-mass balance

The mass balance of the gaseous components within the particle is given by:

$$\frac{\partial C_i}{\partial t} + \frac{1}{r^2} \frac{\partial}{\partial r} \left[D_e(\varepsilon) r^2 \frac{\partial C_i}{\partial r} \right] = R_i \quad (5.20)$$

The first term is the mass accumulation, the second term is the effective diffusivity and third term is the mole generation by the chemical reaction. The convection inside the particle is assumed to be negligible [13].

Where ,

C_i = local component concentration, kmol/m³

t = time, s

r = radius coordinate, m

$D_e(\varepsilon)$ = effective diffusion coefficient, m²/s

ε = particle porosity

R_i = the sum of the rate of chemical production of component i

$$R_i = \sum \alpha_{ij} r_j \quad (5.21)$$

Where ,

α_{ij} = stoichiometric coefficient of ith component in the jth reaction

The rates of chemical production of component i (R_i) for the different gas species available in the model are given below where (n) is used as a subscript to represent naphthalene.

$$\begin{aligned} R_n &= -r_n \\ R_{H_2O} &= -r_{H_2O} - r_{sh} - 10r_n \\ R_{H_2} &= r_{H_2O} - 2r_{H_2} + r_{sh} + 14r_n \\ R_{CO} &= r_{H_2O} + 2r_{CO_2} + r_{sh} + 10r_n \\ R_{CO_2} &= -r_{CO_2} + r_{sh} \\ R_{CH_4} &= r_{H_2} \end{aligned} \quad (5.22)$$

The above equations represent mass balances for the gas components naphthalene, H₂O, H₂, CO, CO₂, and CH₄. Further, a total mass balance (including the mentioned components and N₂) can be formulated where the sum of the mole fractions of the gas components is equal to one.

$$\sum_{i=1}^7 x_i = 1 \quad (5.23)$$

The initial concentration of all the gaseous components inside the particle is zero. Further, the derivative of the concentration of the gas component in the center of the particle is zero because of the particle symmetry. The rate of diffusion at the surface of the particle is equal to the rate of mass diffusion in the gas film surrounding the particle. The initial and boundary conditions of the gaseous mass balance equation are expressed as follows:

Initial condition:

$$t = 0, \quad C_i = 0 \quad (5.24)$$

Boundary conditions:

$$r = 0, \quad \frac{\partial C_i}{\partial r} = 0 \quad (5.25)$$

$$r = R_o, \quad D_{e,i} \frac{\partial C_i}{\partial r} = k_{g,i} (C_{i,b} - C_{i,s}) \quad (5.26)$$

Where ,

$C_{i,b}$ = bulk concentration of the gas component, kmol/m³

$C_{i,s}$ = surface concentration of the gas component, kmol/m³

$k_{g,i}$ = mass transfer coefficient of component i in the gas film, m/s

The mass transfer coefficient of component (i) in the gas film ($k_{g,i}$) can be estimated using the Sherwood number:

$$Sh_i = \frac{k_{g,i} d_p}{D_i} \quad (5.27)$$

Where,

Sh_i = Sherwood number of gas component i

d_p = particle diameter, m

D_i = Binary diffusion coefficient of gas component i, m²/s

The correlation of Kunii and Suzuki [14] for packed beds at low Reynolds numbers is used to estimate the Sherwood number.

$$Sh_i = \frac{\phi_s}{6(1 - \varepsilon_b)\xi} \frac{u_o d_p}{D_i} \quad (5.28)$$

Where,

ϕ_s = shape factor which is the surface area divided by πd_p^2

ξ = ratio of average channeling length to particle diameter

ε_b = bed porosity, usually taken as 0.45 [15]

u_o = superficial gas velocity, m/s

d_p = particle diameter, m

D_i = binary diffusion coefficient, m²/s

Solid-mass balance

The carbon mass balance of the char particle is given in eq. (5.29). The carbon concentration in the particle is expressed in terms of the density of the carbon:

$$\frac{\partial \rho_C}{\partial t} = M_C R_C \quad (5.29)$$

Where,

- ρ_C = density of char particle, kg/m³
- M_C = molecular weight of the carbon, kg/kmol
- R_C = rate of chemical carbon conversion, kmol/m³.s

$$R_C = -r_{H_2O} - r_{CO_2} - r_{H_2} \quad (5.30)$$

The carbon mass balance equation requires only an initial condition:

$$t = 0, \quad \rho_C = \rho_{C,o} \quad (5.31)$$

Internal diffusion

To estimate the effect of the pore diffusion resistance on the overall reaction rate, the effectiveness factor was used. It is defined as the ratio of the actual reaction rate including the pore diffusion resistance to the reaction rate excluding pore diffusion resistance [15]. For spherical particles and a first order reaction the effectiveness factor is given by the following equation [13]:

$$\eta = \frac{1}{\Phi_T} \left(\frac{1}{\tanh(3\Phi_T)} - \frac{1}{3\Phi_T} \right) \quad (5.32)$$

Where,

- η = effectiveness factor
- Φ_T = Thiele modulus

The Thiele modulus Φ_T is the ratio of the surface reaction rate and the pore diffusion rate. For small Φ_T ($\ll 1$) the reaction kinetics are controlling the overall reaction rate, whereas for large Φ_T ($\gg 1$) the pore diffusion is the dominating process. The general Thiele modulus for nth order rate equation and a sphere is [15]:

$$\Phi_T = L \sqrt{\frac{(n+1) k C_s^{n-1}}{2 D_e}} \quad (5.33)$$

Where,

- L = characteristic length; equivalent to $(d_p/6)$ for a sphere, m
- d_p = particle diameter, m
- n = order of reaction
- k = rate constant, $s^{-1} \cdot (\text{kmol}/\text{m}^3)^{n-1}$
- C_s = surface concentration, kmol/m^3
- D_e = effective diffusion coefficient, m^2/s

External diffusion

To estimate the effect of the external diffusion, the Biot number is used [16]. This number represents the ratio between the external and the internal diffusion and it is defined as follows:

$$Bi_m = L \frac{k_g}{D_e} \quad (5.34)$$

Where,

- L = characteristic length, for a sphere: $(d_p/6)$, m
- k_g = mass transfer coefficient, m/s
- D_e = effective diffusion coefficient, m^2/s

For $Bi_m \gg 1$ the internal pore diffusion is the controlling transport mechanism, while for $Bi_m \ll 1$ the external diffusion is controlling.

Summarizing [17]:

- $\Phi_T \ll 1$: kinetically controlled
- $\Phi_T \gg 1$: $Bi_m \gg \Phi_T$, internal diffusion controlled
- $Bi_m \ll \Phi_T$, external diffusion controlled

5.2.3 Energy balance

The temperature profile inside the char particle can be found from the energy balance equation. The considered energy balance considers heat accumulation, heat conduction and heat generation by reaction as follows [17]:

$$\frac{\partial}{\partial t} [\rho_{p,t} (1 - \varepsilon) c_{p,C} T] = \frac{1}{r^2} \frac{\partial}{\partial r} \left[\lambda_e(\varepsilon) r^2 \frac{\partial T}{\partial r} \right] - \sum r_j (-\Delta H_j) \quad (5.35)$$

Where,

$$\begin{aligned} T &= \text{local particle temperature, K} \\ \rho_{p,t} &= \text{true density of the char particle, kg/m}^3 \\ C_{p,C} &= \text{specific heat of the char, kJ.kg}^{-1}.\text{K}^{-1} \\ \lambda_e(\varepsilon) &= \text{effective heat conductivity, kJ.s}^{-1}.\text{m}^{-1}.\text{K}^{-1} \\ &(\lambda_e(\varepsilon) \text{ is discussed in Appendix A}) \\ \Delta H &= \text{heat of reaction, kJ/kmol} \end{aligned}$$

The heat of reaction can be estimated from the enthalpies of the products and reactants as follows:

$$\Delta H_j = \sum_i \alpha_{ij} H_i \quad (5.36)$$

Where,

$$\alpha_{ij} = \text{stoichiometric coefficient of component } i \text{ in reaction } j$$

The heats of reaction for the different reactions presented in the model (reactions 5.1, 5.5, 5.6, 5.12 and 5.16) discussed in section 5.2.1 are expressed as follows:

$$\begin{aligned} \Delta H_{5.1} &= 14H_{H_2} + 10H_{CO} - 10H_{H_2O} - H_n \\ \Delta H_{5.5} &= H_{H_2} + H_{CO} - H_{H_2O} - H_C \\ \Delta H_{5.6} &= H_{CH_4} - 2H_{H_2} - H_C \\ \Delta H_{5.12} &= 2H_{CO} - H_{CO_2} - H_C \\ \Delta H_{5.16} &= H_{CO_2} + H_{H_2} - H_{H_2O} - H_{CO} \end{aligned} \quad (5.37)$$

H_i is the molar enthalpy of the i^{th} component and it is estimated from the molar heat of formation (H_f) in kJ/kmol and the specific sensible heat (H_s) in kJ/kg. H_s is converted to kJ/kmol by multiplying it by the molecular weight of the component (M_i) as follows:

$$H_i = H_{f,i} + M_i H_{s,i} \quad (5.38)$$

$$H_{s,i} = \int_{T_0}^T C_{p,i} dT \quad (5.39)$$

Where,

$$C_{p,i} = \text{heat capacity of component } i, \text{ kJ.kg}^{-1}.\text{K}^{-1}$$

The initial temperature inside the particles is assumed to be similar to the bulk temperature in the reactor as, during the experiments, char particles are heated inside

the reactor until they reach the desired temperature. At any time, the temperature gradient in the center of the particle is zero because of the particle symmetry. At the surface of the particle, the heat flux by conduction in the particle is equal to the heat flux by external convection. The initial and boundary conditions are summarized as follows:

Initial condition:

$$t = 0, \quad T = T_b \quad (5.40)$$

Boundary conditions:

$$r = 0, \quad \frac{\partial T}{\partial r} = 0 \quad (5.41)$$

$$r = R_o, \quad \lambda_e(\varepsilon) \frac{\partial T}{\partial r} = h(T_s - T_b) \quad (5.42)$$

Where,

T_s = surface particle temperature, K

T_b = bulk temperature, K

h = heat transfer coefficient in the gas film, $\text{kJ.m}^{-2}.\text{s}^{-1}.\text{K}^{-1}$

The heat transfer coefficient in the gas film (h) can be estimated using Nusselt number:

$$Nu = \frac{hd_p}{\lambda_g} \quad (5.43)$$

Where,

Nu = Nusselt number

d_p = particle diameter, m

λ_g = gas mixture thermal conductivity, kJ/s.m.K

The correlation of Kunii and Suzuki for packed beds at low Reynolds numbers is used to estimate the Nusselt number [14].

$$Nu = \frac{\phi_s}{6(1 - \varepsilon_b)\xi} \frac{u_o d_p \rho_g C_{p,g}}{\lambda_g} \quad (5.44)$$

Where,

- ϕ_s = shape factor
- ξ = ratio of average channeling length to particle diameter
- ε_b = bed porosity, taken as 0.40 [15]
- u_o = superficial gas velocity, m/s
- d_p = particle diameter, m
- ρ_g = gas density, kg/m³
- $C_{p,g}$ = heat capacity of the gas, kJ/ kg.K
- λ_g = gas thermal conductivity, kJ/s.m.K

The mass and energy balance equations were solved simultaneously to obtain the gaseous concentration profiles, particle density and temperature gradient inside the particle and other properties at different times and operating conditions.

5.2.4 Physical properties and parameters estimation

In this section, the physical properties that strongly affect the model results are discussed and the other properties are discussed in Appendix A. The properties of the biomass char particle used in the experiments of chapter four are used as an input for the model calculations. Unavailable data are taken from literature.

Char porosity

The initial porosity of the biomass char particle (ε_o) can be estimated from the apparent and true densities of the particle.

$$\varepsilon_o = 1 - \frac{\rho_p}{\rho_{p,t}} \quad (5.45)$$

Where,

- ρ_p = apparent particle density, kg/m³
- $\rho_{p,t}$ = true particle density, kg/m³

A porosity value of (0.75) reported for the wood char [18] was used in the model. The porosity changes according to the carbon conversion inside the particle with time. The dependency on the carbon conversion can be related as follows [18]:

$$\varepsilon = 1 - (1 - \varepsilon_o) \left(\frac{\rho_p}{\rho_{p,o}} \right) \quad (5.46)$$

Where,

ρ_p = particle density at a certain time and position, kg/m³

$\rho_{p,o}$ = initial particle density, kg/m³

Char surface area

In chapter four, it was found that the micropores mainly contribute to the total surface area (TSA) of the biomass char. This also agrees with the findings of Guo [19] who found that the wood char particle is microporous and has a complex structure of interconnecting and tortuous pores. The TSA was measured by physical adsorption of nitrogen (BET-surface area, see Table 4-1 and Table 4-4). However, the reaction takes place on the active sites in the pores and, as concluded in the previous chapter, the active surface area (ASA) is mainly concentrated in the larger pores (mesopores and macropores). Moreover, during the gasification, the pore structure is changing and micropores develop into mesopores and macropores. It is reported that the concentration of active sites (ASA/TSA) is typically 1-4 % [13].

The ASA is not constant and changes with carbon conversion. The change in the ASA is because of the change of the pore structure. Moreover, the ASA changes in a different way from the TSA. Mostly, it decreases initially and then increases substantially as reported by Laurendeau [13]. Because the initial ASA is not known, a relevant surface area can be used and defined as follows [20]:

$$a = \frac{\text{available pore surface area per unit weight at any stage of conversion}}{\text{initial available pore surface area per unit weight}}$$

In chapter four, it was found that the ASA for the naphthalene conversion reaction was not the same as the ASA for the char gasification reaction. The ASA for naphthalene reaction most likely did not change during the eight hours experiment (Figure 4-7) at temperature above 800 °C. In the present model, the ASA for the naphthalene reaction was assumed to be constant.

On the other hand, the ASA for the carbon gasification reactions was changing with carbon conversion. In chapter four (Figure 4-22), an experiment was done to measure the carbon conversion as a function of time at 850 °C. The data can be used to find the rate of carbon conversion (R) relative to the initial rate (R_o). The ratio (R/R_o) is, in fact, the relative surface area (a) as shown in Figure 5-1.

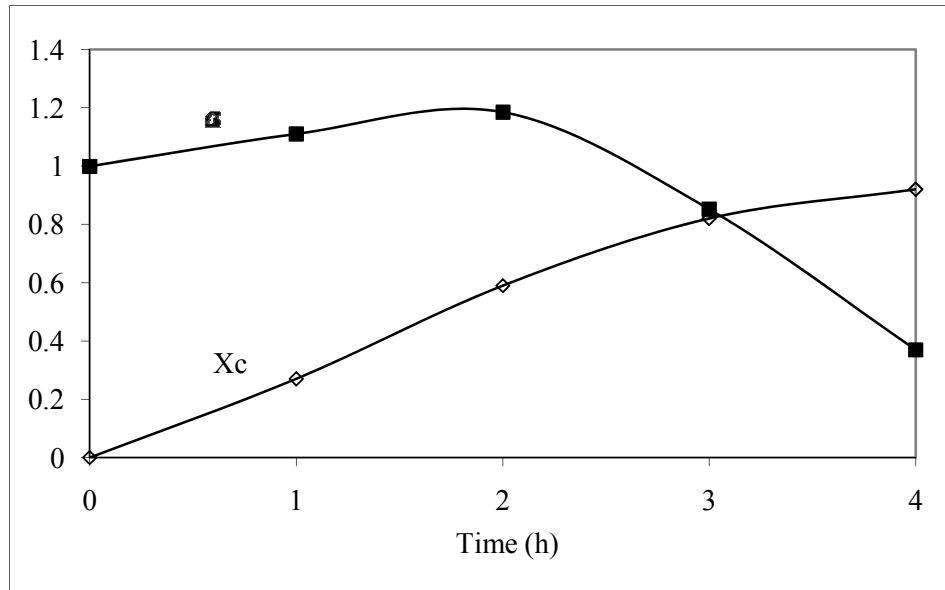


Figure 5-1 the relative surface area a and carbon conversion as function of time, T : 850 °C, d_p : 600 μm

To express the relative surface area as function of the carbon conversion, a fit for the data was done. The following polynomial equation that fits the data was used in the model and assumed to be valid for other conditions:

$$a(X_c) = -4.361X_c^3 + 3.752X_c^2 - 0.391X_c + 1.0 \quad (5.47)$$

Effective diffusion coefficient

The mass transfer of gas components within the porous structure of the biomass char can be modeled by two basic approaches: macroscopic and microscopic [13].

The macroscopic approach is used in most of the models and is based on an empirical correlation for the effective diffusion coefficient that represents the flow resistance throughout the whole particle. This approach mostly uses a constant value for the effective diffusivity that considers the deviation from the ideal path, such as zigzag, constrictions, overlap and other effects [13, 21]:

$$D_e = \frac{\varepsilon}{\tau} D \quad (5.48)$$

Where,

ε = porosity

τ = tortuosity

The tortuosity can be approximated with the following expression [19, 21, 22]:

$$\tau = 1/\varepsilon$$

The microscopic approach considers diffusion through a single pore rather than the entire porous particle, which is described by an appropriate combination of pores. The flow in a single pore is modeled using the capillary diffusion theory that involves

molecular diffusion and Knudson diffusion. Molecular diffusion (D_M), discussed in Appendix A, becomes the dominant diffusion mechanism when the pore size is large compared with the mean free path of the i^{th} diffusing reactant ($\delta / \lambda_i > 10$). On the other hand, Knudson diffusion becomes the dominant when the pore size is small compared with the mean free path ($\delta / \lambda_i < 0.1$). For a smooth pore, the Knudson diffusion coefficient ($D_{K,i}$) is given by the kinetic theory [13]:

$$D_{K,i} = \frac{\delta}{3} \sqrt{\frac{8RT}{\pi M_i}} \quad (5.49)$$

Where,

δ = pore diameter, nm

M_i = molecular weight of i^{th} gas component, kg/kmol

The combined effect of both diffusing mechanisms can be modeled to a good approximation for an isobaric system by using the overall pore diffusing coefficient [13]:

$$D_i = \left(\frac{1}{D_{M,i}} + \frac{1}{D_{K,i}} \right)^{-1} \quad (5.50)$$

The combined diffusivity can be converted to the effective diffusivity using eq. (5.48)

The macroscopic approach was used in the present model as a first approach.

5.2.5 Numerical solution

The model is solved numerically using the chemical engineering module in the software package FEMLAB [23]. The gas and solid mass balance equations and the energy balance equation were applied in the software as three application modes in 1-D geometry. The convective and diffusion mode is used for solving the mass balance equations. On the other hand, the convective and conduction mode is used for solving the energy balance equation.

In each application mode, the dependent variables are set. For the gas mass balances, the following dependent variables are set: H_2O , H_2 , CO , CO_2 , CH_4 , and Naphthalene, respectively. These variables represent the local concentration of the gas species inside the particle. Further, a total mass balance equation is used where the sum of the mole fractions of the gas components is equal to one.

For the char mass balance, the apparent density of the char particle (ρ) is set as the dependent variable. For the energy balance, the particle temperature (T_p) is set as the dependent variable. For the three balances (application modes), the independent variable is set as the particle radius (r). The three equations are solved together using a time-dependent solver. The applied time step is the default value of the solver. The

geometry of the model is 1-D divided into smaller intervals (or mesh elements). The maximum element size is $1 \cdot 10^{-5}$.

The rate equations of the steam and dry gasification of the char contain powers. These powers are a source of instability because powers of negative numbers can occur when the concentration is close to zero. The problem was overcome by using absolute values for the concentrations raised to powers.

5.2.6 Reference conditions

The single char particle model was developed to get more insight in the naphthalene reduction by an active and porous char particle in the environment of H_2O , H_2 , CO , CO_2 , CH_4 and N_2 . The influence of different parameters on the naphthalene and char conversion were studied. The real tar experimental conditions used in chapter four were used in the model as reference conditions. The values of these parameters are given in Table 5-1.

Table 5-1 Reference values of the model parameters

Parameter	Symbol	Value
Pressure	P (atm)	1
Tar	$C_{10}H_8$	Naphthalene
Reactor temperature	T_R ($^{\circ}C$)	850
Gas residence (space) time	τ (s)	0.3
Superficial gas velocity	U (m/s)	0.08
Char particle size	d_p (μm)	600
Standard gas mixture composition (STD) (vol.%)		
CO		13
CO ₂		11
H ₂ O		11
H ₂		6
CH ₄		4
$C_{10}H_8$		0.2
N ₂		Balance

5.2.7 Results of the single particle model

The naphthalene and char gasification reactions inside the char particle are endothermic. Thus, heat needs to be transferred from the bulk gas to the particle and within the particle via conduction. Because of the low thermal conductivity of the carbon and gas, a temperature gradient inside the particle exists. The temperature differences in the particle will affect the local kinetic rate of the reactions inside the particle. The energy balance equation, solved with the gas and char mass balance

equations, gives the temperature profile inside the particle for different bulk temperatures. In Figure 5-2,a the initial temperature profile inside the particle at ($X_c = 0$) is given. Laurendeau [13] reported that when the maximum temperature difference between the surface and the center of the particle is less than 5% of the surface temperature, the particle can be considered as isothermal (see eq. 5.51). The model calculations in Figure 5-2,b show that isothermal conditions can be assumed up to a bulk temperature of about 1160 °C. These calculations were done as described in section (5.2.5) where the energy balance is solved with the mass balance. Thus, at our standard conditions (i.e. 850 °C) the system can be considered isothermal and the energy balance needs not to be solved any more. This also will be applicable during carbon conversion as it only affects the relative surface area and the rate of gasification reactions as shown in Figure 5-1. Thus, at high carbon conversion the temperature difference between the surface and the center of the particle will be lower than at low carbon conversion.

$$\beta = \left| \frac{T_c - T_s}{T_s} \right|_{\max} \quad (5.51)$$

Where,

β = non-dimensional temperature difference

T_c = temperature at the center of the particle, K

T_s = temperature at the surface of the particle, K

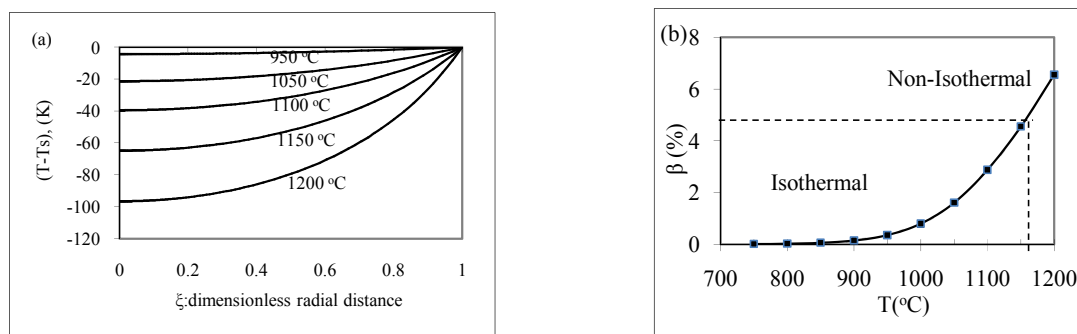


Figure 5-2 Temperature gradient within the particle at different bulk temperatures, d_p : 600 μm ; $X_c = 0$, (a) temperature gradient inside the particle, (b) non-dimensional temperature difference defined by eq. (5-51)

Figure 5-3 shows the effect of internal mass transfer limitations on the naphthalene reduction. The line ($\Phi_T = 1$) shows the temperatures and the corresponding particle sizes at which the Thiele modulus equals unity. The operation at a bulk temperature and a particle size that gives a Thiele modulus below one means that the reaction is kinetically limited. On the other hand, operating at conditions that give a Thiele modulus above one, means that the reaction is mass transfer limited. At the reference temperature (850 °C) and the reference particle size (600 μm), it is clear from Figure 5-3 that the naphthalene reduction reaction is kinetically controlled ($\Phi_T < 1$).

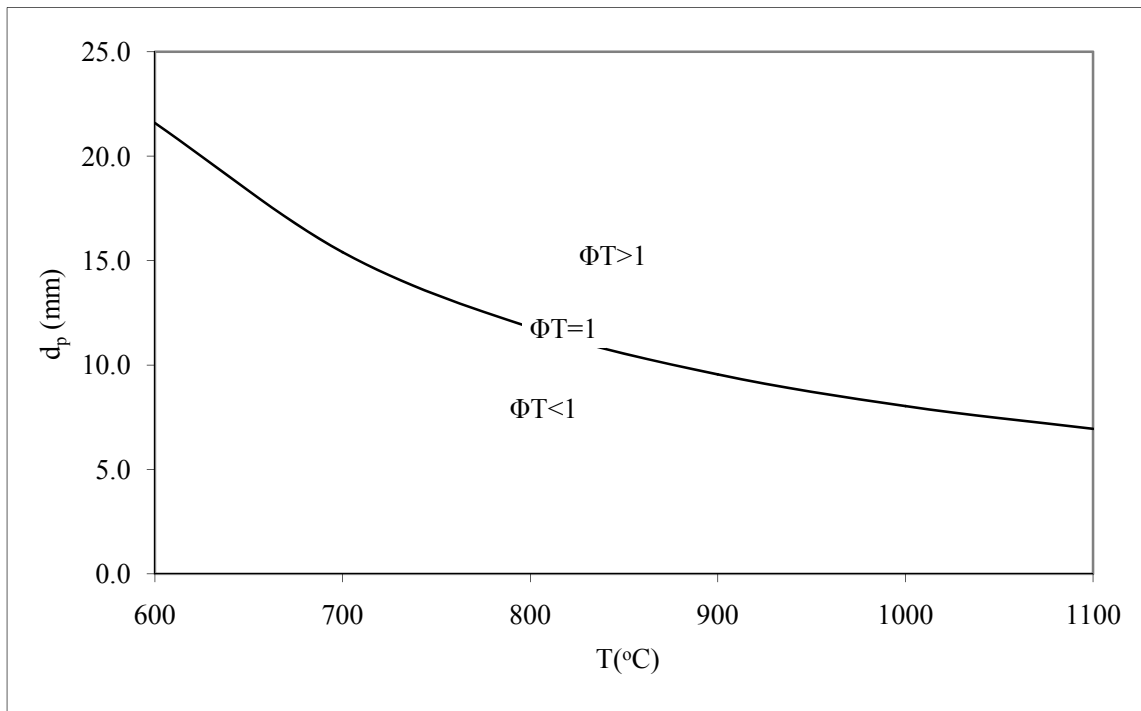


Figure 5-3 Thiele modulus (Φ_T) of the naphthalene reduction reaction as a function of bulk temperature and particle size, reference conditions (T_R : 850 °C; d_p : 600 μm)

The effect of mass transfer is also studied for the steam and dry gasification reactions of the char (see Figure 5-4). At the reference conditions, it is clear that also the steam and the dry gasification reactions of char are kinetically controlled ($\Phi_T < 1$).

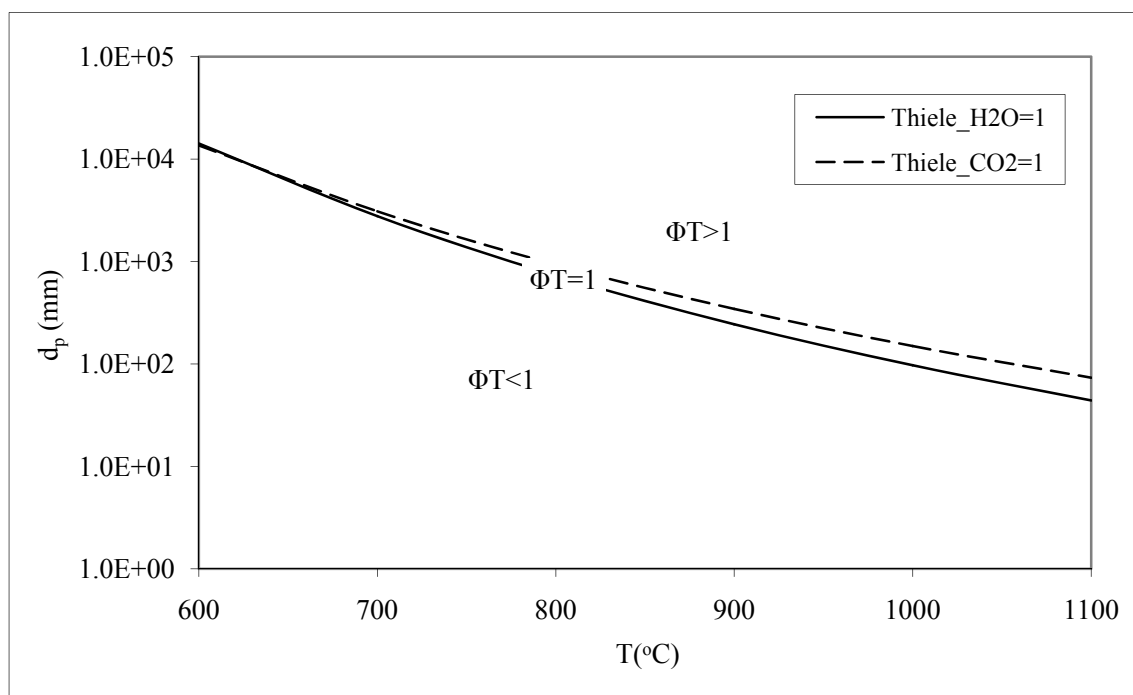


Figure 5-4 Thiele modulus (Φ_T) of the steam and CO_2 gasification reaction as a function of bulk temperature and particle size, reference conditions (T_R : 850 °C; d_p : 600 μm)

The char particles in the tar cracker are continuously gasified by steam and CO_2 content in the producer gas. The gasification of the char consumes the carbon content of the char particles and thus changes the pore structure of the particles. The porosity increases with the carbon conversion because the particle does not shrink in the ($\Phi_T < 1$) region. Thus, more voids are created. The increased porosity increases the relative effective diffusion coefficient because of the less resistance, and thus, the Thiele modulus is decreasing with time on stream as shown for the naphthalene reduction reaction in Figure 5-5 for three different bulk temperatures. The Thiele modulus stays kinetically limited ($\Phi_T < 1$) and reaches its lowest value after almost two hours on stream.

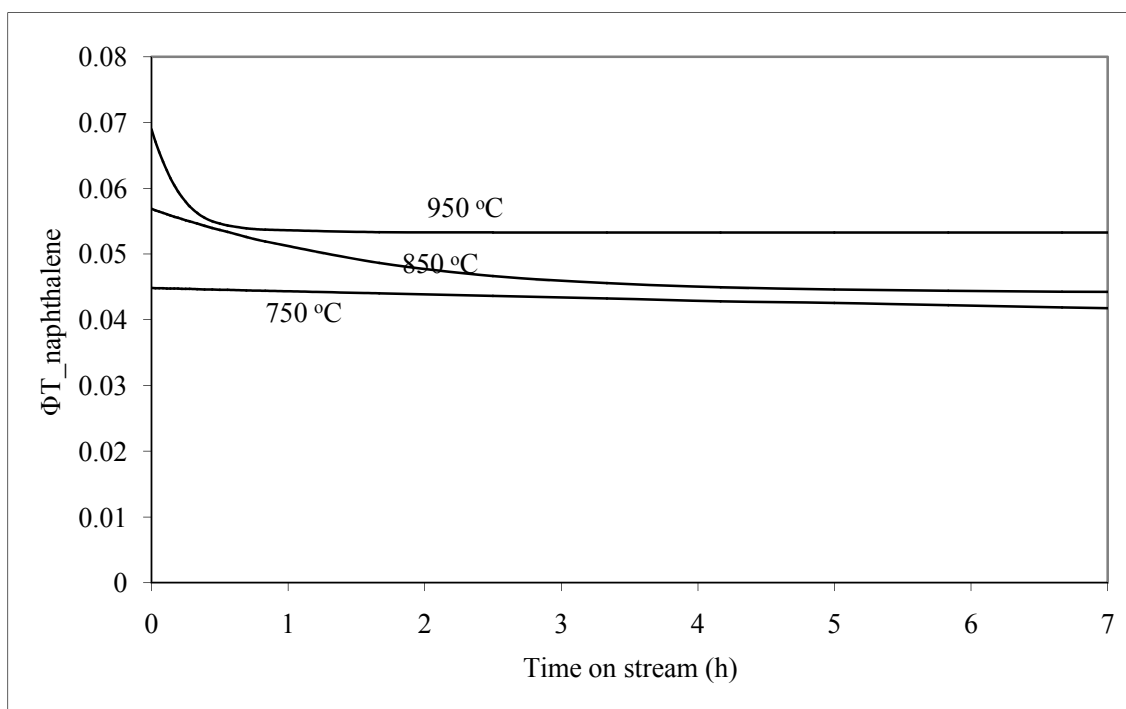


Figure 5-5 Effect of time on stream on the Thiele modulus of the naphthalene reduction reaction at different bulk temperatures

5.3 Reactor model

The single char particle model describes the processes that occur inside the char particle in the atmosphere of the producer gas containing tars such as naphthalene. However, it does not describe the changes in the gas composition and the char conversion along the height of the char bed. Therefore, the single char particle model was extended to a fixed (packed) bed reactor model. Moreover, the model results were validated with the experimental results presented in chapter four for tar reduction in a fixed bed.

Reactor model formulation

The single char particle model was used as a base for the reactor model. The producer gas passes through a differential volume in the reactor (ΔV). The gas diffuses inside the particle and may react. The consumption of certain components, such as, naphthalene, H_2O and CO_2 causes an inward flux from the bulk gas to the particle. On the other hand, the production of certain components, such as, H_2 and CO causes an outward flux from the particle to the bulk gas. These fluxes change the bulk concentration of the components along the height of the bed (z) as shown in Figure 5-6.

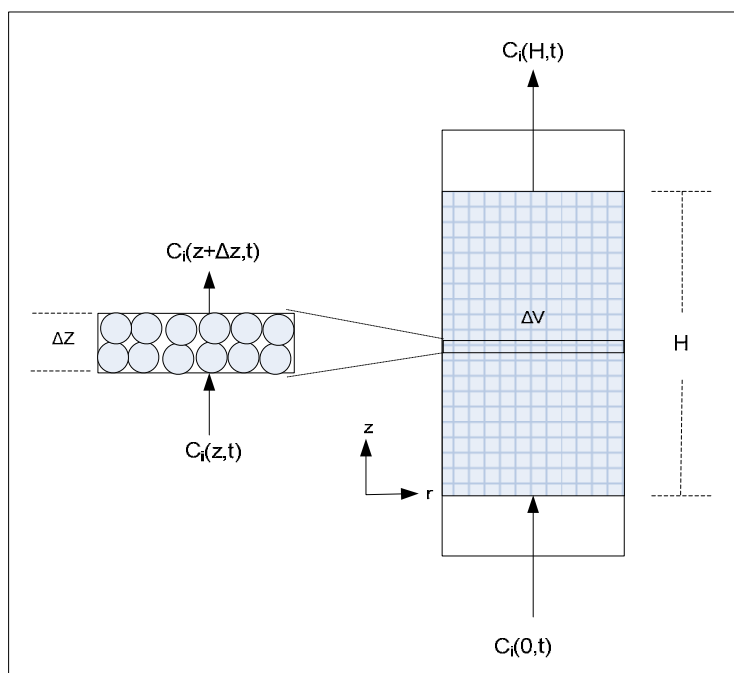


Figure 5-6 Set-up of reactor model

Reactor model Assumptions

In the reactor model, the following assumptions were made:

1. The model is 1-D (only function of the bed height). This assumption is based on the fact that the expected radial concentration gradients are small compared with the axial concentration gradients ($Pe > 3.5$, see section 6.2.1).
2. The gas flow in the fixed bed was assumed a plug flow. This assumption is justified by the calculation of the dispersion coefficient that shows negligible dispersion (see section 6.2.1).
3. Isothermal bed conditions. This assumption is based on the fact that the char particle is isothermal (see section 5.2.7).
4. No mass transfer limitations as found in the particle model results (see section 5.2.7).
5. The hydrogasification reaction is neglected as during the experiments no significant production of methane is measured.

Reactor mass balance

The concentration of the gaseous components and the carbon conversion along the bed can be calculated at any time by solving the mass balance equations.

At any time, the mass balance of the gaseous components on a differential height in the bed becomes:

$$\frac{\partial c_i}{\partial t} + \frac{\partial}{\partial z} (-D_e \frac{\partial c_i}{\partial z} + c_i \cdot u) = R_i \quad (5.52)$$

The first term represents the accumulation. Although, in general, the accumulation of gas is small compared with the accumulation of the solid carbon, the accumulation term is included in the gaseous mass balances as the char properties change with time. The second term represents the gas diffusion in the char bed. The third term represents the effect of convection because of the gas velocity. The right-hand term represents the net generation of the gas components because of the chemical reactions. The above mass balance equation can be used to generate five expressions for the molar concentrations of the gas components H₂O, H₂, CO, CO₂ and naphthalene. Further, a total mass balance equation (including N₂) can be formulated, where the sum of the mole fractions of the gas components is equal to one.

$$\sum_{i=1}^6 x_i = 1 \quad (5.53)$$

Because there is no solid carbon fed or taken out of the bed, the solid (carbon) mass balance of the bed becomes:

$$\frac{\partial \rho_b}{\partial t} = M_C R_C \quad (5.54)$$

The initial conditions of the reactor are a zero inlet molar flow rate (F) and a solid bed density equal to the original one:

$$\begin{aligned} t = 0 \quad F = 0, \text{ or } (c_i = 0) \\ \rho_b = \rho_{b,o} \end{aligned} \quad (5.55)$$

The inlet molar flow rate at the bottom of bed is constant during the experiment (F_o) and represents the producer gas flow that comes from the gasifier. Thus, the boundary conditions can be summarized as follows:

$$z = 0 : \quad F = F_o, \text{ or } (c_i = c_{i,o}) \quad (5.56)$$

Where,

F = molar feed flow rate, kmol/s

ρ_b = bed density, kg/m³

z = distance along the bed height, m

Convective flux was assumed at the exit of the bed.

Tuning the reactor model

The reactor model can be used to estimate the naphthalene and carbon conversion along the bed height and time on stream. The kinetics for the naphthalene conversion reaction is based on the experimental results given in chapter three and four. On the other hand, the number of experimental results for the carbon conversion rate is not

enough to estimate the kinetic constants for the carbon conversion by the steam and dry gasification reactions. Therefore, the kinetics for the carbon gasification reactions were taken from literature [4, 5] and fitted by multiplying the pre-exponential factor with a factor to fit the experimental results.

The tuning factor was estimated by validating the estimated carbon conversions at different temperatures for the experiments presented in chapter four at the reference conditions given in Table 4-2 and Table 5-1. For both the steam and dry gasification kinetics, the same tuning factor has been applied. The results are given in the “low coke factor” column of table 5-2. For experiments at a relatively low temperature (i.e. < 850 °C) or a relatively high gas residence time (i.e. > 0.3 s), the model results overestimate the experimental results. This overestimation can be related to the higher coke formation in and on the char particles. Therefore, the influence of the coke formation was considered by estimating a different tuning factor “High coke factor” for the kinetics at these specific “coke” conditions (see Table 5-2).

Table 5-2 Tuning factor of the pre-exponential constants of the naphthalene and char conversion reactions at different “coke” conditions

	Low coke factor	High coke factor
Naphthalene gasification	1.0	0.94
Steam gasification	0.15	0.033
Dry gasification	0.15	0.033

Coke formation turns out to be an important issue and needs to be investigated more thoroughly. In the present model, the coke formation is simply modeled with a tuning factor to get a preliminary insight in the quantitative influence of the coke formation on the different reaction rates.

5.3.1 Reactor model validation

Solving the gas and carbon mass balance equations gives the concentration of the different gas components, naphthalene reduction and carbon conversion along the bed height. The effects of temperature, gas residence time, particle size and time on stream on the naphthalene and carbon conversion were calculated and validated with experimental results presented in chapter four. As shown in Figure 5-7 to Figure 5-13 the model results agree well with the experiments.

Figure 5-7 shows a comparison between the measured naphthalene conversion as function of temperature and model calculations at high and low coke conditions. It is found that the coke formation does not significantly affect the naphthalene conversion.

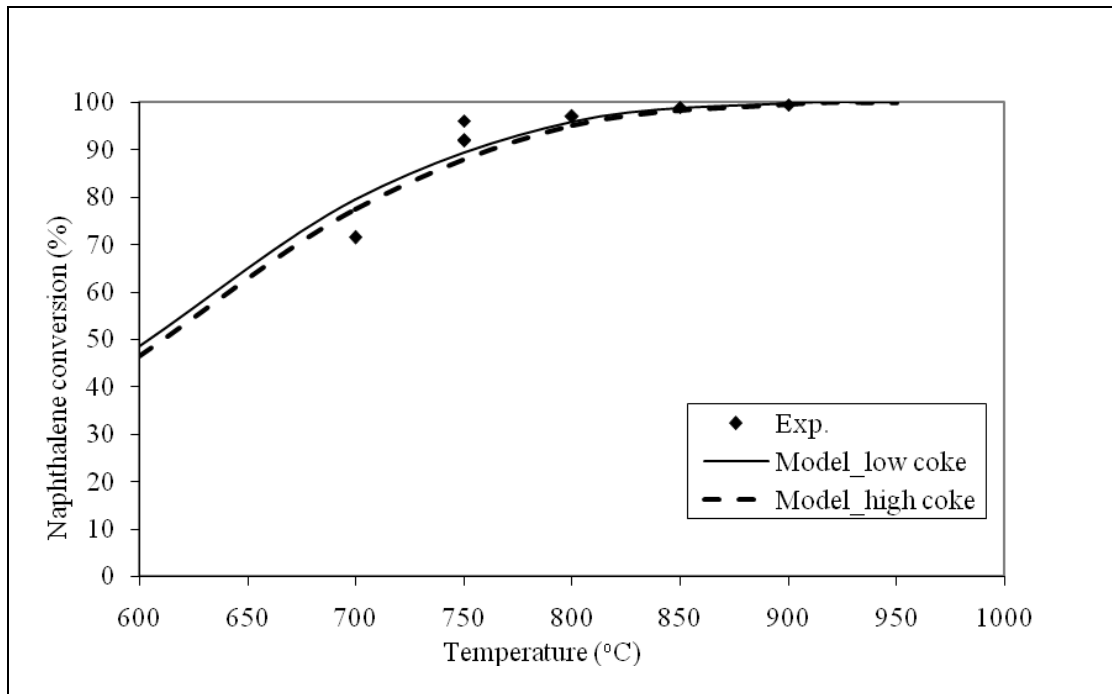


Figure 5-7 Validation of the model calculations with the tuning factor for both the low and high coke situation (Table 5-2) for the naphthalene conversion as a function of temperature with experimental results, τ : 0.3 s; d_p : 500-800 μ m; Gas mixture: Table 4-2; time on stream: 15 min

Figure 5-8 shows a comparison between the measured carbon conversion as function of temperature and model calculations at high and low coke conditions. It is found that the model calculations at low coke conditions fit the real tar experiments carried out at short residence time and the model calculations at high coke conditions fit the naphthalene experiments carried out at long residence time. This means that a longer residence time causes a higher coke formation.

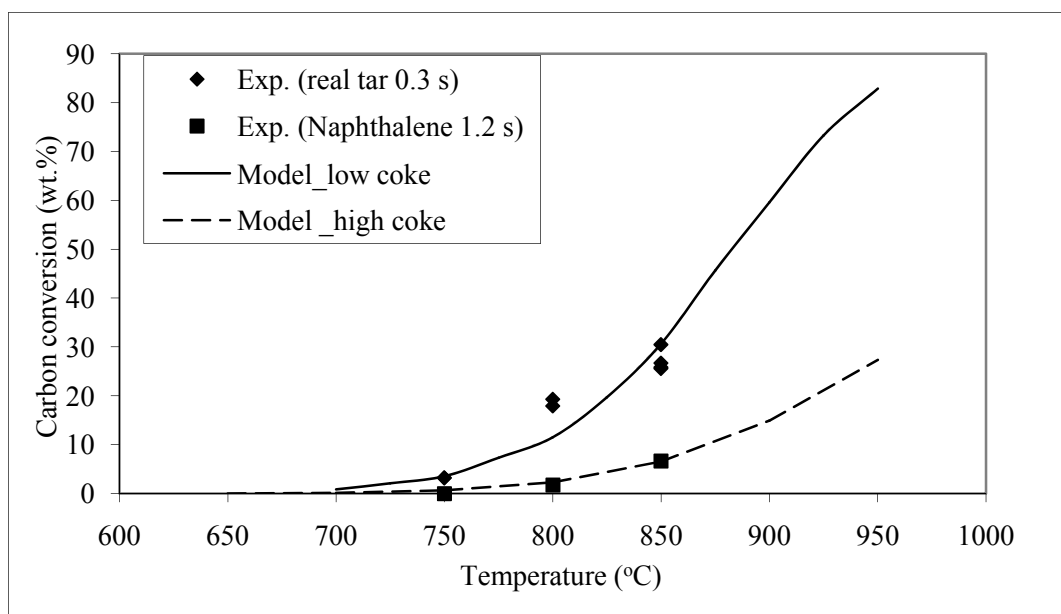


Figure 5-8 Validation of the model calculations with the tuning factor for both the low and high coke situation (Table 5-2) for the carbon conversion as a function of temperature with experimental results. Naphthalene: τ : 1.2 s; d_p : 500-630 μm ; Gas mixture: Table 4-2. Real tar: τ : 0.3 s; d_p : 500-630 μm ; Gas mixture: Table 5-1; time on stream: 60 min

Figure 5-9 shows a comparison between the measured naphthalene conversion as function of gas residence time and the model calculations at high and low coke conditions. The experiments were carried out at a low temperature of 750 °C. It is found that the model calculations at high coke conditions fit experiments carried out at low temperature better than and the model calculations at low coke conditions. This validates that at low temperatures, a higher coke formation occurs.

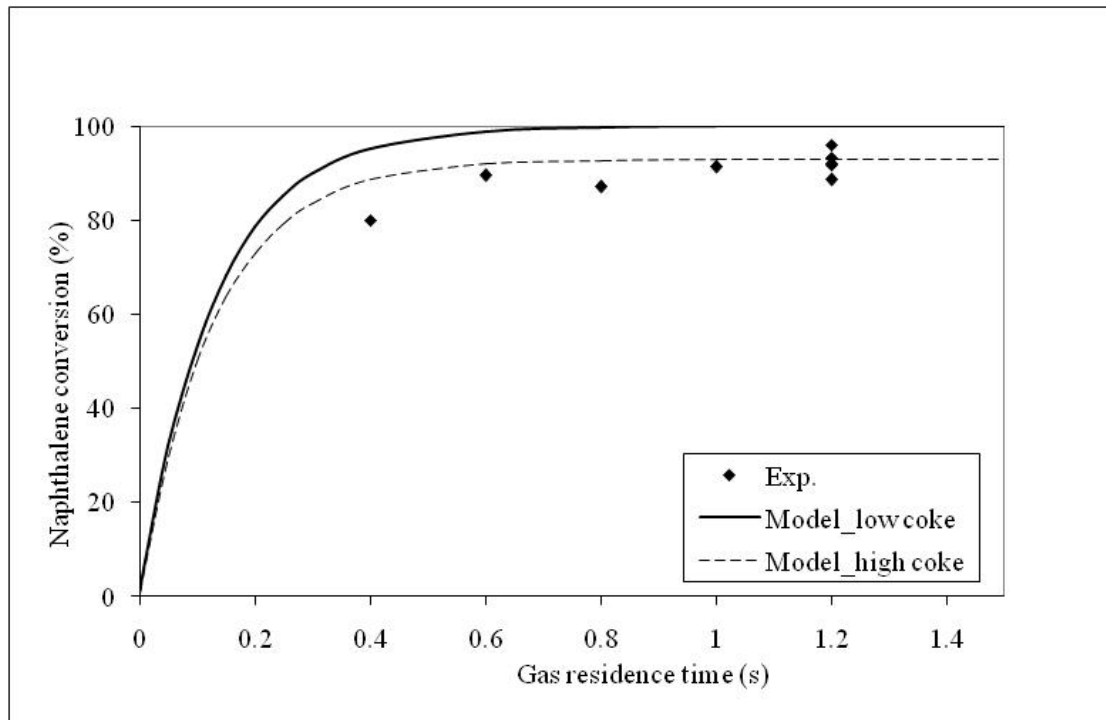


Figure 5-9 Validation of the model calculations with the tuning factor for both the low and high coke situation (Table 5-2) for the naphthalene conversion as a function of gas residence time with experimental results. T_R : 750 °C; d_p : 1000-1180 μm ; Gas mixture: Table 4-2; time on stream: 15 min

Figure 5-10 shows a comparison between the measured carbon conversion as function of the gas residence time and the model calculations at high and low coke conditions. It is found that the model calculations at low coke conditions fit best with the real tar experiments carried out at low residence times, while the model calculations at high coke conditions fit best with the naphthalene experiments carried out at long residence times. This validates that at short residence times, low coke formation occurs and at long residence times, high coke formation occurs.

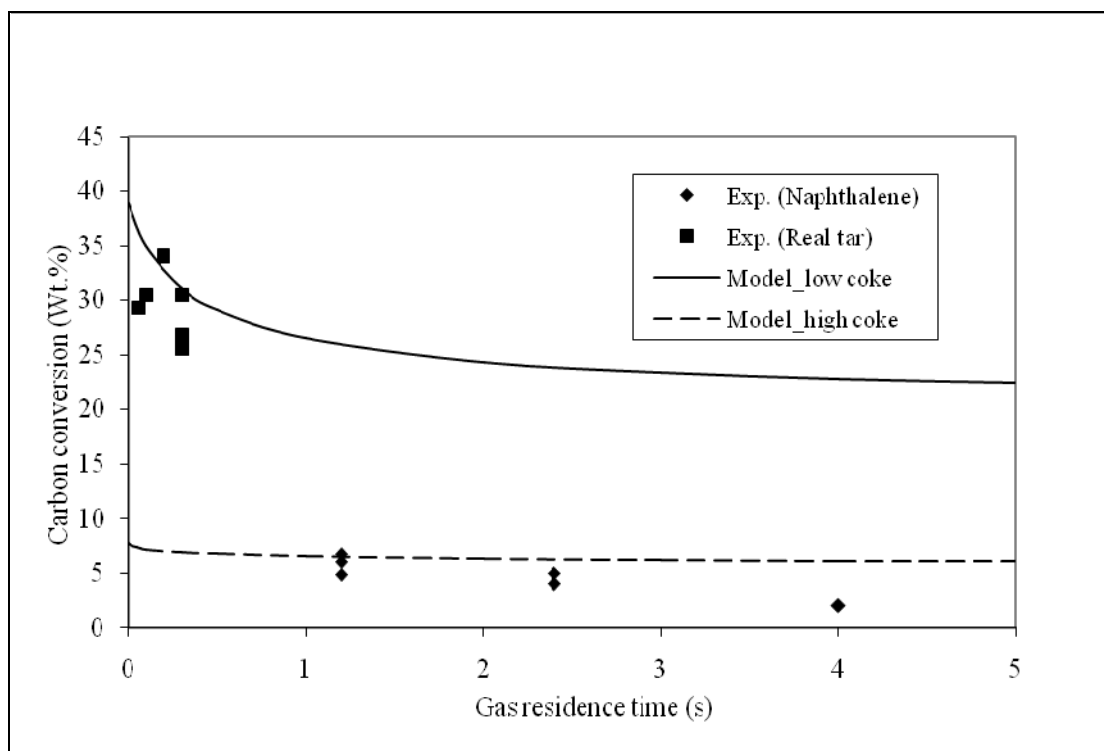


Figure 5-10 Validation of the model calculations with the tuning factor for both the low and high coke situation (Table 5-2) for the carbon conversion as a function of gas residence time with experimental result. Exp. (Naphthalene): T_R : 850 °C; d_p : 500-630 μm ; Gas mixture: Table 4-2; time on stream: 60 min. Exp. (Real tar): T_R : 850 °C; d_p : 500-630 μm ; Gas mixture: Table 5-1; time on stream: 60 min

Figure 5-11 shows a comparison between the measured naphthalene conversion at long residence time as function of particle size and the model calculations at high and low coke conditions. It can be seen that the model calculations at high coke conditions fit best with the naphthalene conversion experiments carried out at low temperature (750 °C). This validates that low temperatures and long residence time cause higher coke formation. Further, the particle size has no significant effect on the naphthalene conversion at these conditions as the conversion is kinetically limited.

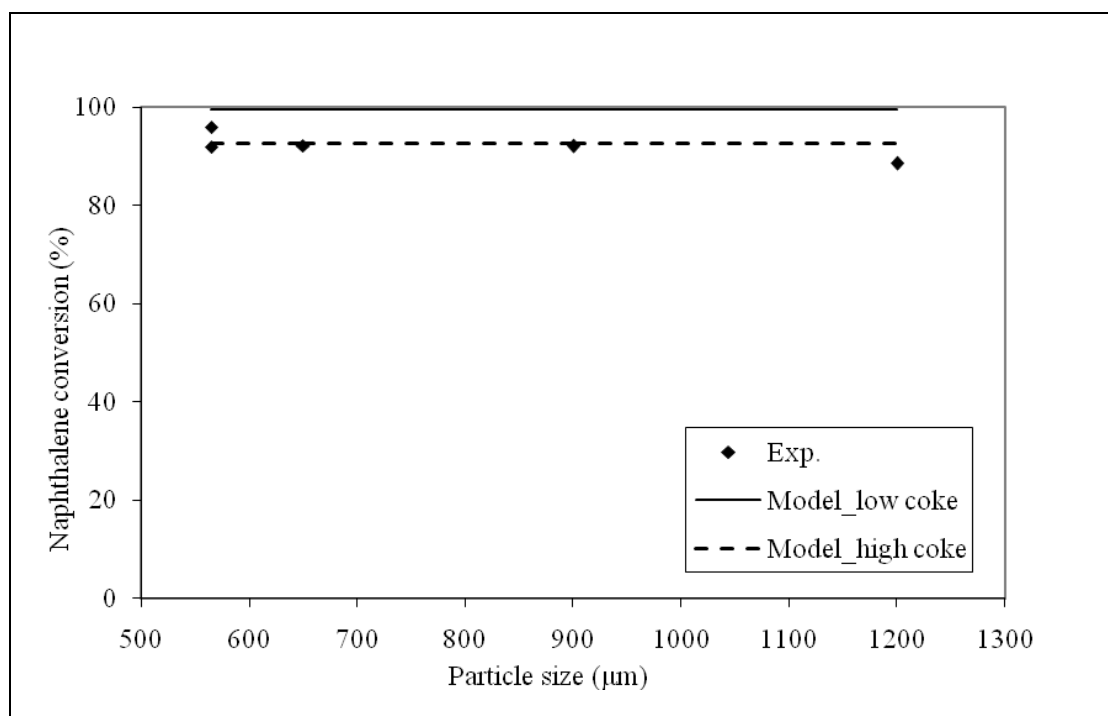


Figure 5-11 Validation of the model calculations with the tuning factor for both the low and high coke situation (table 5-2) for the naphthalene conversion as a function of particle size with experimental results. T_R : 750 °C; τ : 1.2 s; Gas mixture: Table 4-2, time on stream: 15 min

Figure 5-12 shows a comparison between the measured carbon conversion as function of time on stream for a long residence time (1.2 s) and two particle sizes (500-630 μm and 1400-1700 μm) and the model calculations at high and low coke conditions. It can be seen that the model calculations at high coke conditions fit best with the experiments for both particle sizes. This validates that long residence times cause high coke formation whereas the particle size has no effect on the carbon conversion.

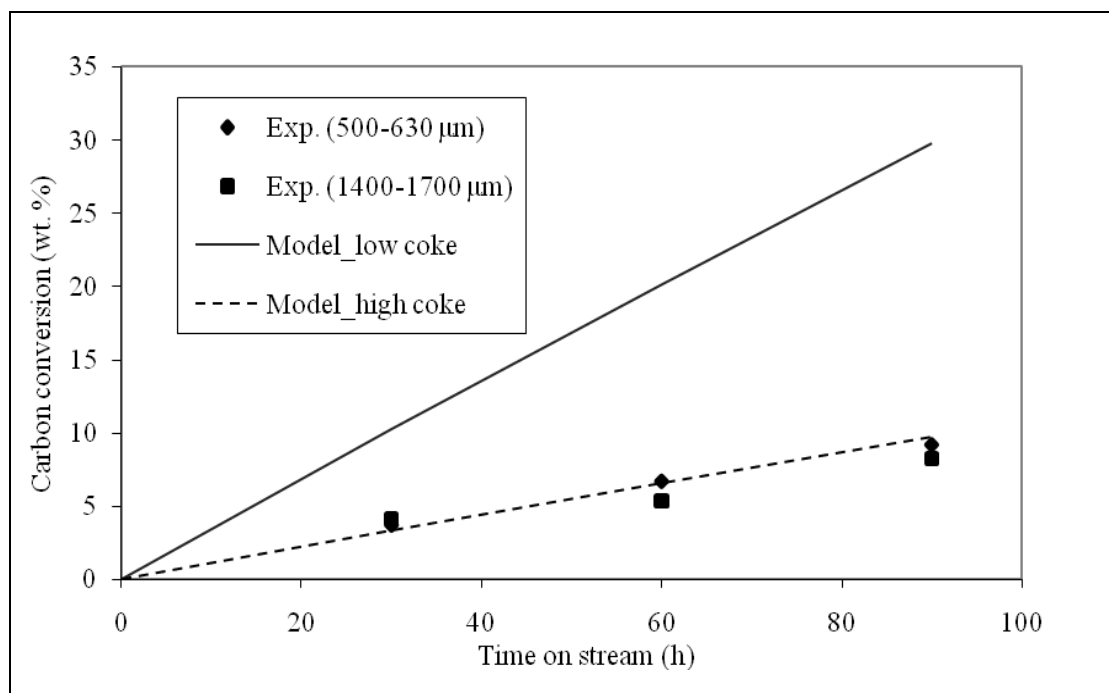


Figure 5-12 Validation of the model calculations with the tuning factor for both the low and high coke situation (table 5-2) for the carbon conversion as a function of particle size with experimental results. T_R : 850 $^{\circ}\text{C}$; τ : 1.2 s; Gas mixture: Table 4-2

Figure 5-13 shows the carbon conversion as function of time on stream for the carbon conversion experiments carried out at long residence time (2.4 s for naphthalene) and short residence time (0.3 s for real tar) and the model calculations at high and low coke conditions. It can be seen that the model calculations at high coke conditions fit best with the experiments carried out at long residence time for naphthalene, and the model calculations at low coke conditions fit best with the experiments carried out at short residence time for real tar. This validates that at long residence times occurs high coke formation whereas at short residence times low coke formation occurs.

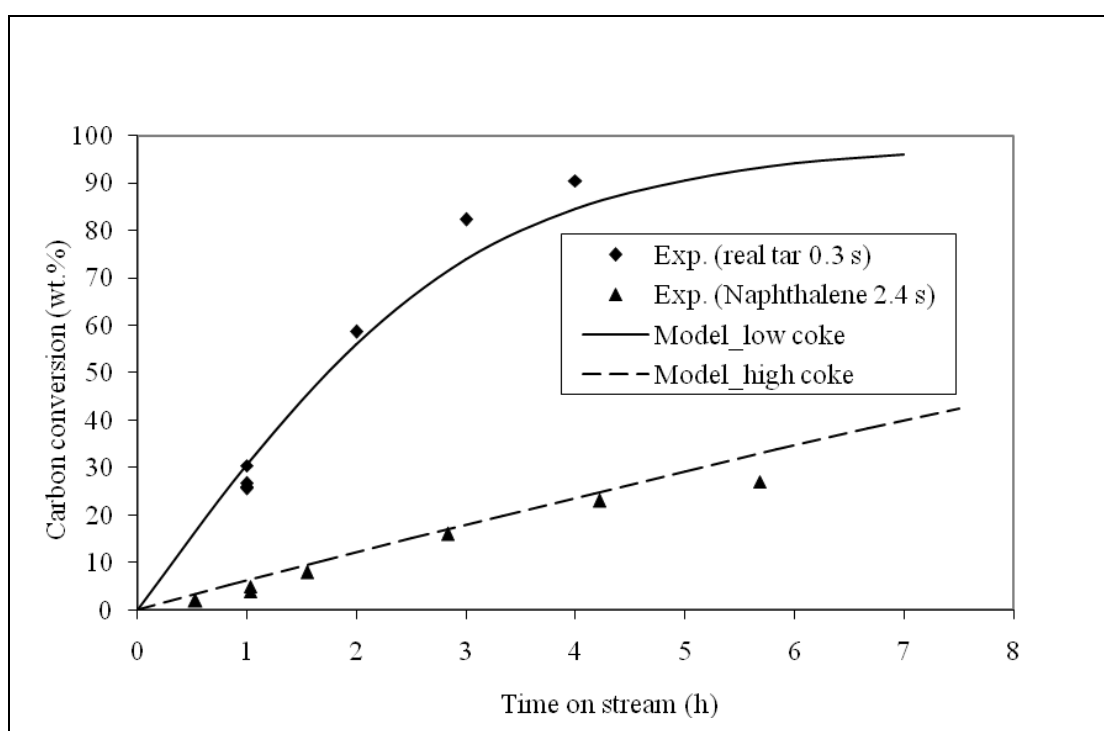


Figure 5-13 Validation of the model calculations with the tuning factor for both the low and high coke situation (table 5-2) for the naphthalene conversion as a function of time on stream with experimental results. Exp. (Naphthalene): T_R : 850 °C; τ : 2.4 s; d_p : 500-630 μm ; Gas mixture: Table 4-2. Exp. (Real tar): T_R : 850 °C; τ : 0.3 s; d_p : 500-630 μm ; Gas mixture: Table 5-1

From the validation results in Figure 5-7 to 5-13, it can be concluded that the effect of coke on tar and carbon conversion is significant at low reactor temperatures and high gas residence times. In addition, the model results agree well with the experimental results.

5.3.2 Key parameters for optimal design

The main criteria for an optimum design of a tar cracker with a fixed char bed are high tar reduction, low energy consumption and high gas throughput. Thus, the key parameters for an optimum design are: temperature, gas residence time in the bed and the time on stream. The temperature is dominating the naphthalene conversion and the

energy consumption; the gas residence time is important for the gas throughput; and the time on stream affects the amount of char refreshment of the char bed. The developed reactor model has been used to investigate the aforementioned key parameters.

Temperature

The naphthalene reduction and the carbon conversion reactions are kinetically controlled. The maps for the effect of the temperature on the naphthalene and carbon conversion are given in Figure 5-14 and Figure 5-15. The lowest temperature that gives complete naphthalene removal is the favored one to reduce energy cost. A temperature of 850 °C can be considered a good selection because of 1) almost complete naphthalene conversion (> 98%), 2) low coke influence on tar conversion and 3) moderate carbon consumption.

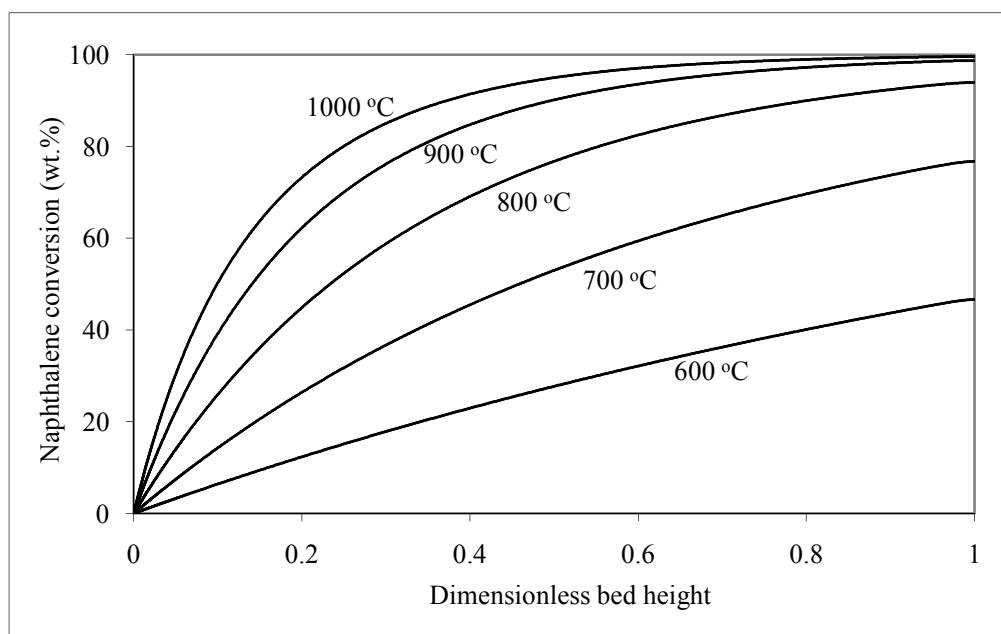


Figure 5-14 Effect of the bulk temperature on the naphthalene conversion along the dimensionless bed height. d_p : 600 μm ; Gas mixture: Table 5-1; time on stream: 1 s

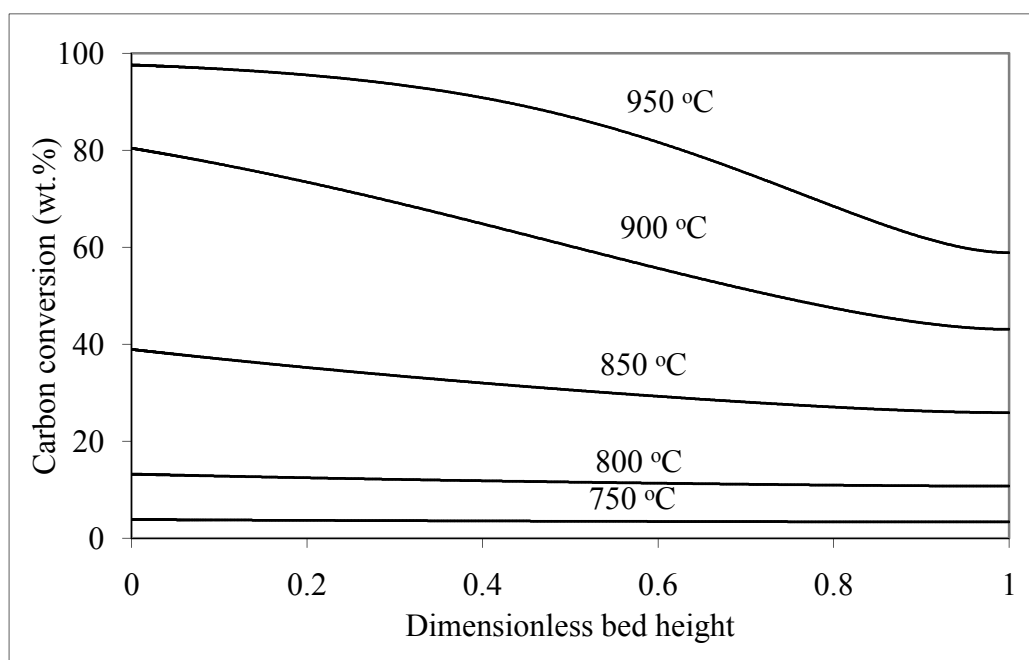


Figure 5-15 Effect of the bulk temperature on the carbon conversion along the dimensionless bed height. T_R : 850 °C; d_p : 600 μm ; Gas mixture: Table 5-1; time on stream: 60 min

Gas residence time

The tar conversion reaction is not very fast. Thus, we have to insure that the tar has enough time in the catalyst bed to be converted. Several definitions for residence time have been used in literature. Here, the residence time (τ) in the catalyst bed with respect to the empty catalyst bed volume is selected. The gas residence time in the reactor is varied by varying the superficial gas velocity. The effect of the gas residence time on the naphthalene and char conversion is given in Figure 5-16 and Figure 5-17. This parameter affects the concentration profile of the gases along the bed height. Because the concentration of the steam and CO_2 is decreasing along the bed height, the carbon conversion decreases as well. Thus, decreasing the gas residence time by increasing the gas velocity flattens the gas concentration profile along the bed height and flattens the carbon conversion profile as well. A more flat profile means a better overall use of the char bed. On the other hand, increasing the gas residence time increases the naphthalene conversion, which is kinetically limited. Thus, the higher the tar residence time, the higher is the tar conversion. However, going for higher residence times increases the size of the tar cracker. A value of 0.3 s gas residence time seems to be a good selection because it almost insures a complete tar conversion at 850 °C. However, for a moving char bed, one could decide to choose a higher residence time because this will result in the consumption of the lower part of the bed. In this situation, the bed temperatures could be lowered further. Here, we decide for a gas residence time of 0.3 s and a temperature of 850 °C.

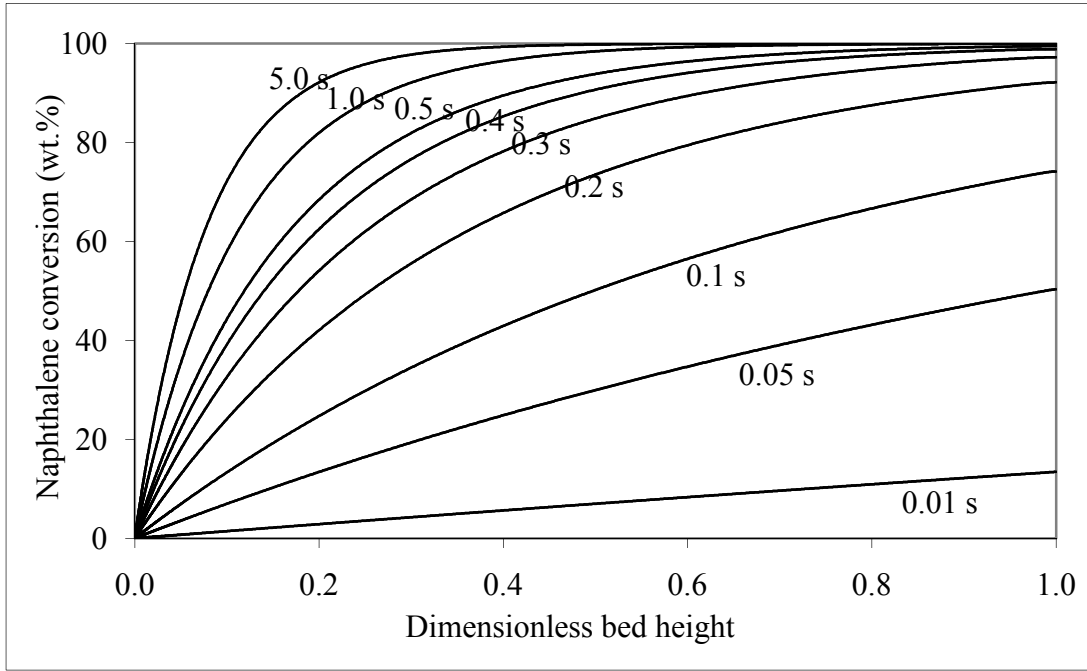


Figure 5-16 Effect of the gas residence time on the naphthalene conversion along the dimensionless bed height. T_R : 850 °C; d_p : 600 μm ; Gas mixture: Table 5-1; time on stream: 1 s

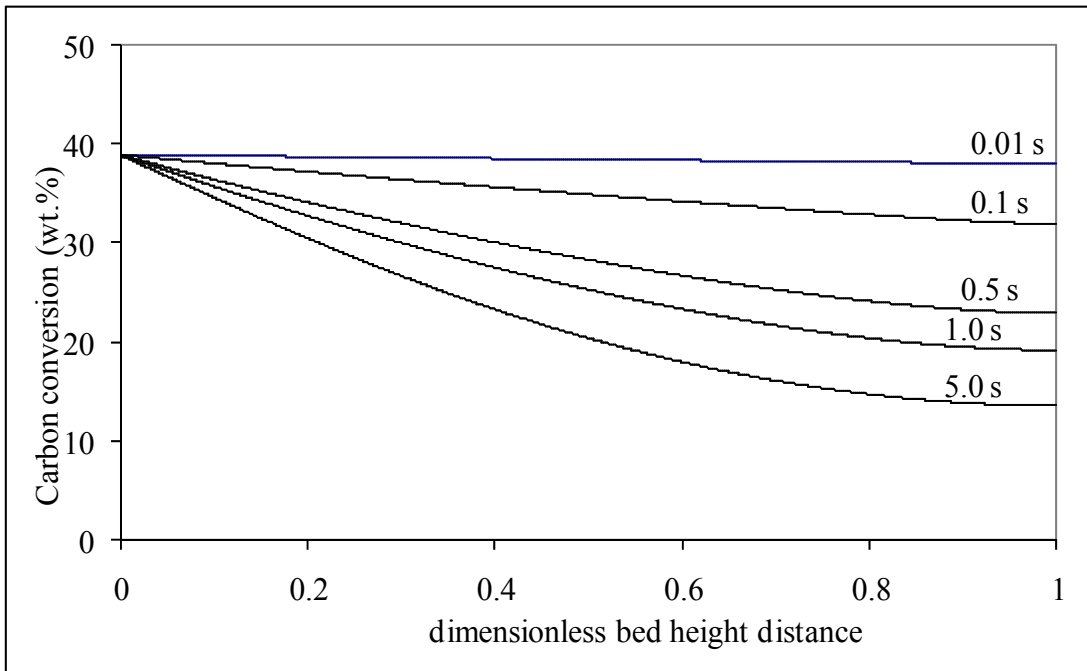


Figure 5-17 Effect of the gas residence time on the carbon conversion along the dimensionless bed height. T_R : 850 °C; d_p : 600 μm ; Gas mixture: Table 5-1; time on stream: 60 min

Time on stream

The time on stream is an important parameter because it reveals the time-dependent characteristics of the char in the tar cracker. In this way, the char consumption of the tar cracker may be calculated. Thus, for a successful design of the tar cracker, the consumed char should be continuously compensated by the char produced in the biomass gasifier. The maps for the effect of the time on stream on the naphthalene and carbon conversion are given in Figure 5-18 and Figure 5-19. Although it cannot be seen in Figure 5-18, the naphthalene conversion is independent of the time on stream because of the char activity that was found to be constant at a temperature of 850 °C or above.

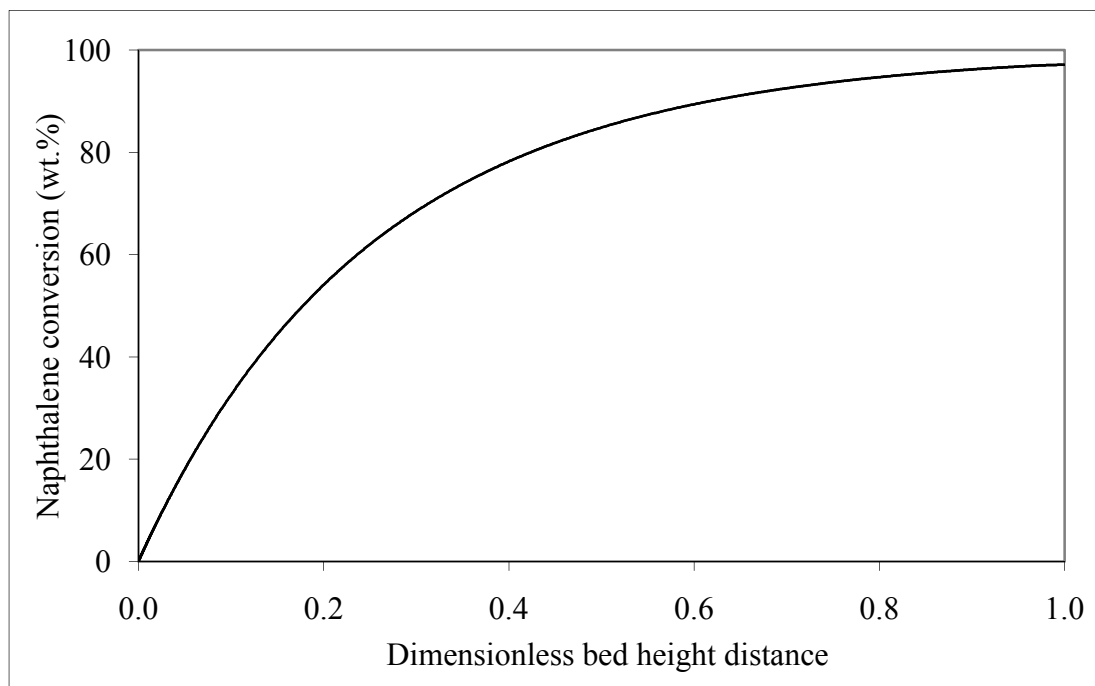


Figure 5-18 Effect of the time on stream (lines coincide with one another) on the naphthalene conversion along the dimensionless bed height. T_R : 850 °C; τ : 0.3 s; d_p : 600 μm ; Gas mixture: Table 5-1

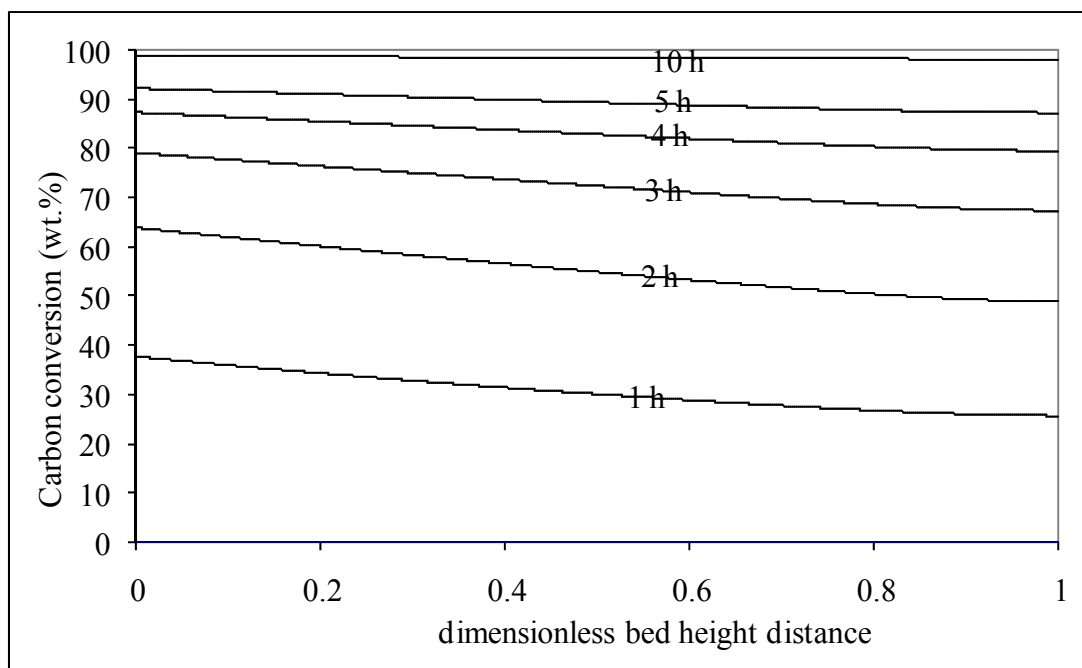


Figure 5-19 Effect of the time on stream on the carbon conversion along the dimensionless bed height. T_R : 850 °C; τ : 0.3 s; d_p : 600 μm ; Gas mixture: Table 5-1

5.4 Evaluation

In chapter four, several parameters that affect the tar reduction and the carbon conversion were experimentally investigated. The knowledge gained from the previous chapter is used here to develop a model for the naphthalene reduction by biomass char for both particle and reactor scale. Moreover, the models are used to validate and further explain the experimental results of the previous chapter.

The experimental results given in chapter four show that the naphthalene and carbon conversion reactions are kinetically limited. The experiments also show that the internal mass transfer has a minor effect. In this chapter, the particle model calculations support this result and show that there are no internal or external mass transfer effects on the naphthalene and carbon conversions.

From the experiments in chapter four, it was shown that for temperatures of 850 °C or higher, the activity of the char bed for the naphthalene conversion does not depend on the time on stream. Therefore, the reactor model calculations for the naphthalene concentration profile along the bed height can be simplified to a plug flow reactor ($C = C_o e^{-k\tau}$). So that, we have only two parameters that affect the naphthalene conversion: the naphthalene residence time in the char bed and the temperature of the char bed.

On the other hand, the carbon is converted because of the gasification reactions with steam and CO_2 . The rate of these reactions is highly dependent on the temperature because they are kinetically limited. Moreover, the physical properties of the char particle and the pore structure change with the carbon content conversion.

Therefore, the reaction surface area within the particle is changing with time on stream. Thus, the activity of the carbon conversion reactions changes with the time on stream. Because the concentration of the steam and CO₂ is decreasing along the bed height, the carbon conversion decreases as well. Thus, decreasing the gas residence time by increasing the gas velocity flattens the gas concentration profile along the bed height and flattens the carbon conversion as well.

To get insight in the integration of a fixed bed tar cracker downstream of a biomass gasifier, a preliminary design was made. The tar cracker was integrated with the gasifier by compensating the char consumption in the tar cracker with the produced ash from the gasifier that contains mainly char. A scheme of such integration is shown in Figure 5-20.

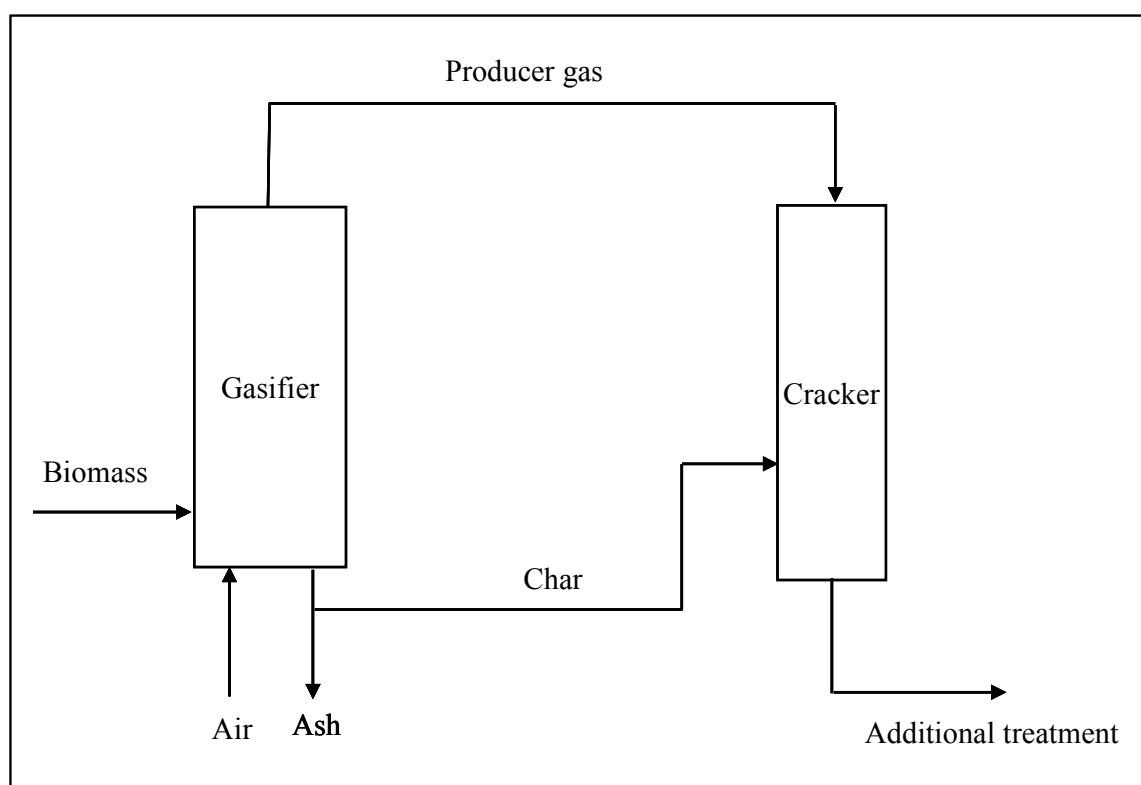


Figure 5-20 Scheme of the integrated fixed bed tar cracker downstream the biomass gasifier

Fixed beds are commonly used for small scale processes. Thus, the fixed bed tar cracker is integrated with a fixed bed gasifier. The values of the key parameters (i.e. temperature and gas residence time) discussed in the previous section were used in the design of the tar cracker. The particle size of the char particles was selected to be 5 mm in order to increase the particles minimum fluidization velocity and prevent blowing out the particles. Nevertheless, the internal mass transfer is expected to be negligible as found earlier. For small scale gasification processes, the downdraft gasifier is often used. Here a capacity of 10 MWth was selected. A summary of the integrated gasification process parameters is given in Table 5-3 and Table 5-4.

Table 5-3 Summary of the input parameters of the integrated gasification process

	Unit	Value
Gasifier		
Type		downdraft fixed bed
Capacity	MW th	10
Heating value of biomass(Beech wood) [24]	MJ/kg	18
Biomass supply	ton/h	1.96
Carbon conversion of the biomass feed	%	90
Tar concentration in the producer gas	mg/Nm ³	1000
Gas production per kg biomass [25]	Nm ³ /kg	2
Cracker		
Temperature	T(°C)	850
Gas residence time	τ (s)	0.3 s
Char particle size	d_p (mm)	5

Table 5-4 Summary of the output results of the integrated gasification process

	Unit	Value
Gasifier		
Rate of total ash production	ton/h	0.196
Cracker		
Tar concentration in the output gas	mg/Nm ³	13
Rate of consumed char	ton/h	0.194

The output tar content from the tar cracker was estimated to be 13 mg/Nm³. This concentration is clean enough for power production applications. The tar reduction degree is 98.3%. Moreover, the rate of biomass char consumed in the cracker is found to be lower than the ash produced in the gasifier assuming 90 % carbon conversion of the biomass [28].

The sizing of the tar cracker can be done by making a mass balance on the integrated gasification process (see Table 5-5). The superficial gas velocity was assumed to be 80 % of the minimum fluidization velocity ($U = 0.8 \cdot U_{mf}$). The cross section area was estimated from gas flow to the tar cracker and the gas superficial velocity ($A = v/U$). The bed diameter can be calculated from the bed area. On the other hand, the height of the char bed was estimated using the gas residence time and the gas superficial velocity ($H = \tau \cdot U$).

Table 5-5 Sizing of the fixed bed tar cracker

	Symbol	Value
Volume of the char bed	$V_R(\text{m}^3)$	1.11
Diameter of the char bed	$D(\text{m})$	0.98
Height of the char bed	$H(\text{m})$	1.46
Height to bed ratio	$H/D(-)$	1.48

The height to diameter ratio (H/D) of the tar cracker is dependent on the particle size. As the particle size increases the minimum fluidization velocity increases and thus more gas can flow through the area of the cracker. This gives a lower bed diameter and a higher bed height as shown in Figure 5-21. From this preliminary design it could be seen that the resulting cracker is very compact.

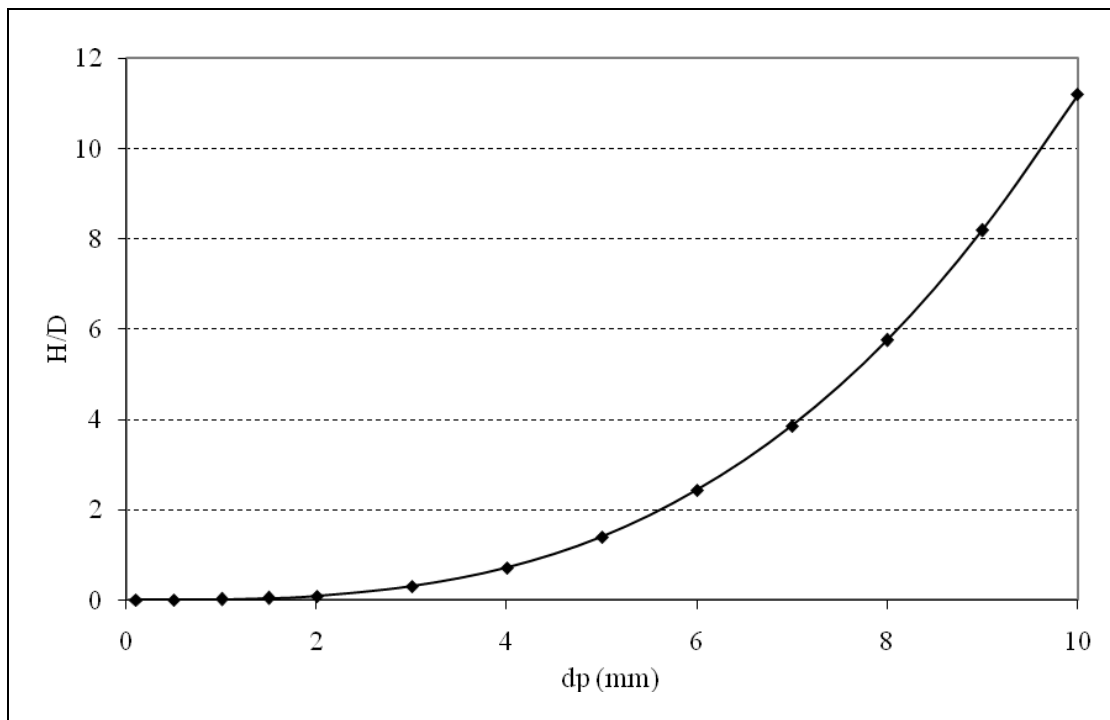


Figure 5-21 Effect of the char particle size on the height to bed ratio of the cracker

5.5 Concluding Remarks

For the naphthalene reduction with a fixed char bed, the following conclusions can be drawn:

- Isothermal conditions can be assumed.
- The naphthalene and char gasification reactions are kinetically limited.
- The main parameters that affect the naphthalene conversion are: the char bed temperature and gas residence time. Optimum values for these parameters are 850 °C and 0.3 s, respectively.
- The main parameters that affect the char conversion are: the char bed temperature, gas residence time and steam flow.
- Operating at a high gas residence time (> 0.3 s) and a low char bed temperature (< 850 °C) causes higher coke formation and significantly reduces the carbon conversion and naphthalene reduction.
- A more sophisticated model for the coke formation needs to be developed.
- A preliminary design of a fixed bed gasifier and a fixed bed tar cracker has been developed. Model results show a naphthalene (tar) reduction degree of 98.3%.

References

1. Dasappa, S., et al. *Wood-Char Gasification: Experiments and Analysis on Single Particles and Packed Beds*. in *Twenty-Seventh Symposium (International) on Combustion / The Combustion Institute*. 1998.
2. Wurzenberger, J.C., S. Wallner, and H. Raupenstrauch, *Thermal Conversion of Biomass: Comprehensive Reactor and Particle Modeling*. AICHE, 2002. **48**(10): p. 2398-2411.
3. Wang, Y.F. and S.K. Bhatia, *A generalised Dynamic Model for Char Particle Gasification with Structure Evolution and Peripheral Fragmentation*. *Chemical Engineering Science*, 2001. **56**: p. 3683-3697.
4. Barrio, M., et al. *Steam Gasification of Wood Char and the Effect of Hydrogen inhibition on the Chemical Kinetics*. in *Progress In Thermochemical Biomass Conversion*. 2001. Tyrol, Austria: Blackwell Science Ltd.
5. Barrio, M. and J.E. Hustad. *CO₂ Gasification of Birch Char and the Effect of CO Inhibition on the Calculation of Chemical Kinetics*. in *Progress In Thermochemical Biomass Conversion*. 2001. Tyrol, Austria: Blackwell Science Ltd.

6. Bartholomew, C.H., *Mechanism of Catalyst Deactivation*. Applied Catalysis A: General, 2001. **212**: p. 17-60.
7. Katta, S. and D. Kerlins, *Study of Kinetics of Carbon Gasification Reactions*. Ind. Eng. Chem. Fundam., 1981. **20**: p. 6-13.
8. Messenbk, R.C., D.R. Dugwell, and R. Kandiyoti, *CO₂ and Steam-Gasification in a High-Pressure Wire-Mesh Reactor: The Reactivity of Daw Mill Coal and Combustion Reactivity of its Chars*. Fuel, 1999. **78**: p. 781.
9. Devi, L., *Catalytic Removal of Biomass Tars; Olivine as Prospective in-Bed Catalyst for Fluidized-Bed Biomass Gasifiers*. 2005, Technical University of Eindhoven: Eindhoven, The Netherlands.
10. Jess, A., *Catalytic Upgrading of Tarry Fuel gases: A Kinetic Study with Model Components*. Chemical Engineering and Processing, 1996. **35**: p. 487-494.
11. Srinvas, B., *Model Studies on Single Partcile Char Gasification and Combustion*, in *The Faculty of Department of Chemical Engineering*. 1980, University of Houston.
12. Neogi, D., et al., *Study of Coal Gasification in an Experimental Fluidized Bed Reactor*. AIChE Journal, 1986. **32**(1): p. 17-28.
13. Laurendeau, N.M., *Heterogeneous Kinetics of Coal Char Gasification and Combustion*. Prog. Energy Combust. Sci., 1978. **4**: p. 221-270.
14. Kunii, D. and Y. Suzuki, *Particle-to-Fluid Heat and Mass Transfer in Packed Beds of Fine Particles*. International Journal of Heat and Mass Transfer, 1967. **10**: p. 845.
15. Levenspiel, O., *Chemical Reaction Engineering*. Second Edition ed. 1972, Singapore: Wiley & Sons, Inc. 472.
16. Bird, R.B., W.E. Stewart, and E.N. Lightfoot, *Transport Phenomena*. Second ed. 2002, New York: John Wiley & Sons, Inc.
17. Valk, M., ed. *Atmospheric Fluidized Bed Coal Combustion: Research, Development and Application*. Coal Science and Technology, ed. L. Anderson. Vol. 1. 1995, Elsevier: Amsterdam. 71.
18. Groeneveld, M.J. and W.P.M. Van Swaaij, *Gasification of Char Particles with CO₂ and H₂O*. Chemical Engineering Science, 1980. **35**: p. 307-313.
19. Guo, J., *Pyrolysis of Wood Powder and Gasification of Wood-Derived Char*. 2004, Technical University of Eindhoven: Eindhoven, The Netherlands.
20. Dutta, S., C.Y. Wen, and R.J. Belt, *Reactivity of Coal and Char. 1. In Carbon Dioxide Atmosphere*. Ind. Eng. Chem. Process Des. Dev., 1977. **16**(1): p. 20-30.
21. Hong, J., *Modeling Char Oxindation as a Function of Pressure using an Intrinsic Rate Equation*, in *Department of Chemical Engineering*. 2000, Brigham Young University.

22. Srinivas, B., *Model Studies on Single Particle Char Gasification and Combustion*, in *Chemical Engineering*. 1980, University of Houston.
23. www.comsol.com.
24. <http://www.ecn.nl/phyllis/>.
25. van der Drift, A., C.M. van der Meijden, and S.D. Srating-Ytsma. *Ways to Increase Carbon Conversion of a CFB-Gasifier*. in *12th European Conference on Biomass for Energy, Industry and Climate Protection*. 2002. Amsterdam, The Netherlands: ETA-Florence.

Chapter 6

Tar Reduction in a Bubbling Fluidized Char Bed

Abstract

In this chapter, the tar reduction performance of biomass char at fluidized bed conditions is discussed. First, a model on the naphthalene removal in a bubbling fluidized char bed is presented and then the model is validated against experimental results. The model is used to study the effect of the following parameters on the naphthalene conversion: the particle size, temperature, and height of the fluidizing char bed. Mass transfer of the naphthalene between the bubble and dense phase is the main factor for the naphthalene removal. It can be increased by increasing the particle size, bed height and bed temperature. The model results agree well with the experimental results.

Finally, a novel experiment is presented where biomass was gasified in a fluidized char bed. In this situation, the char production by the gasification reaction and its catalytic activity for tar cracking take place simultaneously inside the gasifier. It was found that this in-situ biomass gasification in a char bed seems to be very promising for (partial) solving of the tar problem. In this preliminary experiment, a producer gas with tar content below 300 mg/Nm³ was produced at a gasification temperature of 850 °C. This corresponds to more than 97 % tar reduction compared with gasification in a fluidized bed of inert sand particles.

6.1 Introduction

Fixed bed experiments reported in chapter four proved that the biomass char is a catalyst of high potential. It is active and can be produced in the gasification process itself (low-cost). It would be interesting to explore the biomass char as a catalyst in medium scale gasification processes. The common types of reactor for medium scale are fluidized beds. The main advantages of the fluidization technology are the avoidance of hot spots, high rates of heat transfer and excellent gas-solid contacting [1, 2]. Fluidized bed reactors may operate in several fluidization regimes: bubble, turbulent, fast and pneumatic fluidization [3]. For this study, a bubbling fluidized bed was selected for further investigation. For the modeling of the hydrodynamics of the bubbling bed, a model which also covers the turbulent regime has been developed by Thompson and is called the GBT model (Generalized Bubbling/Turbulent) [4]. Besides that, the process was modeled using a simple two-phase reactor model. We used the model to study the effect of the bed height (gas residence time) and the particle size on the gases concentration profiles along the height of the reactor and estimate the naphthalene and the carbon conversion. The model was validated against experimental results concerning naphthalene reduction in a fluidized char bed. Finally, a novel experiment was carried out where biomass was fed in a fluidized char bed. In this way the biomass char was simultaneously used as a catalyst and bed material inside the fluidized bed biomass gasifier.

6.2 Model Development

The rate of tar conversion in the fluidized bed can be controlled by two phenomena: the mass transfer between the different phases (e.g., bubble and emulsion, and mass transfer in and around the char particle) and the chemical reaction rate. The hydrodynamics control the mass transfer in the bed, while the rate of the chemical reaction is controlled by the amount of catalyst (char). For slow reactions, the chemical kinetics control the conversion rate, while for very fast reactions the conversion is controlled by hydrodynamics. For intermediate reaction rates (such as the tar reduction reaction), both, the chemical reaction and the hydrodynamics are controlling the tar conversion rate. A model is developed for the case that producer gas containing tar is supplied to a downstream fluidized char bed cracker. In the model, it is assumed that the tar is supplied to the fluid bed via the inlet gas flow. Therefore, a part of the tar will directly enter the emulsion phase (e) and the other part will go into gas bubbles (b), see Figure 6-1. In the bed, an exchange of gases between the bubble and the dense phase occurs. This mass transfer can be described with the inter-phase mass exchange factor (K_{be}). In the emulsion phase, it is assumed that there is complete mixing in the radial direction. The mass transfer around the particle and pore diffusion within the particles is also taken in account in the model. The tar is assumed to react on the char surface or to deposit as coke. The kinetic model used in the fixed bed reactor model (see section 5.2.1) is also used here.

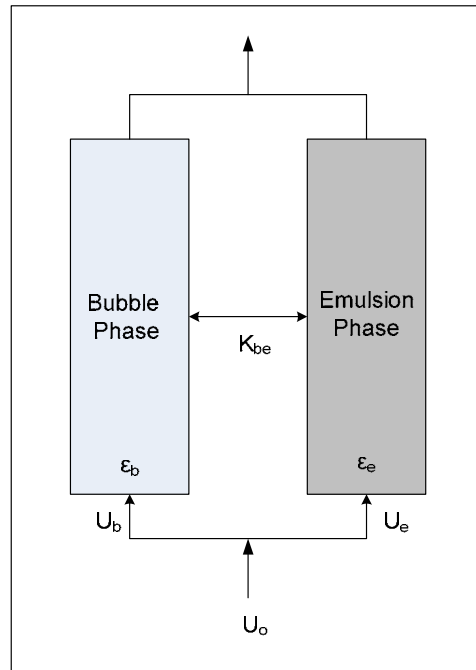


Figure 6-1 Two-phase fluidization model

In the following section, the hydrodynamics model used in the reactor model is described.

6.2.1 Hydrodynamics

The hydrodynamics model is a part of the reactor model that describes the effect of the mass transfer on the gas-char reactions. The degree of back-mixing of the gas in the axial direction in the reactor determines the selection of the hydrodynamics model. Therefore, it is needed to calculate the dimensionless Peclet number (Pe) to determine the type of flow.

$$Pe = v \cdot \frac{L}{D_l} \quad (6.1)$$

$Pe \rightarrow 0$ large dispersion, hence mixed flow

$Pe \rightarrow \infty$ negligible dispersion, hence plug flow

Where,

L = length of the bed, m

v = velocity, m/s

D_l = dispersion coefficient, m^2/s

To determine the dispersion coefficient (D_l), the Chung and Wen [5] correlation is used. They correlated the axial dispersion coefficients using many data in literature, both for fixed and fluidized beds. The correlation can be used for the present conditions.

$$\varepsilon \cdot Bo \cdot \frac{Re}{Re_{mf}} = 0.2 + 0.011 \cdot Re^{0.48} \quad (6.2)$$

(*Bo*) is Bodenstein number and is defined as:

$$Bo = v \cdot d_p / D_l \quad (6.3)$$

Where,

d_p = particle size, m

D_l = coefficient of longitudinal dispersion, m²/s

Re = Reynolds number

v = velocity, m/s

m_f = minimum fluidization, m/s

From the above two correlations D_l and thus the Pe-number can be estimated. For the considered experimental conditions given in Table 6-2, the Pe-number was found to be relatively high (> 3.5) and thus the gas flow behaves like a plug flow.

The hydrodynamics are described by the selected two-phase model as shown previously in Figure 6-1. The model describes the fluidized bed as a two-phase system consisting of an emulsion phase and a solid-free bubble phase. The gas velocity in the emulsion phase is equal to the minimum fluidization velocity of the bed. The gas flow through the bubble phase is characterized by the bubble rise velocity in the bed. The gas flow through each phase will be a plug flow like, because the axial dispersion is low compared with the axial velocity. All catalyst particles are assumed to be in the emulsion phase and the excess gas passes the bed through the bubble phase. More information on the hydrodynamics of the two-phase model can be found in the references [6-8].

The bubble velocity (U_b) in fluidized bed situation (Davidson and Harrison, 1963) is calculated with[6]:

$$U_b = U - U_{mf} + U_{b\infty} \quad (6.4)$$

Where,

U = superficial gas velocity, m/s

U_{mf} = minimum fluidization velocity, m/s

$U_{b\infty}$ = bubble rise velocity, m/s

The minimum fluidization velocity for small particles and Reynolds number at minimum fluidization ($Re_{p,mf} < 20$) is given by the relation [9]:

$$U_{mf} = \frac{d_p^2 (\rho_s - \rho_g) g}{150 \mu} \frac{\varepsilon_{mf}^3 \phi^2}{1 - \varepsilon_{mf}} \quad (6.5)$$

Where,

- ρ_s = solid particle density, kg/m³
- ρ_g = gas density, kg/m³
- g = acceleration of gravity, m/s²
- ε_{mf} = void fraction at minimum fluidization
- ϕ = shape factor of particle
- μ = gas viscosity, kg/m · s

The bubble rise velocity is estimated using the following correlation [6]:

$$U_{b\infty} = 0.711 \cdot (g \cdot d_b)^{0.5} \quad (6.6)$$

Where,

- g = gravitational acceleration, m/s²
- d_b = bubble diameter, m

It is assumed that the bubbles reach their maximum size quickly after gas enters the bed, hence the model works with a constant bubble size diameter equal to $d_{b,max}$. The maximum bubble diameter can be estimated by [10]:

$$d_{b,max} = 0.65 \cdot \left(\frac{\pi}{4} \cdot d_t^2 \cdot (U - U_{mf}) \right)^{0.4} \quad (6.7)$$

Where,

- d_t = bed diameter, m

The fraction of the bubble phase (ε_b) is [6]:

$$\varepsilon_b = \frac{U - U_{mf}}{U_b} \quad (6.8)$$

The gas interchange coefficient (K_{be} , s⁻¹) is defined as the volume of gas going from the bubbles to the emulsion or from the emulsion to the bubbles per unit volume of bubbles in bed per unit time [11]. For intermediate particle size and intermediate bubble velocity, the following correlation can be used [11]:

$$K_{be} = 4.5 \cdot \left(\frac{U_{mf}}{d_b} \right) \quad (6.9)$$

6.2.2 Solving the mass balances

For every gaseous component there are two mass balances, one for the dense phase and another for the bubble phase, see Figure 6-2. An additional mass balance for the carbon/char in the dense phase was made. The mass transfer between the two phases is controlled by the gas interchange coefficient. This makes ten differential mass balances for the gases in total and one for the solid char. These balances were

then solved simultaneously in a commercial program called Matlab. The applied ODE45 solver is based on a Runge-Kutta solving procedure with a self-seeking step size.

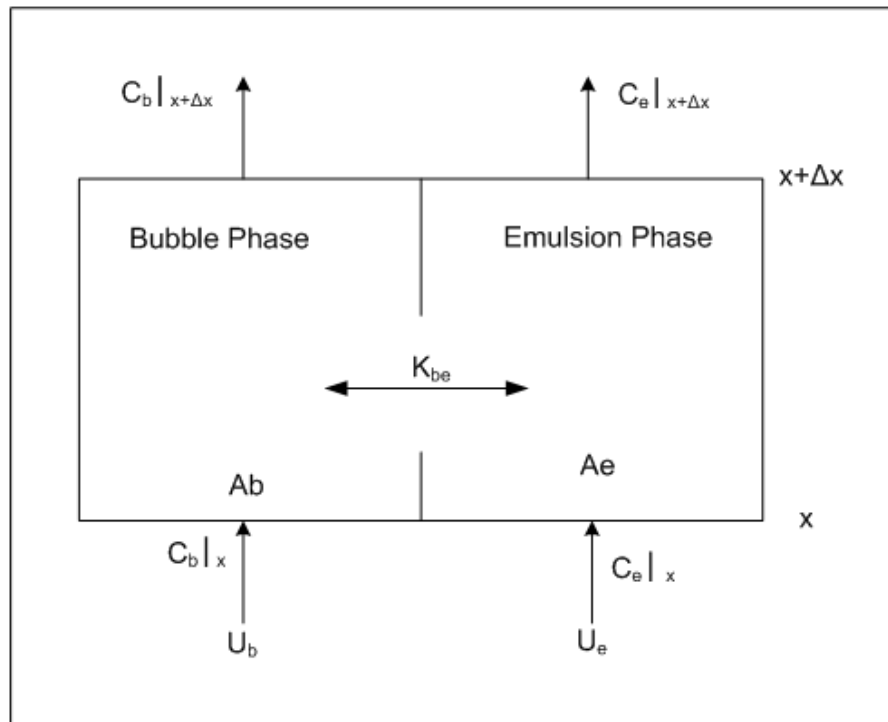


Figure 6-2 Differential mass balance over an infinitesimal section of the fluidized bed.

The general mass balance for the gas component (i) is made over a differential bed volume ($A_0\Delta x$), where (A_0) is the area of the bed and (Δx) is the differential height.

The bed area consists of an emulsion phase area (A_e) and a bubble phase area (A_b). As the bubble fraction in the bed is (ε_b), then:

$$A_e = A_0(1 - \varepsilon_b) \quad (6.10)$$

$$A_b = A_0\varepsilon_b \quad (6.11)$$

For each phase, a general mass balance over the volume ($A_0\Delta x$) can be set up. Every gas component is represented by $i = 1 - 5$ that corresponds to the components: Naphthalene, H_2O , CO , H_2 and CO_2 .

The general mass balance equation for the emulsion phase is:

Accumulation = Convection + Gas interchange + Diffusion + Reaction

$$\begin{aligned} \frac{\partial}{\partial t}(A_e\Delta x C_{i,e}) &= (U_e A_e C_{i,e} \Big|_x - U_e A_e C_{i,e} \Big|_{x+\Delta x}) + A_b \Delta x K_{be} (C_{i,b} - C_{i,e}) + \\ &(-D_{i,e} A_e \frac{\partial C_{i,e}}{\partial x} \Big|_x + D_{i,e} A_e \frac{\partial C_{i,e}}{\partial x} \Big|_{x+\Delta x}) + A_e \Delta x \sum R_{i,e} \end{aligned} \quad (6.12)$$

In solving the general mass balance equation, the following assumptions were made:

- Steady state conditions for the gas components as the transient term of the gas components are small compared with the transient term of the char.
- No axial dispersion
- Constant gas velocity in both phases
- The gas fraction in the emulsion phase equals the gas fraction at minimum fluidization velocity; the excess gas is in the bubbles
- The char is ideally mixed over the total volume of the emulsion phase
- The convection term can be approximated by Taylor series
- At $x = 0$, $C_e = C_b$

When applying the above assumptions the general mass balance equation of the emulsion phase can be reduced to:

$$U_e \frac{dC_{i,e}}{dx} = \sum R_{i,e} + \frac{\varepsilon_b}{1 - \varepsilon_b} K_{be} (C_{i,b} - C_{i,e}) \quad (6.13)$$

The rates of the reactions that take place in the emulsion phase are multiplied with the solid fraction ($1 - e_{mf}$). This is because the rates of the reactions depend mainly on the gas contact with the solid char that works as a catalyst. The water gas shift reaction was not multiplied by the solid fraction because it occurs in the gas and the solid phase and the rate of the reaction is not enhanced by the contact with the solid (catalyst).

$$\sum_{i=1}^6 R_{i,e} = \alpha_{i,sh} r_{sh} + \sum_{j=1}^3 \alpha_{ij} r_j (1 - e_{mf}) \quad (6.14)$$

The same procedure can be applied for the bubble phase, which results in:

$$U_b \frac{dC_{i,b}}{dx} = \sum R_{i,b} - K_{be} (C_{i,b} - C_{i,e}) \quad (6.15)$$

The only reaction that takes place in the bubble phase is the water gas shift reaction.

6.3 Model results

The two-phase reactor model was developed to study the performance of the biomass char for naphthalene reduction in a bubbling fluidized bed in the environment of H₂O, CO₂ and N₂. The model was used to study the effect of the following parameters on the naphthalene conversion: (1) the char particle size, (2) bed temperature and (3) bed height (residence time). The standard conditions used in the model are the same as the experimental conditions that will be discussed in section 6.4.1. These conditions are summarized in Table 6-1.

Table 6-1 Reference values of the model parameters

Parameter	Symbol	Value
Tar	$C_{10}H_8$	Naphthalene
Pressure	P (atm)	1
Reactor temperature	T_R ($^{\circ}C$)	900
Gas residence time	τ (s)	0.3
Height of char bed	H(m)	0.09
Gas superficial velocity	U (m/s)	0.30
Char particle size	d_p (μm)	1000
Standard gas mixture (STD) (vol.%)		
		CO ₂ 7
		H ₂ O 7
		Naphthalene 0.2
		N ₂ Balance

6.3.1 Effect of particle size

The two-phase behavior of a bubbling bed can be influenced by the particle size of the bed material. For small particles, the gas is mainly transported through the bubble phase. In that case, the contact between the gas in the bubbles with the char catalyst in the dense phase is not very good. This effect can be explained by the two-phase reactor model. In Figure 6-3 and Figure 6-4 the naphthalene concentration in both, the bubble and dense phase are plotted for the two different particle sizes, 1000 and 600 μm . The superficial gas velocity was kept constant at 0.3 m/s. The minimum fluidization velocity decreases from 0.10 to 0.04 m/s for the two particle sizes. In the figures, it is clearly shown that there is a remarkable difference in the naphthalene concentration between the dense and the bubble phase. For the small particles, the higher gas slips through the bubbles and results in a higher naphthalene concentration in the gas leaving the bed.

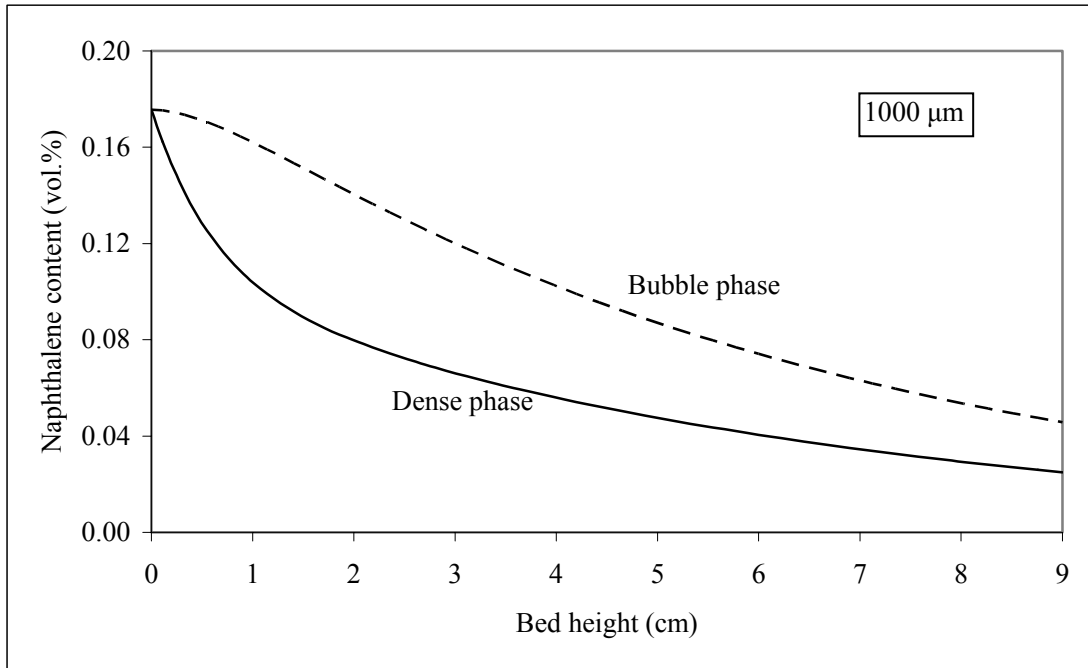


Figure 6-3 Model estimation of naphthalene content in the dense and the bubble phase as function of bed height, T: 900 °C, τ : 0.3 s; d_p : 1000 μm ; U/U_{mf} : 3.0; feed gas (7 % H₂O, 7 % CO₂, 0.2 % Naphthalene, balance N₂)

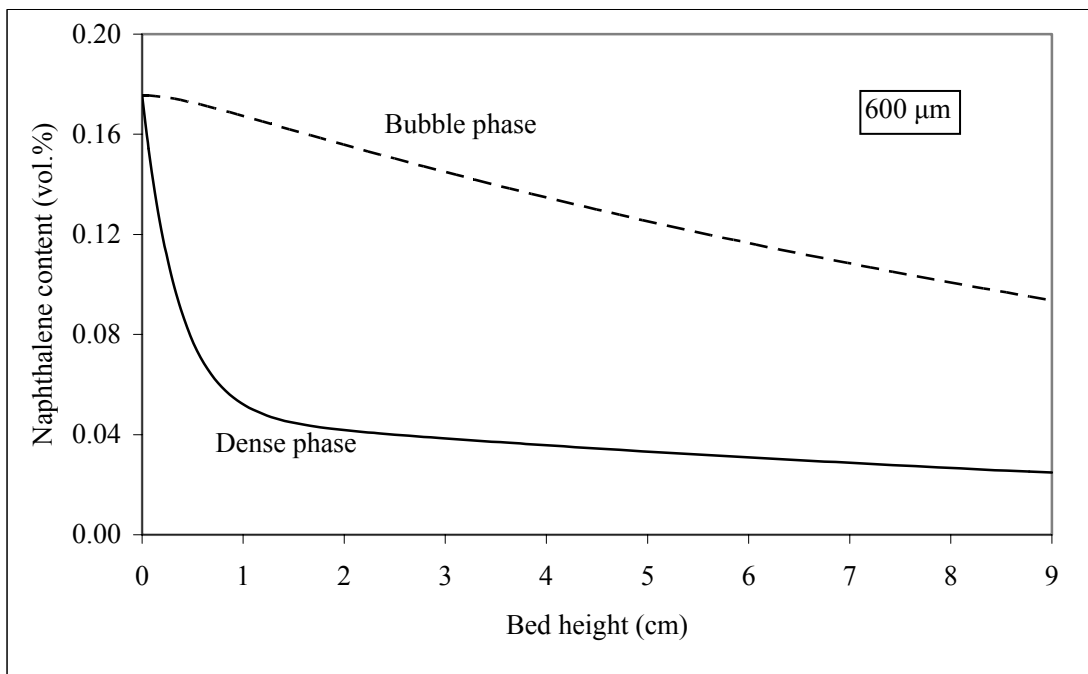


Figure 6-4 Model estimation of naphthalene content in the dense and the bubble phase as function of bed height, T: 900 °C, τ : 0.3 s; d_p : 600 μm ; U/U_{mf} : 8.3; feed gas (7 % H₂O, 7 % CO₂, 0.2 % Naphthalene, balance N₂)

The effect of the particle size on the naphthalene conversion is shown in Figure 6-5. The largest particle size used in the figure is the one at which the superficial velocity equals the minimum fluidization velocity ($U/U_{mf} = 1$). Thus, above this particle size, no fluidization can occur and fixed bed conditions prevail. The naphthalene conversion increases with the particle size as shown in Figure 6-5. The increase is steep up to 1000 μm above which the increase is not that significant. The maximum conversion occurs at the largest particle size where we have fixed bed conditions.

Using larger particle sizes has different effects: an increase of the gas transfer from the bubble phase to the dense phase, and a higher gas flow through the dense phase. Both effects increase the naphthalene conversion. Thus, the hydrodynamic is the dominating mechanism that affects the naphthalene conversion.

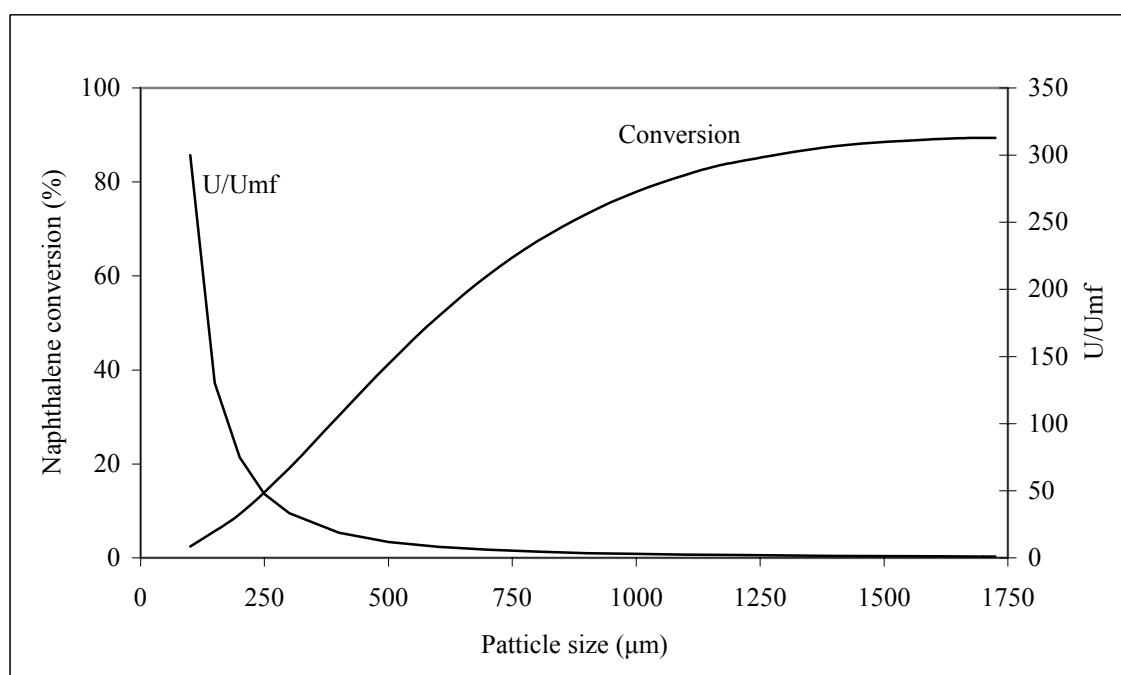


Figure 6-5 Effect of particle size on naphthalene conversion at different feed gas superficial velocities, $T: 900\text{ }^{\circ}\text{C}$, $\tau: 0.3\text{ s}$; feed gas (7 % H_2O , 7 % CO_2 , 0.2 % Naphthalene, balance N_2)

6.3.2 Effect of bed temperature

The naphthalene conversion as function of the bed temperature is shown in Figure 6-6. As expected, the conversion is increasing with bed temperature because of the higher reaction rate of the cracking reaction at higher temperatures. The conversion is increasing to a level of about 85 % at a bed temperature of 1000 $^{\circ}\text{C}$ and a bed particle size of 1000 μm . A complete conversion could not be achieved in this case because of limitation of the two-phase flow behavior of the bed. Also, the ratio between kinetics and mass transfer will be different for different particle sizes.

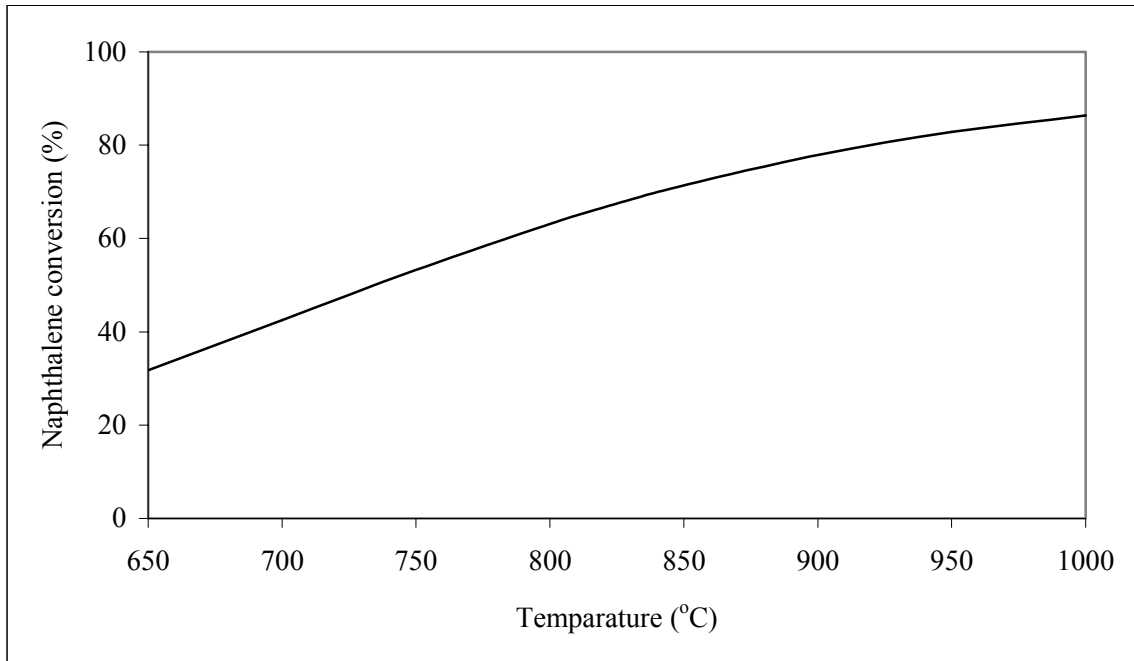


Figure 6-6 Effect of temperature on naphthalene conversion, τ : 0.3 s; d_p : 1000 μm ; feed gas (7 % H_2O , 7 % CO_2 , balance N_2)

6.3.3 Effect of the bed height

Changing the char bed height while keeping the superficial gas velocity constant affects the gas residence time in the char bed. The model was used to calculate the output naphthalene and other gases concentrations in the output gas and the first hour carbon conversion. Figure 6-7 shows the model estimations.

The naphthalene conversion is assumed constant over time as found in the previous chapter. The total carbon conversion over the whole bed, after one hour is estimated based on the rate of the steam and CO_2 consumption.

The naphthalene conversion increases with the char bed height. This is because the naphthalene conversion depends besides the bed temperature mainly on the gas residence in the char bed. It is remarkable that for higher temperatures, the naphthalene conversion is limited to 85% at relatively high temperature (1000 °C) as shown previously in Figure 6-6. While for higher bed heights (residence times), the naphthalene conversion could reach a complete conversion (100%). Normally, the temperature has a higher effect than the residence time. Thus, this case is clearly mass transfer limited.

On the other hand, the first hour carbon conversion decreases with increasing bed height because of decreasing reactant concentrations as the bed height (residence time) increases: CO_2 and H_2O are lower in the upper part of the bed.

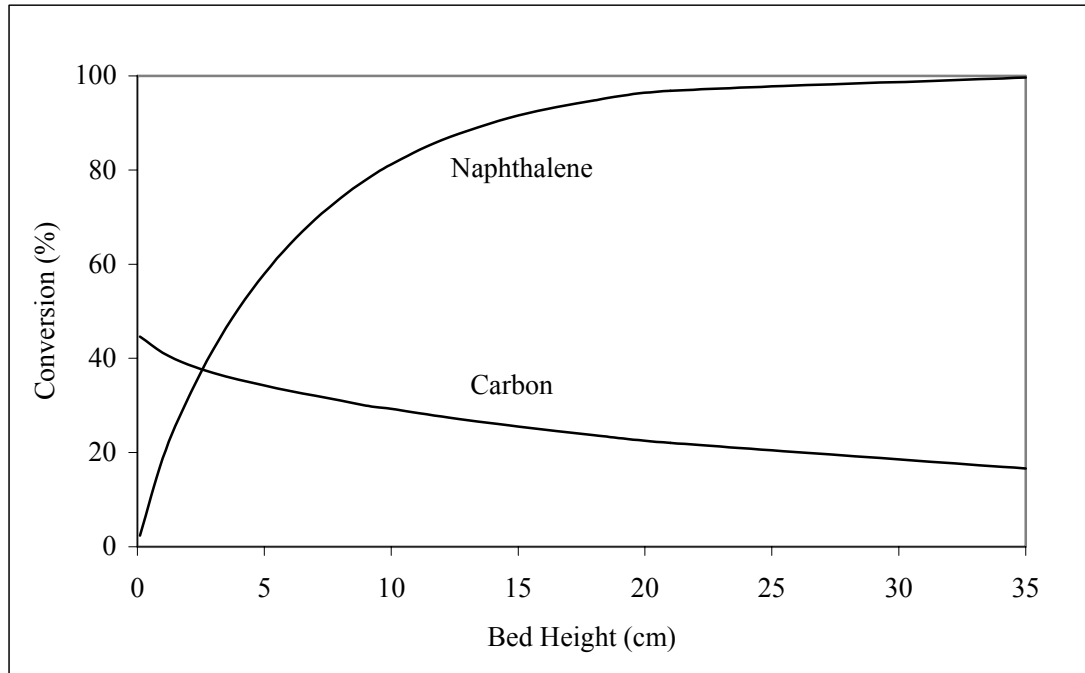


Figure 6-7 Estimation of initial naphthalene and first hour carbon conversion as function of bed height, $T: 900\text{ }^{\circ}\text{C}$, $\tau: 0-1.13\text{ s}$; $d_p: 1000\text{ }\mu\text{m}$; feed gas (7 % H_2O , 7 % CO_2 , balance N_2)

The CO and H_2 increased on behalf of the H_2O , CO_2 and naphthalene concentrations. The naphthalene concentration decreased because of the steam and dry reforming reactions with the carbon. The produced CO and H_2 are caused by the gasification reactions of the char and to a less extent because of the naphthalene reforming reaction.

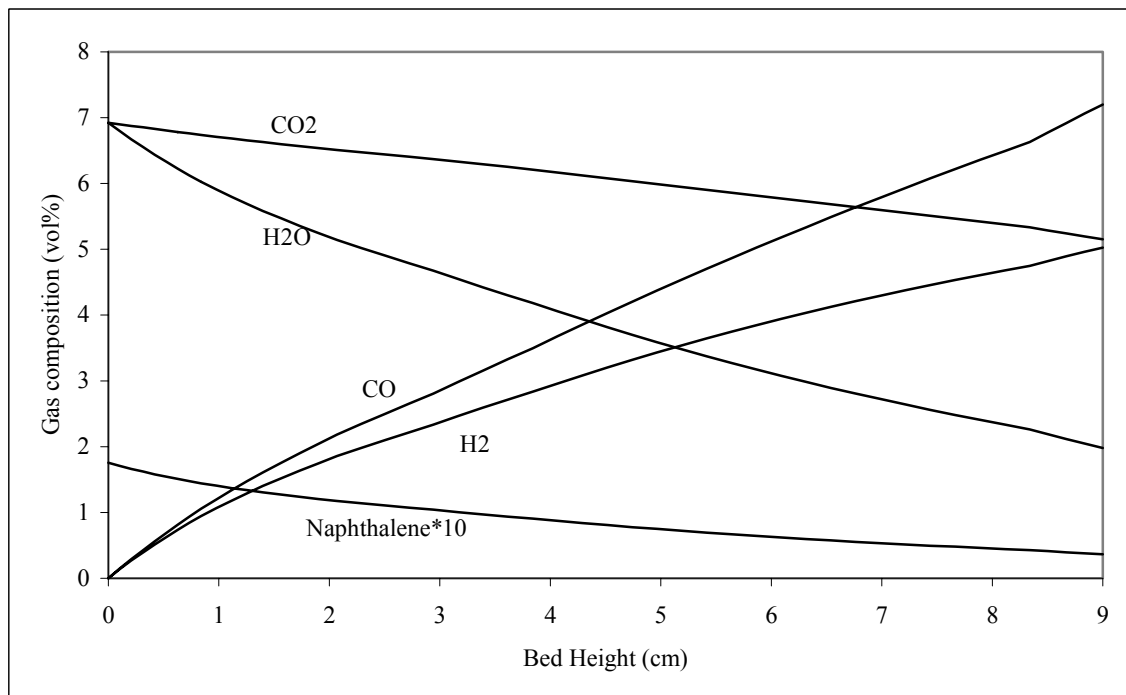


Figure 6-8 Model estimation of gas composition as function of bed height, $T: 900\text{ }^{\circ}\text{C}$, $\tau: 0.3\text{ s}$; $d_p: 1000\text{ }\mu\text{m}$; feed gas (7 % H_2O , 7 % CO_2 , 0.2 % Naphthalene)

6.4 Experimental results

Experiments have been carried out to study the performance of the biomass char for the naphthalene reduction in a bubbling fluidized bed. The effect of bed height and particle size of the char bed on the naphthalene conversion was studied.

6.4.1 Experimental setup

These experiments were carried out utilizing the same setup used in the fixed bed experiments given in chapter three; only the gas velocity was increased above the minimum fluidizing velocity. The feed gas flow rate in the fluidized bed experiments was about 315 NI/h instead of 70 NI/h in the fixed bed experiments. The biomass char used and most of the experimental conditions are the same as those given in chapter three. The simultaneous carbon conversion and the output gas composition were measured.

The naphthalene conversion measurements were based on the concentrations measured after (15 min) time on stream during the experiment. On the other hand, the carbon conversion is based on (1 h) time on stream, which is the total time of every experiment. The final weight of char is determined after each experiment. The experimental conditions are listed in Table 6-2.

Table 6-2 Reference conditions applied for the naphthalene removal in the bubbling fluidized char bed experiments

Parameter	Symbol	Value
Tar	C ₁₀ H ₈	Naphthalene
Pressure	P (atm)	1.0
Temperature	T (°C)	900
Gas residence time	τ (s)	0.3
Bed height	H (m)	0.09
Gas flow rate	v _o (NI/h)	315
Particle size	d _p (μm)	1000-1250
Reference gas composition (STD):		
CO ₂	(vol %)	7
H ₂ O	(vol %)	7
N ₂	(vol %)	balance
Naphthalene	(g/Nm ³)	10-20

The bed temperature chosen for these experiments was higher compared with the fixed bed experiments given in chapter four and five (900 °C instead of 850 °C). The higher temperature was chosen to compensate for the lower conversion at BFB conditions. The standard gas contains only H₂O and CO₂ as gasification agents

because the other components have minor effect as found in the previous chapters. The biomass char used in these experiments is pinewood biomass char produced in our laboratory and not the commercial biomass char. The chemical and physical properties of this char are given in chapter three in Table 3-5 and Table 3-6.

6.4.2 Synthetic tar results

6.4.2.1 Effect of particle size

In this experiment, we studied the influence of the particle size on the naphthalene and carbon conversion. Three different particle size ranges were selected: 800-1000 μm , 1000-1250 μm and 1400-1700 μm . The pinewood biomass char particles were produced at the same pyrolysis conditions discussed in chapter three (3.2.5).

Figure 6-9 shows the effect of the char particle size on the produced gas composition and the conversion of naphthalene and carbon over the first hour. The naphthalene conversion increased with increasing particle size. This can be explained by the increased gas flow through the dense phase and thus a more efficient contact between the naphthalene and the char. The increase in carbon conversion was not significant for larger bed particles. This is because the carbon conversion mainly depends on the H_2O and the CO_2 concentrations that are available at relatively high concentrations compared with the naphthalene.

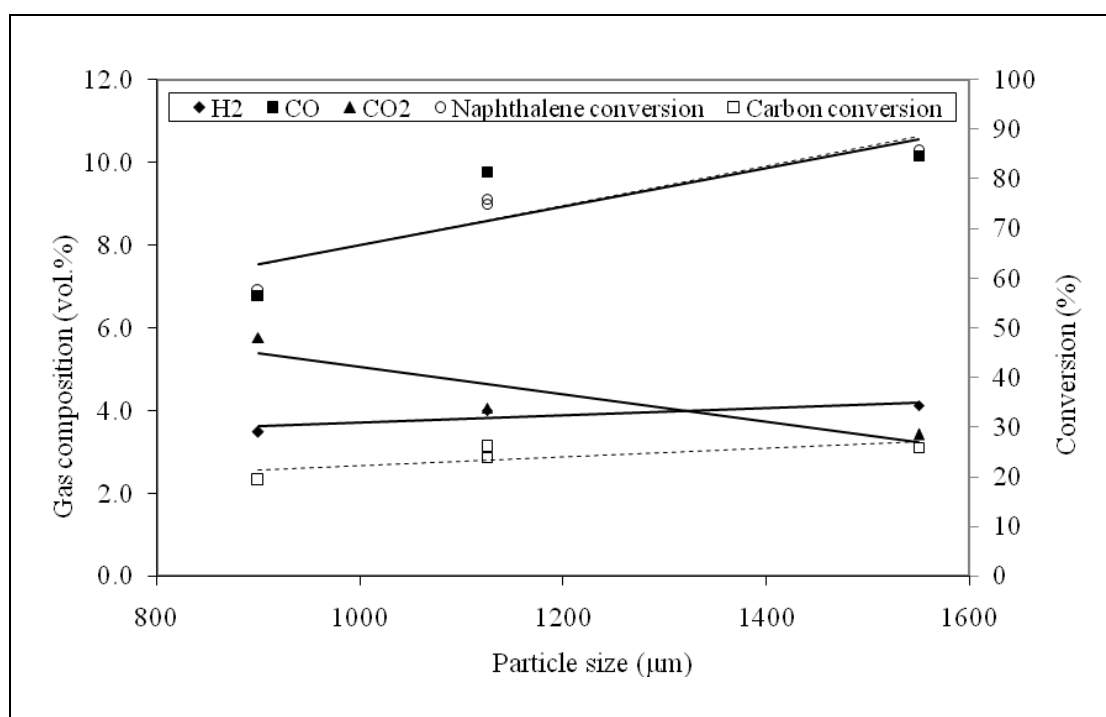


Figure 6-9 effect of particle size on initial naphthalene and first hour carbon conversion in a fluidized bed, T : 900 $^{\circ}\text{C}$, τ : 0.3 s; H : 9 cm, feed gas (7 % H_2O , 7 % CO_2 , 0.2 % Naphthalene, balance N_2)

Larger particle sizes gave higher H_2 and CO content and less CO_2 content. This is related to the higher naphthalene conversion for larger particles.

6.4.2.2 Effect of bed height

Changing the char bed height while keeping a constant superficial gas velocity affects the gas residence time in the char bed.

Figure 6-10 shows the naphthalene and other gas concentrations in the output gas and the first hour carbon conversion at different bed heights. The naphthalene conversion increased with the char bed height. This is because the naphthalene conversion depends on the reaction kinetics (temperature) and the gas residence time. The carbon conversion over the first hour slightly decreased with increasing bed height because of decreasing reactant concentrations as the bed height increases.

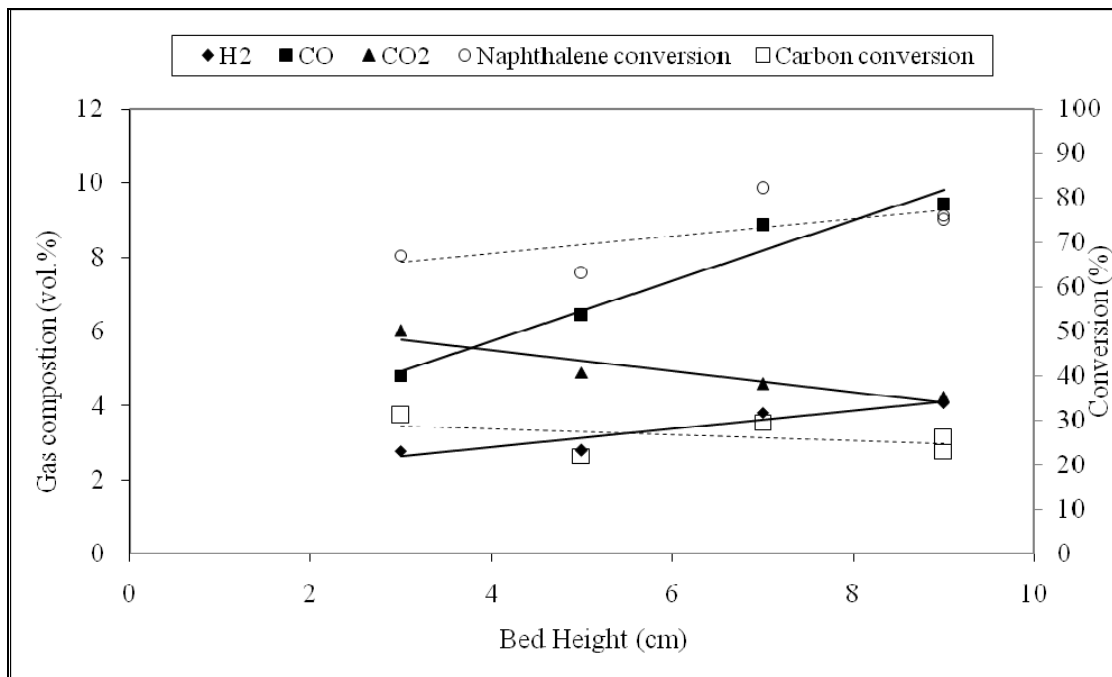


Figure 6-10 Effect of bed height on initial naphthalene and first hour carbon conversion in a fluidized bed, T: 900 °C, d_p : 1000-1250 μm , feed gas (7 % H₂O, 7 % CO₂, 0.2 % Naphthalene, balance N₂)

The CO and the H₂ increased with increasing bed height because of the consumption of CO₂ and H₂O by the dry and steam reforming of char. The CO concentration is higher than the H₂ concentration mainly because the dry reforming reaction produces moles of CO that are twice the amount of H₂ moles produced by steam reforming reaction of the carbon.

6.5 Validation of the model

To validate the fluidized bed model, the predictions are compared with the experimental data presented in the previous section (6.4). The measured conversion of carbon, naphthalene, and gas composition at different bed heights are put side by side with the model predictions.

First, the carbon and naphthalene conversion are compared with the model predictions. As can be seen from Figure 6-11 the trend is predicted well for both naphthalene and carbon conversion. However, the model slightly overestimates the carbon conversion. This will result in lower carbon availability for tar cracking and thus underestimating the naphthalene concentration.

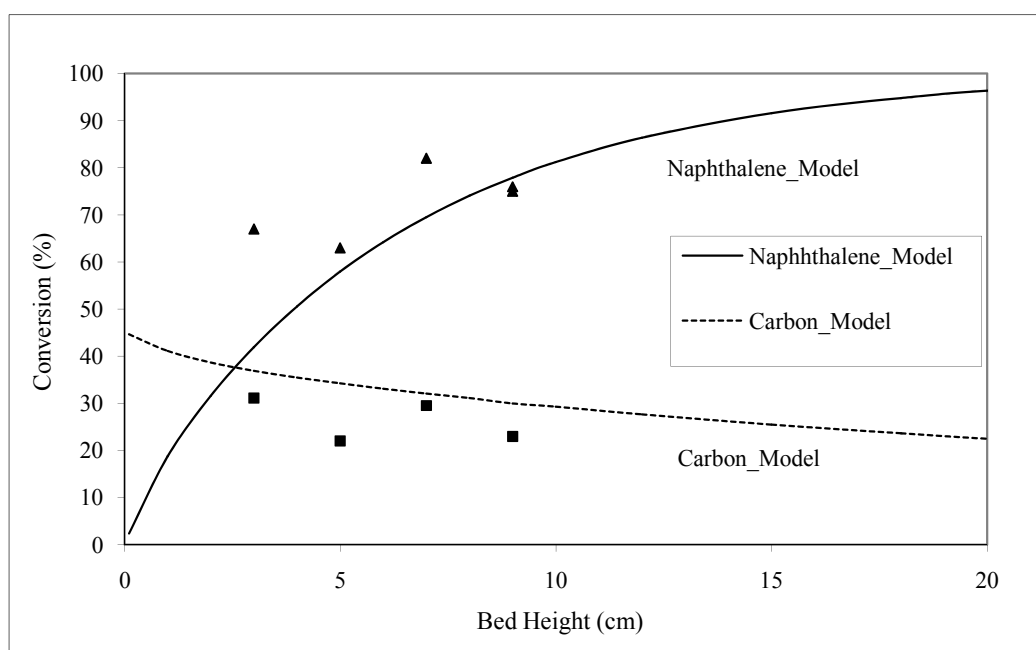


Figure 6-11 Validation of the model on initial naphthalene and first hour carbon conversion as function of bed height, Experiments and model conditions: T: 900 °C, d_p : 1000-1250 μm ; feed gas (7 % H_2O , 7 % CO_2 , 0.2 % Naphthalene, balance N_2); (see experiments in section 6.4)

The composition of the produced gas is reasonably predicted by the model as shown in Figure 6-12. However, the model slightly underestimates the CO content. This is related to the model overestimation of the carbon conversion discussed above.

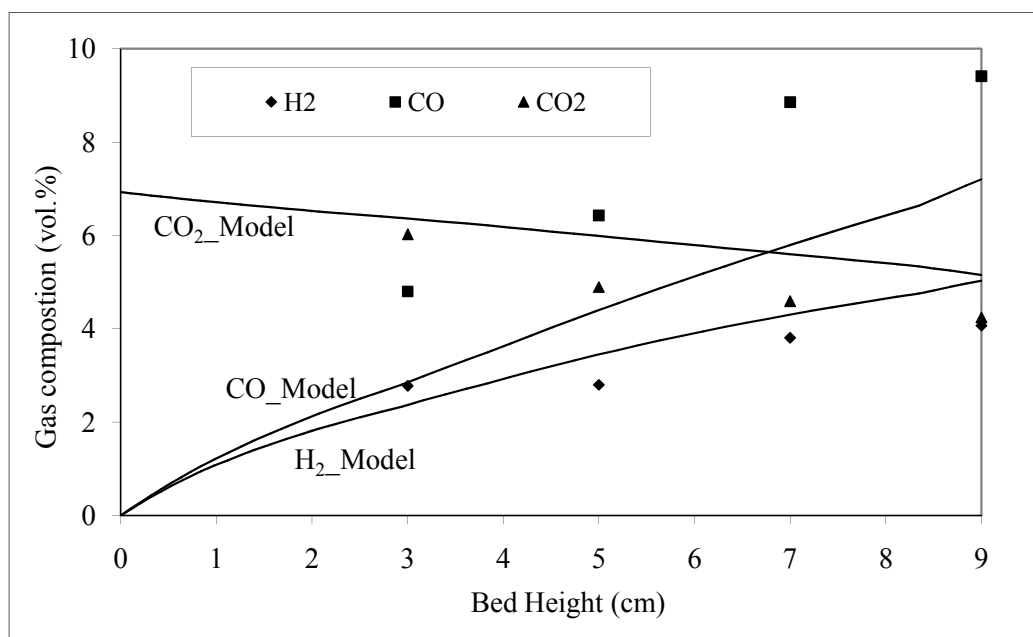


Figure 6-12 validation of the model estimation for gas composition with experiments, Experiments and model conditions: T: 900 °C; d_p : 1000-1250 μm ; time: 15 min; feed gas (7 % H₂O, 7 % CO₂, 0.2 % Naphthalene, balance N₂). (see experiments in section 6.4)

6.6 In-situ Real Tar Reduction

The biomass char shows a good performance for the naphthalene reduction at bubbling fluidized bed conditions. The combination of the char as tar cracking agent and its natural production inside the gasifier makes it a good primary additive to minimize the tar formation inside the fluidized bed gasifier itself. Therefore, a novel experiment was carried out to investigate the effectiveness of the biomass char for tar reduction inside the bubbling fluidized bed gasifier.

6.6.1 Gasifier

This setup is the same real tar setup presented in chapter four with some modifications. The silica sand bed material was replaced with the commercial biomass char as shown in Figure 6-13. The biomass particles are fed on top of the char bed.

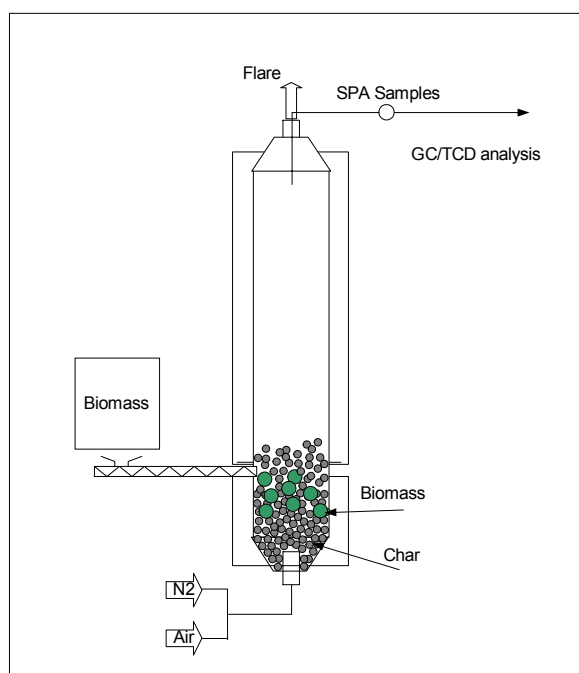


Figure 6-13 Biomass gasification in a biomass char bed

The in-situ tar reduction was tested in a biomass bubbling fluidized bed gasifier where the biomass char was used as a bed material. The biomass particles (1.5-3.0 mm) were fed on top of the char bed. The gasification was carried out at 850 °C and an equivalence ratio (ER) of 0.3. A constant superficial air velocity of 0.3 m/s was used in these experiments. Two char bed particle sizes were used: 1.0 and 1.5 mm. The superficial gas velocity was difficult to be increased for better fluidization when using the larger char particle size because of the instability of the setup. High flame was produced from the top of the gasifier, which made it difficult to continue the experiment. The chemical and physical properties of the commercial biomass char used in this experiment is given in chapter three in Table 3-5 and Table 3-6. Further, a summary of the experimental conditions is given in Table 6-3.

Table 6-3 Applied conditions in biomass gasification in a biomass char bed

Parameter	Value
Tar	Real
Pressure (atm)	1.0
Temperature (°C)	850
Biomass particle size (μm)	1500-3000
Biomass char particle size (μm)	1000, 1500
Min. fluidization velocity (m/s)	0.10, 0.27
Superficial velocity (m/s)	0.3
Equivalence Ratio (ER)	0.3
gas composition	Producer gas

6.6.2 Experimental results

These experiments are indicated by the ratio between the superficial velocity (U) and the minimum fluidization velocity (U_{mf}).

Table 6-4 In-situ char bed experiments

Experiment	Average char particle size (μm)	U/U_{mf}
1	1500	1.1
2	1000	3.0

To be able to evaluate the performance of the in-situ use of the biomass char for tar removal, the results were compared with the inert sand bed gasification; results presented in chapter four. The biomass gasification in a silica sand bed gave an average tar concentration in the producer gas of 9000 mg/Nm^3 . The tar composition of the different experiments presented in Figure 4-19 is averaged and presented in Figure 6-14.

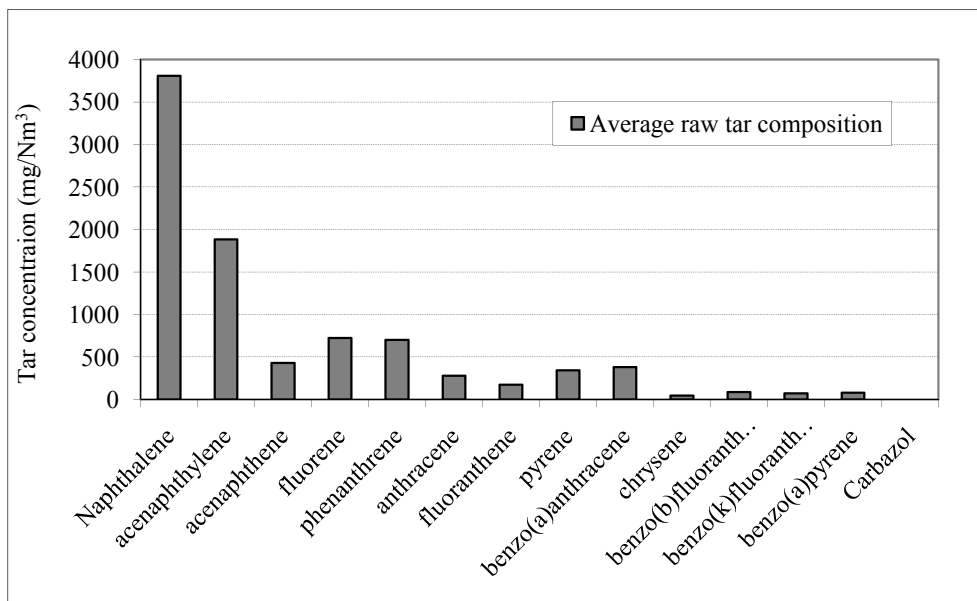


Figure 6-14 The average tar composition of the raw gas produced in sand bed biomass gasification, Real tar; T_R : $850 \text{ }^\circ\text{C}$; ER: 0.3; biomass d_p : $1500\text{-}1300 \text{ }\mu\text{m}$; sand bed d_p : $200 \text{ }\mu\text{m}$; gas composition: producer gas

The tar composition of the first in-situ char experiment (1500 μm) is given in Figure 6-15. The total concentration was found to be 315 mg/Nm^3 . Only four tar components were detected: naphthalene, acenaphthene, anthracene, and benzo(a)pyrene.

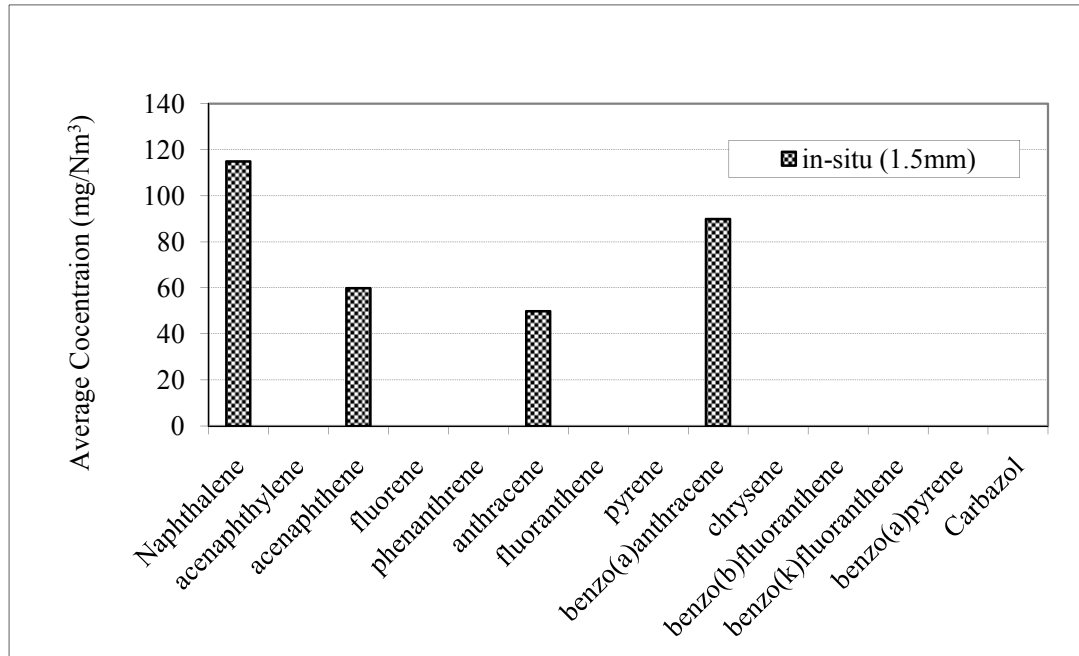


Figure 6-15 Tar composition of in-situ (1500 μm) char bed gasification experiment, Real tar; TR: 850 $^{\circ}\text{C}$; ER: 0.3; biomass dp: 1500-1300 μm ; char dp: 1500 μm , U/U_{mf} : 1.1

The fluidization of the bed in the experiment described above was rather smooth, $U = 1.1 U_{\text{mf}}$. In the second experiment (smaller particles), the fluidization is more turbulent. This will improve the mixing behavior of the bed with the fresh biomass particles. For the small bed particles the total concentration was found to be 260 mg/Nm^3 . Only two tar components were detected: acenaphthylene, and carbazol (Figure 6-16). Therefore, improving the fluidization conditions increased the tar removal. The volatiles are released below the bed surface within the bed and this gives a higher contact time between the devolatilized tar components and the char particles.

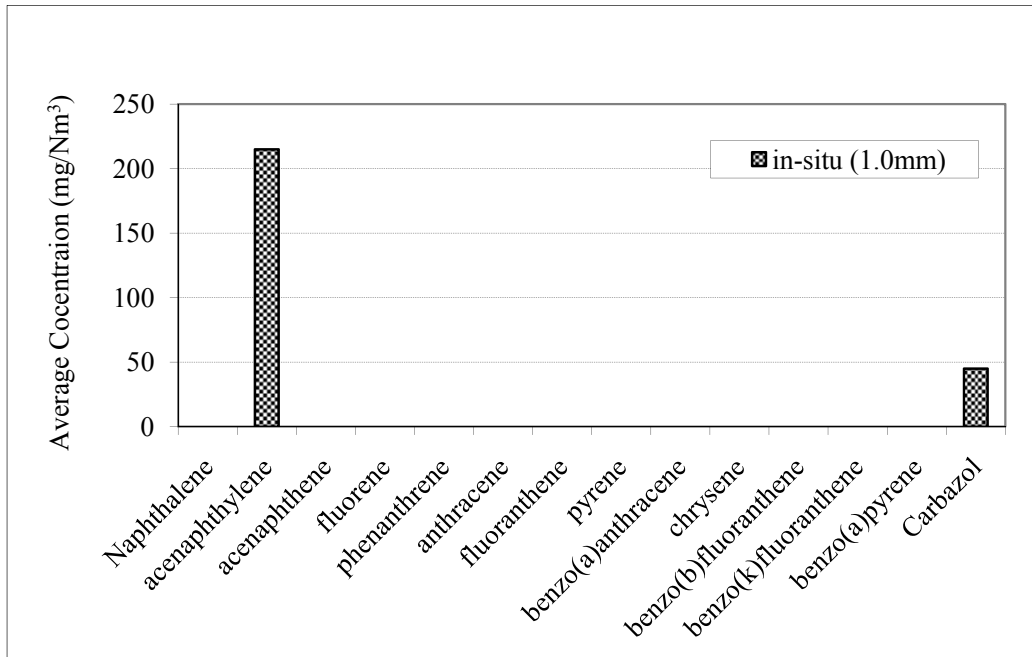


Figure 6-16 Tar composition of in-situ (1000 μm) char bed gasification experiment, Real tar; T_R : 850 $^\circ\text{C}$; ER: 0.3; biomass d_p : 1500-1300 μm ; char d_p : 1000 μm , U/U_{mf} : 3

The gasification in the char bed gave a highly reduced tar concentration in the range of 260 mg/Nm^3 which corresponds to an average conversion of more than 97 %. This is very promising and more experiments are needed to investigate thoroughly the performance of the biomass char as a bed material in the gasifier.

6.7 Evaluation

In this chapter, the performance of biomass char as a catalytic bed material in a bubbling fluidized bed reactor was investigated. The biomass char was tested both as a bed material for naphthalene removal in a downstream fluidized bed reactor (secondary measure) and as a bed material inside the biomass gasifier itself (primary measure).

6.7.1 Naphthalene removal in a secondary fluidized bed

Experiments were carried out to investigate the performance of biomass char for the naphthalene removal in a downstream bubbling fluidized bed. In these experiments the effect of the bubbling fluidized bed hydrodynamics on the naphthalene conversion were measured. The hydrodynamics were studied by changing the char bed height (gas residence time in the char bed) and the particle size at a constant gas superficial velocity.

It was found in the experiments that the naphthalene conversion increased with increasing the char bed particle size (Figure 6-9) and with increasing the char bed height (Figure 6-10). Whereas, the first hour carbon bed conversion decreased with

increasing particle size and bed height. With the developed model the hydrodynamics was described as a two-phase system consisting of an emulsion phase and a solid-free bubble phase. The gas velocity in the emulsion phase is equal to the minimum fluidization velocity of the bed and the gas in excess of the minimum fluidizing velocity goes through the bubble phase. The gas flow through each phase was found to be in plug flow, because of the negligible axial dispersion compared with the axial velocity.

The model shows that the hydrodynamics has a significant effect on the overall naphthalene conversion. The model clarifies the effect of the particle size on the naphthalene conversion. It shows that increasing the particle size till U/U_{mf} approaches unity improves the naphthalene conversion (Figure 6-5). For the coarse bed particle size of 1.5 mm ($U/U_{mf} = 1.1$), the bubble rise velocity turned out to be lower than the minimum fluidization velocity (dense phase velocity). Thus, in this situation the gas flows mainly through the dense phase of the bed where the char particles are, (Figure 6-3), and this leads to a higher naphthalene conversion. For the fine bed particle size of 1.00 mm ($U/U_{mf} = 3$), the bubble rise velocity is higher than the minimum fluidization velocity. Then, the gas flows as a two-phase flow and the naphthalene partly slips via the bubbles through the bed causing less conversion (Figure 6-3 and Figure 6-4). A higher char bed is then needed to allow the naphthalene in the bubble phase to diffuse to the dense phase for better conversion.

The model shows that the gas residence time of the naphthalene in the char bed is an important parameter that affects the naphthalene conversion. A gas residence time of at least 1 s (30 cm bed height in this case) is needed to get more than 99 % naphthalene conversion. This is supported by experiments: (Figure 6-10). The first hour carbon conversion decreases with increasing bed height because of lower reactant concentrations (CO_2 and H_2O) as the bed height (residence time) increases.

6.7.2 Comparison of the naphthalene removal in a fixed and a fluidized bed

The naphthalene conversions in the bubbling fluidized bed (BFB) experiments are, in general, significantly lower than those in the fixed bed experiments presented in chapter four. The naphthalene conversion in the fluidized bed was 76 % at 900 °C and 0.3 s gas residence time (Figure 6-9). Whereas, the fixed bed gave more than 98 % naphthalene conversion with comparable temperature and gas residence time, (Figure 4-23). This indicates the importance of the mass transfer in the BFB.

The effect of the particle size on the naphthalene conversion in the BFB is opposite to that in the fixed bed. The fixed bed favors smaller particle sizes to decrease the effect of internal diffusion limitations. On the other hand, the BFB favors larger particle sizes to decrease the naphthalene bypass through the bubbles. The optimum particle size is almost equal to the largest particle size that corresponds to a gas superficial velocity approaching the minimum fluidization velocity as explained above.

The BFB requires longer residence time of the tar in the char bed to get the same conversion in the fixed bed. This is caused by the bubble formation in the BFB which allows the naphthalene to slip via the bubbles without contacting the char. Thus, a higher bed (more char) is needed to allow the naphthalene in the bubbles to diffuse to the dense phase of char.

The carbon conversion in both types of beds decreases with increasing bed height (gas residence time) because of lower reactant concentrations as the bed height (residence time) increases. Further, the carbon conversion in both beds is comparable and low, and can be compensated with the produced char in the biomass gasifier.

The BFB reactor has a poor overall gas solid contact efficiency which reduces the tar conversion. In order to improve the tar conversion in bubbling fluidized bed conditions, the contact between the gas and the char should be improved. The improvement can be done by either improving the reactor conditions or changing the reactor type. The reactor conditions can be improved by using conditions that give smaller bubble size and increase the contact between gas and solid (char). This can be done by, e.g. larger bed particle size and internals in the bed to hinder bubble growth and cut down bubble size [11]. Another option could be the use of a circulating fluidized bed with a better contact efficiency between the solid and the gas.

6.7.3 Biomass gasification in a char bed

The biomass char showed high tar conversion degrees for both fixed bed and fluidized bed conditions. Moreover, char is a product of biomass gasification. Thus, biomass char can be easily integrated in the gasification process for tar removal. An innovative use of the biomass char as a primary measure for tar removal was reported in this chapter. The biomass gasification was carried out in a BFB of biomass char instead of silica sand.

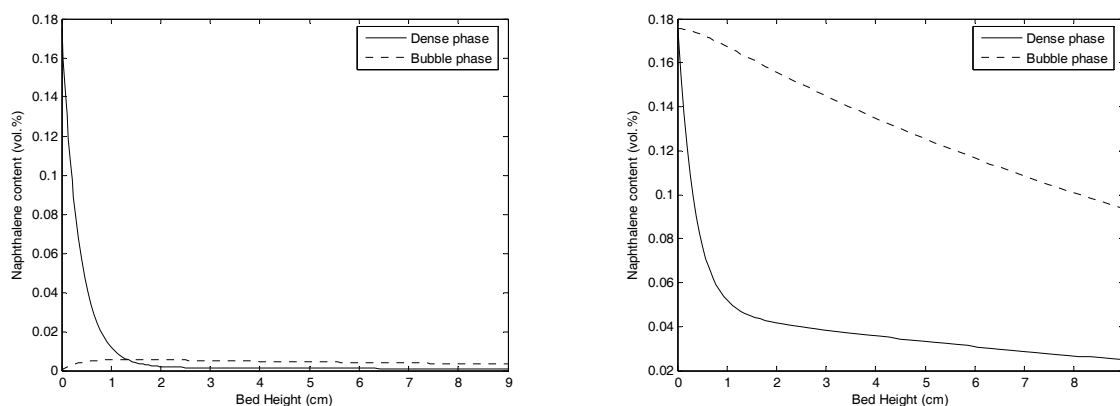
The biomass is directly injected in the char bed and is converted into gas, tar and char. If the char stays in the bed it can catalytically remove the tar that is produced in the bed. The extent of the tar removal depends on the efficiency of the contact between the tars and the char. The longer the residence time of these tars in the char bed the higher the conversion. Thus, the hydrodynamics and the position of the biomass feeding to the char bed will be important.

In the experiments, the biomass was fed on top of the char bed in the gasifier. The char was comparable with the char used in the fixed bed experiments discussed in chapter four. The in-situ gasification experiments were carried out at 850 °C. The preliminary experiments showed a high tar reduction, which is more than 97 % corresponding to an outlet tar concentration of 260 mg/Nm³ (Figure 6-16). Further optimization of the process conditions is possible: higher bed, lower biomass feeding, larger bed particles, etc.

The tar conversion in the in-situ gasification in the char bed is remarkably higher than the naphthalene conversion in the secondary bubbling fluidized bed of char (76 %). The high tar conversion in the in-situ tar removal is related to two reasons. Firstly, the char is a gasification product. Thus, more char is formed and accumulated during the in-situ gasification, which gave the tars longer residence time in the char

bed, which leads to a higher conversion. This supports feeding the biomass at the bottom of the char bed to give the devolatilized tars a higher residence time for complete tar conversion. Secondly, the devolatilized tars are formed in the dense phase where direct contact with the char is possible. Thus, the tars can react before slipping to the bubbles whereas in the secondary fluidized bed the naphthalene slips directly into the bubble phase. This reason can be further explained by the model.

For the in-situ tar removal in the char bed, the direct contact between the devolatilized tars and the char gives higher tar conversion in the case of small particle size. This is because the gas interchange coefficient between the bubble and the dense phase is dependent on the minimum fluidization velocity and the bubble diameter. Thus, a smaller particle size means lower minimum fluidization velocity which decreases the naphthalene diffusion from the dense phase to the bubble phase and increases the naphthalene conversion. So the tar is locked in the dense phase. In Figure 6-17, the naphthalene concentration profile along the bed height is plotted. Part (a) represents the case of in-situ gasification in the char bed where the tar may contact the char before it slips to the bubble phase. Thus, at the bottom of the bed the tar concentration in the bubble phase is assumed to be zero. Part (b) represents the case of a downstream BFB tar cracker where the naphthalene is directly divided over the dense and bubble phase. The conversion is 51 % in case of the downstream BFB (Figure 6-17, b) and 86 % in case of the in-situ gasification (Figure 6-17, a).

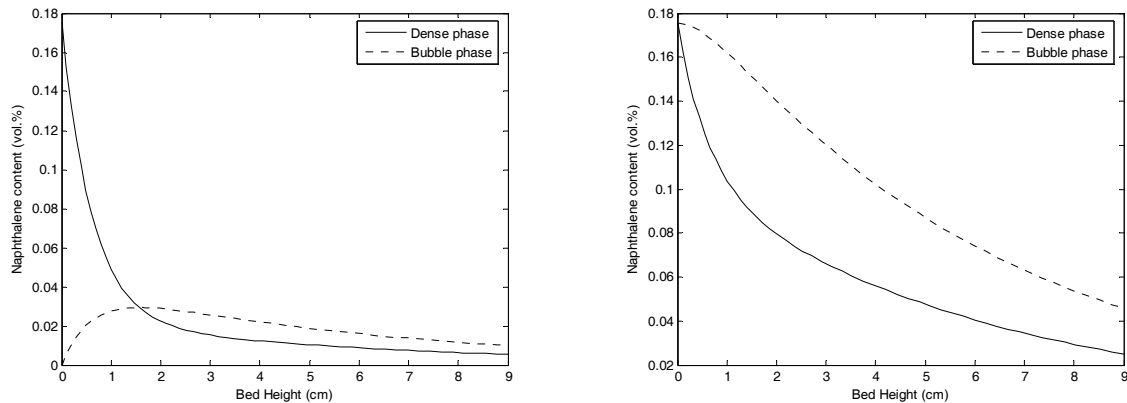


(a) In-situ: Naphthalene conversion: 86 %, d_p : 600 μm

(b) BFB: Naphthalene conversion: 51 %, d_p : 600 μm

Figure 6-17 The naphthalene concentration in the bubble and dense phase along the small particles bed height for the (a) in-situ gasification and (b) downstream BFB tar cracker at the same conditions, T: 900 °C; superficial velocity: 0.3 m/s; feed gas (7 % H₂O, 7 % CO₂, 0.2 % Naphthalene, balance N₂)

In the case of the coarse char particle size, the diffusion of naphthalene from the dense phase to the bubble phase is very fast. The naphthalene conversion is then 78 % in case of the downstream BFB tar cracker (Figure 6-18, b) and stays 86 % in case of the in-situ gasification (Figure 6-18, a). Thus, the effect of the initial direct contact with the char is relatively small. There seems to be no overall influence of the particle size on the naphthalene conversion for the in-situ gasification case.



(a) In-situ: Naphthalene conversion: 86 %, d_p : 1000 μm

(b) BFB: Naphthalene conversion: 78 %, d_p : 1000 μm

Figure 6-18 tar concentration in the bubble and dens phase along the large particles bed height of for the (a) in-situ gasification and (b) downstream BFB tar cracker at the same conditions, T: 900 °C; superficial velocity: 0.3 m/s; feed gas (7 % H₂O, 7 % CO₂, 0.2 % Naphthalene, balance N₂)

Both char and dolomite can be used for tar removal for an in-situ gasification process. The aim of both processes is to remove the tars inside the gasifier. However, there are some differences in the application and the results. In the in-situ use of the dolomite, a certain percent of the dolomite is mixed with the sand bed (gasifier bed material) whereas in the present concept the whole sand bed is replaced with the biomass char. Corella and his co-workers studied the in-situ use of the dolomite and obtained a reduction of the tar concentration in the producer gas to a level of about 1.2 g/Nm³. A tar concentration below this limit was not reached with dolomites by these authors [12, 13], whereas Gil et al. [14] obtained a tar concentration below 1 g/Nm³ with 15 and 30 wt. % of dolomite, with the rest being silica sand. Thus, the gasification in the char bed as done here achieved a much better result as the tar concentration in the producer gas was reduced to 260 mg/Nm³. Moreover, the dolomite is sensitive to the coke formation whereas the biomass char is not that sensitive because of the continuous activation and formation of the biomass char.

In the conventional gasification processes, the char is produced because of incomplete carbon conversion. On average, about 90 % of the incoming carbon is converted to gases in CFB gasifiers [15]. The amount of produced char is enough for a complete tar removal, but it should be used in the most effective way. To have a complete investigation of the biomass char as a bed material in the gasifier, the following effects needs to be further investigated:

Effect of fluidization conditions, such as, char bed particle size and superficial gas velocity, on the tar outlet composition and concentration: It was found that increasing the U/U_{mf} from 1.1 to 3.0 by decreasing the char bed particle size from 1500 to 1000 μm decreased the tar outlet concentration from 315 to 260 mg/Nm³ and also changed the outlet tar composition. Thus, more experiments can give insight to what extent the tar concentration can be lowered and how the tar composition is affected.

Also, the influence of internals or baffles in the char bed on the naphthalene removal should be studied.

Effect of the position of the biomass feeder on the tar output composition and concentration: The biomass was fed on top of the char bed. This gives the devolatilized tar a low contact time with the char particles. Moreover, smaller biomass particles will be gasified in the freeboard of the gasifier, where almost no char is available, and this results in a higher tar concentration in the outlet gas. Other feeding locations need to be explored, such as, the middle and the bottom of the bed.

Effect of the char mechanical strength under different fluidization conditions on the gasifier performance: The biomass char has low mechanical strength compared with silica sand and FCC catalyst. On the other hand, it is similar to the calcined dolomites which have low mechanical strength. The low mechanical strength of the char can cause fines. The amount of fines increases with increasing the severity of fluidization. Therefore, improved cyclone efficiency will be needed to separate the fine char particles. However, the fines can act as an adsorbent on the downstream filters for tars reduction at low temperatures. The fine particles can be afterwards recycled back to the gasifier, thus, increasing the gasification efficiency.

Effect of coke formation on the tar removal under different gasification temperatures: The sensitivity of char to coke formation is found to be much less than other catalysts such as nickel, dolomite, FCC or olivine. In chapter four it was found that the biomass char kept its catalytic activity for tar removal at a temperature of 800 °C or above. This is because of the continuous reactivation of the char by the gasification reactions with steam and CO₂. Moreover, during the gasification in the char bed, a new and active char is produced from the gasified biomass. Therefore, there is no need for catalyst regeneration or external supply of fresh catalyst. Further, the coke that deposits on the char stays in the gasifier to be gasified. Thus, the gasification efficiency is not decreased because there is no loss of coke, i.e. no energy loss.

Effect of using gasification in a char bed using a circulating fluidized bed gasifier: This reactor can be used for large scale applications and it overcomes the problem of tar diffusion to the bubble phase before being completely converted. The flow of gas and char is close to co-current plug flow where finer particles are used and higher conversion is possible. Moreover, fine char particle size can be used which increases the tar conversion per kg char. This reactor has very high superficial velocities which can be compensated by the large height of the CFB-raiser to make sure that tars have enough residence time to be converted.

Effect of sampling method on tar composition and quantization: The sample points were clean and depositions were not found at these experiments. This means no heavy tars were expected in the outlet gas which makes the difference between the results of the SPA and the standard method insignificant.

6.8 Application

The biomass gasification in a char bed seems to be very promising both technically and economically. It has the potential to save the cost of a secondary reactor for removing the tar, because 97 % tar conversion with a tar concentration in the producer gas of 260 mg/Nm³ was found. This result is comparable with tar cracker from the Swedish company TPS AB which has more than 95 % tar conversion with a concentration of 200 mg/Nm³. However, the TPS result required a secondary circulating fluidized bed reactor of dolomite that is close-coupled with the circulating fluidized bed gasifier.

For using the producer gas in a power production application, the tar concentration in the producer gas needs to be further decreased to a level less than 100 mg/Nm³ [16]. To decrease further the tar concentration in the producer gas of the biomass gasification in a char bed to acceptable limits, either the process conditions in the gasifier need to be optimized or a more efficient reactor type should be selected.

Improving the process conditions can be done by improving the contact between the tars and the char. This can be done by decreasing the bubbles size (e.g. by increasing bed particle size) and breaking the bubbles by inserting internals into the bed to hinder bubble growth and cut down bubble size [11]. Moreover, the tars residence time in the char bed can be increased by changing the position of the biomass feeder to the bottom of the gasifier. Thus, the tars produced from the biomass have longer residence time in the char bed to be removed. Another possibility is the co-gasification. The feed to the gasifier can also be a mixture of coal and biomass. The coal produces a char of higher activity (higher metal content) than biomass. Thus, the tar removal can be increased further.

The biomass char has a low mechanical strength. Thus, fines are expected to be formed. To separate the fine particles, cyclones of improved efficiencies are needed. The gas can be further cleaned using filters that trap the fine chars which also act as adsorbents for the remaining tar in the gas.

The coke deposition on the char is not considered a problem because of the continuous activation and production of char. Moreover, the coke that is deposited on the char stays in the gasifier or recycled back to be gasified. Thus, the gasification efficiency is not decreased because there is no loss of coke, i.e. no energy loss.

This process can be used for power production in a medium to large scale where an IC-engine can be used in the lower scale and a gas turbine in the upper scale.

6.9 Concluding Remarks

In this chapter, the performance of biomass char as a catalyst for tar removal under fluidized bed conditions was studied. The main conclusions are:

- The biomass gasification in a char bed (in-situ gasification) seems to be very promising for (partial) solving of the tar problem. It has the potential to give more than 97 % tar conversion at 850 °C.
- Further improving of the fluidization conditions in the in-situ gasification may further increase the tar removal.
- The tar conversion in the in-situ gasification (97% at 850 °C) is remarkably higher than the naphthalene conversion in the secondary bubbling fluidized bed of char (76 % at 900 °C)
- The mass transfer of the naphthalene between the bubble and dense phase is the main factor that affects the naphthalene removal in bubbling fluidized bed conditions.
- The naphthalene conversion in bubbling fluidized bed conditions can be increased by increasing: the particle size, bed height (i.e. the gas residence time) and bed temperature.
- The bubbling fluidized bed reactor has a poor overall gas solid contact efficiency which reduces the naphthalene conversion to 76 % at 900 °C and 0.3 s gas residence time. Thus, the hydrodynamics is more important than the kinetics for the catalytic removal of the naphthalene in bubbling fluidized bed conditions.
- The improvement of the contact between gas the char can be done by either improving the reactor conditions or changing the reactor type (circulating fluidized bed).

References

1. Kunii, D. and O. Levenspiel, *Fluidization Engineering*. Second ed. Series in Chemical Engineering, ed. H. Brenner. 1991, Boston: Butterworth-Heinemann. 491.
2. Neogi, D., et al., *Study of coal gasification in an experimental fluidized bed reactor*. AIChE J., 1986. **32**(1): p. 17-28.
3. Kunii, D. and O. Levenspiel, *Fluidization Engineering*. Second ed. 1991, Boston: Butterworth-Heinemann.
4. Thompson, M.L., H. Bi, and J.R. Grace, *A generalized bubbling/turbulent fluidized-bed reactor model*. Chemical Engineering Science, 1999. **54**(13-14): p. 2175-2185.
5. Westerterp, K.R., et al., *Chemical reactor design and operation*. 2nd ed. 1984: Wiley.
6. Davidson, J.F. and D. Harrison, *Fluidization*. 1977, London and New York: Academic Press.

7. Mostoufi, N., H. Cui, and J. Chaouki, *A Comparison of Two- and Single-Phase Models for Fluidized-bed Reactors*. Ind. Eng. Chem. Res., 2001. **40**: p. 5526-5532.
8. Grace, J.R., *High velocity Fluidized Bed Reactors*. Chemical Engineering Science, 1990. **45**(8): p. 1953-1966.
9. Katta, S. and D. Kerlins, *Study of Kinetics of Carbon Gasification Reactions*. Ind. Eng. Chem. Fundam., 1981. **20**: p. 6-13.
10. Mori, S. and C.Y. Wen, *Estimation of Bubble Diameter in gaseous fluidized beds*. AIChE J., 1975. **21**: p. 109.
11. Levenspiel, O., *Chemical Reaction Engineering*. Second Edition ed. 1972, Singapore: Wiley & Sons, Inc. 472.
12. Orio, A., J. Corella, and I. Narvaez, *Performance of Different Dolomites on Hot Raw Gas Cleaning from Biomass Gasification with Air*. Ind. Eng. Chem. Res., 1997. **36**: p. 3800-3808.
13. Corella, J., et al., *Biomass Gasification in Fluidized Bed: Where to Locate the Dolomite?* Energy & Fuels, 1999. **13**(6): p. 1122-1127.
14. Gil, J., et al., *Biomass Gasification with Air in a Fluidized Bed: Effect of the In-Bed Use of Dolomite under Different Operating Conditions*. Ind. Eng. Chem. Res., 1999. **38**: p. 4226-4235.
15. van der Drift, A., C.M. van der Meijden, and S.D. Srating-Ytsma. *Ways to Increase Carbon Conversion of a CFB-Gasifier*. in *12th European Conference on Biomass for Energy, Industry and Climate Protection*. 2002. Amsterdam, The Netherlands: ETA-Florence.
16. Hasler, P. and T. Nussbaumer, *Gas Cleaning for IC Engine Applications from Fixed Bed Biomass Gasification*. Biomass and Bioenergy, 1999. **16**: p. 385-395.

Chapter 7

Conclusions and Recommendations

7.1 Conclusions

In chapter two, a review was presented for the various types of catalysts that have been used in several research programs on tar reduction in producer gas from a gasification process. It was concluded that calcined rocks and transition metal-based catalysts give the highest tar reduction. They are used as a reference for the catalytic cleaning methods of most institutions and companies working on biomass gasification. On the other hand, biomass char can be a good alternative catalyst for tar removal. The attractiveness of biomass char for solving the tar problem is related to its low cost, natural production inside the biomass gasifier, its catalytic activity for tar reduction and the possibility to be integrated in the gasification process itself.

In chapter three, the reviewed catalysts were tested to evaluate how competitive biomass char can be. The comparison is based on both the activity for model tar components removal in a fixed bed reactor and catalyst stability. Biomass chars gave the highest naphthalene conversion among the low cost and active catalysts.

In chapter four, naphthalene conversion was found to be comparable with the real tar conversion over biomass char at temperatures above 800 °C, but clearly higher at lower temperatures (700-750 °C). A temperature of 800-850 °C seems to be optimal for high tar conversion degree and a limited carbon conversion degree.

It is noted from the experimental results that the char activity for naphthalene reduction did not decrease during the carbon conversion process. Possible explanations are: 1) during the conversion of the carbon, the char micropores grow to meso pores and macro pores which are more effective for the removal, and 2) the metal content concentration of the remaining char increases with the char conversion. Thus, the decrease in the total surface area is (partly) compensated by the increase of the effective surface area for tar conversion or by an increase of the kinetic constant of the reaction.

The mechanism of the tar reduction by char was investigated. The tar or naphthalene is adsorbed on the active sites of the char particle surface. The adsorbed

tars can have two parallel pathways. The first path is a catalytic conversion of naphthalene or tar to form CO and H₂ by steam and dry gasification reactions. The exact mechanisms of the steam and dry reforming reactions of tar are not well known. Nevertheless, tar can have longer residence time when adsorbed on the surface of char. The metal content of char catalyzes the reforming reactions of tar. The second path is a decomposition of tars to form free radicals that enter polymerization reactions and form coke deposited on char surface. Char has the activity to remove the hydrogen atom from the tar component to form a free radical. This free radical participates in the heavy hydrocarbon polymerization reactions while the reaction products are deposited as coke on the surface of char. The tendency toward coke formation is related to the number of aromatic rings in the tar component. The larger the number of aromatic rings, the larger is the tendency for coke formation. The tar reforming reactions probably produce insensitive coke which can be effectively controlled by adapting the operating conditions in such a way that the gasification rate of coke is higher than the production rate.

In chapter five, the knowledge gained from the experimental work is used to develop a model for the naphthalene reduction by biomass char for both particle and reactor scale. Moreover, the models are used to validate and further explain the experimental results of the previous chapter. The particle model calculations support experimental results and show that internal and external mass transfer has a minor effect on naphthalene and carbon conversions. Further, the particle model shows that isothermal conditions can be assumed.

From the experiments in chapter four, it was shown that for temperatures of 850 °C or higher, the activity of the char bed for the naphthalene conversion does not depend on the time on stream. Therefore, the reactor model calculations for the naphthalene concentration profile along the bed height can be simplified to a plug flow reactor ($C = C_o e^{-k\tau}$). Thus, only two parameters affect the naphthalene conversion: the naphthalene residence time in the char bed and temperature of the char bed.

On the other hand, carbon is converted because of gasification reactions with steam and CO₂. The rate of these reactions is highly dependent on the temperature because they are kinetically limited. Moreover, the physical properties of the char particle and the pore structure change with the carbon content conversion. Therefore, the reaction surface area within the particle is changing with time on stream. Thus, the activity of the carbon conversion reactions changes with the time on stream. Because the concentration of the steam and CO₂ is decreasing along the bed height, the carbon conversion decreases as well. Thus, decreasing the gas residence time by increasing the gas velocity flattens the gas concentration profile along the bed height and flattens the carbon conversion as well.

To get insight in the integration of a fixed bed tar cracker downstream of a biomass gasifier, a preliminary design was made. The tar cracker was integrated with the gasifier by compensating the char consumption in the tar cracker with the produced ash from the gasifier that contains mainly char. Fixed beds are commonly used for small scale processes. Thus, the fixed bed tar cracker is integrated with a fixed bed gasifier. The values of the key parameters (optimum values for these

parameters are 850 °C and 0.3 s, respectively). The particle size of the char particles was selected to be 5 mm in order to increase the particles minimum fluidization velocity and prevent blowing out the particles. Nevertheless, the internal mass transfer is expected to be negligible as found earlier. For small scale gasification processes, the downdraft gasifier is often used. Here a capacity of 10 MW_{th} was selected. The output tar content from the tar cracker was estimated to be 13 mg/Nm³. This concentration is low enough for power production applications. The tar reduction degree is 98.3%. Moreover, the rate of biomass char consumed in the cracker is found to be lower than the char produced in the gasifier assuming 90 % carbon conversion of the biomass.

In chapter six, the performance of biomass char as a catalytic bed material in a bubbling fluidized bed reactor was investigated. The biomass char was tested both as a bed material for naphthalene removal in a downstream fluidized bed reactor (secondary measure) and as a bed material inside the biomass gasifier itself (primary measure).

The naphthalene conversions in the bubbling fluidized bed (BFB) experiments are significantly lower than those in the fixed bed experiments. The naphthalene conversion in the fluidized bed was 76 % at 900 °C and 0.3 s gas residence time, whereas, the fixed bed gave more than 98 % naphthalene conversion with comparable temperature and gas residence time. This indicates the importance of the mass transfer in the BFB.

Biomass char can be easily integrated in the gasification process for tar removal because it is a product of the gasification process. An innovative use of the biomass char as a primary measure for tar removal was presented. The biomass gasification was carried out in a BFB of biomass char instead of silica sand. The preliminary in-situ gasification experiments, carried out at 850 °C, showed a high tar reduction, which is more than 97 % corresponding to an outlet tar concentration of 260 mg/Nm³. Further optimization of the process conditions is possible: higher bed, lower biomass feeding, larger bed particles, etc. Thus, the biomass gasification in a char bed seems to be very promising both technically and economically. It has the potential to save the cost of a secondary reactor for removing the tar, because 97 % tar conversion with a tar concentration in the producer gas of 260 mg/Nm³ was found.

7.2 Recommendations

The char source is an important parameter for the tar reduction. Especially, the presence of metals like iron and alkalis in the ash have a major influence on the tar reduction. Also, the method of char production seems to be important. Unfortunately, because of the high naphthalene conversion degrees, no influence of the heating rate and the final pyrolysis temperature could be recognized in the present experiments. These parameters will certainly influence the tar-char reaction. More research in this area is required.

Coke formation turns out to be an important issue and needs to be investigated more thoroughly. In the reactor model presented in chapter five, the coke formation is simply modeled with a tuning factor to get a preliminary insight in the quantitative influence of the coke formation on the different reaction rates. A more sophisticated model for the coke formation needs to be developed.

The preliminary in-situ gasification experiments showed a high tar reduction. To get a complete investigation of the biomass char as a bed material in the gasifier, the following effects need to be further investigated:

- Effect of fluidization conditions, such as, char bed particle size and superficial gas velocity, on the tar outlet composition and concentration.
- Effect of the position of the biomass feeder on the tar output composition and concentration.
- Effect of the char mechanical strength under different fluidization conditions on the gasifier performance.
- Fluidization behavior of a char bed.
- Effect of coke formation on the tar removal under different gasification temperatures.
- Effect of using gasification in a char bed using a circulating fluidized bed gasifier.
- Effect of sampling method on tar composition and quantization.

Nomenclature

Acronyms

ABD	Apparent bulk density
APS	Average particle size
ASA	Active surface area
BET	Brunauer-Emmet-Teller
BFB	Bubbling fluidized bed
BIGCC	Biomass integrated gasification combined cycle
BTG	Biomass technology group BV
C.B. char	Commercial biomass char
CEN	European Committee for Standardization (Comité Européen de Normalisation)
CFB	Circulating fluidized bed
CHP	Combined heat and power
daf	Dry-ash free
DTU	Technical University of Denmark
ECN	Energy research center of the Netherlands
EF	Entrained flow
Eq.	Equation
ER	Equivalence ratio
EU	European union
Exp.	Experiment
FCC	Fluid catalytic cracking
FID	Flame ionization detector
GBT	Generalized Bubbling/Turbulent
GC	Gas chromatography
HPAH	Heavy poly aromatic hydrocarbon
IEA	International energy agency
K-L	Kunii-Levenspiel
KTH	Royal institute of technology, Stockholm
LAH	Light aromatic hydrocarbon
LPAH	Light poly aromatic hydrocarbon

MSA	Matrix surface area
MS	Mass spectrometry
NREL	National renewable energy laboratory
PAH	Poly aromatic hydrocarbon
p.s	Particle size
RDF	Refused derived fuel
SA	Surface area
SDE	Agency for research in sustainable energy
SPA	Solid phase adsorption
STD	Standard
TCD	Thermal conductivity detector
ThW	Thermal engineering department (Thermische Werktuigbouwkunde)
TGA	Thermogravimetric analysis
TNO	The Netherlands organization for Applied Scientific Research "Toegepast natuurwetenschappelijk onderzoek"
TPS	Termiska Processor AB
TSA	Total surface area
UT	University of Twente
VTT	Technical Research Centre of Finland (Valtion Teknillinen Tutkimuskeskus)

Latin

a	Relative surface area of the char particle, see eq. (5.45)	m^2 / m^2
A_b	Bubble phase area	m^2
A_e	Emulsion phase area	m^2
A_0	Cross section area of the bed	m^2
Bi_m	Biot number	—
Bo	Bodenstein number	—
C_b	Gas component concentration in the bubble phase	$kmol / m^3$
C_e	Gas component concentration in the emulsion phase	$kmol / m^3$
C_i	Gas component concentration	$kmol / m^3$
$C_{i,b}$	Bulk concentration of the gas component	$kmol / m^3$
$C_{i,s}$	Surface concentration of the gas component	$kmol / m^3$
C_{in}	Inlet concentration	$kmol / m^3$

C_n	Naphthalene concentration	$kmol / m^3$
C_{out}	Outlet concentration	$kmol / m^3$
$C_{p,C}$	Specific heat capacity of the char	$kJ / kg.K$
$C_{p,i}$	Specific heat capacity of the gas component i	$kJ / kg.K$
$C_{p,g}$	Specific heat capacity of the gas	$kJ / kg.K$
C_s	Surface concentration of the gas	$kmol / m^3$
d_b	Bubble diameter	m
D_e	Effective diffusion coefficient	m^2 / s
D_i	Binary diffusion coefficient of the gas component i	m^2 / s
D_K	Knudson diffusion coefficient	m^2 / s
D_l	Coefficient of longitudinal dispersion	m^2 / s
D_M	Molecular diffusion coefficient	m^2 / s
d_p	Particle diameter	m
d_t	Tube diameter	m
E_{app}	Apparent activation energy	$kJ / kmol$
e_{mf}	Void fraction at minimum fluidization velocity	—
F	Molar feed flow rate	$kmol / s$
f_1	Tuning factor for the steam reforming reaction of the char	—
f_2	Tuning factor for the dry reforming reaction of the char	—
g	Acceleration of gravity	m / s^2
H	Height of char bed	m
h	Heat transfer coefficient in the gas film around the particle	$kJ / m^2.s.K$
H_f	Molar heat of formation	$kJ / kmol$
H_i	Molar enthalpy	$kJ / kmol$
H_s	Specific sensible heat	kJ / kg
k	Kinetic rate constant	$s^{-1} . (kmol / m^3)^{n-1}$
k'	Intrinsic rate coefficient on area basis	$kg / m^2.s$
k_{app}	Apparent kinetic rate constant of the naphthalene reforming reaction	s^{-1}

K_{be}	Gas interchange coefficient	s^{-1}
$k_{g,i}$	Mass transfer coefficient of the gas component i in the gas film	m / s
$k_{n,true}$	True kinetic rate constant of the naphthalene reforming reaction	s^{-1}
$k_{o,app}$	Frequency factor of the rate constant of the naphthalene steam reforming reaction	s^{-1}
k_{sh}	Kinetic rate constant of the forward direction in the gas shift reaction	$m^3 / kmol \cdot s$
k_{-sh}	Kinetic rate constant of the backward direction of the gas shift reaction	$m^3 / kmol \cdot s$
L	Length of the char bed	m
L	Characteristic length; equivalent to $(dp/6)$ for a sphere	m
M_i	Molecular weight of the i^{th} gas component	$kmol / kg$
M_C	Molecular weight of the carbon	$kmol / kg$
n	Apparent reaction order with respect to the gas component	—
Nu	Nusselt number	—
Pe	Peclet number	—
P_i	Partial pressure of component i	Pa, atm
P_{tot}	Total pressure in the bed	Pa, atm
Q_{in}	Inlet volumetric flow rate	m^3 / s
r	Radius coordinate	m
r	Intrinsic volumetric gasification rate	$kmol / m^3 \cdot s$
r_n	Rate of naphthalene conversion reaction	$kmol / m^3 \cdot s$
R	Gas constant	$kJ / kmol \cdot K$
R_C	Sum of the rates of the chemical carbon conversion	$kJ / kmol \cdot K$
R_i	Sum of the rates of the chemical production of gas component i	$kJ / kmol \cdot K$
Re	Reynolds number	m
R_o	Outside particle diameter	—
S	Effective surface area of the char at a certain carbon conversion	m^2 / kg
S_o	Initial total surface area of the char	m^2 / kg
Sh	Sherwood number	—
t	Time on stream	s
T	Local particle temperature	K
T_b	Temperature of the bulk gas	K

T_c	Temperature of the center of the particle	K
T_R	Temperature of the reactor	$^{\circ}C, K$
T_s	Temperature of the surface of the particle	K
U	Superficial gas velocity	m / s
U_{mf}	Minimum fluidization gas velocity	m / s
u_o	Superficial gas velocity	m / s
$U_{b\infty}$	Bubble rise velocity	m / s
$V_{R,cat}$	Volume of the catalyst bed with respect to the volume of empty reactor	m^3
v	Average actual fluid velocity	m / s
v_o	Volumetric feed gas flow rate	l / min
w_C	Carbon content in the char particle (0.88)	—
W_0	Weight of the char bed at reactor temperature and time zero	g
W_t	Weight of the char bed at reactor temperature and time on stream	g
x_i	Gas component mole fraction	—
X	Tar conversion	—
$X_{c,t}$	Carbon conversion at a certain time on stream	—
y_c	Carbon content of the treated char	—
z	Distance along the bed height	m

Greek

α_{ij}	Stoichiometric coefficient of the i^{th} component in j^{th} reaction	—
β	Non-dimensional temperature difference	—
ε	Porosity of the particle	—
ε_b	Porosity of the bed (0.4)	—
ε_b	Bubble fraction in the bed	—
ε_{mf}	Void fraction at minimum fluidization conditions	—
δ	Pore diameter	nm
Φ_T	Thiele Modulus	—
ϕ_s	Shape factor: (surface area of the particle / πdp^2)	—
η	Effectiveness factor	—

λ_e	Effective thermal conductivity	$\text{kJ} / \text{s.m.K}$
λ_g	Gas mixture thermal conductivity	$\text{kJ} / \text{s.m.K}$
μ	Gas viscosity	$\text{kg} / \text{m} \cdot \text{s}$
$\langle \nu \rangle$	Kinematic viscosity	m^2 / s
ρ_b	Density of the bed	kg / m^3
ρ_C	Density of the char particle	kg / m^3
ρ_g	Density of the gas	kg / m^3
ρ_p	Density of the particle at a certain time and position	kg / m^3
$\rho_{p,o}$	Initial density of the particle	kg / m^3
$\rho_{p,t}$	True density of the particle	kg / m^3
ρ_s	Density of the solid in the particle	kg / m^3
τ	Tortuosity	—
τ	Gas residence time (space time)	s
τ'	Gas weight time	$\text{kg} \cdot \text{h} / \text{m}^3$
ξ	Ration of average channeling length to particle diameter	—
ξ	Dimensionless radial distance	—
Δx	Differential bed height	m
ΔH	Heat of reaction	kJ / kmol

Subscripts and superscripts

app	Apparent
<i>b</i>	Bulk conditions, bed or bubble
C	Carbon
c	Center
Cat.	Catalyst
e	Effective or emulsion
eff	Effective
f	formation
g	Gas
i	Gas species index
in	inlet
j	Reaction index

l	Longitudinal
mf	Minimum fluidization conditions
o, 0	Initial conditions or outside
n	Naphthalene
out	outlet
p	Particle
R	Reactor
s	Surface
sh	Forward shift reaction
_sh	Backward shift reaction
t	Time on steam or true
th	Thermal
tot	Total

Appendix A

Physical Properties Estimation

A.1 Char density

The bulk density of the char is the weight of the sample divided by the volume displaced by the sample, which includes the micro and macropores inside the particle and voids between the particles.

$$\rho_p = \frac{\rho_b}{1 - \varepsilon_b} \quad (\text{A.1})$$

Where,

- ρ_p = apparent particle density, kg/m³
- ρ_b = bulk density, kg/m³
- ε_b = bed voidage, usually taken as 0.45 [1]

The particle apparent density (ρ_p) is based on the volume defined by the external surface of the particle that includes the pores. The true particle density ($\rho_{p,t}$) is calculated by eliminating that portion of the total volume in the pores (V_{pores}). The ratio of the volume of the pores to the total volume of the particle is defined as the particle porosity.

A.2 Carbon content

The carbon content (w_c) in the char particle used is based on the ultimate analysis of treated biomass char given in Table 4-5.

A.3 Gas density

Assuming ideal gas, the density of the gas component (ρ_i) is

$$\rho_i = \frac{P_i M_i}{RT} \quad (\text{A.2})$$

Where,

- P_i = partial pressure of component i, atm
 M_i = molecular weight of component i, kg/kmol

The density of the gas mixture is:

$$\rho_g = \sum_i \rho_i \quad (\text{A.3})$$

The mean molecular weight of the gas mixture (M_g) is:

$$M_g = \left[\sum_i \frac{\rho_i}{M_i \rho_g} \right]^{-1} \quad (\text{A.4})$$

Where,

- ρ_i = density of gas component i, kg/m³
 ρ_g = density of the gas mixture, kg/m³

A.4 Gas Diffusion coefficient

The gaseous reactants are assumed diluted species in the inert component N₂ which is about 60 vol. % of the gas mixture. This assumption allows the use of the binary diffusion theory for our system, which is a multi-component system. The binary diffusion coefficient is estimated using the following expression [1]. The values of the diffusion coefficients for the different components are given in Table A-1.

$$\frac{pD_{AB}}{(p_{CA}p_{CB})^{1/3} (T_{CA}T_{CB})^{5/12} (1/M_A + 1/M_B)^{1/2}} = a \left(\frac{T}{\sqrt{T_{CA}T_{CB}}} \right)^b \quad (\text{A.5})$$

Where,

- p, p_C = pressure, critical pressure, atm
 D_{AB} = binary diffusion coefficient of reactant A in B (i.e. N₂), cm²/s
 T, T_C = temperature, critical temperature, K
 M = molecular weight, kg/kmol

For non-polar gases: (H₂, CO, CO₂, CH₄, naphthalene)

$$a = 2.74 \cdot 10^{-4}, \quad b = 1.823$$

For polar gases (H₂O)

$$a = 3.640 \cdot 10^{-4}, \quad b = 2.334$$

Table A-1 The physical properties needed to calculate the diffusion coefficient at 850 °C of the components [2]

	H₂	H₂O	CO	CO₂	CH₄	Naphthalene	N₂
T _c (K)	33.18	647	134.45	304.18	190.6	748	126.2
P _c (bar)	13	220.64	34.9875	73.8	46.1	41	33.978
M (g/mol)	2	18	28	44	16	128	28
D (cm ² /s)	8.96	5.85	2.29	1.76	2.46	0.80	2.33

Laurendeau reported that that the binary diffusion coefficient values can be approximated at other temperatures with high accuracy as follows [3]:

$$D(T, P) = D(T_o, P_o) \left(\frac{T}{T_o} \right)^{7/4} \left(\frac{P}{P_o} \right) \quad (\text{A.6})$$

Where,

T_o, T = initial and new temperature, K

P_o, P = initial and new pressure, atm

A.5 Thermal conductivity

The effective thermal conductivity can be estimated by [4]:

$$\lambda_e = (1 - \varepsilon)^2 \lambda_c + \varepsilon^2 \lambda_g \quad (\text{A.7})$$

Where,

λ_c = char thermal conductivity, kJ/s.m.K

λ_g = gas thermal conductivity, kJ/s.m.K

ε = porosity of the char particle

Many researchers have reported values for the thermal conductivity of wood char [5-9]. However, these values are difficult to compare because of the incomplete specifications at which these values can be applied. These specifications lack mostly the source type of biomass char, density and temperature. Moreover, there is a mix sometimes in the specification whether the reported data is for the solid char or the char particle. The value reported by Dasappa et. al. [6] for wood char carbon was used because they modeled the wood char in a close temperature range.

$$\lambda_c = 1.85 \cdot 10^{-3} \quad (\text{kJ} / \text{s} \cdot \text{m} \cdot \text{K}) \quad (\text{A.8})$$

The thermal conductivity of the gases in the producer gas is based on a fit for experimental data [10]. Because of the linearity of the thermal conductivity with temperature, these correlations are assumed to be valid for the temperature range from

273 k (or boiling point) to 1273 K. The thermal conductivity of naphthalene (n) is approximated with that of benzene.

$$\begin{aligned}
 \lambda_n &= -2.150 \cdot 10^{-5} + 1.039 \cdot 10^{-7} T \\
 \lambda_{H_2O} &= -2.694 \cdot 10^{-5} + 1.253 \cdot 10^{-7} T \\
 \lambda_{H_2} &= 3.988 \cdot 10^{-5} + 4.861 \cdot 10^{-7} T \\
 \lambda_{CO} &= 1.234 \cdot 10^{-5} + 5.055 \cdot 10^{-8} T \\
 \lambda_{CO_2} &= -5.031 \cdot 10^{-6} + 7.617 \cdot 10^{-8} T \\
 \lambda_{CH_4} &= -5.77 \cdot 10^{-6} + 1.50 \cdot 10^{-7} T \\
 \lambda_{N_2} &= 1.00 \cdot 10^{-5} + 5.562 \cdot 10^{-8} T
 \end{aligned} \tag{A.9}$$

The thermal conductivity of the gas mixture can be approximated using the empirical law [11]:

$$\lambda_g = \frac{1}{2} \left[\sum_i x_i \lambda_i + \left(\sum_i \frac{x_i}{\lambda_i} \right)^{-1} \right] \tag{A.10}$$

Where,

- λ_g = thermal conductivity of gas mixture, kJ/s.m.K
- λ_i = thermal conductivity of gas component i, kJ/s.m.K
- x_i = mole fraction of gas component i

A.6 Heat capacity

The heat capacity of char in ($kJ / kg.K$) is estimated based on the correlation reported for charcoal derived for the temperature range 273-1273 K [9]:

$$C_{p,C} = 0.42 + 2.09 \cdot 10^{-3} T + 6.85 \cdot 10^{-7} T^2 \tag{A.11}$$

The heat capacity of the different gas components in the system in ($kJ / kg.K$) is given in the set of equations below. The naphthalene heat capacity is approximated by benzene heat capacity. The temperature range of validity is 273-1373 K [9, 12].

$$\begin{aligned}
C_{p,n} &= -0.10 + 4.4 \cdot 10^{-3} T - 1.57 \cdot 10^{-6} T^2 \\
C_{p,H_2O} &= 1.67 + 6.4 \cdot 10^{-4} T \\
C_{p,H_2} &= 13.925 + 1.3 \cdot 10^{-3} T \\
C_{p,CO} &= 0.767 + 4 \cdot 10^{-4} T \\
C_{p,CO_2} &= 0.9784 + 2 \cdot 10^{-4} T \\
C_{p,CH_4} &= 1.508 + 2.9 \cdot 10^{-3} T \\
C_{p,N_2} &= 0.97 + 2.0 \cdot 10^{-4} T
\end{aligned} \tag{A.12}$$

The average heat capacity of the gases is

$$C_{p,g} = \frac{\sum_i C_{p,i} \rho_i}{\rho_g} \tag{A.13}$$

A.7 Enthalpy

The heat of formation (H_f°) in ($kJ / kmol$) of the different components in the system is [10]:

$$\begin{aligned}
H_{f,C}^\circ &= 0 \\
H_{f,n(g)}^\circ &= 1.56 \cdot 10^5 \\
H_{f,H_2O}^\circ &= -2.41826 \cdot 10^5 \\
H_{f,H_2}^\circ &= 0 \\
H_{f,CO}^\circ &= -1.10603 \cdot 10^5 \\
H_{f,CO_2}^\circ &= -3.93777 \cdot 10^5 \\
H_{f,CH_4}^\circ &= -7.48977 \cdot 10^4
\end{aligned} \tag{A.14}$$

The sensible heat (H_s) in (kJ / kg) of the different components in the system is estimated according to eq. (5-39).

$$\begin{aligned}
H_{s,C} &= -2.24 \cdot 10^2 + 0.42T + 1.045 \cdot 10^{-3}T^2 + 2.283 \cdot 10^{-7}T^3 \\
H_{s,n} &= -1.517 \cdot 10^2 - 0.1T + 2.2 \cdot 10^{-3}T^2 - 5.233 \cdot 10^{-7}T^3 \\
H_{s,H_2O} &= -5.052 \cdot 10^2 + 1.6T + 3.2 \cdot 10^{-4}T^2 \\
H_{s,H_2} &= -4.2074 \cdot 10^3 + 13.925T + 6.5 \cdot 10^{-4}T^2 \\
H_{s,CO} &= -2.004 \cdot 10^3 + 0.767T + 2 \cdot 10^{-2}T^2 \\
H_{s,CO_2} &= -3.0133 \cdot 10^2 + 0.9784T + 1 \cdot 10^{-4}T^2 \\
H_{s,CH_4} &= -5.781 \cdot 10^2 + 1.508T + 1.45 \cdot 10^{-3}T^2
\end{aligned} \tag{A.15}$$

A.8 Dynamic viscosity

The dynamic viscosity of the components expressed in ($kJ/m.s$) and the temperature in (K) is given for the temperature range 273-1273 K. The dynamic viscosity of N_2 is approximated by that of air and that of naphthalene is approximated with that of benzene.

$$\begin{aligned}
\mu_n &= -3.7310^{-7} + 2.62 \cdot 10^{-8}T \\
\mu_{H_2O} &= -1.47 \cdot 10^{-6} + 3.78 \cdot 10^{-8}T \\
\mu_{N_2} &= 9.12 \cdot 10^{-6} + 3.27 \cdot 10^{-8}T \\
\mu_{CO} &= 9 \cdot 10^{-6} + 3 \cdot 10^{-8}T \\
\mu_{CO_2} &= 7 \cdot 10^{-6} + 3 \cdot 10^{-8}T
\end{aligned} \tag{A.16}$$

For H_2 , the correlation is based on a fit for temperature range 273-1073 K [12] and for CH_4 , the correlation is based on a fit for temperature range 273-772 K [12]. It is assumed that these correlations are valid to model range up to 1273 K.

$$\begin{aligned}
\mu_{H_2} &= 5 \cdot 10^{-6} + 2 \cdot 10^{-8}T \\
\mu_{CH_4} &= 4 \cdot 10^{-6} + 3 \cdot 10^{-8}T
\end{aligned} \tag{A.17}$$

The average dynamic viscosity of the gas mixture is:

$$\mu_g = \frac{\sum_i \mu_i \rho_i}{\rho_g} \tag{A.18}$$

A.9 Physical properties at standard conditions

At the standard gas composition and temperature, the physical properties are evaluated and summarized in Table A-2. Moreover, the physical properties of the gas mixture at standard composition in the temperature range 750 to 950 °C are evaluated and summarized in Table A-3

Table A-2 Physical properties of components at standard composition and temperature (850 °C)

	H ₂	H ₂ O	CO	CO ₂	CH ₄	Naphthalene	N ₂	Mixture
x	0.06	0.11	0.13	0.11	0.04	0.002	0.548	
M (kg/kmol)	2	18	28	44	16	128	28	26.82
D (m ² /s)·10 ⁵	89.6	58.5	22.8	17.6	24.6	8.02	23.3	
C _p (kJ/kgK)	15.38	2.39	1.20	1.22	4.76	2.86	1.19	1.452
ρ (kg/m ³)	0.0013	0.0212	0.0390	0.0518	0.0069	0.0027	0.1643	0.2873
μ (kg/m·s)·10 ⁵	2.75	4.10	4.27	2.95	3.77	2.90	4.58	4.17
λ (kJ/ s·m·K)·10 ³	0.586	0.114	0.069	0.081	1.163	0.095	0.072	0.097

Table A-3 Physical properties of standard gas mixture at different temperatures

T (°C)	C _{p,g} (kJ/kgK)	ρ _g (kg/m ³)	μ _g (kg/m·s)·10 ⁵	λ _g (kJ/ s·m·K)·10 ³	λ _c (ε ₀) (kJ/s·m·K)·10 ³
750	1.418	0.3153	3.86	0.089	0.057
800	1.435	0.3006	4.02	0.0931	0.059
850	1.452	0.2873	4.17	0.0971	0.061
900	1.470	0.2750	4.32	0.101	0.063
950	1.487	0.2638	4.47	0.105	0.066

References

1. Szekely, J., Evan, J.W. and Sohn, H.Y., *Gas-Solid Reactions*. 1976, New York: Academic Press.
2. <http://www.nist.gov/>.
3. Laurendeau, N.M., *Heterogeneous Kinetics of Coal Char Gasification and Combustion*. Prog. Energy Combust. Sci., 1978. **4**: 221-270.
4. Stoirchos, S. and Burganos, V.N., *Intraparticle Diffusion and Char Combustion*. Chemical Engineering Science, 1986. **41**(6): 1599.
5. Gupta, M., Yang, J. and Roy, C., *Specific Heat and Thermal Conductivity of Softwood Bark and softwood Char Particles*. Fuel, 2003. **82**: 919.

6. Dasappa, S., Paul, P.J., Mukunda, H.S. and Shrinivasa, U. *Wood-Char Gasification: Experiments and Analysis on Single Particles and Packed Beds*. in *Twenty-Seventh Symposium (International) on Combustion / The Combustion Institute*. 1998.
7. Koufopoulos, C.A., Papayannakos, N., Maschio, G. and Lucchesi, A., *Modeling of the Pyrolysis of Biomass Particles. Studies on Kinetics, Thermal and Heat Transfer Effects*. The Canadian Journal of Chemical Engineering, 1991. **69**: 907-915.
8. Bryden, K. and Hagge, M., *Modeling the Combined Impact of the Moisture and Char Shrinkage on the Pyrolysis of a Biomass Particle*. Fuel, 2003. **82**: 1633.
9. Gronli, M.G., *A Theoretical and Experimental Study of the Thermal Degradation of Biomass*, in *Mechanical Engineering*. 1996, The Norwegian University of Science and Technology: Trondheim, Norway.
10. <http://webbook.nist.gov/chemistry/>.
11. Warnatz, J., Maas, U. and Dibble, R.W., *Combustion: Physical and Chemical Fundamentals, Modeling and Simulation, Experiments, Pollution Formation*. 2001, Berlin: Springer.
12. Raznjevic, K., *Handbook of Thermal Tables and Charts*. 1976, Washington: McGraw-Hill Book Company.

List of publications

Abu El-Rub, Z., Bramer, E.A., Brem, G., “Evaluation of Catalysts for Tar Elimination in Biomass Gasification Processes”, *Ind. Eng. Chem. Res.*, 2004, 43, 6911-6919.

Abu El-Rub, Z., Bramer, E.A., Brem, G., “Experimental Comparison of Biomass Chars with other Catalysts for Tar Reduction”, *Fuel*, in press.

Abu El-Rub, Z.Y, Bramer, E.A., Brem, G., “Modeling of Tar Reduction in Biomass Gasification Using Biomass Char as a Catalyst” published in *Science in Thermal and Chemical Biomass Conversion*, Victoria, Vancouver Island, BC, Canada, 30 Aug to 2 Sep 2004.

Abu El-Rub, Z.Y, Bramer, E.A., Brem, G., “Tar Reduction in Biomass Gasification Using Biomass Char as a Catalyst” Proceeding of Conference and Technology Exhibition on Biomass for Energy, Industry and Climate Protection, 10-14 May 2004, Rome, I.S.B.N 88-89407-04-2, p.p. 1046-1049.

Abu El-Rub, Z., Bramer, E.A., Brem G., Tar Removal in Fixed Bed with Application to Biomass Gasification. International Nordic Bioenergy 2003 Conference, Proceeding of an Expert Meeting. 2 September – 5 September 2003, Jyväskylä, Finland, I.S.B.N 952-5135-26-8, p.p. 443-447.

Abu El-Rub, Z., Bramer, E.A., Brem G., Tar Removal in an Entrained Flow Cracker (EFC) with Application to Biomass Gasification. Pyrolysis and Gasification of Biomass and Waste, Proceeding of an Expert Meeting. 30 September – 1 October 2002, Strasbourg, France, I.S.B.N 1 872691 7 3, p.p. 337-346.

Abu El-Rub, Z., Bramer, E.A., Brem, G. Removal of Naphthalene as the Model Tar Compound on Calcined Dolomites, Olivine and Commercial Nickel Catalyst in a Fixed Bed Tubular Reactor, Applied For biomass Gasification. 12th European Conference and Technology Exhibition on Biomass for Energy, Industry and Climate Protection, June 2002, Amsterdam, I.S.B.N. -88-900442-5-X, p.p. 607-610.

Acknowledgements

Time has past so quickly since I have started my PhD. It was a rich experience full of joy and pain at the same time. But, finally I could reach the end line of this journey. There were many people along the way who stood beside me and without their support and faith in me I could not make it. These words are just for them to express my gratitude and appreciation for their help.

Initially, I would like to thank Prof. Gerrit Brem my advisor for selecting me for doing the PhD with him, teaching me many things and supporting me all the time. I would like also to thank Ir. Eddy Bramer, my daily supervisor, for his continuous help and his good company. Moreover, I would like to thank Prof. Theo van der Meer, the head of our group for his guidance, support and understanding.

Along the way also many people in the field have helped me with their feedback during discussions in the conferences and emails. I would like to thank my friend Dr. Nader Padban from TPS who was an ex-college in my department, Prof. Corella from University Complutense of Madrid, Spain and Dr. Arij van Berkel from TNO. I would like also to thank the catalyst suppliers companies A/S OLIVINE, Norway and Lhoist, The Netherlands.

The Thermal Engineering Department was my second home in which I spent most of my time. I spent good times thanks to the people their, who have made my stay easy and pleasant. Thanks to our secretary Sally Kloost for her help in many administrative issues. Eise Veenstra for his support in computer related issues. Chris Bakker for his support in building the experimental setups. My roommates Bram de Jager and Bogdan Albrech for their nice company. My students who carried out a part of my PhD work (alphabetical order): Akos, Ashraf, Johnny, Jorke, Isabella, Lambert, Mathijs and Owen. Jan Veneman and all the members of the Thermal Engineering Department.

The social life in the University of Twente and the city of Enschede made my life away from home and family easy and pleasant. Thanks to the Islamic society of University of Twente (ISUT) and the Islamic society of Enschede (Baito allah lelmoslemeen). Also I would like to thank many dear friends for their care and friendship: M. Jadallah, M. Alhaj Ali, M. Alsaleh, T. Ismail, A. Nasr, M. Habash, M. Khatib, Marouf, A. Wazwaz, , K. Sor, Sagheir, K. Azzam, Hadi, Moad, Ibrahim, M. Dahli, R. Dahli, R. Yaiz, Sheikh Omar, Jawhar, Jamari, Wail, Salaheddin, Asheq, and Nader.

Last but not least, I would like to thank my parents, brothers and sisters who always support me and believe in me. I would like also to thank my dear wife (Maisa'a) for her patience and support. Finally, all the gratitude is to Allah Almighty.

Curriculum Vitae

Ziad Abu El-Rub was born on April 21, 1975 in Rusaifah, Jordan. In 1993 he completed his high school. In 1998, He finished his Bachelor of Chemical Engineering with distinction from the University of Jordan. He continued his master study in the same department where he took courses without thesis. At the same time he worked as a Quality Control Manager in the National's Paints Factory in Amman, Jordan. In February 2000, he started his Professional Doctor in Engineering (PD.Eng.) which was previously called Master of Technical Design in the Process Development School, University of Twente, The Netherlands.

In February 2001, he started his thesis of PD.Eng. as the first year of his Ph.D. in the Thermal Engineering Department in the University of Twente. His project aims to remove tar from producer gas of biomass fuelled gasifiers using biomass char as an in-situ catalyst.

Since Feb 2007, Ziad has been working as a Business Development Manager at KGL Petroleum Company in Kuwait. He is heading the company's projects and is directly responsible for planning, evaluating and carrying out projects assessment.